Exchange processes between the Ems river and estuary

Results of EDoM measurement campaigns 2018 & 2019

Exchange processes between the Ems river and estuary
Results of EDoM measurement campaigns 2018 & 2019

Author(s)
Bas van Maren
Julia Vroom
Daan van Keulen
Roy van Weerdenburg

Exchange processes between the Ems river and estuary
Results of EDoM measurement campaigns 2018 & 2019

Client	Rijkswaterstaat Water, Verkeer en Leefomgeving
Contact	mevrouw ir. C.A. Schmidt
Reference	WR09 2021
Keywords	Ems Estuary, Field measurements, turbidity, data analysis

Document control	
Version	2.0
Date	22-12-2021
Project nr.	11203742-000
Document ID	11203742-000-ZKS-0002
Pages	195
Status	final

Author(s)		
	Bas van Maren	
	Daan van Keulen	
	Julia Vroom	

Doc. version	Author	Reviewer	Approver	Publish
1.0	Bas van Maren	Thijs van Kessel	Toon Segeren	28-10-2020
1.1	Bas van Maren	Thijs van Kessel	Toon Segeren	3-12-2021
2.0	Bas van Maren	Thijs van Kessel	Toon Segeren	23-12-2021

Summary

The Ems estuary is a water body on the Dutch-German border with a turbidity that is considered undesirably high as a consequence of human interventions in the past. As part of the ED2050 programme, solutions are being developed and implemented to reduce the turbidity in the estuary. Deltares contributes to this programme by developing numerical models aiming to understand the mechanisms responsible for changes in turbidity and quantifying the long-term impact of potential sediment solutions. One of the uncertainties in these models was identified to be the interaction of the Ems estuary with the lower Ems River. The lower Ems river is a very turbid system connected to the Ems estuary through the Fairway to Emden. Large amounts of sediment are annually transported from the Ems estuary to the lower Ems river, reflected in continuous dredging requirements. However, the mechanisms responsible for this up-estuary transport are poorly known, even as to what extent the lower Ems river influences the sediment dynamics in the Ems estuary. To better quantitatively understand these mechanisms, a large-scale measurement campaign was set-up: the EDoM 2018-2019 measurement campaign.

This report synthesizes the main findings of the measurement campaign, specifically addressing three research questions related to this exchange: (1) which mechanisms and transport patterns are responsible for the up-estuary transport through the Fairway to Emden, (2) what is the effect of the high sediment concentrations in the lower Ems River on the sediment concentrations in the Ems estuary, and (3) why the maintenance dredging volumes in the transition zone (i.e. the Fairway to Emden) are so high.

Based on the analysis of collected data, it is concluded that the exchange between the lower Ems river and the Ems estuary is influenced by a sediment flux over the Geise dam, transporting sediment from the Dollard into the Fairway to Emden. During conditions with high river discharge, the effect of salinity-induced vertical and cross-sectional circulation also contributes to transport from the Ems estuary to the lower Ems river. The high maintenance dredging volumes in the Fairway to Emden are explained with sediment transport convergence patterns, with a superimposed seasonal variation which is probably strongly influenced by flocculation dynamics. In contrast to earlier hypotheses, flushing of sediments from the Ems River into the Ems Estuary seems to occur continuously.

The report concludes with important lessons learned from such an extensive measurement campaign with recommendations on (1) how insights of the EDoM campaign may further increase our understanding of turbidity in the Ems Estuary, (2) what future measuring campaigns should additionally be executed, and (3) new solutions to reduce turbidity and interpret the effectiveness of existing sediment solutions.

Contents

List of abbreviations and parameters

ETM	Estuarine Turbidity Maximum
SSC	Suspended Sediment Concentration
NLWKN	Niedersächsischer Landesbetrieb für.Wasserwirtschaft Küsten
BAW	Bundesanstalt für Wasserbau
EDoM	Ems-Dollard Measurements
ADCP	Acoustic Doppler Current Profiler
CTD	Conductivity Temperature Depth
NTU	Nautical Turbidity Units (measure for turbidity)
PSU	Practical Salinity Units (measure for salinity)

1 Introduction

1.1 Background

The Ems estuary, located on the Dutch-German border, is heavily modified by human activities. Its sediment concentration has increased in the past decades (de Jonge et al., 2014, van Maren et al., 2015a), but the reasons for this increase are still under debate. Proper understanding of the physical system and its response on human interventions is paramount for management of the estuary, which focusses on the improvement of the ecological system.

The Ems estuary is connected to the lower Ems River. The present-day lower Ems River is characterized by a thick layer of mobile fluid mud with concentrations up to 200 kg/m^3 (Papenmeier et al., 2013) which migrates up- and down-estuary with the tide over a distance of about 10 km. At low river flow high sediment concentrations are measured up to Herbrum, where a weir in the river has been constructed (Talke et al., 2009). The suspended sediment concentration has increased in the past decades as well (de Jonge et al., 2014), even stronger than in the Ems estuary. The river likely became hyper-turbid somewhere in the 1990’s. The transition towards hyperturbidity is most likely related to channel deepening (Chernetsky et al., 2010). The mechanisms responsible for the transition towards hyperturbidity are becoming better understood (Winterwerp and Wang, 2013; Winterwerp et al., 2013; van Maren et al., 2015b). In addition to deepening, also the construction of the upstream weir at Herbrum (Schuttelaars et al., 2013) and changing dredging activities in the beginning of the 1990’s (van Maren et al., 2015a) may have contributed.

In order to sustainably manage the Ems Estuary, the role of the Ems River on turbidity changes needs to be better understood. However, as will be elaborated in more detail hereafter, detailed knowledge on exchange mechanisms between the Ems Estuary and lower Ems River is still insufficient to accurately predict the effect of future (and past) human interventions (such as removal of mud from the system to reduce turbidity). This has motivated the execution of an ambitious measurement programme of which the main results are reported here.

1.2 Dominant physical processes in the estuary

Regions of elevated sediment concentration within an estuary are referred to as Estuarine Turbidity Maxima (ETM’s) and result from converging sediment transport mechanisms. These converging mechanisms are driven by estuarine circulation and lag effects (Dyer, 1994). Estuarine circulation is the combined effect of gravitational circulation (Postma, 1967 – see Box 1), internal tidal asymmetry (Jay and Musiak, 1994) due to tidal straining (Simpson et al., 1990), lateral tidal residual flows (Lerczak and Geyer, 2004) and river flow; the relative importance of each component is strongly site-specific. Residual transport by time lag effects (such as settling lag and scour lag) are the result of sediment properties (settling velocity, critical shear stress for erosion) in combination with asymmetries in the hydrodynamics (asymmetries in space or time). Sediment properties vary throughout the tidal cycle, and – especially at high sediment concentrations – influence the hydrodynamics (diffusivity, viscosity). An ETM is typically centred near the tip of the salt wedge (Allen et al. 1980), although in tide-dominated systems the ETM may be transported further up-estuary by tide-induced processes into the fresh water region, up to the tidal limit (Uncles et al. 2006).

Box 1 Gravitational circulation
Horizontal salinity gradients generate horizontal gradients in the near-bed hydrostatic pressure (driving a near-bed flow directed to areas with low salinity) and a sloping free water surface (driving a seaward directed current near the surface). In most estuaries, this gives rise to a vertical gravitational circulation with landward-directed currents near the bed, and seaward-directed currents near the water surface. With sediment concentrations typically higher close to the bed, this gravitational circulation leads to net landward transport of sediment.

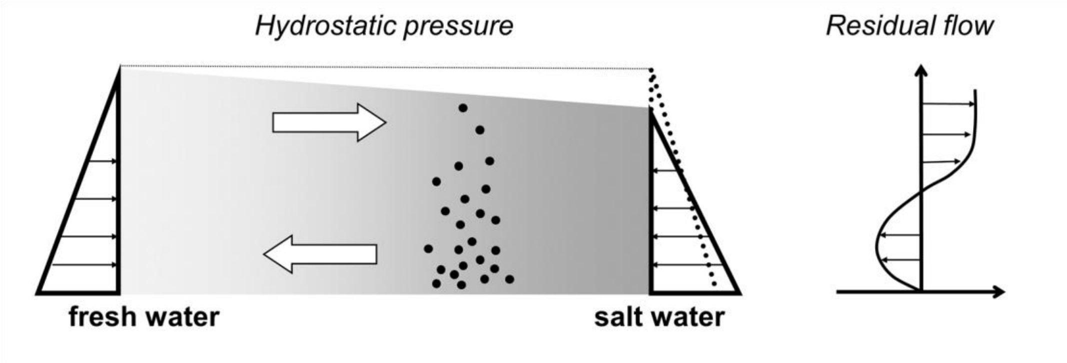

Figure 1-1 Hydrostatic pressure gradients of fresh and salt water (left, with equal total hydrostatic pressure in both the salt and fresh water triangles) and resulting residual flow (right). From Winterwerp et al., 2021.

Up-estuary transport mechanisms
The location of the ETM of the Ems River used to be located near the tip of the salt wedge (De Jonge et al., 2014) but fluid mud is presently observed many km landwards of the salt intrusion limit (Talke et al., 2009). The transport of sediment landwards of the salt limit may be the result of sediment-induced density currents (Talke et al., 2009), tidal asymmetry (Chernetsky et al., 2010; van Maren, 2015b), lag effects (Chernetsky et al., 2010), or trapping of sediments in the fluid mud layer: a combination of these processes seems most likely. Seawards of the turbidity maximum (in the outer Ems estuary) the tides are more symmetrical (although still flood-dominant; Pein et al., 2014), and salinity-driven gravitational circulation (van Maren et al., 2015b) and tide-induced residual flows (van de Kreeke and Robazewska, 1993) also contribute to residual landward sediment transport (van Maren et al., 2015b). However, the tides in the water body connecting the lower Ems River and the outer Ems estuary (i.e. the Fairway to Emden) are ebb-dominant (Pein et al., 2014). The Fairway to Emden is characterised by a steep horizontal concentration gradient (from several 0.1 g/l near the Ems Estuary to several g/l near the Ems River). Given ebb-dominant tides, a major question is why large quantities of sediment are transported against the horizontal sediment concentration gradient. This may be the result of gravitational circulation. However, baroclinic sediment transport models (such as van Maren, 2015a) fail to reproduce the strong up-estuary transport in this area, suggesting that either the nature of the salinity-driven currents or the sediment transport processes here are insufficiently understood in detail. An important aspect may be the effect of temporal and vertical variations in turbulent energy on flocculation: it was hypothesized by Winterwerp (2011) that tidal asymmetries in flocculation lead to a pronounced up-estuary sediment transport. With flocculation dynamics strongly linked to current shear and turbulence (Winterwerp et al., 2006), more quantitative insight in hydrodynamics and sediment dynamics is required in the Fairway to Emden.

Impact on the Ems estuary
Although the residual sediment transported is directed from the Ems Estuary to the lower Ems River (resulting in regular dredging of the lower Ems River and Fairway to Emden), sediment may

also be transported from the lower Ems River to the estuary. There are indications that such seaward transport takes place during high discharge events (Spingat and Oumeraci, 2000; van Maren et al., 2015b). However, it may also be that the tides are so flood-dominant that even during high discharge events sediment remains trapped in the upper reaches of the lower Ems River (Winterwerp et al., 2017). The effect of river discharge on sediment dynamics requires detailed observations of sediment transport parameters during or shortly after high and low river discharge.

A second mechanism through which the high sediment concentration in the lower Ems River influences those in the Ems estuary is shear dispersion. Mixing of a lateral concentration gradient by tidal currents generates a net transport flux that is proportional to the concentration gradient (and directed to the area with the lowest sediment concentration, i.e. the Ems estuary).

Storage in the Fairway to Emden

The transition between the lower Ems River and the outer Ems estuary, i.e. the Fairway to Emden, is sheltered from waves by the intertidal flats on which the Geise dam was built (the Geisesteert). The larger part of this ~12 km long channel is also the navigational route to the port of Emden, which is dredged to -10 m NAP to provide access to the port. The length of the channel along the Geise dam is close to the tidal excursion length, which implies that during the tidal cycle a large part of the sediment is kept within this channel and moves back and forth with the tide. Sediment may deposit during slack tide and remobilised during the following ebb and flood currents, with asymmetries in either settling or resuspension potentially generating residual sediment transport. Therefore, the water-bed interaction in this area is important for exchange processes between the lower Ems River and the Ems estuary. Although the flow velocities in the Fairway to Emden are high, sedimentation rates are also high. Approximately 1.6 million tons of fine-grained sediments are annually dredged from the fairway and disposed in the estuary. It is not known why so much sediment accumulates in the fairway, and neither how this impacts the transport into the lower Ems River. Existing complex 3D transport models such as used by van Maren et al. (2015a) fail to reproduce these sedimentation rates, and apparently miss the dominant physical transport mechanisms.

1.3 Research questions

The previous section provides an overview of the most likely main sediment transport mechanisms in the Fairway to Emden and the interactions of the fairway with the Ems estuary and the lower Ems river. Knowledge gaps have been identified. The current study aims to increase our understanding of the exchange between the Ems river and the estuary (including the Dollard bay), to be able to better understand its effect on the turbidity and the related high dredging and disposal volumes. We therefore formulated three research questions which will be addressed in this report:

1. What are the mechanisms responsible for the large up-estuary transport through the Fairway to Emden?
2. What is the effect of the high sediment concentrations in the lower Ems River on the sediment concentrations in the Ems estuary?
3. Which mechanism are responsible for the high maintenance dredging volumes in the Fairway to Emden?

The EDoM measurement campaign has been setup in such a way that they provide sufficient information to address these research questions, including detailed observations of the vertical structure of the currents and sediment dynamics (13 hrs ship observations) and timescale varying from a spring-neap cycle (continuous frame observations deployed for 1-2 spring-neap cycles) to seasonal variations (with a measurement campaign during high and low discharge conditions) with sufficient spatial coverage to generate a synoptic pattern of transport mechanisms (8 ships and 8 frame observations).

1.4 Outline of the report

The full analysis of data is provided in the appendixes, both in figures as in detailed textual descriptions. The main report primarily addresses the main integral outcome of the EDoM measurements, focussing on the research questions provided above.

The structure of this report is as follows. The EDoM campaigns are shortly introduced in Chapter 2, whereas the main results are provided in Chapter 3. The main body of the report finalises with conclusions, recommendations, and lessons learned. More details of the data are given in the appendices. Appendix A provides details on the EDoM measurements. More detailed visualizations and interpretation of data during the 13-hr surveys follows in Appendix B. Dredging volumes are summarized in Appendix C. All analysed data is visualized in Appendix D without any data interpretation. All data reporting flow and sediment transport over the Geise Dam resulting from the EDoM measurements but also earlier campaigns are reported in Appendix E. Appendix F provides the data from the flocculation camera.

1.5 Acknowledgements

This report compiles and describes data collected as a joint effort by a large group of people. We are grateful for all boat and survey crews for their help in collecting the data. We would especially like to acknowledge the help of Jan-Willem Mol (for coordinating the measurements from Rijkswaterstaat and postprocessing of ADCP data), Christian Maushake (for coordinating the measurements from the German side, and postprocessing of ADCP data), Andy Manning (for carrying out the floc experiments), and Petra Dankers (for general coordination of the measurement campaign).

2 The EDoM campaigns

The EDoM (Ems-Dollard Measurements) campaign was carried out in the summer of 2018 and the winter of 2019. The aim of the summer campaign is to document exchange during low discharge conditions (~30 m^3/s, see Figure 2-1) between the Ems River and the Ems estuary, whereas the winter campaign targets conditions of higher discharge (50-250 m^3/s, see Figure 2-1). Also, the wave conditions matter when considering sediment transport in the area of interest. Wave height measurements show that the wave height during both deployment periods was fairly comparable, and the wave height during the January 2019 deployment is slightly lower than average winter conditions (Figure 2-1). Measurements consisted of (1) moorings operated by BAW and RWS, measuring for one to two spring-neap tidal cycles, and (2) simultaneous shipborne observations carried out during a 13-hrs period (see Figure 2-2 for the location of all surveys). The 13-hrs measurements were executed on 28 August 2018 and 24 January 2019, with the longer moorings deployed prior and after the 13-hrs measurements.

Unfortunately, the discharge of the Ems river was relatively low during the winter of 2019 (see also the discharge of the previous year in Figure 2-1) and started late. Note that the 13-hrs measurements on 24 January were carried out in-between two peaks in the river discharge at Versen.

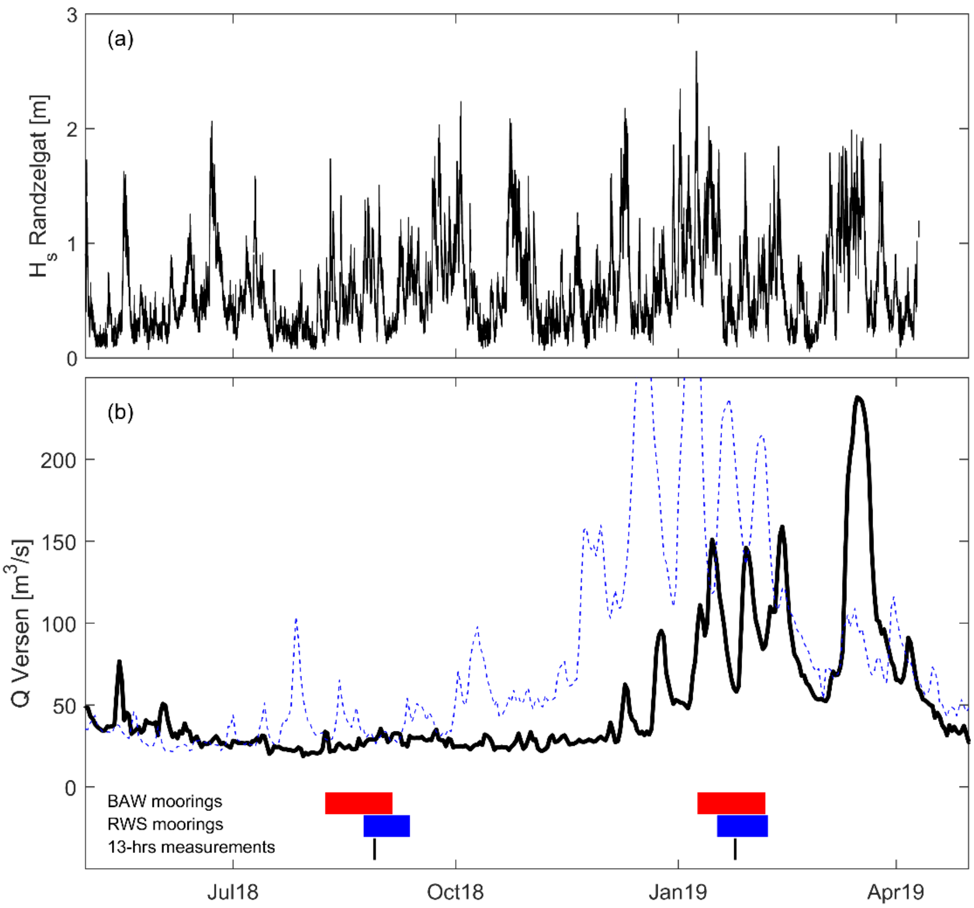

Figure 2-1 Wave height H_s measured at station Ranzelgat (a) and discharge of the Ems river at Versen (b) from 1 May 2018 to 1 May 2019, with deployment dates of BAW frames, RWS frames, and the 13-hrs measurements added to (b). The dashed blue discharge in (b) is the discharge of the period 1 May 2017 to 1 May 2018.

Table 2.1 Explanation of abbreviations for survey type and location

Measurement type		**Location**	
CS_	Cross-section	GAT	Gatjebogen
SB_	Stationery Boat	KNO	Knock
BM_	Bottom Mount	DOL	Dollard
MC_	Mooring Chain	EFW	Emder Fahrwasser (Fairway to Emden)
RS_	RWS bottom frame	EMD	Emden
		POG	Pogum

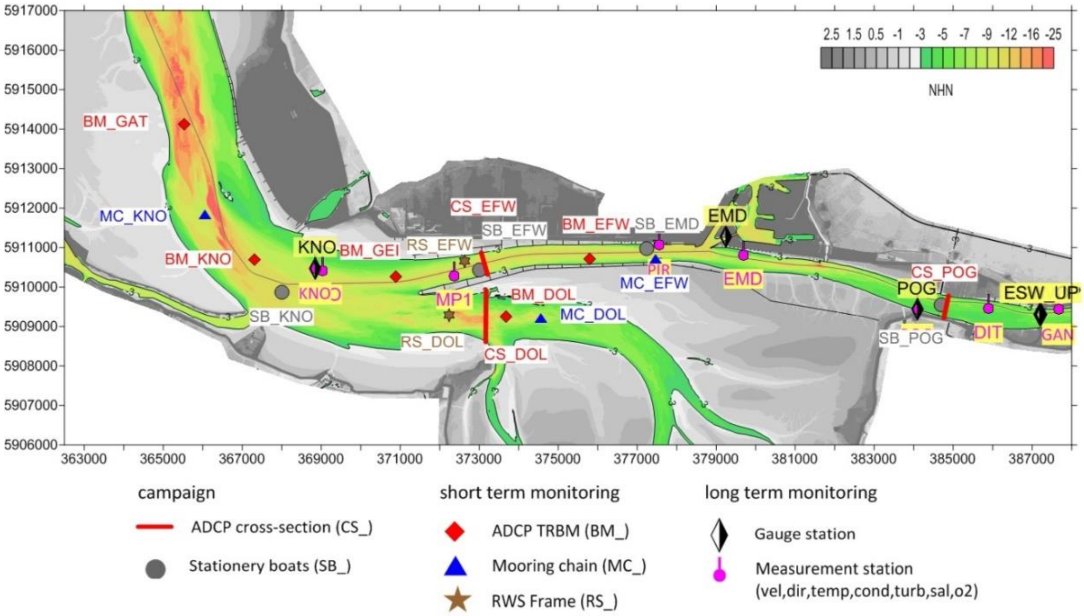

Figure 2-2 Location of all observation stations during the EDoM campaigns (see Table 2.1 for explanation of abbreviations). From Maushake and Dankers (2018).

Three types of boat surveys were executed during the 13-hrs measurements: stationary measurements, cross-sections, and a longitudinal survey. During stationary measurements, the boat remains anchored for the full measurement period of 13 hours. This allows surveying of the water column with profilers (salinity, temperature, turbidity, fall velocity, turbulence properties) and collection of water samples. During cross-sections, profiling is not possible and only flow velocity and echo intensity profiles are measured using ADCPs. The longitudinal profile was sailed from Borkum to Papenburg during flood, and back during ebb. All 13-hrs measurements started 20 minutes before low water and continued until low water slack of the following tide (see Figure 2-3). Low water is progressively later in the up-estuary direction, and therefore the various boat surveys started at slightly different times.

One aspect that arose during the elaboration of the collected data (as will be elaborated in more detail in this report) was that the role of flows over the Geise dam was important for the sediment budget. Therefore, additional measurements were executed on the Geise dam in January 2019 (Western Geise dam) and in March 2020 (Eastern Geise dam).

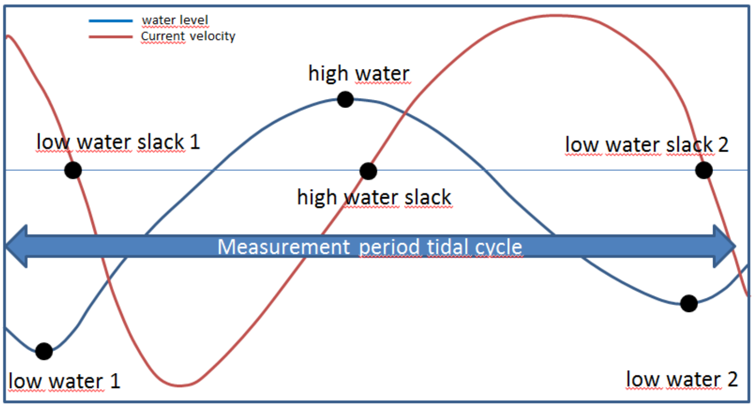

Figure 2-3 Definition of the measurement period of the 13-hrs surveys (from Maushake and Dankers, 2018).

The BM frames were equipped with an upward-looking ADCP and sensors measuring salinity, temperature and turbidity close to the bed. The RS frames were additionally equipped with a downward-looking ADCP (measuring the velocity close to the bed) and a second sensor for measuring salinity, temperature, and turbidity. The mooring chains (MC) measured velocity, salinity, temperature, and turbidity at three locations in the vertical. A summary of all observations is provided in Table 2.2. All data was processed initially by the institute responsible for executing the measurements. This initial processing phase includes calibration and validation, conversion to a standard format, and adding of metadata in a separate data report (Wunsche, 2019) or read me files (most data). The data was subsequently uploaded to an FTP server from which data can be disseminated among project partners.

Table 2.2 Summary of executed measurements per location

Observation station	Measurements
BM_GAT	Velocity profile; salinity, temperature, turbidity at 1 vertical position
BM_KNO	Velocity profile; salinity, temperature, turbidity at 1 vertical position
BM_GEI	Velocity profile; salinity, temperature, turbidity at 1 vertical position
BM_DOL	Velocity profile; salinity, temperature, turbidity at 1 vertical position
BM_EFW	Velocity profile; salinity, temperature, turbidity at 1 vertical position
MC_KNO	Velocity, salinity, temperature, and turbidity near-bed, middle, and near-surface
MC_DOL	Velocity, salinity, temperature, and turbidity near-bed, middle, and near-surface
MC_EFW	Velocity, salinity, temperature, and turbidity near-bed, middle, and near-surface
RS_DOL	Velocity profile (also near-bed); salinity, temperature, turbidity at 4 vertical positions
RS_EFW	Velocity profile (also near-bed); salinity, temperature, turbidity at 4 vertical positions
SB_KNO	Profiles of salinity, temperature, turbidity, velocity, settling velocity (LISST) and turbulence (fall velocity and turbulence only in 2018); water samples near-surface, near-bed, and in the middle
SB_EFW	Profiles of salinity, temperature, turbidity, velocity; water samples near-surface, near-bed, and in the middle
SB_EMD	Profiles of salinity, temperature, turbidity, velocity, settling velocity using LISST (only in 2019), settling velocity from camera; water samples near-surface, near-bed, and in the middle
SB_POG	Profiles of salinity, temperature, turbidity, velocity; water samples near-surface, near-bed, and in the middle
CS_DOL	Profiles of flow velocity and echo intensity
CS_EFW	Profiles of flow velocity and echo intensity
CS_POG	Profiles of flow velocity and echo intensity
Long	Near-surface salinity, temperature and turbidity; profiles of echo intensity and velocity

3 Results and discussion

We start out with answering the research questions (as introduced in section 1.3) in section 3.1, based on a more extensive analyses addressed in the sections thereafter. We focus on a horizontal circulation identified as part of the measurements in section 3.2, and evaluate transport patterns within the Fairway to Emden in more detail in section 3.3.

3.1 Answers to research questions

3.1.1 What are the mechanisms responsible for the large up-estuary transport through the Fairway to Emden?

The persistent dredging required in the lower Ems River are clear evidence of a net sediment transport from the Ems Estuary to the lower Ems River. It was *a priori* believed that this sediment is conveyed through the Fairway to Emden, and especially during summer conditions – sediment transport would be in opposite direction during winter conditions because of higher river discharge. However, the tides in the fairway are ebb-dominant and therefore tidal asymmetry does not generate landward transport. During winter conditions, tides do lead to landward transport through a large sediment availability of sediment around low water slack, possibly related to lateral sediment supply (transport over the Geisesteert).

Analysis of the EDoM measurements reveals the following (numbers referring to sketches in Figure 3-1)

- The sediment fluxes suggest that sediment is transported *out* of the fairway during summer conditions (1). Some sediment may be imported during winter conditions because of estuarine circulation (a salinity-driven landward-directed bottom current, (1)) and a landwards increasing sediment availability around high water slack (2)
- A very persistent sediment flux exists into the Dollard due to higher sediment concentrations during flood than during ebb (3)
- A significant residual water flow exists from the Dollard to the fairway over the Geisesteert, probably generating a residual transport of sediment from the Dollard to the fairway (4).

The Dollard does not fill up with sediments, and therefore the sediment flux into the Dollard probably flows back into the fairway over the Geisesteert. This sediment is transported over the Geise dam around high water, and therefore most of this sediment flux is subsequently diverted seawards with the onset of ebb. Along the southern bank of the Fairway to Emden, flood currents are larger than ebb currents. Therefore, sediments flowing over the Geise dam may be temporally deposited on the bed and transported into the lower Ems river during the flood. Of particular importance hereby is the large availability of sediment in the Emden fairway around low water slack, which probably originates from the Dollard mudflats.

During winter (storm) conditions, it is expected that more water will flow over the Geise dam. With high suspended sediment concentrations resulting from wave-induced resuspension of the Dollard mudflats, sediment is efficiently transported into the Fairway to Emden, and part of the sediment is advected into the lower Ems River. However, this effect could not be substantiated with observations carried out in the winter of 2020.

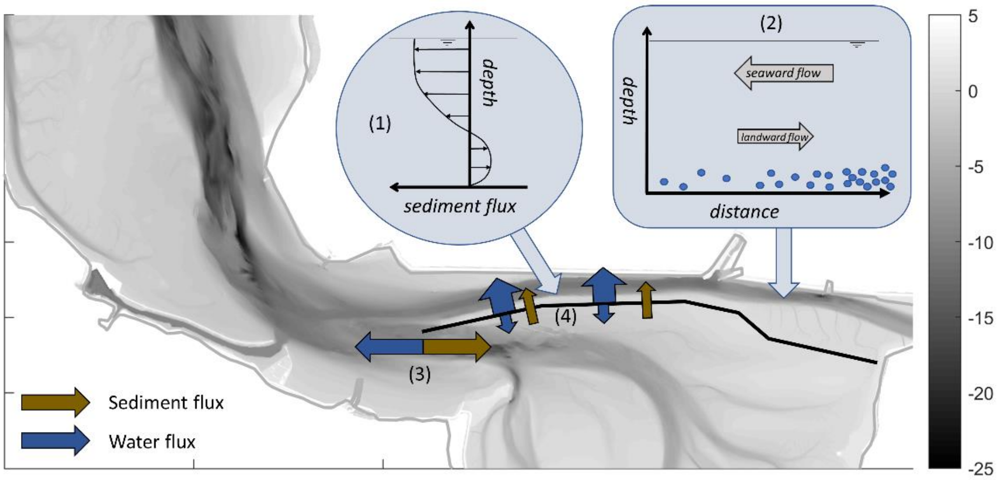

Figure 3-1 Sketch with main processes driving the up-estuary transport through the Fairway to Emden. See text for details.

3.1.2 What is the effect of the high sediment concentrations in the lower Ems River on the sediment concentrations in the Ems Estuary?

Sediment is transported from the Ems estuary to the lower Ems river through the Fairway to Emden. However, sediment is also transported in the seaward direction during ebb flows, especially in combination with high discharge conditions. The EDoM measurements have revealed the following impact of the lower Ems River on the sediment concentration in the Ems Estuary (numbers referring to sketches in Figure 3-2):

- The sediment concentrations at the mouth of the Fairway to Emden (near Knock) are 2-3 times higher in winter than in summer (1).
- The higher winter concentrations (also those flowing out of the fairway into the Ems Estuary) are related to (a) wave-induced resuspension of the mudflats in the Dollard (2), (b) seaward flushing of sediment by high river discharge (1), and (c) lower settling velocities (1). As long as the discharge in the lower Ems River is high, and/or wave-induced resuspension is pronounced, the sediment concentration at Knock during winter will progressively increase (as the observations indeed suggest).
- During summer conditions, sediment is gradually deposited in the Dollard (2). Less sediment enters the Fairway to Emden and is subsequently transported into the Ems Estuary, and then the Dollard. This may at least partly explain the lower sediment concentration in the Ems estuary and the Fairway to Emden during summer (Figure 3-18; see also Smits and van Maren, 2021). Other factors are lower sediment resuspension rates by waves, and higher settling velocities in summer.

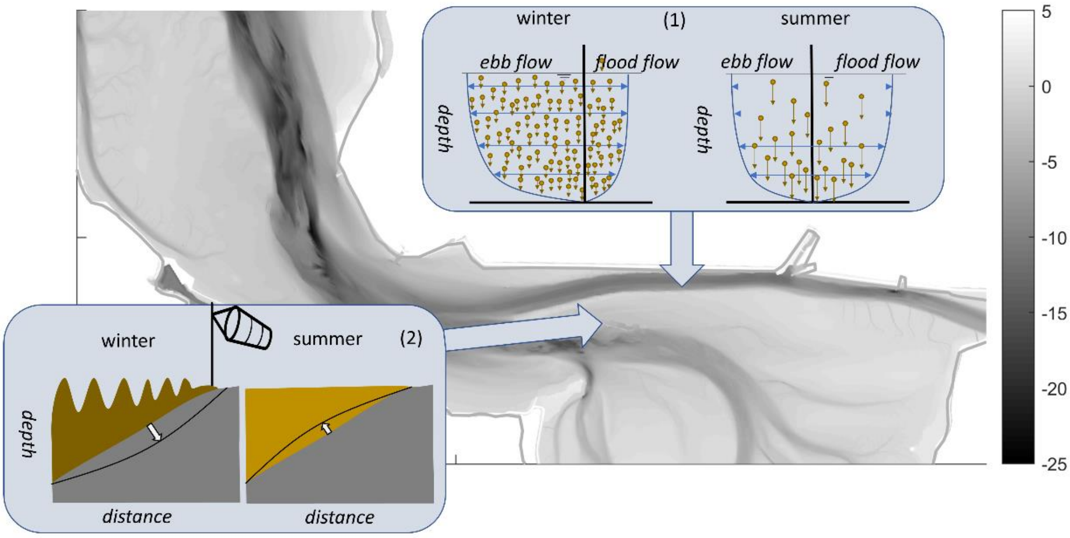

Figure 3-2 Sketch with main influences of the lower Ems River on the Ems Estuary. See text for details.

3.1.3 Which mechanisms are responsible for the high maintenance dredging volumes in the Fairway to Emden?

In summer, most dredging takes place in the Fairway to Emden between km 45 and 50. In winter, dredging shifts seawards, with a peak between km 50 and 53 (between the Fairway to Emden and Knock). More sediment is dredged in summer (defined as May through October): 3.4 million m^3 in 2018 and 3.3 million m^3 in 2019 compared to 2.5 million m^3 and 1.3 million m^3 in winter, for the same years. Analysis of the EDoM data has revealed the following relationships between dredging and sediment transport processes (numbers referring to sketches in Figure 3-3):

- The location of dredging corresponds to areas of sediment convergence ((1), also compare Figure 3-4 with Figure C.1). The sediment flux from the Dollard over the Geise dam feeds the pronounced seaward sediment transport from the Fairway to Emden to the estuary in both summer and winter; probably more in winter than in summer (1a).
- Further seaward transport of the zone with elevated suspended sediment concentration is counterbalanced by salinity-driven residual flows (2). The resulting landward-directed near-bed current effectively traps sediment at the head of the estuary, especially just after high river discharges.
- The sediment flux from the Dollard over the Geise dam also directly causes high deposition rates within the Fairway to Emden by directly depositing in the fairway after flowing over the Geise dam (1b).
- Dredging volumes are influenced by the seasonal variation in floc density and settling velocity, with dense, fast settling flocs leading to the deposition of (fluid) mud requiring maintenance dredging; the less dense, slowly settling flocs in winter generate highly concentrated near-bed suspensions which do not need to be dredged (and are easily transported into the lower Ems River).

Sediment convergence may lead to higher sediment concentrations or to dredging, depending on the local bed shear stresses and the strength of the sediments on the bed. The higher dredging volumes in summer compared to winter are probably caused by differences in settling velocity and density of flocs. The settling velocity in summer is about 50% larger than in winter, and the density of flocs is, on average, more than two times larger (so the mass settling flux is three times larger). Larger density implies that the flocs are more compact. In summer, these depositing flocs may rapidly gain strength due to their higher density and are not easily eroded. In winter, the flocs remain in suspension for a longer period of time (partly explaining the higher sediment concentrations in winter) and probably form a highly concentrated benthic suspension (fluid mud) which may not need to be dredged and is easily transported by tidal currents and by salinity-driven flows (leading to landward transport).

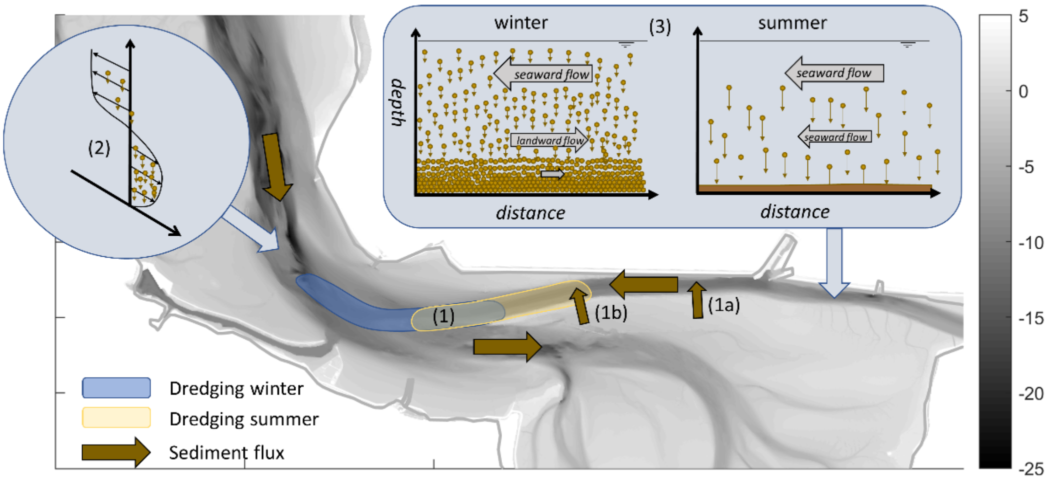

Figure 3-3 Sketch with main mechanisms influencing dredging volumes in the Fairway to Emden. See text for details.

3.2 Large scale transport patterns

3.2.1 Circulation of sediments between the Dollard, the Fairway to Emden, and the Ems Estuary

The sediment fluxes computed from both the frame (BM and RS) and the mooring chain (MC) deployments provide a consistent picture of the large-scale sediment transport (Figure 3-4). Both during low and high discharge conditions, sediment is transported landwards in the Dollard and mostly seawards in the Fairway to Emden (although the transport directions are more complex in the fairway during high discharge conditions, which will be discussed in more detail in section 3.3). Extrapolating the fluxes computed over a tidal cycle or a spring-neap cycle to the period of a year (see box 2 for methodology) suggests that approximately 6 million ton/y is transported from the estuary into the Dollard, and 6 million ton/y out of the Fairway to Emden into the estuary (Figure 3-5). All residual mass fluxes are expressed in ton (or kg) dry matter.

Note that the sediment concentration for most of the mooring locations (BM and RS) was only measured near the bed, and these concentrations were used over the whole profile to estimate the sediment flux. With sediment concentrations generally being higher close to the bed, this simplification overestimates the surface sediment flux. Only the mooring chains (MC) provide fluxes based on depth-varying flow velocity and sediment concentration.

By considering tidal asymmetry in sediment concentrations, we can understand the direction of the sediment fluxes from the different areas. Sediment export from the Fairway to Emden is not only the result of a seaward-directed residual flow (generated by the river discharge itself, see appendix 7D.1 and 7D.2) but primarily by a higher sediment concentration during ebb than during flood. A first estimate of the residual flow component can be obtained by multiplying the average river discharge with the typical ambient sediment concentration: using Q = 60 m^3/s and C = 0.5 g/l leads to export of 1 million tons of sediment. The majority of export results therefore from a tidal asymmetry in the sediment concentration: a slightly higher SSC during ebb already leads to a large residual transport of sediment.

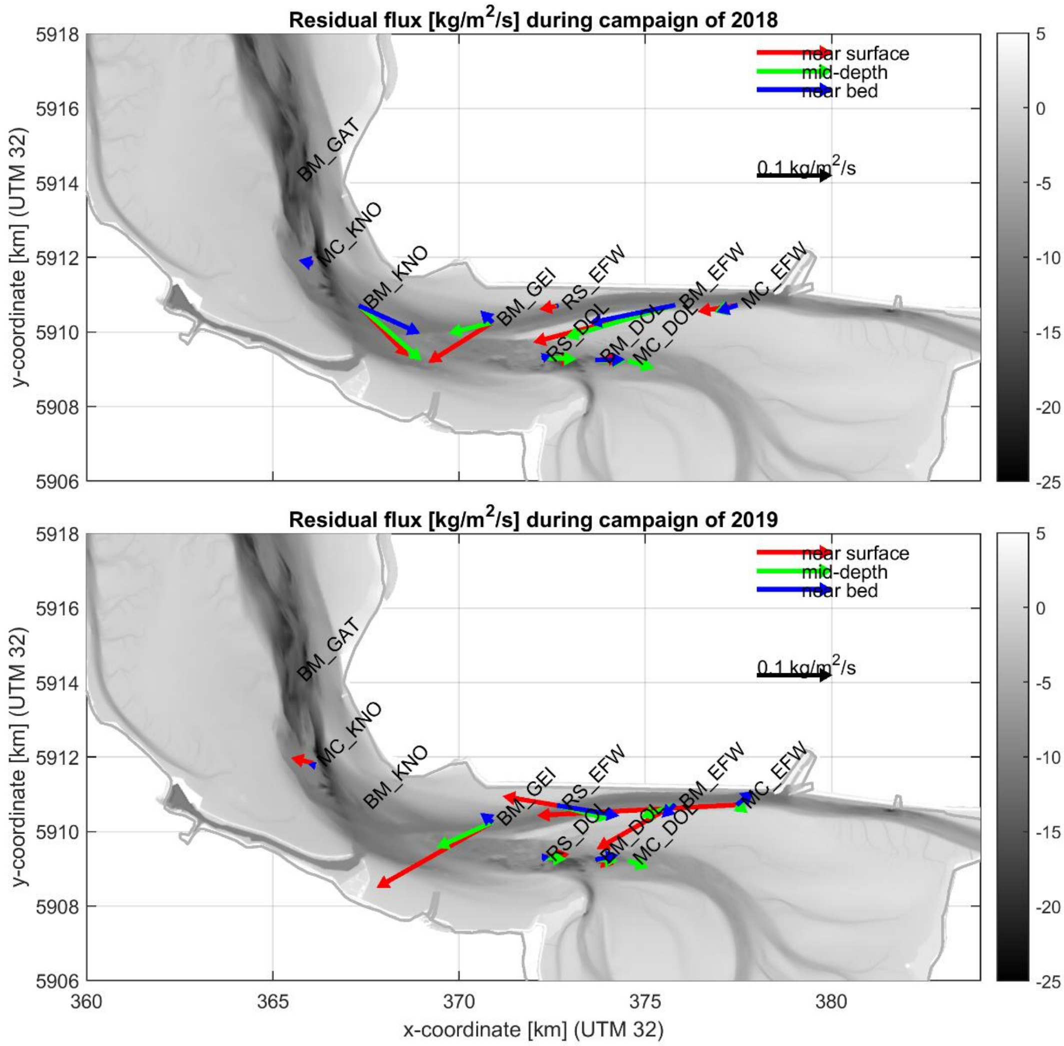

Figure 3-4 Residual sediment transports [kg/m²/s] computed at all observation stations with a length exceeding the duration of a spring-neap cycle, in 2018 and 2019 for which velocity and SSC observations are available. At MC stations, velocities at 3 positions in the vertical are multiplied with SSC at the same position. At other locations velocity profiles, as collected by an ADCP are multiplied with near bed SSC.

Residual sediment transport into the Dollard is also mostly the result of an ebb-flood asymmetry in the sediment concentration. The residual flow in the entrance to the Dollard is very low and therefore not driving residual transport. However, the sediment concentration during flood is markedly higher than during ebb (Appendix 7B.4). This higher sediment concentration during flood is likely the result of a large sediment supply from the Fairway to Emden delivered by the previous ebb phase: sediment transported out of the Fairway to Emden remains in suspension or settles on the bed and is transported into the Dollard bay during the subsequent flood period. In addition, there is also a short period (~30 mins) around low water when the water is still flowing out of the Fairway to Emden, and already into the Dollard bay (Figure 3-10 and also shown by flow velocities for the various stations in appendix B.3).

Box 2 Computation of fluxes
The annually averaged cross-sectional sediment fluxes are computed from point observations, which requires several steps and underlying assumptions.

Step 1: depth-averaging
The way each depth-averaged sediment flux is computed depends on the available type of observations. For the boat surveys, profiles of velocity *u* (with *u* being a 2-dimensional vector) and sediment concentration *c* have been collected every half hour. The depth-averaged sediment flux is then computed by depth-integrating the product of u_z and c_z between the ADCPS blanking range near the bed ($z_{b,b}$) and surface ($z_{b,s}$): $F = \int_{z=z_{b,b}}^{z=z_{b,s}} u_z c_z dz$. Note that no correction has been applied for the sediment flux above the near-surface blanking range and below the near-bed blanking range.
A velocity profile with a point concentration profile close the bed is available for near bed frame observations. Here the depth-averaged flux is computed by multiplying the flow velocity profile with the near-bed sediment concentration instead of the depth-varying concentration. The mooring chains were equipped with velocity sensors and turbidity sensors at three depths. The depth-averaged flux is here defined as the average of the product of *u* and *c* at three height.

Step 2: time-averaging
The short-term moorings provide timeseries of fluxes for a period of 1-2 spring-neap cycles (depending on deployment). The yearly averaged fluxes are obtained by selecting a spring-neap tidal period during which all moorings were deployed during a particular measurement campaign, computing the time-averaged flux, and multiplying this flux with the number of spring/neap cycles in a year.

Step 3: width-averaging
The depth-and time averaged flux is subsequently multiplied with the width of the cross-section. This step introduces the greatest uncertainty because (1) the flow velocity is not constant over the cross-section, (2) the water depth is not constant over the cross-section (and the depth-integrated flux can be assumed to be larger in deep water), and (3) the transport processes vary over the cross-section (with typically most salinity-driven transport in deep water). The distribution of flow (averaged over the flood, ebb, and tide) over a cross-section is compared with the nearby point-measurements in Appendix D.1.11 and D.2.1.11.

The large export from the Fairway to Emden is surprising, because we know that sediment is transported from the Ems estuary into the lower Ems River and large volumes of sediment are dredged from the Fairway to Emden. The computed exporting flux from the Fairway to Emden can be explained in two ways: (1) the budgets are not representative and/or (2) a large amount of sediment is transported over the Geise dam. We will first elaborate on the accuracy of the computed fluxes, followed by transport over the Geise dam.

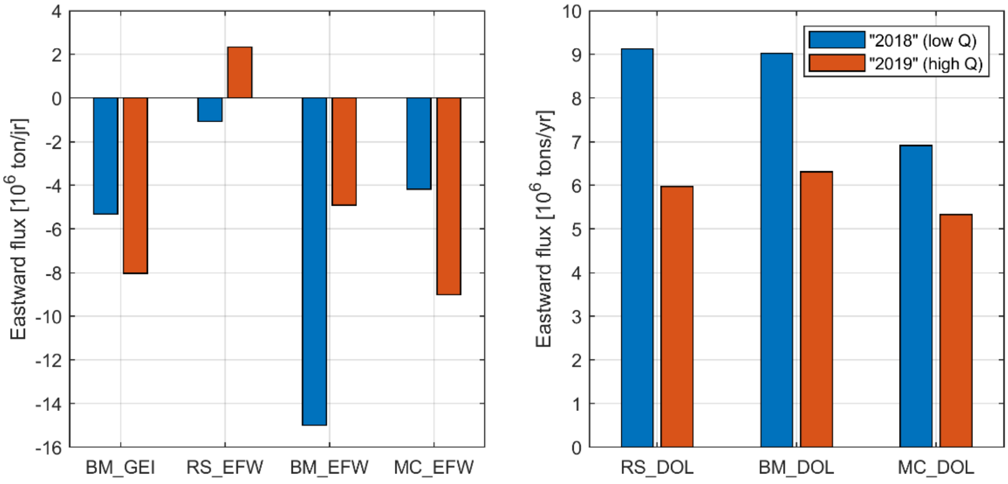

Figure 3-5 Annually averaged sediment flux in the Fairway to Emden (left) and Dollard (right) in 2018 (blue) and 2019 (red), obtained by extrapolating the flux measured over one spring-neap cycle over time, and multiplying with the average width and depth of the cross-section.

3.2.1.1 Accuracy of flux computations

Errors in the fluxes may result from spatial and temporal extrapolations and measurement errors. If the gross flux (the amount of sediment transported during ebb and during flood) is large compared to the net flux (the difference between the gross ebb and flood flux), then relatively small errors in either the ebb or flood flux have a large impact on the net flux. Typically, the gross fluxes are three to seven times higher than the net sediment fluxes (Figure 3-6). Hence, the net fluxes are fairly large compared to the gross fluxes, and therefore methodological errors in computing the gross fluxes are unlikely to influence the direction of residual transport. Even more, the consistency of both the direction and magnitude of the computed fluxes (especially in the Dollard) suggests that both the directions and the order of magnitude of the net and gross fluxes are fairly accurate. However, the absolute value of the fluxes still has a uncertainty of at least several 10's of percent, resulting from natural variability over time and space and measurement errors.

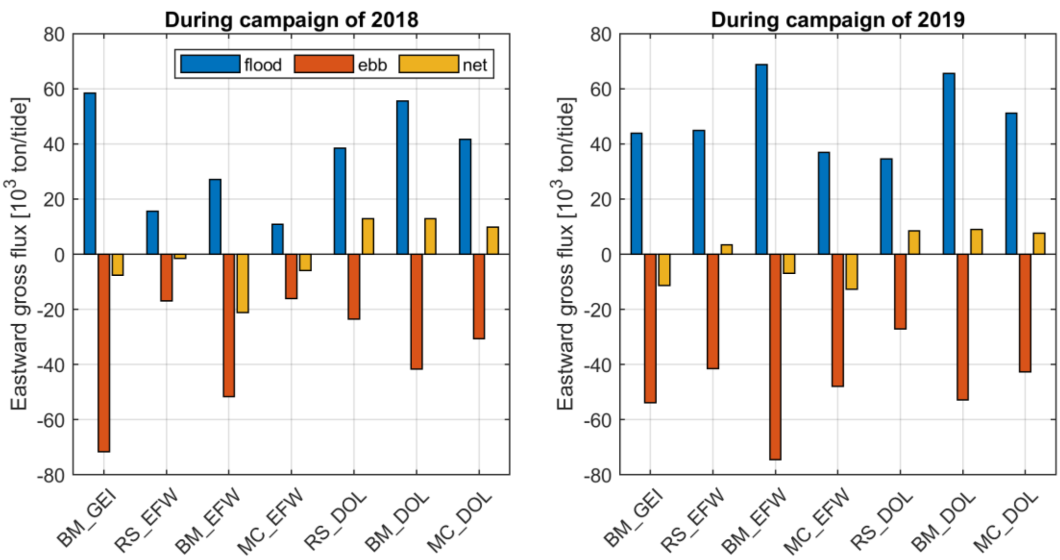

Figure 3-6 Gross and net fluxes per tide, based on one spring-neap cycle of observations from the long term moorings, in 2018 and 2019. Positive fluxes are directed in the flood direction.

In order to evaluate the importance of the cross-sectional averaging, we also provide flux estimates based on ADCP transect observations (carried out in the entrances of the Dollard, the Fairway to Emden, and the lower Ems River at Pogum), see Figure 3-7. The Dollard transects provide a residual transport around 4,000 (2018) and 6,000 (2019) ton/tide in the flood direction, corresponding to 2.8 and 4.2 million ton/year. These transect fluxes are approximately 2-3 times lower than the fluxes computed with the long-term moorings, but still in the same direction. Also the flow measured at the Dollard point observations is representative for the flow over the whole cross-section (measured during transect surveys), while the concentration distribution is fairly homogeneous over the cross-section during both ebb and flood (see details in Appendices 7D.1.1.11 and 7D.2.1.11).

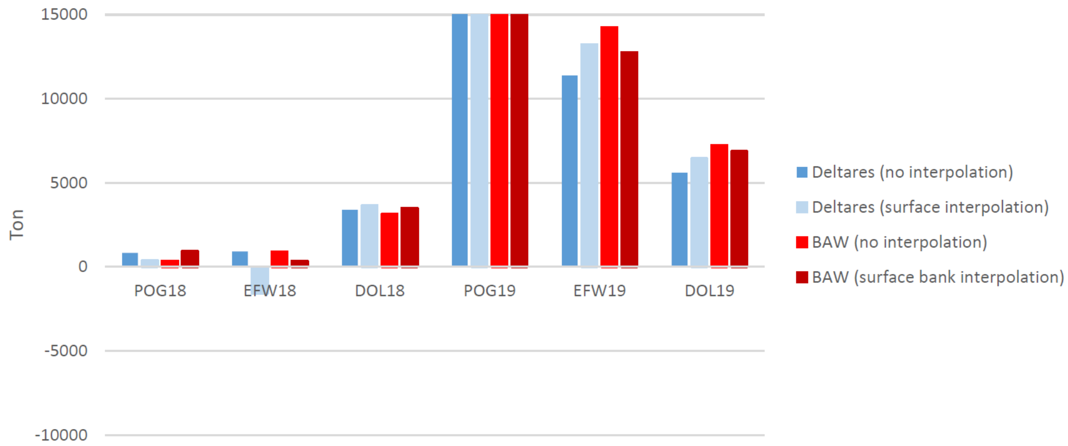

Figure 3-7 Residual flux computed from the 13-hour measurements at the entrances of the Dollard, the Fairway to Emden, and the lower Ems River in 2018 and 2019. N.B. Four methodologies are compared, differing in executing partner (BAW / Deltares) and with or without extrapolation (where Deltares only extrapolates to the surface, and BAW also towards the river banks and bed). Positive fluxes are directed in the flood direction. All fluxes computed for Pogum are capped at 15000 ton for readability, but equal to 2471, 27027, 60991 and 60881 (resp.) ton for Deltares without, Deltares with, BAW without, and BAW with interpolation.

The residual flux at EFW is close to zero in 2018 (Figure 3-7), and around 12,000 ton/tide (8.5 million ton/year) in the flood direction in 2019. This is a substantial difference with the residual fluxes computed at mooring stations BM_EFW (20,000 ton/tide in ebb direction in 2018 and close to zero in 2019) and RS_EFW (close to zero in both years). The differences between the transect fluxes and the moorings can be explained by four aspects:

1. ADCP backscatter is not always a good measure for SSC. This is exemplified by Figure 3-8, where water samples show that the SSC is two times higher during ebb than during flood, whereas the echo intensity of the ADCP provides nearly equal ebb and flood SSC. The water samples therefore suggest ebb-dominant sediment transport, whereas the ADCP-based estimate has a negligible flux (and the net direction results from small differences between the ebb and flood SSC or residual flow). For fine-grained sediments, the OBS (as used by the moorings) typically provides a more reliable estimate.
2. The duration of the survey is short, and therefore easily influenced by (1) the averaging period and (2) non-representative conditions. Although the period of the dominant M2 tide is 12.41 hours, the hydrodynamic conditions after exactly 12.41 hours are rarely identical because of the impact of other tidal constituents and because of meteorological conditions. For cross-section EFW, the residual flow was directed landwards in both 2018 and 2019 (without extrapolation) which is not realistic from a physical point of view as the river is delivering water to the estuary. Non-representative conditions include nearby dredging activities, increased wave height and set-up or river discharge.

3. The transect observations also cover the deep channel, whereas continuous observations are not allowed to measure in the deep channel not to hinder navigation. Close to the bed in the deeper parts of the channel, the flow and transport is typically directed landwards (see also section 3.2). For this aspect, transect measurements are therefore more accurate.
4. The ADCP echo intensity accounts for the full SSC profile, which the moorings do not cover. This aspect is therefore more accurate for transect observations (although there may be a large error in the absolute value of the SSC observations, as explained under point 1).

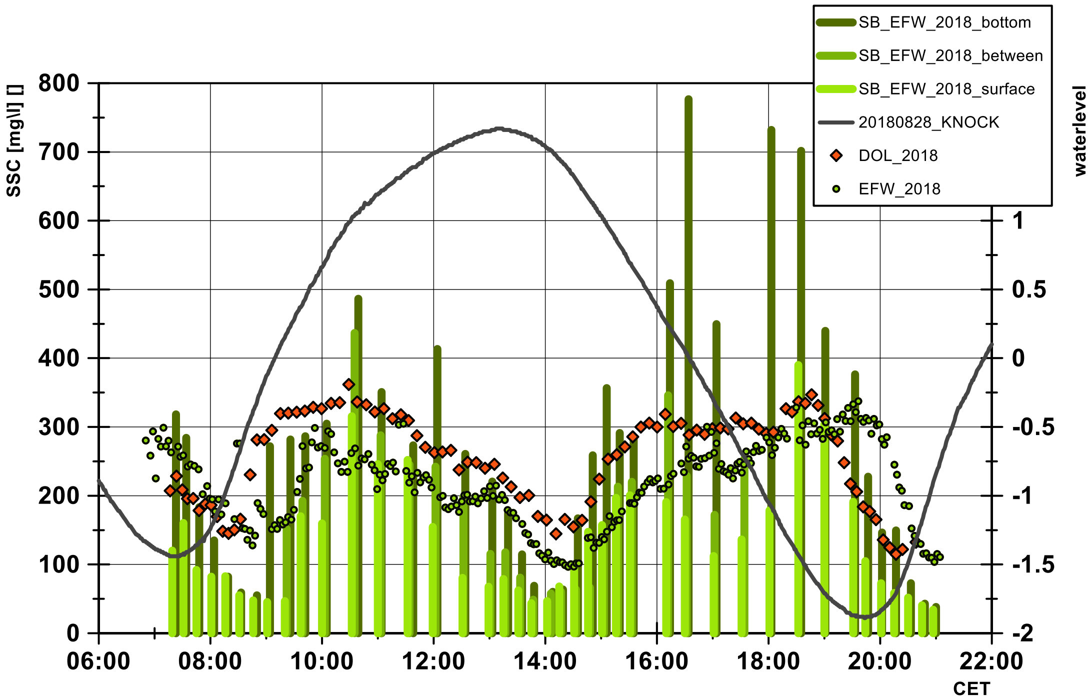

Figure 3-8 Sediment concentration at EFW in 2018 based on water samples (dark / light green bars) and SSC based on ADCP echo intensity at EFW (green dots). Figure provided by BAW.

It is difficult to determine which of these aspects is most important, and therefore which method is most accurate. The tidal variability in the difference between the ADCP backscatter and observations is so large for EFW2018 that this observation cannot be used for residual fluxes (typically the residual is 10-20% of the gross flux, so a factor 2 error in the gross flux leads to very unrealistic residual fluxes). However, for most other transect observations the differences are more subtle. Gravitational circulation generates a near-bed landward directed current likely resulting in sediment import through the Fairway to Emden (although not as large as suggested by the EFW transect, given the seaward flux measured by most other observation methods). This will be elaborated in more detail in section 3.2.

The sediment fluxes vary over the year (resulting from variability in discharge, wave and wind conditions, offshore sediment supply and biological effects). Nevertheless, the fluxes computed over a spring-neap period during the two measurement campaigns are remarkably similar, even though the river discharge conditions differed significantly (see Figure 2-1).

Dyer et al. (2000) revealed that the residual flux in the Dollard depends on wind and wave conditions, with sediment transport in the flood direction during calm conditions and transport in the ebb direction during periods with wave-induced resuspension. We did not observe a seaward flux from the Dollard during the EDoM surveys. The wave height during both deployment periods was fairly comparable, and the wave height during the January 2019 deployment was slightly lower than average winter conditions (Figure 2-1). The residual transport in the flood direction measured in the Dollard may therefore reverse direction during more wave-dominated conditions.

But despite this dependence on wave height, the computed fluxes seem sufficiently realistic to conclude that several million ton per year is transported into the Dollard. All observations predict export from the Fairway to Emden in summer, whereas the direction of the residual flux in the winter period depends on the methodology. Since only the transect measurement and a single point measurement suggest import and other point measurements suggest export during this period, it is likely that sediment is also exported from the Fairway to Emden. The time-variation in this flux introduces an uncertainty in the absolute yearly fluxes, and therefore we will hereafter refer to a landward transport into the Dollard and seaward transport from the Fairway to Emden of 'several million ton'. The most likely mechanism explaining the large transport fluxes into the Dollard and out of the Fairway to Emden is then a considerable transport of sediment over the Geise dam.

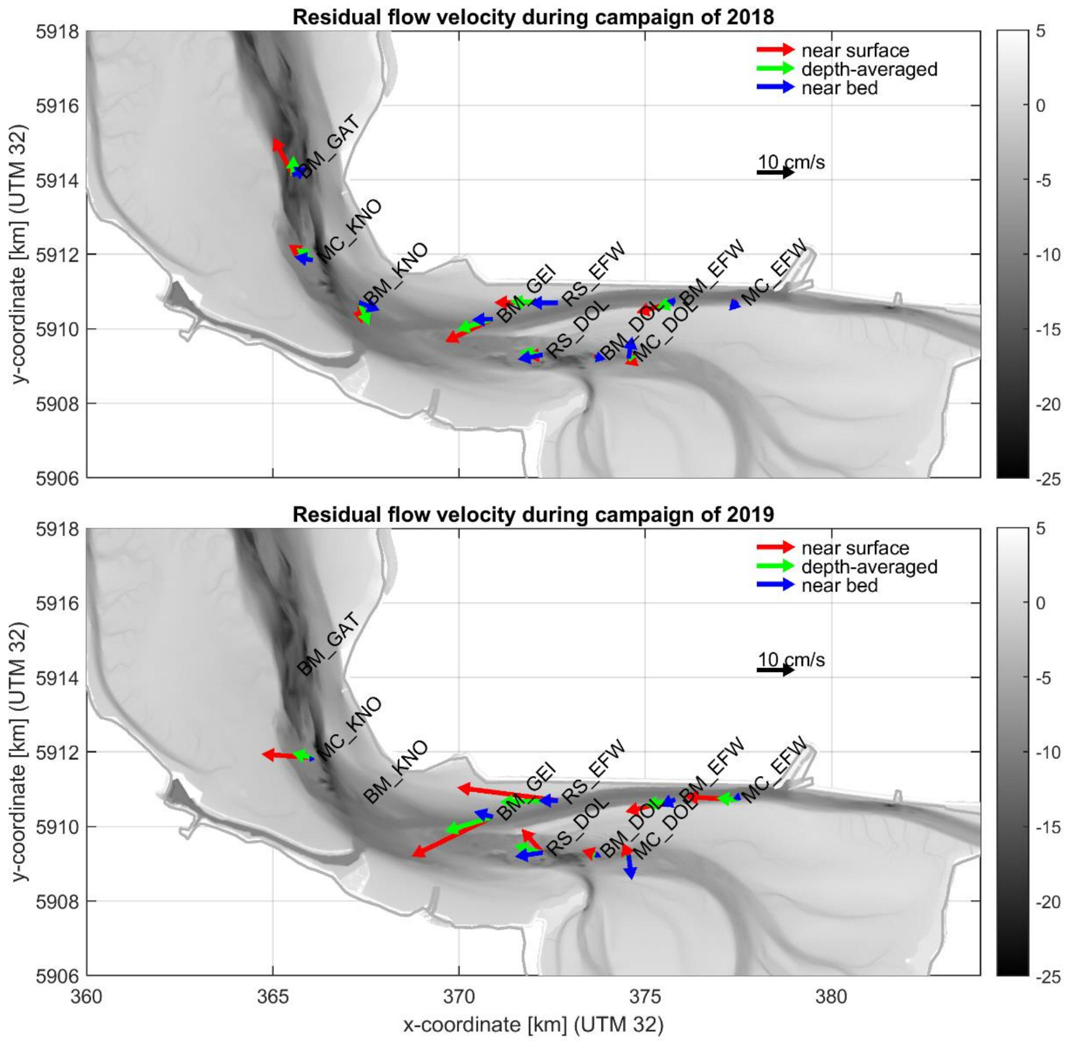

Figure 3-9 Residual flow velocity computed for the same period and locations as in Figure 3-4.

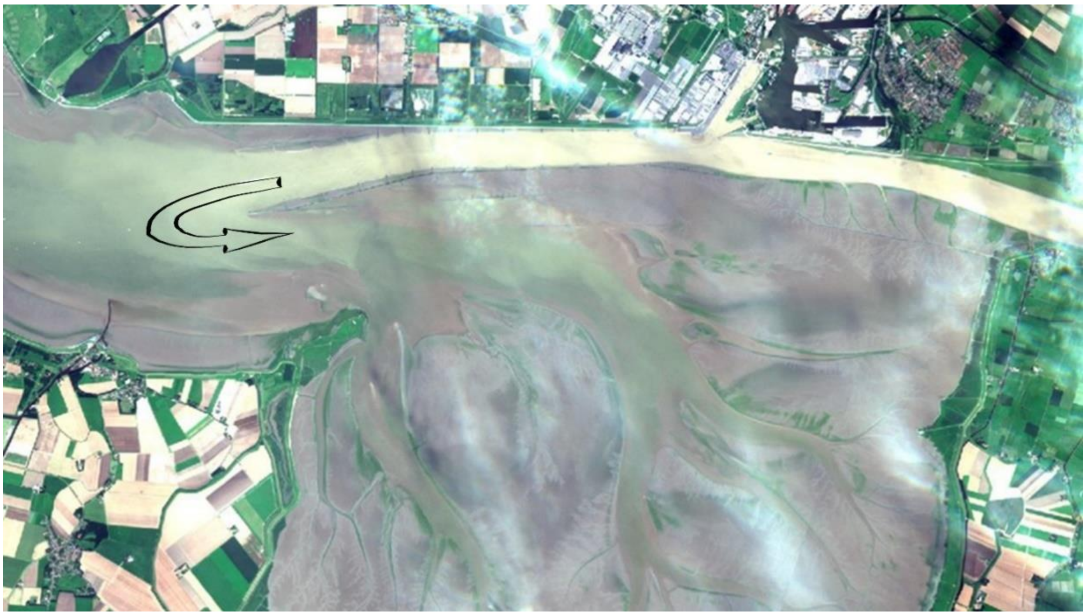

Figure 3-10 Satellite image taken around low water, illustrating outflow of turbid water from the Fairway to Emden and transport of turbid water into the Dollard (from presentation Water Insight)

3.2.1.2 *Transport over the Geisesteert and Geise dam*

Both the EDoM channel measurements and the satellite image (Figure 3-10) suggest a transport of sediment from the Fairway to Emden into the Dollard bay via the Ems estuary. However, long-term bathymetric observations demonstrate that the Dollard is not a permanent sediment sink (Appendix D). The mass balance can therefore only be closed with a sediment flux from Dollard to the Fairway to Emden, over the Geisesteert and Geise dam. Flow and transport over the Geisesteert is indicated by the topography of the Geisesteert (Figure 3-11), revealing tidal channels intersecting the Geise dam. Three sources of information are available on transport of water and sediment over the Geisesteert, collected in 1999, 2001, and in 2019/2020 as part of the EDoM campaign. During these campaigns, a sediment transport from the Dollard to the Fairway to Emden equivalent to of 1-4 million ton/year after extrapolation was registered. This is on the lower side to close the circulation cell. During storm conditions (not in the measurement campaigns), the sediment transport may increase.

Figure 3-11 Aerial view over the Geisesteert at low water showing the Geise dam, the tidal creeks crossing the Geise dam, openings in the Geise dam (near the white arrows), and the bathymetric depression of the Geisesteert in the more wave-exposed western flats (white dashed line). Photo by Lars Plumeyer (fotocommunity.de).

The 1999 measurements

Eight observation stations were installed over the full length of the Geisesteert between 8 and 10 November 1999, recording flow velocity, water depth and suspended sediment concentration (Klebanowski and Jurgens, 2001; see Appendix E.1). Extrapolating their computed sediment flux (Figure 7-27) to a full year yields a transport of 4 million ton/year from the Dollard to the Fairway to Emden.

The 2001 measurements

Eight observation stations were deployed on 13 March 2001 (Jensen et al. 2002; see Appendix E.2). Jensen et al. focussed on water volumes, concluding that 15 million m^3 of water flows from the Dollard to the fairway whereas 10 million m^3 flows back during the tidal cycle on 13 March 2001. They also measured the turbidity (in NTU) but did not calibrate turbidity to SSC. However, a first-order estimate of the suspended sediment concentration can be obtained by assuming that 1 NTU is 1 mg/l (typically 1 NTU varies between 0.5 and 2 mg/l). Using 1 NTU = 1 mg/l and extrapolating their single-tide observation to annual values, yields a transport rate of 1.25 million ton/year from the Dollard to the Fairway to Emden.

The EDoM measurements

Two tripods were deployed in January 2019 (Appendix E.3) and seven tripods were deployed in March 2020 (Appendix E.4) as part of the EDoM (follow-up) measurements. The observed flow velocities are graphically displayed in Figure 3-12.

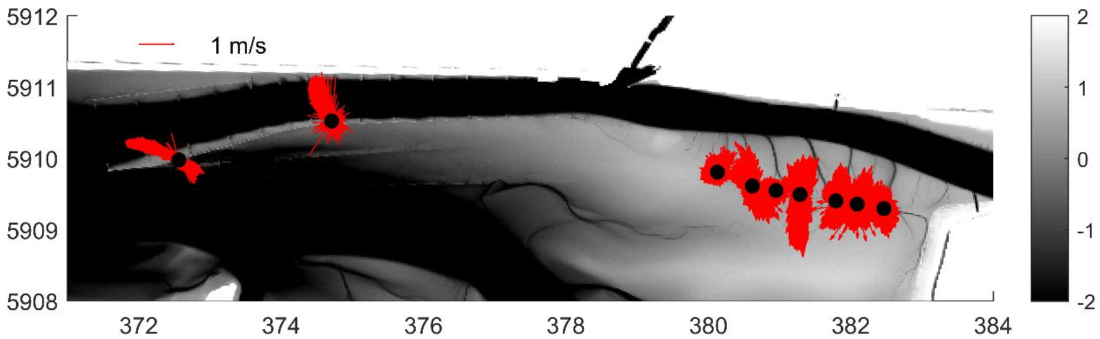

Figure 3-12 Observed flow velocities (in red) with the bed level (in m below NAP) as background. The two observation stations on the western Geise dam collected data in January 2019, the seven stations on the eastern Geise dam collected data in March 2020.

The two January 2019 observations (western part of Geisesteert) were not equipped with OBS's and only provide flow velocities and volumes. The flow direction is strongly directed from the Dollard to the Fairway to Emden. With some crude estimates on ambient SSC (200 mg/l during ebb and flood) these observations can be used to provide a first-order budget: between 13 January and 3 March 2.1 and 6.6 10^4 ton are transported over the section represented by both observation stations (Figure 7-34). On a yearly basis this corresponds to 1.6 million ton.

The sediment flux measured in March 2020 over the eastern Geisesteert is directed from the Fairway to Emden to the Dollard (Appendix E.4 and Figure 3-13), similar to the observations of Klebanowski and Jurgens (2001) and Jensen et al. (2002). The measured sediment fluxes in this section are largely confined to the gullies and can therefore not be easily extrapolated. Given the creek patterns, the transport of sediment from the Dollard to the Fairway to Emden seems unlikely. An important observation is that the direction of residual transport is equal to the direction of residual flow, suggesting that the assumption of equal SSC during flow from the Dollard to fairway and vice versa (used above) is reasonable.

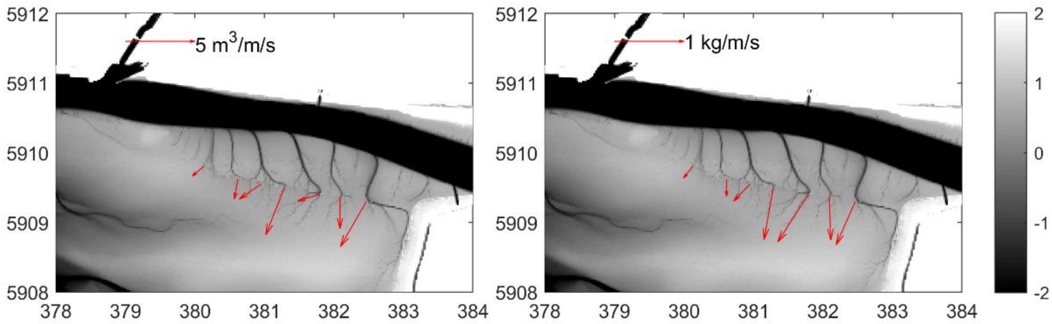

Figure 3-13 Residual discharge (in m³/m/s; left) and residual sediment flux (in kg/m/s) based on the March 2020 Geisesteert measurements

<u>Storm conditions</u>
A significant additional amount of water and sediment must be exchanged during storm conditions. The height of the Geise dam varies between 0 (west) and 1 meter (east) above MSL and will therefore only be limitedly inundated under normal conditions (high water level varying from approximately 1 to 2 meters from neap to spring). A storm setup adds 1 to 2 meters of water leading to a complete submergence. Even more, storm setup is accompanied by more intense wave resuspension, leading to high SSC in the shallow Dollard (probably several g/l). Under these conditions, large quantities of sediment can be transported from the Dollard to the Fairway to Emden. The northern flats of the Dollard may hereby serve as a temporal storage of sediment during calmer conditions.

The tidal flats bordering the Fairway to Emden (Geisesteert) are much lower at the western end than at the eastern end (also explaining why the tidal creeks (Figure 3-11) are better developed at the eastern side). The elevation of this depression (highlighted with white dashed lines in Figure 3-11) is constant over longer timescales, as revealed by long-term bathymetric surveys. Likely, sedimentation is prevented by episodic wave-induced erosion, as these flats are exposed to the wind waves generated in and propagating through the Ems estuary. Recent detailed observations in an equally muddy, more westward located part of the Wadden Sea (near the port of Harlingen) reveals that temporal sediment deposits are crucial for long term transport dynamics, dominated by meteorological events. They observed that with fine sediments deposited temporally on tidal divides and the upper tidal flats for prolonged periods (weeks, possibly longer), but is massively remobilised and transported elsewhere even during fairly low-energetic wind and wave conditions (Colosimo et al., 2020). At what wind and wave conditions the sediment transport over the Geisesteert intensify is not known at the moment, but this may well be different then at the location near Harlingen due to other local bathymetry and geometry. As the Ems estuary is more confined (smaller fetch lengths), we expect that higher wind speeds are needed to generate high transport storm conditions.

The exchange over the Geisesteert is therefore hypothesized to be as follows. During tide-dominated conditions, the sediment flux entering the Dollard is partly flowing over the Geisesteert (~1 million ton/year). The remaining mass deposits temporarily on the Geisesteert (Figure 3-14). This sediment mass is remobilised during periods with more energetic wave conditions and set up and transported into the Fairway to Emden (Figure 3-15). The episodic character of the flux over the Geisesteert cannot be determined from the EDoM measurements and requires additional future observations (see Chapter 5).

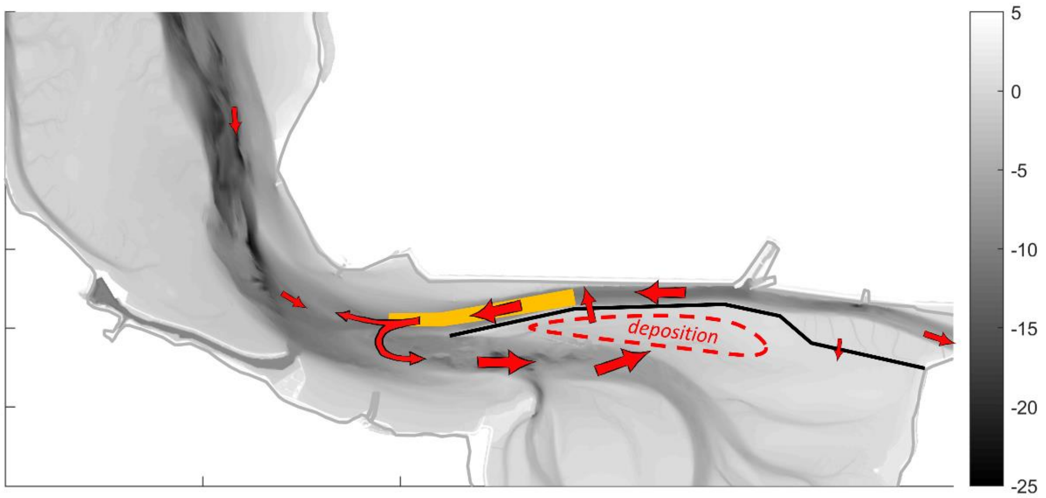

Figure 3-14 Counter-clockwise residual sediment transport pattern during summer conditions (low wind/waves and river discharge). Most sediment exported from the Fairway to Emden into the Ems estuary during ebb is transported towards the Dollard during the following flood period. Some of this sediment flows over the Geisesteert, some deposits on its shallow flats. Most sediment is transported over the Geisesteert during high water and is transported back towards the Ems Estuary during the following ebb. Part of the sediment is picked up by flood currents and transported into the lower Ems River. The orange polygon indicates the area with highest maintenance dredging in summer (see section 3.2.3). Dredge disposal sites are at Ems km 65 and 70 (slightly North of the map)

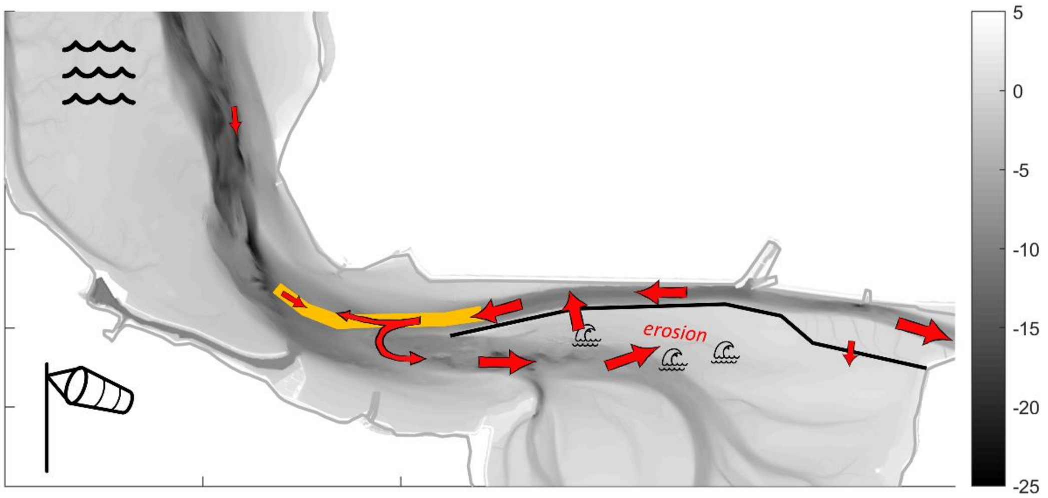

Figure 3-15 As Figure 3-14 but for winter conditions with more wind and wave-induced resuspension of fine sediments over the Geisesteert and subsequent transport over the Geise dam. Sediment transport into the lower Ems River is larger in winter than in summer for reasons explained in more detail in section 3.3.4. The orange polygon indicates the area with highest maintenance dredging in winter (which is lower than in summer; see section 3.2.3).

Summarizing, our main hypothesis explaining the observed fluxes is that a counter-clockwise circulation cell exists transporting several million ton on a yearly basis. The magnitude of the fluxes forming this circulation cell is variable due to:

- wave-induced resuspension during larger wind speeds (occurring more frequently in winter) transporting sediments from the Dollard to the Fairway to Emden (as in Figure 3-15);
- flushing of sediments from the lower Ems river and Fairway to Emden into the Ems estuary;

- variations in discharge, with higher discharges causing larger near-bed landward sediment fluxes (see Figure 3-4).

Assuming all sediment entering the Dollard is transported over the Geisesteert into the Fairway to Emden would yield 5-9 million ton/year, although extrapolation of observations on the Geisesteert yields only 1 to 4 million ton/year. There are no clear alternative hypotheses explaining the computed annual sediment fluxes. The computed annual fluxes are subject to measuring errors and variations in cross-sectional and temporal sediment transport. However, with the presently available data (with comparable patterns of transport along the southern and northern banks of the Fairway to Emden, and fairly uniform flow in the entrance to the Dollard) the computed fluxes seem realistic.

3.2.2 Exchange between circulation cell, the Ems estuary and lower Ems River

The circulation cell above explains how much sediment is transported into the Fairway to Emden from the Dollard, and through which processes. Questions that remain are how sediment is exchanged between the Ems estuary and this circulation cell, and how sediment is transported from the circulation cell into the lower Ems river.

3.2.2.1 Exchange between the circulation cell and the Ems estuary

The point measurements in the Ems estuary (Knock) reveal a landward-directed residual sediment flux (Figure 3-4). The Knock fluxes have not been extrapolated to cross-sectionally and yearly averaged fluxes, because of the large width and resulting cross-sectional variation. Therefore we only discuss the results of our point measurement. The landward transport results from a phase difference between maximal flow velocity and maximal sediment concentration (illustrated with summer observations at Knock in Figure 3-16). The sediment concentration peaks around low water during both the end of ebb and the beginning of flood (Figure 3-16c). However, flow velocities are maximal at the *beginning* of ebb and the beginning of flood (Figure 3-16b). High flow velocities therefore coincide with high SSC only during flood, resulting in a large up-estuary sediment flux (Figure 3-16d). The asymmetry in the current velocity is the result of tidal asymmetry (or a flow asymmetry resulting from topographic constraints). However, the asymmetry in SSC results from an asymmetry in sediment supply: if the SSC peaks would be generated by local resuspension then the peaks in SSC and velocity would coincide. The asymmetry in sediment supply results from the higher sediment concentration flowing out of the Fairway to Emden. Apparently, the typical asymmetry of tidal currents in the Ems estuary (with high flow velocities at the beginning of flood but not the end of ebb) is of such a nature that it effectively counterbalances a greater sediment supply conveyed by the slower ebb currents.

It is noted that this tidal velocity asymmetry is not very commonly observed. The most common velocity asymmetries are (1) a shorter period of the flood compared to ebb, with resultingly higher flood flow velocities, or (2) a velocity peak at the beginning of flood and the end of ebb (HW slack asymmetry), or (3) a velocity peak at the beginning of ebb and the end of flood (LW slack asymmetry). The observed velocity asymmetry deviates from these types, possibly due to bathymetric effects or density differences. The mechanisms driving this asymmetry at Knock need to be further investigated (see section 5.2).

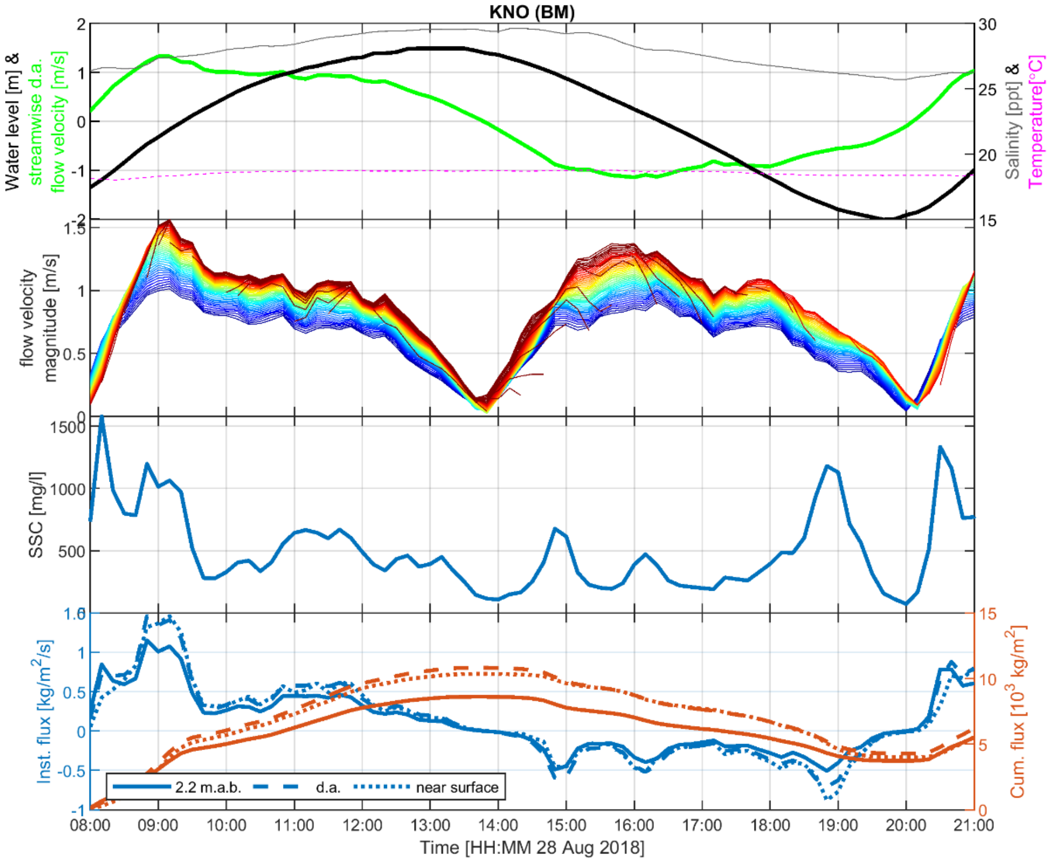

Figure 3-16 Tidal cycle observations at Knock, showing the water level (black), salinity (grey), depth-averaged flow velocity (green) and temperature (pink, top panel), the depth-varying flow velocity (red near the surface, blue near the bed, second panel), the sediment concentration near the bed (third panel), and instantaneous and cumulative sediment flux (landwards positive; lower panel).

The role of river flushing on export of sediment can be estimated from observed salinity and SSC variations at the permanent observation station Knock. Years with high SSC at Knock (2016, 2018) are characterized by a low salinity whereas the salinity is higher in years with lower SSC (2017, 2019). This suggest that the primary driver for elevated SSC concentrations at Knock is river flow. The importance of river flow is further supported by the longitudinal distribution of SSC (Figure 3-17, revealing a seaward shift of high sediment concentrations in winter) and by maintenance dredging volumes (section 3.2.3 and Appendix C, revealing a shift of dredging requirements from the Fairway to Emden in summer towards the Ems estuary in winter). This more pronounced seaward flushing was also observed during the EDoM campaigns (especially near-surface, see Figure 3-5). During winters with higher discharge this seaward flushing will be more pronounced. This is further supported by the sediment concentrations at Knock which were also lower at the time of the EDoM winter measurements (relatively low discharge) compared to years with high discharge (2016 and 2018, see Figure 3-18).

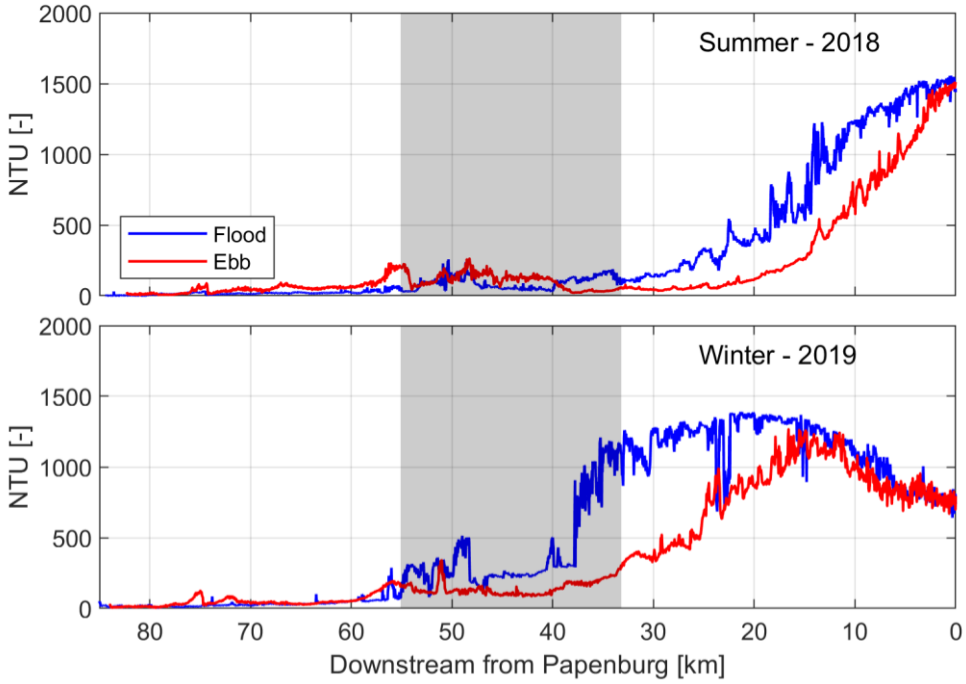

Figure 3-17 Longitudinal near-surface NTU distribution observed in 2018 (top) and 2019 (bottom), during the flood (blue) and during the ebb (red) cruise. The survey starts at km 85 at the beginning of flood and reaches Papenburg around the transition from flood to ebb after which it sails back for 6 hours with the ebbing tide. The grey-shades area denotes the focus area of the EDoM campaign. Observations were made with a near-surface sensor towed by the ship, and therefore no near-bed observations are available.

3.2.2.2 Exchange between the circulation cell and the lower Ems River

A question is which mechanism is responsible for the transport to the lower Ems river further upstream. Especially since most sediment flows over the Geisesteert during high water, and is then transported in ebb direction during the subsequent ebb period. The dredging volume in the lower Ems River is 1 to 1.5 million ton/year (Vroom et al., 2021), which provides an approximation of the long-term residual transport. This total sediment mass into the lower Ems River approximates the lower bound of the sediment flux over the Geisesteert (1 million ton/year) but is about 20% of the upper bound (the 5-9 million ton/tear entering the Dollard).

During the EDoM campaign, the observations in the lower Ems River appeared to be unreliable, suffering from strong oscillations in SSC. Also only part of the water column was registered by the ADCP (the ADCP measurements suffered from the high concentrations, not capturing near bed part of the water column). As a result, there are no accurate residual fluxes based on ADCP and / or OBS observations. However, the water samples (see also Figure 3-30 and Figure 3-31) do reveal that the near-bed sediment concentration near Pogum is so high (>20 g/l) during the flood tide winter period that the residual sediment transport during the winter campaign was probably directed landward.

The responsible mechanism may be the observed cross-sectional variation in ebb-flood asymmetry in the fairway: the currents in the Fairway to Emden along its southern banks are – in contrast to the currents in the centre and along the northern banks - flood-dominant, so close to the Geise dam (Figure 3-25a; see more details in section 3.3.2). Sediment transported over the Geise dam during high water may therefore temporarily deposit on the bed throughout the ebb, whereas the stronger currents during the following flood are able to remobilise the sediment and transport them into the lower Ems river.

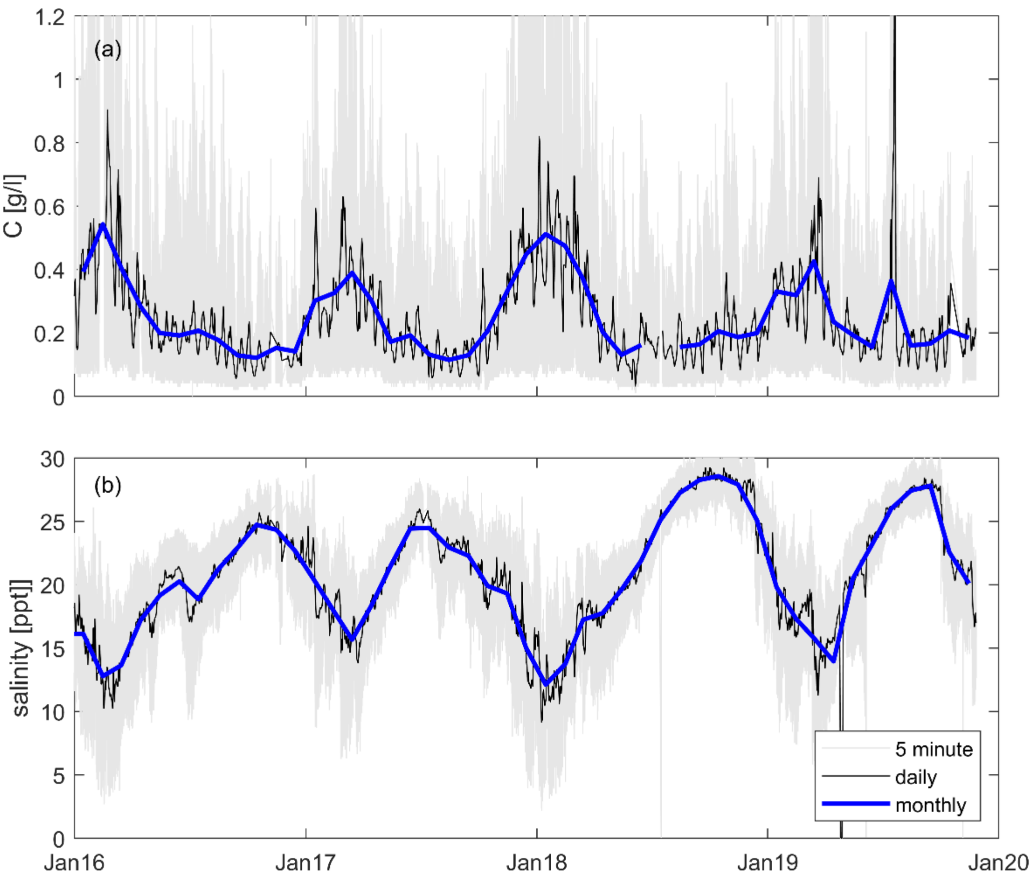

Figure 3-18 Four years of suspended sediment concentration (a) and salinity (b) measured at station Knock (near KNO[BM]) at 5-minute intervals (grey lines). Data has been averaged per day (black lines) and per month (blue lines)

3.2.3 Dredging volumes and residual fluxes

Long-term dredging from the lower Ems River is estimated at 1 - 1.5 million ton of mud per year, which is mostly disposed on land (see van Maren et al., 2016 and Vroom et al., 2021). If the lower Ems River is assumed to be in equilibrium (i.e. no net accretion or increase in turbidity), the residual flux into the lower Ems river also is 1 – 1.5 million ton/year. The flux will be even higher if this area is net accumulating, but no detailed information is available on net bed level changes in the lower Ems River. The total amount of suspended sediment (including the fluid mud layers) is probably around ~1 million ton, so a long-term annual increase in turbidity of several percent per year does not strongly influence this number.

Maintenance dredging volumes in the main navigation channel in the Ems Estuary were 5.9 and 4.6 million m^3/year (primarily muddy, so corresponding to 3 and 2.3 million ton/year using a density of 500 kg/m^3, see Mulder (2013)) in 2018 and 2019, respectively (see more details in Appendix C). Maintenance dredging rates are higher in summer than in winter. In summer dredging is primarily confined to the Fairway to Emden (between km 40.7 and km 50) whereas relatively more sediment is dredged in the estuary during winter (km 50-53; see Figure 3-19). Sediment is disposed close to the port of Eemshaven.

Close to Knock (km 50-53), the landward sediment flux in the estuary meets the seaward directed sediment flux from the fairway to Emden, resulting in sediment convergence. Apparently the resulting deposition flux exceeds the erosion flux, resulting in maintenance dredging (see Figure

3-14 and Figure 3-15). The Fairway to Emden (km 40.7-50) is not an area of longitudinal sediment convergence fluxes (sediment is transported seawards throughout the navigation channel). However, it may be the result of a longitudinal transport gradient or from a sediment influx from the Dollard.

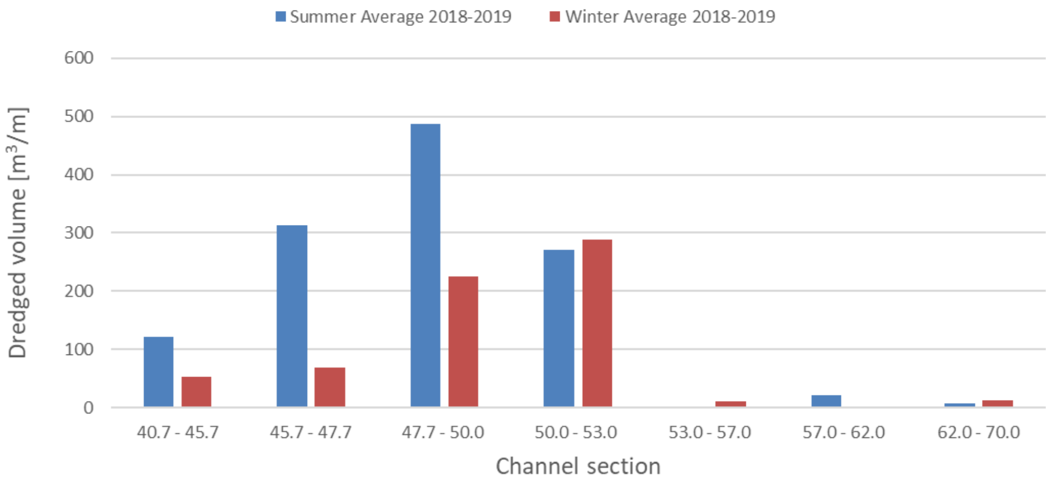

Figure 3-19 Maintenance dredging volumes (in m³/m per section) in summer (defined as the period May through October) and winter (November through April), based on data from 2018 and 2019 (see Appendix C).

The dredging numbers can be used to further refine the residual sediment fluxes in the estuary (Figure 3-20). Between 1 and 1.5 million ton/year annually enters the lower Ems river (Vroom et al., 2021). This means that the sediment flux into the Dollard must be larger than the flux flowing out of the Fairway to Emden (here estimated at ~6 and ~5 million ton/year, but these numbers have a larger uncertainty than dredging numbers). The 2.7 million ton annually dredged from the Fairway to Emden and its approaches (average of 2018 and 2019) must be compensated by a residual flux of the same number (as the Dollard and the lower Ems river do not constitute a long-term source of sediments), to which the net flux into the lower Ems river is added. Therefore, the net up-estuary transport in the Ems estuary is in the order of 4.0 million ton/y.

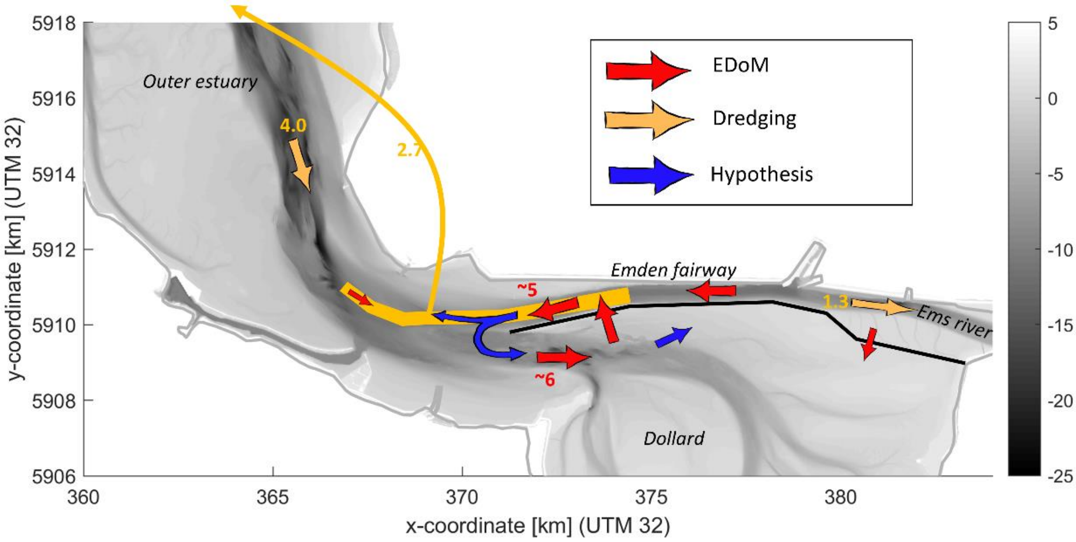

Figure 3-20 Sketch with fluxes (with numbers in million ton/year), based on the EDoM measurements and dredging data. Red arrows are based on the EDoM measurements (with an approximate number for the value of the flux), orange arrows and numbers are based on dredging requirements, and blue fluxes are based on interpretation of all data.

It is not obvious why dredging requirement rates in summer exceed those in winter, since:

- The sediment supply in winter is higher (resulting from seaward flushing of the Ems river ETM, see Figure 3-17 and the expected higher sediment flux over the Geise dam).
- The sediment concentrations within the fairway are comparable or even higher in winter (see Figure 3-17, but also the more detailed observations in Appendix B and D).
- Near-bed sediment transport is directed landwards in winter, but much less so in summer. This would concentrate sediment deposition in the Fairway to Emden in winter, in contrast with observations.

There are three potential mechanisms explaining the higher dredging volumes in summer:

- The settling velocity is higher in summer than in winter. This is evaluated in section 3.3.3.
- Sediment deposition in winter is concentrated over a wider range longitudinally. This results in smaller bed level changes for equal total sediment deposition rates. The wider longitudinal range is the direct result of more pronounced flushing by the Ems river discharge, but also by the more complex structure of the flow. The near-surface currents drive a seaward flux whereas near-bed currents drive a landward flux. The result is a longitudinal spreading of the turbidity maximum.
- During winter, sediment is transported into a more exposed part of the estuary with more wave-induced resuspension and hence lower dredging volumes.

3.3 Transport mechanisms in the Fairway to Emden

The previous section explained the large-scale recirculation pattern of sediment to and from the Fairway to Emden. This section addresses sediment transport mechanisms within the Fairway to Emden, and their implication for residual transport of sediment. It is important to realise that residual transport of sediment may be generated by hydrodynamics (residual flows or tidal asymmetries) but also by tidal asymmetries in sediment properties and availability. The first two sections hereafter address the role of salinity-driven residual flows in the longitudinal (section 3.3.1) and the lateral direction (section 3.3.2). The last two sections focus on asymmetries in sediments, focussing on flocculation (section 3.3.3) and sediment availability (section 3.3.4).

3.3.1 Longitudinal salinity-driven residual flow

Longitudinal salinity-driven currents are primarily driven by the horizontal salinity gradient. The observed horizontal salinity gradient (Figure 3-21) in the transition from the lower Ems river and the Ems estuary was comparable between winter surveys (between 8 and 19 ppt) and the summer surveys (19-28 ppt). In winter, the salinity gradient is steeper in the middle reaches of the estuary (seaward of km 55) whereas in summer it is steeper in the lower Ems River. Therefore the estuarine salinity-driven currents are stronger in winter than in summer (Appendix D.1.1.3).

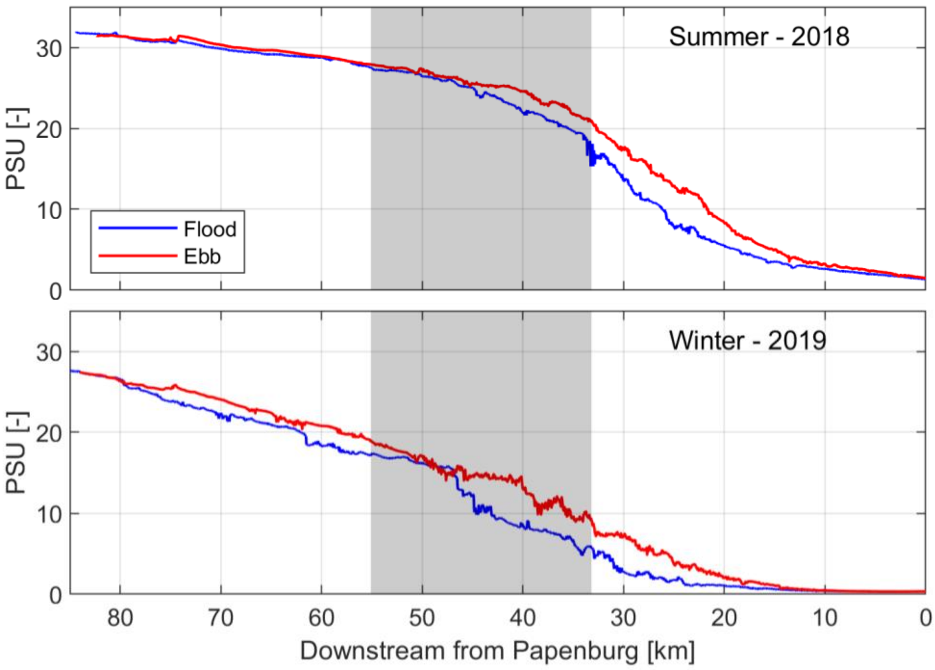

Figure 3-21 Longitudinal near-surface salinity distribution observed in 2018 and 2019, during the flood (blue) and during the ebb (red) cruise. The survey starts at km 85 at the beginning of flood and reaches Papenburg around the transition from flood to ebb after which it sails back for 6 hours with the ebbing tide. The grey-shades area denotes the focus area of the EDoM campaign. Observations were made with a near-surface sensor towed by the ship, and therefore no near-bed observations are available.

The observations also revealed a temporal variation in the gravitational circulation, with most pronounced landward-directed near-bed currents shortly after a high discharge event (Figure 3-22). *During* high discharge conditions, the residual flow is seawards (especially near the water surface, but also close to the bed). The pulse of fresh water into the Ems estuary leads to large horizontal gradients in salinity. Therefore, *after* the high discharge event, pronounced salinity-driven currents develop with a strong landward-directed current near the bed.

These residual flow patterns are effectively trapping sediments at the head of the estuary, which is schematically visualized in Figure 3-23. *During* the high discharge event, the sediment concentration is probably high (Figure 3-23a). *After* the high discharge event the near-bed currents are directed landwards while particles flushed out during the discharge event are settling from suspension. These settling particles are then transported landwards by near-bed salinity-driven flows, providing a mechanism for trapping sediments at the head of the estuary. The effect of the salinity-driven flow is larger when sediment is additionally resuspended by tidal currents.

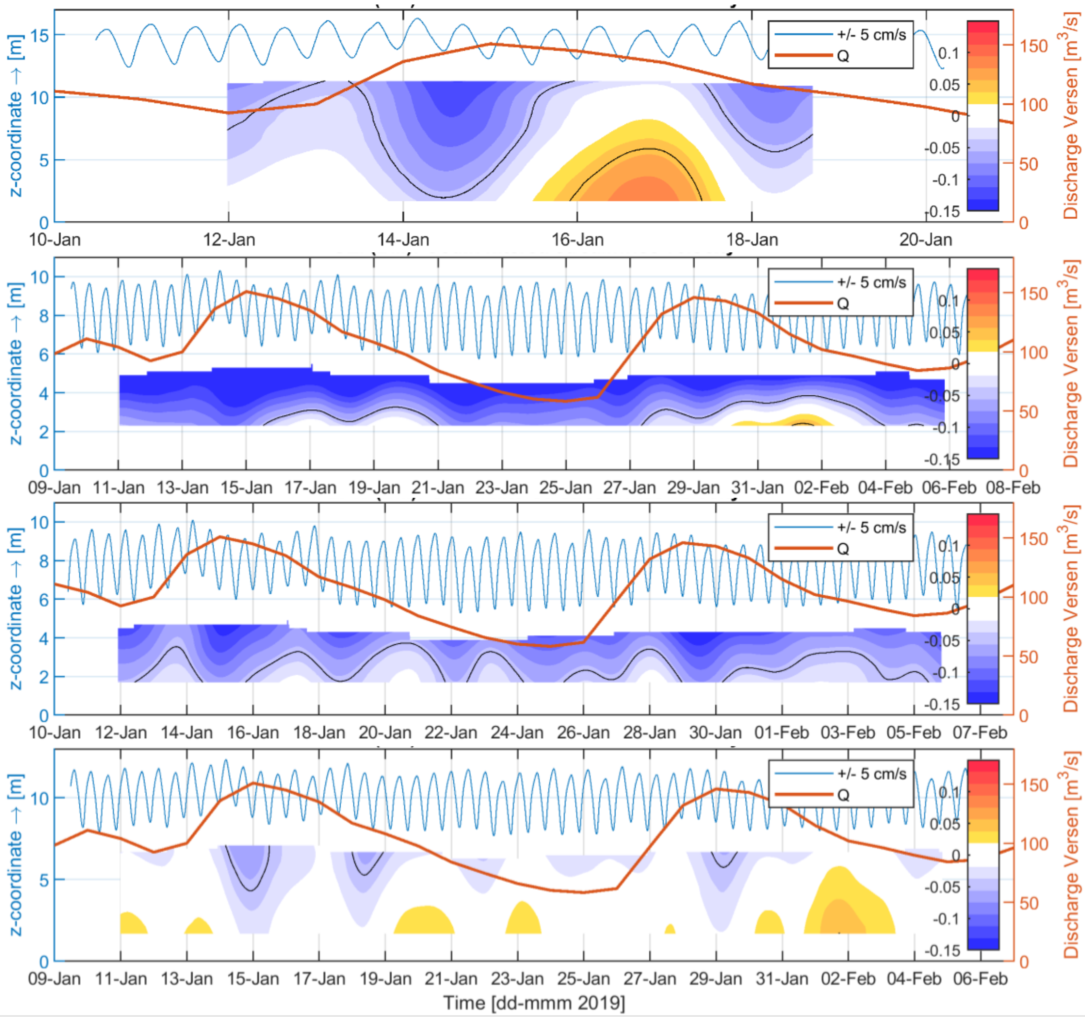

Figure 3-22 Godin-filtered residual longitudinal flows (landwards positive) measured with the bottom-mounts (BM) at stations GAT (panel 1), GEI (panel 2), EFW (panel 3) and DOL (panel 4) in 2019. A Godin low-pass filter removes tidal flow velocities from the observation, showing temporal variations of the average flow velocity.

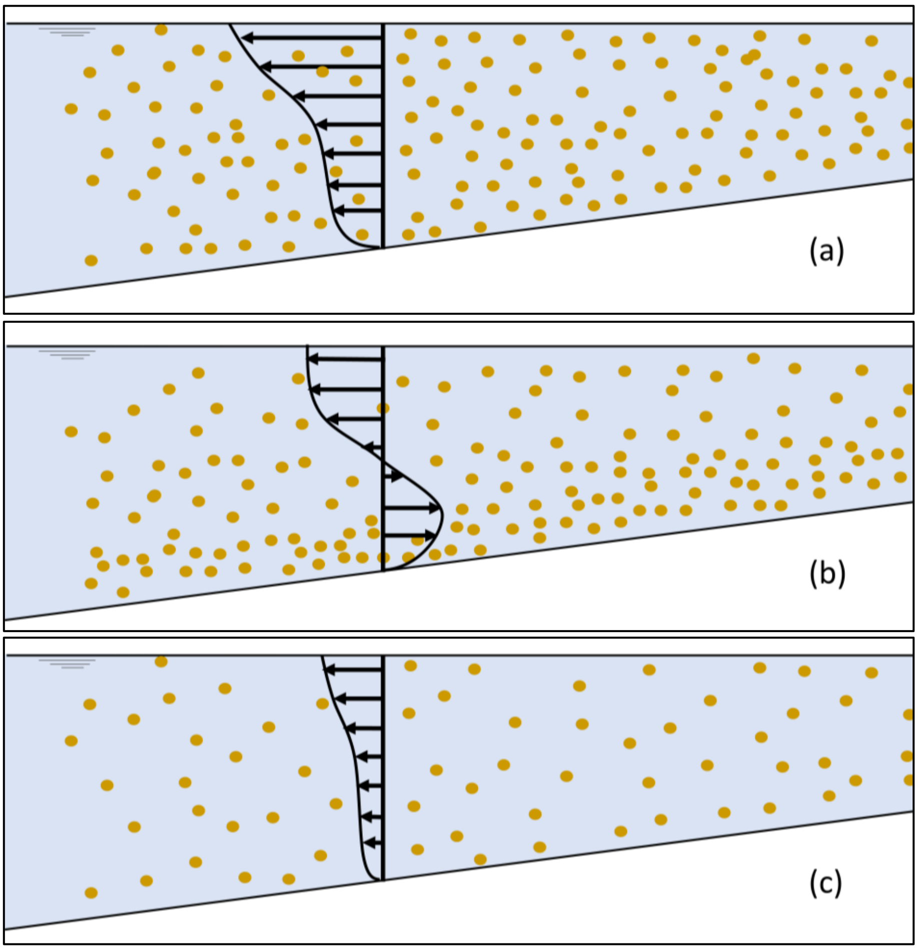

Figure 3-23 Landward transport after a high river discharge: turbid water flows out of the lower Ems river by seaward-directed currents and high sediment concentration (a). Sediment settles from suspension in the Ems estuary, where it is transported landwards by a near-bed current generated by salinity differences resulting from the pulse of freshwater flow (b). For comparison: in absence of a large river discharge the residual flow velocity is weaker and the suspended sediment concentration lower (c).

3.3.2 Lateral salinity-driven residual flow

When combining all observations (13-hrs and frame deployments), the residual fluxes and flows in the Fairway to Emden are more complex than the schematic pictures of Figure 3-14 and Figure 3-15 suggest (see Figure 3-24 for residual flows, Appendix D for fluxes). The residual flow is directed seawards, whereas the sediment flux is directed landwards along the Northern banks of the Fairway to Emden (Figure 3-24, but see details in Figure 3-25). Along the southern bank, both the residual flow and fluxes are in opposite direction: the residual flow is directed landwards, and the sediment flux is directed seawards (Figure 3-26b).

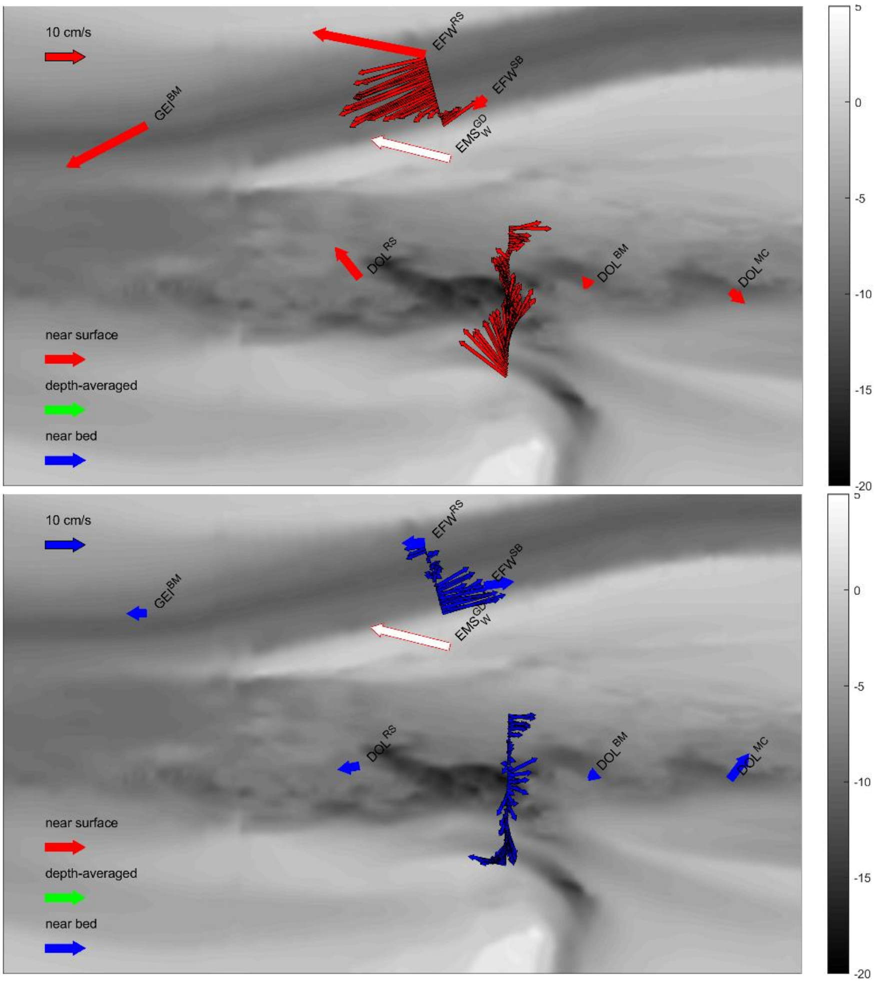

Figure 3-24 Residual flow velocity near-surface (top) and near-bed (below) over the 13-hr measurement period on 24 January 2019, including moorings (GEI^{BM}, EFW^{RS}, DOL^{RS}, DOL^{BM}, DOL^{MC}) and the Geisesteert frame (EMS^{GD}), shipborne stationary observations (EFW^{SB}) and the transects in the Fairway to Emden and in the Dollard.

The observation that the direction of the residual sediment fluxes is opposite to the direction of residual flow can be explained with the sediment concentration (lower panels in Figure 3-25). Along the northern bank, the sediment concentration during flood is much higher than during ebb, resulting in landward fluxes despite a net flow in the seaward direction. It is not likely these patterns are influenced by agitation dredging in the port of Emden, because the port entrance is 8 km landwards of the observation transect

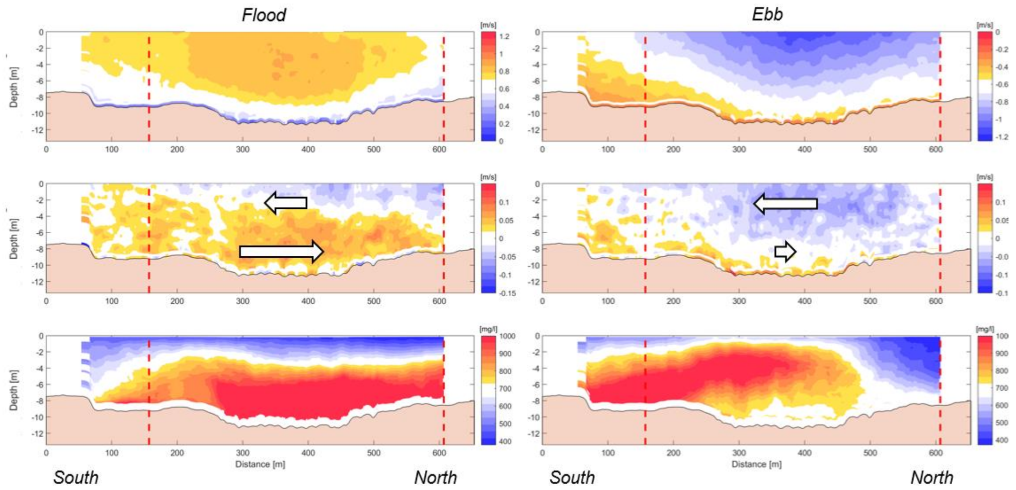

Figure 3-25 Velocity and SSC measured at the EFW cross-section in 2019 averaged over the flood (left panels) and ebb (right panels). Top panels: measured along-channel current velocities; middle panels: cross-channel current velocities (northward positive) and lower panels: sediment concentration based on ADCP backscatter conversion (not scaled). The arrows in the middle panels provide indicative velocity magnitudes and directions.

The mechanism causing asymmetry in sediment concentrations is complex and therefore visualized in Figure 3-26. The ebb flow is stronger along the northern bank (probably because of the slight curvature of the channel), and therefore the salinity is lower along the north bank (the stronger ebb flows transport more low-saline water seawards). At station EFW^{RS} (North, frame observation) the near-bed salinity varied from 5-18 ppt on 24 January 2019 whereas it varied between 10 and 20 ppt during the concurrently measuring 13-hrs boat survey (EFW^{SB}) 500 meter to the South-east, supporting this hypothesis (although it should be realized that comparing the permanent sensor on the frame observation to the CTD cast is prone to errors). Along the southern bank, the flood velocities are larger (bringing in saline water). This drives a cross-sectional circulation with a persistent northward current close to the bed (most pronounced during the flood, see Figure 3-25) , and southward close to the surface. Since the sediment concentration is highest close to the bed, the northward near-bed currents transport sediments northwards, leading to high SSC values along the northern bank during flood. It is not known why the northward near-bed current is more strongly developed during the flood than during the ebb.

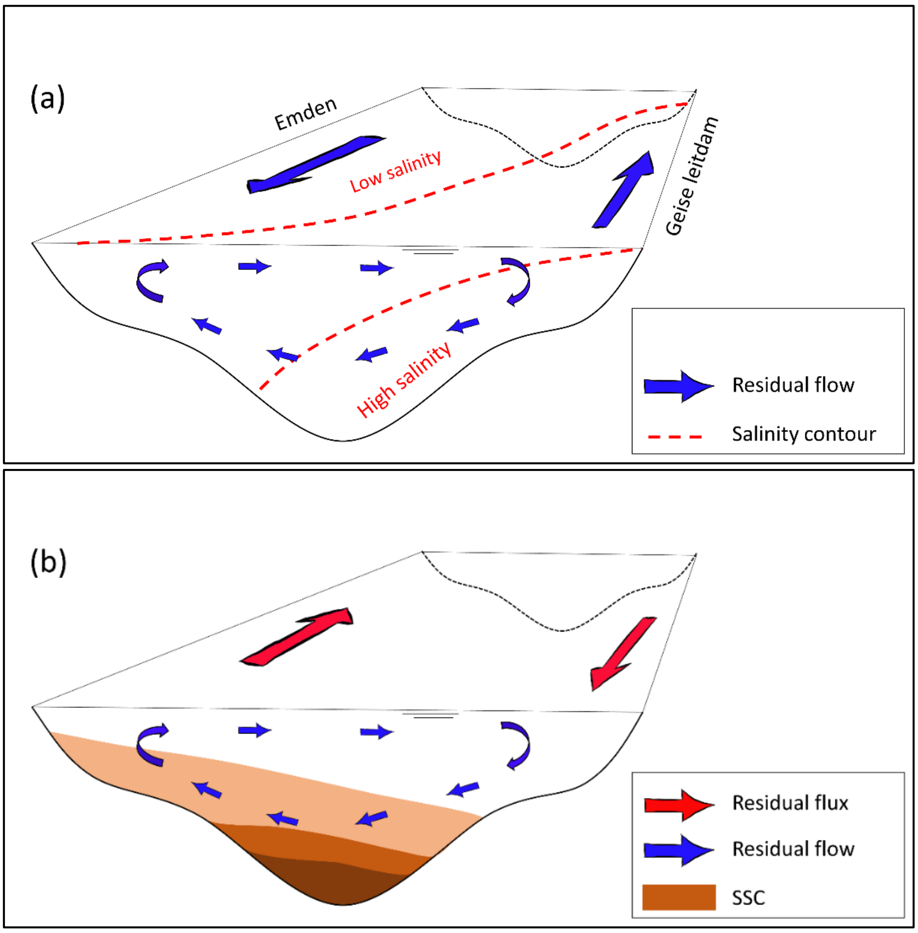

Figure 3-26 Graphical presentation of salinity-driven lateral and vertical sediment transport processes. Panel (a): a net seaward-directed residual flow leads to lower salinities in the northern bank (Emden) and residual inflow to higher salinities near the southern bank (Geise). This drives a lateral salinity-driven circulation with near-bed northward flow towards the northern bank. Panel (b): this northward near-bed flow pushes the high near-bed SSC towards the northern bank, especially during flood, leading to landward residual sediment fluxes in the North. Because of relatively low SSC during flood along the southern banks, the residual flux is directed seawards.

3.3.3 Flocculation

Settling velocity observations were carried out using a flocculation camera during both the August 2018 and the January 2019 campaigns onboard SB_EMD.

During the August measurement campaign, the mean settling velocity close to the surface was highest at the end of ebb and the beginning of flood (3-4 mm/s), even during high flow conditions (velocities exceeding 1 m/s). Settling velocities are much lower at the end of flood and the beginning of ebb (between 0.5 and 1.5 mm/s): see Figure 7-36. The settling velocity close to the bed follows a similar trend, albeit with larger settling velocities (1.5 - 4 mm/s). The difference between macrofloc and microfloc settling velocity is small around high water slack and the following ebb but much larger around low water slack and the following flood (Figure 7-38). During the January measurement campaign, the settling velocity was much more constant throughout the tidal cycle (Figure 7-37). However, in contrast to the tidally fairly constant settling velocity of the mean flocs and microflocs , the macrofloc settling velocity does show a clear tidal variation. It peaks around the end of flood, high water slack and the beginning of ebb (Figure 7-38).

Measuring floc properties
The settling velocity is measured using water samples which are analysed directly after sampling using a flocculation camera following the following procedure. A water sample is collected using a Niskin bottle sampler. A subsample taken from this larger sample using a pipette is then inserted into a still and clear water settling column operated onboard, in which the water-sediment mixture settles from suspension. This settling is monitored with a high-resolution video camera. Postprocessing of the camera data reveals the size, shape, and settling velocity of all particles registered with the camera. This provides a population of settling speeds and floc sizes, which can be averaged into a sample-averaged value (see e.g. Manning and Dyer, 2002). The settling velocity can be analysed in more detail by separating into microflocs and macroflocs (with a floc size of less than or more than 160 µm, resp.). Microflocs are typically denser aggregates, with greater resistance to breakup by turbulent shear – they are more persistent and may settle and be eroded from the bed. Macroflocs are larger but also much more fragile, and easily breakup by turbulent shear. Macroflocs cannot be eroded from the bed without breakup: they are therefore the product of the flocculation in the water column. Macrofloc settling velocities may be up to 8 mm/s.

The macrofloc settling velocity reflects conditions in the water column whereas microflocs are aggregates that have been eroded from the bed and only limitedly reflect conditions of the water column. The settling velocity of the macroflocs is influenced by the sediment concentration, turbulence levels, salinity, and by biotic effects. The macrofloc settling velocity is highest around low water / beginning in summer but from the end of flood to halfway ebb in the winter. This suggests that optimum flocculation conditions exist around both these periods (related to the turbulent energy, salinity, SSC, and biotioc effects). In order to identify which factor contributes most to flocculation, the settling velocity (mean, micro, and macro) is related to parameters measured during the surveys (the flow velocity, salinity and the sediment concentration, see Figure 7-39 - Figure 7-45) and Chlorophyll-a.

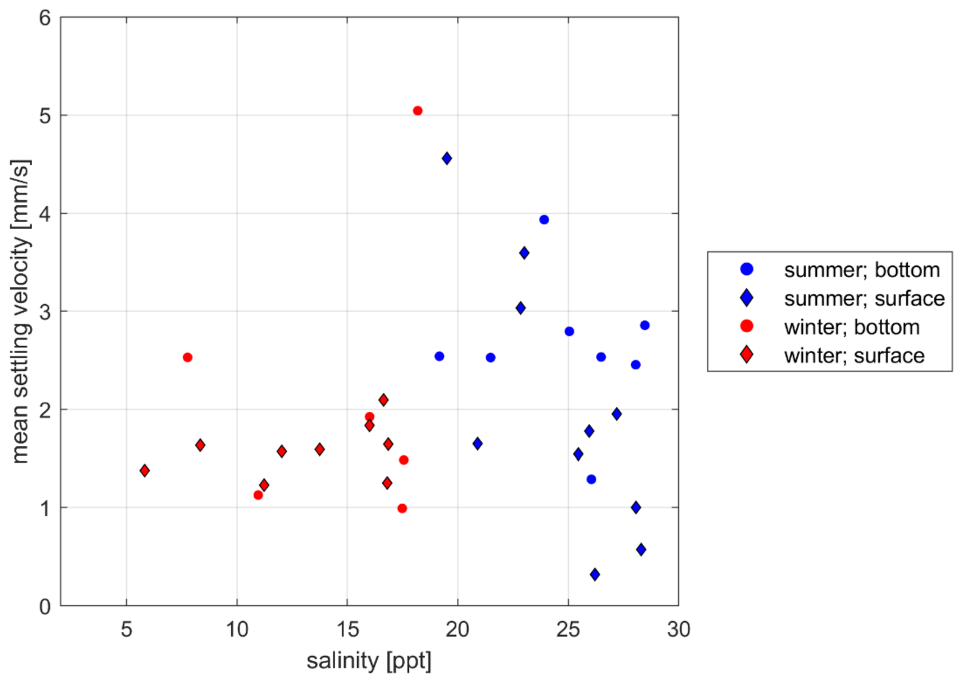

Figure 3-27 Mean floc settling velocity as a function of salinity; both measurement campaigns, near bed and near surface

In general the settling velocity increases with the sediment concentration, but such a relation is not obvious during the August measurements and inverse in January (Figure 7-37 and Figure 7-38). In terms of hydrodynamic energy, an optimum turbulence level exists (at low turbulence levels clay particles do not collide and hence flocs are not formed; at high turbulence levels flocs are destroyed by turbulent shear). A first approximation of turbulence levels is the flow velocity. The settling velocity measured in August seems to be independent of the flow velocity (Figure 7-41), but a weak dependence appears to exist in winter (with highest settling velocity at a flow velocity around 1 m/s).
The strongest correlation between investigated parameters and settling velocity (Figure 7-39 - Figure 7-45) is provided by salinity (see also Figure 3-27). Floc formation is influenced by salinity as the salt ions shield (i.e. compress the electrical double layer of) the negatively charged clay surfaces such that clay particles may approach each other more easily and hence flocculate. However, this shielding effect is already very effective at a salinity of a few ppt. From a physico-chemical point of view the fairly strong relation is not in line with expectations (at low salinity levels there should be a clear relation, but not at salinity levels exceeding 5 ppt).

The variability in the settling velocity in Figure 3-27 probably reflects a seasonal variation in flocculation resulting from algae growth. Flocculation is strongly strengthened by the presence of algae, with organic filaments contributing to floc formation and therefore settling velocity. The effect of algae is the generation of larger flocs compared to a pure sediment floc, but also to promote floc growth seaward of the salt intrusion limit (Deng et al., 2019). In the Ems Estuary, the Chlorophyll-a content (a proxy for phytoplankton biomass) in the water column is several times larger in summer than in winter (Figure 3-28). However, the difference may be an order of magnitude in the sediment substrate and the primary production in the water column is 100 to 1000 times larger in summer than in winter (Brinkman et al., 2014). It is therefore most likely that the higher floc settling velocity in summer results from the higher biologic productivity. An apparent relation with salinity (as in Figure 3-27) only emerges because salinity is also seasonally varying.

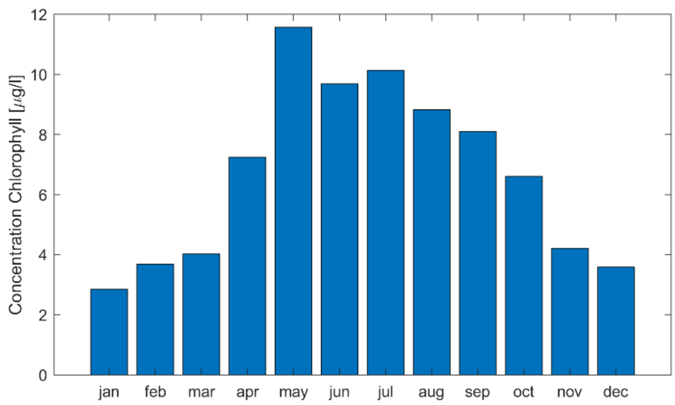

Figure 3-28 Monthly averaged near-surface Chlorophyll-a concentration measured over the period 2000-2020 at MWTL location Groote Gat (Dollard).

However, the relation between salinity and density (Figure 3-29) reveals a similar overall relationship (high density in summer, low density in winter), but also a clearer positive correlation within each season (especially in winter): the higher the salinity, the higher the floc density (so a higher density during summer). This positive correlation between salinity and floc density does not mean salinity is the key factor influencing the density. Water from the Ems river is less saline, but may also contain less algae (resulting in less dense and more slowly settling flocs). It is not clear why such a difference exists because all sediment in the Ems river originates from the Ems estuary. It appears there is a mechanism that reduces the settling velocity of sediments while they are in the Ems River. This may be related to a low oxygen content in the lower Ems River preventing growth of phytoplankton.

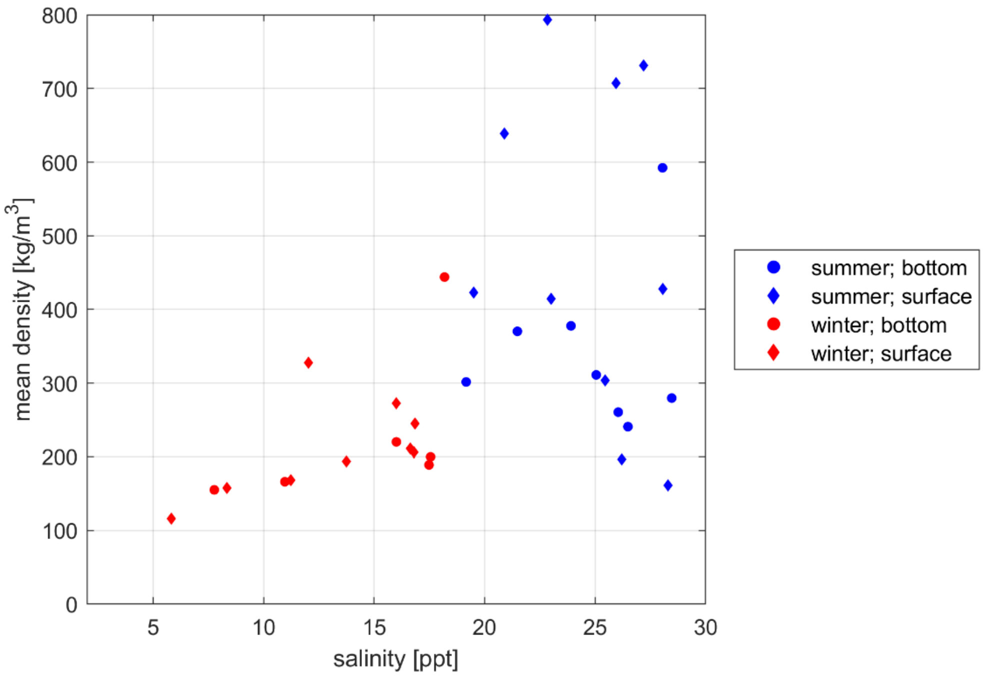

Figure 3-29 Mean floc density as a function of salinity; both measurement campaigns, near bed and near surface

Irrespective of the responsible mechanism, the seasonal variation in floc properties is important for the sediment dynamics in the Ems estuary. Apparently, flocs are relatively denser and faster settling in summer than in winter. This means that in summer the settling particles form a dense fluid mud in the Fairway to Emden whereas in winter a highly concentrated benthic suspension is more likely to develop in the water column close to the bed. Such near-bed suspensions are relatively susceptible for transport by near-bed currents (the estuarine circulation that occurs in winter) which is directed landwards and may hence contribute to sediment transport to the lower Ems River. Secondly, sediments deposited in the Fairway to Emden are much more likely to rapidly consolidate in summer (because of the higher settling velocity but especially because of the higher density), requiring more maintenance dredging.

3.3.4 Sediment availability and tidal asymmetry

During the summer measurement campaign (28 August 2018), the peak ebb flow velocity was higher than flood flow velocity peaks at three stations (BM_GEI, RS_EFW, and SB_EMD) whereas higher peak flood flow velocities were recorded at two stations (SB_EFW and MC_EFW); at station BM_EFW the peak flow velocities were comparable (section B.3.1). In winter (24 January 2019) the peak ebb flow velocities were higher at two stations (BM_GEI, RS_EFW) while peak flood flow velocities were higher at three stations (SB_EFW, BM_EFW, SB_EMD); now station MC_EFW yielded equal ebb and flood flow velocities. The observations that ebb-flood asymmetries in the flow velocities are differing so much over a relatively small area suggests that bathymetric effects are important (either the ebb or flood flow is sheltered by an upstream topographic feature). This is especially prominent for station SB_EMD, where peak ebb currents were 1.6 m/s in August and January, but peak flood currents were 1.1 m/s in August and 1.8 m/s in January. Probably, the location was slightly different. Because of these topographic effects, the water levels are probably a better indicator for tidal asymmetries than the flow velocities.

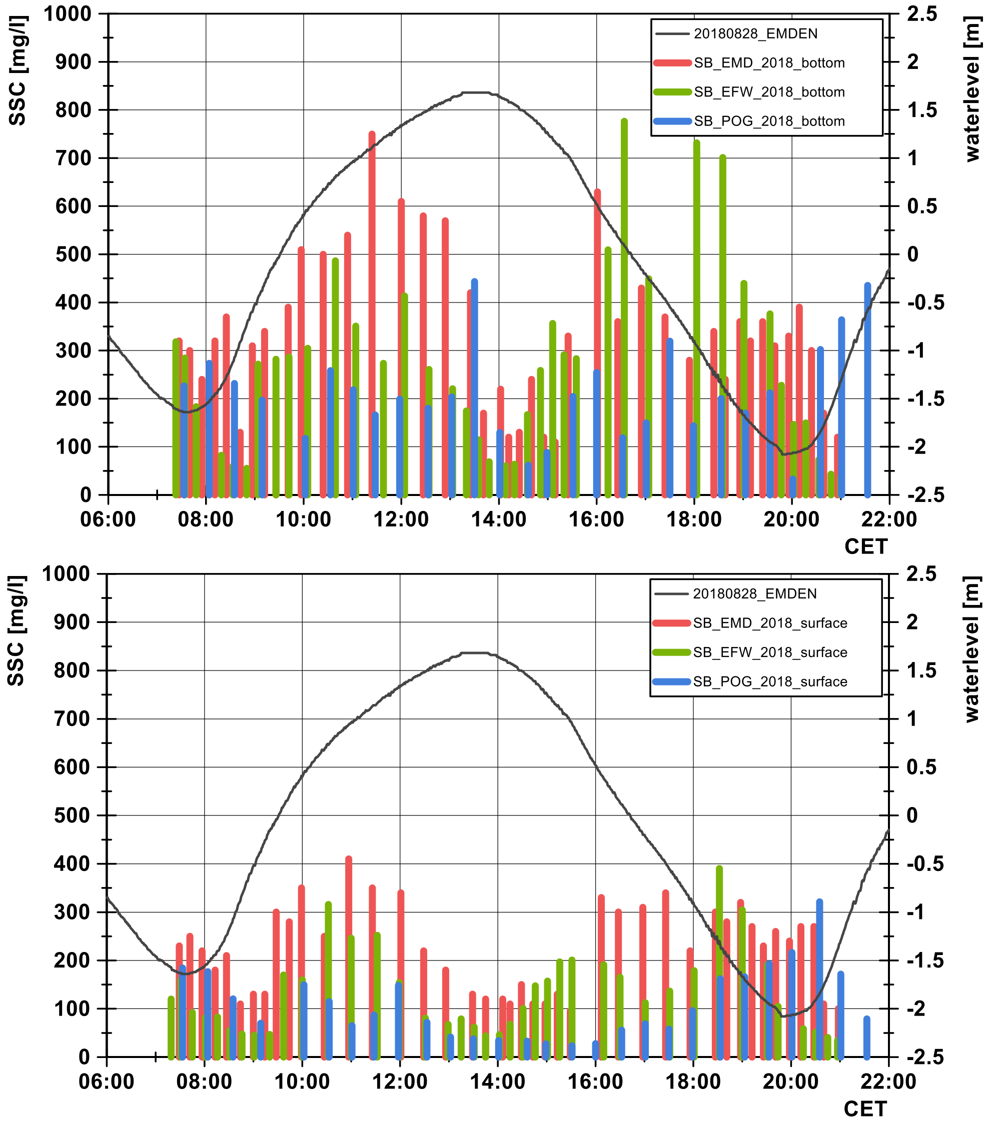

Figure 3-30 SSC based on water samples collected in the Fairway to Emden (station SB_EFW and SB_EMD) and the lower Ems River (SB_POG), on 28 August 2018 near the bottom (top) and near the surface (bottom). Figures provided by BAW.

In August, there is no clear variability in SSC over the tidal cycle (Figure 3-30). The sediment concentration at station Pogum is lower than that at Emden or EFW. In January, the SSC distribution is completely different (Figure 3-31). First, the SSC is highest around low water slack and the beginning of flood. Secondly, the SSC becomes progressively higher (a factor 10) from EFW towards Pogum. Such a variability (both in time and in space) cannot be explained with the observed flow velocities (which did not reveal a pronounced asymmetry). This pattern can only be explained by a large availability of easily erodible sediment in the Fairway to Emden. Sediment is picked up by the flood current as it travels towards the lower Ems River (with the time difference of two hours between the SSC peak at Emden and Pogum corresponding to the approximate travel time of the tidal current). The opposite does not happen during the ebb current. This may be explained in two ways:

1. A large amount of sediment was deposited in the Emden fairway around low water slack. This cannot be a direct result of water flowing over the Geisesteert, because that only

takes place at high water. It may be, however, sediment draining from the gully system north of the Geisesteert (Figure 3-11) which was first deposited at high water.

2. The flow reversal period is shorter around low water slack tide than around high-water slack tide (Figure 3-31). This may have the following implications. Sediments carried by the flood flow that settled on the bed during high water slack have already consolidated so much at the beginning of ebb that they are not easily resuspended. On the other hand, sediments transported seawards by the ebb have had insufficient time to consolidate during low water slack, and are immediately transported in the flood direction.

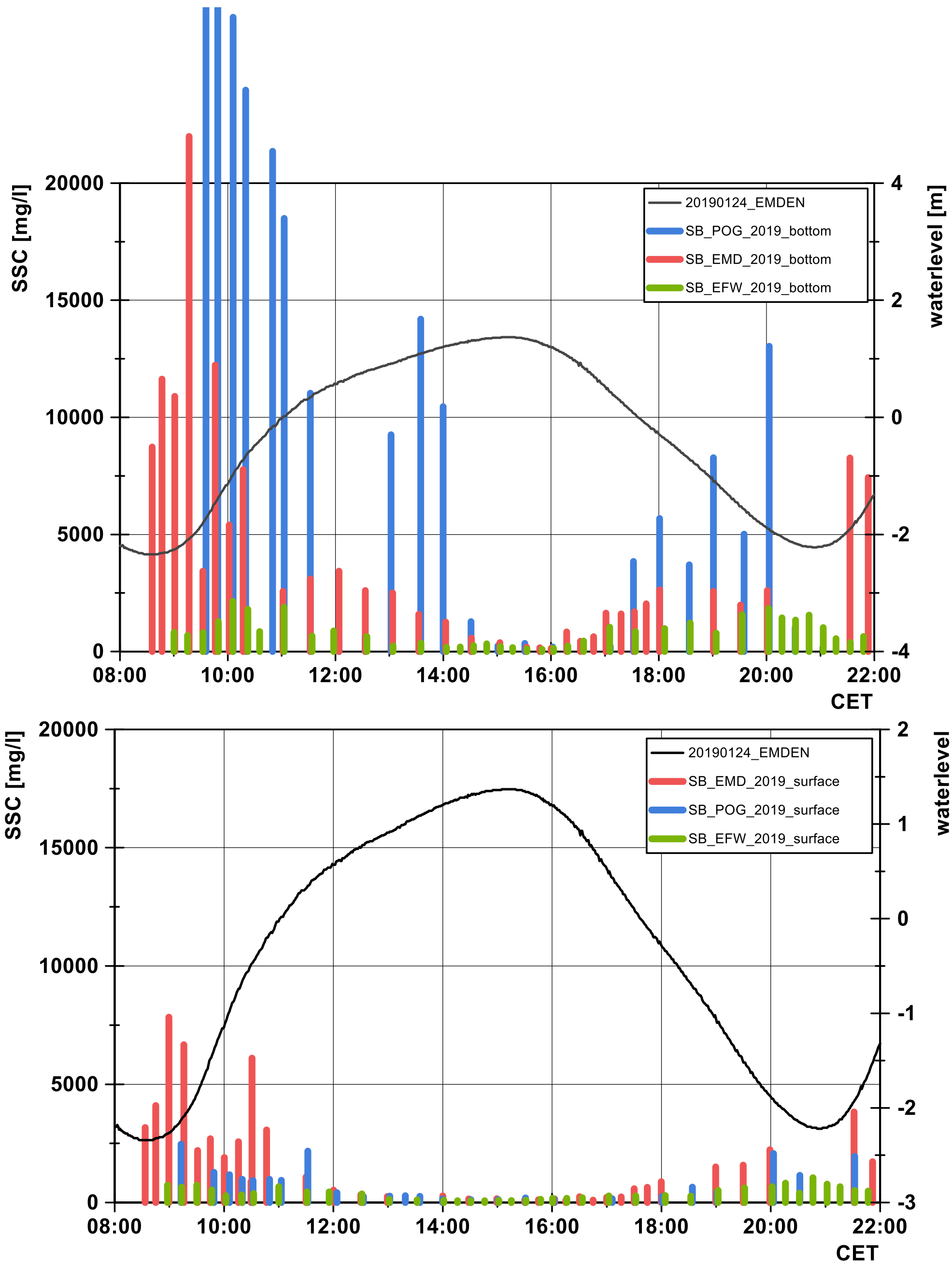

Figure 3-31 SSC based on water samples collected in the Fairway to Emden (station SB_EFW and SB_EMD) and the lower Ems River (SB_POG), on 24 January 2019 near the bed (top) and near the surface (bottom). Figures provided by BAW.

The very pronounced degree of asymmetry in SSC (both in space and time) suggest that explanation 1 is more likely. An asymmetry in slack tide duration (explanation 2) is rather subtle and especially leads to residual transport of sediment when averaged out over many consecutive tidal cycles.

The observation that this asymmetry in SSC is so pronounced during winter but not during summer conditions may be the result of different hydrodynamic conditions, sediment properties, or sediment supply. Hydrodynamic differences are quite small (a larger contribution of salinity-driven flow in winter), unlikely to explain the difference. Also the supply is not a likely explanation: the high dredging requirements in summer reveal that there is sufficient sediment – it is only limitedly resuspended. The most likely explanation is the seasonal variation in sediment properties: the low density, slow settling winter flocs are transported into the lower Ems River whereas the high-density fast-settling summer flocs deposit on the bed of the fairway to Emden and need to be dredged.

4 Conclusions

The main conclusions of the analysis of the EDoM data are as follows:

- Net sediment transport observed during the EDoM surveys was primarily from the Fairway to Emden into the Ems estuary. The net depth-averaged sediment transport was seawards under low discharge conditions from the Ems river. Sediment may be transported in the landward direction during high discharge conditions (inconclusive results due inconsistent observation methods). A landward transport was observed close to the bed at some stations during winter conditions. However, for most observation locations (frames) the sediment fluxes throughout the water column were computed using the suspended sediment concentration observations close to the bed, and therefore the near-surface sediment fluxes (which are always directed seawards) may be overestimated for some stations.
- A net transport from the estuary towards the Dollard has been observed during the EDoM surveys. No sediment accumulates over longer timescales in the Dollard, which implies that most of the sediment transported into the Dollard must be transported towards the Fairway to Emden. One to several million ton/year is transported through and over the Geise dam, depending on the meteorological conditions. During more energetic wave conditions sediment transport from the Dollard to the Fairway to Emden likely increases. The flux into the Dollard may be on the higher side as the observational period was mainly during low wave conditions, and wave-induced resuspension may generate a flux in the opposite direction.
- Longitudinal and cross-sectional variations in salinity-driven residual currents exist in the Fairway to Emden, which influence import and export of sediment. They generate an up-estuary sediment transport component during high-discharge conditions along the northern banks of the Fairway to Emden, and close to the bed.
- During/after high discharge events, residual near-bed to mid-depth importing sediment fluxes are observed in the Fairway to Emden, that are absent, or only occurring very close to the bed, during low discharge conditions. In addition, near the water surface larger seaward residual flows are observed during high discharge periods in the EDoM campaign. The 2019 campaign reflecting high discharge conditions still reflect fairly low discharges, and hence the effect may be even stronger during higher discharge events.
- Largest volumes (per length unit) are dredged at the entrance of the Fairway to Emden, just west of the Geisesteert. The EDoM measurements suggest that this location corresponds to a point of sediment transport convergence. The dredging volumes here are largest in summer. The reason dredging requirements are largest in summer (despite lower sediment availability) is probably mainly a seasonal variation in settling velocity. Additional factors are more pronounced longitudinal spreading of the ETM and transport of the ETM towards a more energetic part of the estuary (preventing sedimentation).

5 Lessons learned and recommendations

5.1 Lessons learned

The most important lessons learned from the preparation, execution, and analysis of the EDoM campaign is that

A. Despite the large group of participants, the EDoM campaign was successful and resulted in a large and very useful dataset. Important for a successful campaign with such a large number of participants is a centrally organized planning by experienced practical surveyors. The planning of practical aspects was picked up by especially Christian Maushake (BAW) in combination with Jan-Willem Mol (RWS); overall planning by Petra Dankers (RHDHV).

B. Frame measurements provided more system understanding than the labor-intensive shipborne stationary measurements. The reason for this is that (1) vertical gradients in SSC and salinity (for which shipborne measurements are needed) were less important than *a priori* estimated and (2) the subtidal variability is high, especially during winter conditions. The greatest use of shipborne cross-section observation was for understanding the cross-sectional variation in longitudinal and lateral flows.

C. The EDoM campaign created a large and valuable dataset and most instruments have delivered proper data. Analysis of such an extensive dataset is labour-intensive, especially when set-ups are different (different instruments and number of instruments per frame and/or ship). New campaigns should try to avoid this as much as possible. The LISST data measured on the SB_EMD proved to be unreliable, and also the high concentrations at Pogum negatively impacted observations there.

D. Converting the originally validated data from the individual project partners into a final coherent dataset takes a large effort because of (1) in practice some additional corrections are needed to the data, and (2) the variation in data format is large (despite efforts to use consistent data formats).

E. Most important finding from the EDoM campaign is that the Fairway to Emden is mostly exporting sediment at its western connection with the estuary. Export is strongest in summer and weakest in winter (in contrast to a priori assumptions)

F. A water and sediment flux from the Dollard to the fairway to Emden through and over the Geise dam plays a crucial role for sediment exchange between the Ems Estuary and the lower Ems River. This lateral flux may be more important than longitudinal import through the fairway to Emden (as *a priori* assumed).

G. Seasonal variations in sediment dynamics (including dredging) are probably strongly influenced by seasonal variation in flocculation. Flocculation should be more prominently investigated in follow-up campaigns (see also the next section).

5.2 Recommendations

The following recommendations are given, (1) on increasing our understanding of turbidity in the Ems Estuary based on insights of the EDoM campaign (2) for future monitoring and measuring campaigns, and (3) how the EDoM measurements provide insights into the effectiveness of solutions aiming at reducing the turbidity in the Ems Estuary.

1 Turbidity

A. The hypothesized large contribution of sediment transport over the Geise dam provides new insights into the sediment dynamics in the Ems estuary. This mechanism influences the effectiveness of measures aiming at strengthening sedimentation in the Dollard, especially in the North (potentially reducing the turbidity in the middle reaches by reducing the sediment flux from the Fairway to Emden), and also implies that transport mechanisms regulating the turbidity in the middle reaches of the Ems estuary are different than previously thought. However, evidence of this circulation cell is now partly indirect (the sediment flux over the Geise dam has not been observed), and also to what extend sediment transported in this transport cell is renewed or recirculates, requires further investigations. In order to better understand the transport cell itself, and its impact on solutions to reduce turbidity, it is recommended to:

- Measure continuous bed level variations at several locations on the Geisesteert (to verify to what degree sediment is temporally stored here during fair weather and remobilized during more energetic conditions) in combination with observations of the water and sediment flux over the Geisesteert during storm conditions (requiring a full winter deployment, preferably in combination with monitoring of bed levels). Preferably, bed level variations of the whole Geisesteert should be monitored at a higher frequency than the current vaklodingen data (monthly observations). Alternatively (or in addition to these soundings), a newly developed techniques to monitor bed level changes using satellite images available in the Google Earth Engine may be explored to monitor spatially varying bed level changes on a high time resolution (~ weekly observations, depending on cloud cover).
- Use numerical models to further quantify the horizontal circulation over the Geisesteert and from the lower Ems river to the Dollard. Such models in combination with observations are also very useful to make a more accurate estimate of long-term residual transport than based on observations only. The extrapolation of gross transport at a few points for a short time towards cross-sectional long-term residual transport can be much better made in this way. Additionally, such a model can be used to (1) determine the impact of flow over the Geisesteert on the turbidity in the middle reaches of the Ems estuary and (2) estimate the amount of sediment available in the system for suspended sediment transport: this is key for predicting the impact of sediment extraction on turbidity.
- Analyse horizontal sediment transport patterns through analysis of satellite images.

B. Transport patterns within the Fairway to Emden have a pronounced vertical but also cross-sectional variability. This variability is important for measures aiming at reducing sediment transport into the lower Ems River (including tidal regulation with the Ems Sperrwerk). However, the EDoM measurements only provide a spatial snapshot of the cross-sectional variability, which may show pronounced longitudinal variation. It is therefore recommended to further analyse the importance and the longitudinal variability of lateral circulations in the Fairway to Emden on residual sediment transport.

C. Compare the observations from the EDoM campaign in more detail with existing long-term monitoring data to point at variations between years and consistency of described transport processes over even longer periods.

D. The hypothesized mechanisms for the seasonal variation in dredging requirements may contribute to a reduction in maintenance dredging costs. It is therefore recommended to further investigate the hypothesized mechanisms for the seasonal variation in dredging requirements in more detail with a numerical model.

E. Investigate the role of flocculation in more detail. The settling velocity observations appear to be more important than estimated before the measurement campaign, and therefore drivers for flocculation (especially organic properties) were not adequately measured. The degree of flocculation appears to influence the formation of fluid mud (and maintenance dredging volumes) and therefore flocculation measurements should preferentially be combined with detailed studies on fluid mud development during summer and winter conditions. Such fluid mud observations would, however, require observation in the central channel (which is constrained by nautical requirements – frames are not allowed in the central channel).

F. Further investigate the role of the phase difference between supply-limited SSC and tidal flow velocity observed at Knock in driving the strong landward sediment transport in the middle reaches of the Ems Estuary.
G. Use the available data to analyse detailed transport mechanisms in more detail in academic studies (e.g. PhD trajectories). Funding for such trajectories may be centrally organized (e.g. by BAW or Rijkswaterstaat) or applied for by academic partners at scientific organizations such as NWO. Topics for such trajectories include:
    - Spatial variation of horizontal asymmetries in the Ems estuary and Fairway to Emden;
    - Lateral and vertical stratification and flow dynamics in the Fairway to Emden;
    - Horizontal vs vertical exchanges between the Dollard, Ems estuary, and lower Ems River.
    - Seasonal and lateral variation in flocculation dynamics
H. The various new insights from the EDoM campaign are important for sediment management in the whole estuary. In order to have these results accepted by a wider audience, it is recommended to
    - Publish the results in a set of scientific papers (for the scientific community)
    - Write a condensed and less technical publication (for managers), possibly as a collaborative effort (multiple project partners)
    - Have a dissemination workshop

2 Monitoring

A. Frame measurements provided more system understanding than the labor-intensive shipborne stationary measurements. Potential future measurements in the Ems estuary (similar to the EDoM locations, but also elsewhere) should therefore especially focus on frame observations in combination with shipborne cross-section observations.
B. The Geisesteert has an important role in temporarily storing sediment and apparently allows for a large exchange between the Dollard and the Fairway to Emden. New monitoring should therefore focus on this area. This is elaborated in more detail as part of recommendation 1A.
C. Try to set-up as many identical measurement frames/ships as possible to reduce time for post-processing.
D. Observations are not allowed in the central channel. Observations in the central sections are crucial however, as this is where most transport takes place (especially by salinity-driven residual flows). It is recommended to involve nautical authorities in an earlier stage, in order to find ways to measure in the central channel.
E. Collect transect observations using multi-frequency ADCP backscatter in the fairway to Emden. A multi-frequency approach makes transect fluxes much more reliable, and therefore provides details on transport in the central channel.

3 Solutions to reduce turbidity in the estuary, Fairway to Emden and Dollard.

A. Minimize dredged sediment disposal that feeds the circulation cell. Only Delfzijl disposes sediment in the circulation cell (Groote Gat), although disposal here has been replaced by airset techniques (where sediment is agitated and flushed into the Ems Estuary) in the past 20 years. This sediment source may still influence the circulation cell. A potential solution to reduce transport into the circulation cell is to dispose sediment dredged from the port of Delfzijl north of the port. This does not neccesarily lead to a reduction in maintenance dredging from the port of Delfzijl. Sediment dredged from the Fairway to Emden is already disposed further seawards (close to Eemshaven).
B. The sediment flux into the Fairway to Emden can be reduced by minimizing sediment transport over the Geisesteert (for instance, by restoring the dam, and/or creation of salt marshes). Less inflow over the dam will probably lead to a lower seaward sediment flux, and hence turbidity in the estuary. The impact of such works on the Dollard are not obvious, however. If the sediment that is no longer transported over the Geisesteert

becomes permanently fixed, the turbidity in the Dollard will probably decrease. If, on the other hand, this sediment remains mobile, the turbidity in the Dollard may increase. Such measures also require more thorough investigations on the impact of the Geisesteert, preferably through a combination of monitoring and modelling (as in recommendation 1A). Note that from satellite images remnants of old salt marsh works on the Geisesteert are visible. It is not known why these works have been built, how they functioned and why they were not maintained.

C. The transport over the Geisesteert may be an important factor preventing infilling of the Dollard. Solutions aiming at promoting infilling of the Dollard (for creation of salt marshes or reducing the tidal prism) should consider examining the role of the Geisesteert.

D. An alternative to blocking sediment transport over the Geisesteert (as in recommendation 3B) is to make the connection between the Dollard and the Fairway to Emden more open. This potential solution may have several positive but also negative aspects. Before considering such a potential solution, the effect of removing the Geise dam and lowering of the Geisesteert should be carefully explored (for instance using a well-calibrated numerical model).

6 Literature

Allen GP, Salomon JC, Bassoulet P, Du Penhoat Y, De Grandpré C (1980) Effects of tides on mixing and suspended sediment transport in macrotidal estuaries. Sediment Geol 26:69–90

Brinkman, AG, R Riegman, P Jacobs, S Kuhn and A. Meijboom (2014). Ems Dollard primary production research: Full data report. Imares report Report C160/14, 280 p.

Chernetsky AS, Schuttelaars HM, Talke SA (2010) The effect of tidal asymmetry and temporal settling lag on sediment trapping in tidal estuaries. Ocean Dyn 60(5):1219–1241

Colosimo, I., P. L.M. de Vet, D. S. van Maren, A.J.H.M. Reniers, J.C. Winterwerp, and B.C. van Prooijen (2020). The Impact of Wind on Flow and Sediment Transport over Intertidal Flats. Journal of Marine Science and Engineering 8 (11).

Deng, Z., He, Q., Safar, Z., and Chassagne, C (2019. The role of algae in fine sediment flocculation: In-situ and laboratory measurements, Marine Geology, Volume 413, Pages 71-84, ISSN 0025-3227,https://doi.org/10.1016/j.margeo.2019.02.003.

Dyer, K.R., Christie, M.C., Feates, N., Fennessy, M.J., Pejrup, M., Vander Lee, W., 2000. An investigation into processes influencing the morphodynamics of an intertidal mudflat, the Dollard Estuary, The Netherlands: I. Hydrodynamics and suspended sediments. Estuar. Coast. Shelf Sci. 50, 607–625

de Jonge, V.N., Schuttelaars, H.M., van Beusekom, J.E.E., Talke, S.A., de Swart, H.E., 2014. The influence of channel deepening on estuarine turbidity levels and dynamics, as exemplified by the Ems estuary. Estuarine, Coastal and Shelf Science 01/2014; DOI:10.1016/j.ecss.2013.12.030.

Dyer, K.R., 1994. Estuarine sediment transport and deposition. In: Pye, K. (Ed.), Sediment Transport and Depositional Processes. Blackwell Scientific Publications, Oxford, pp. 193–218.

Geyer, W. R. (1993), The importance of suppression of turbulence by stratification on the estuarine turbidity maximum, Estuaries, 16(1), 113–125.

Held, P., Schrottke, K., & Bartholomä, A. (2013). Generation and evolution of high-frequency internal waves in the Ems estuary, Germany. Journal of sea research, 78, 25-35.

Jay, D.A., and Musiak, J.D., 1994. Particle trapping in estuarine tidal flows. J. Geophys. Res. 99, 445-461.

Jensen, J., Frank, T., Mudersbach, C. (2002). Dokumentation und Untersuchungen zur Begleitung der Beweissicherungsmessungen Emssperrwerk (Null-Messung). NLWKN report WBL 156 D, 102 p.

Klebanowski, S., and Jurgens, H.H. (2001). Messungen zum Massenaustausch über den Geiseleitdamm vom Oktober bis Dezember 1999: Auszugsergebnisse zu den Überströmungsmengen, Feststoff und Salzfrachten. Report Wasser- und Schifffahrtsamt Emden 4-231.2/UnEm/58

Krebs, M., and Weilbeer, H., 2008. Ems-Dollart Estuary. Die Küste 74, 252-262.

Lerczak, J. A., and W. R. Geyer, 2004: Modeling the lateral circulation in straight, stratified estuaries. J. Phys. Oceanogr., 34, 1410–1428.

Manning, A.J., and Dyer, K.R. (2002). The use of optics for the in situ determination of flocculated mud characteristics. J. Opt. A: Pure Appl. Opt. 4 (2002) S71–S81

Maushake, C. and Dankers, P.J.T. (2018). Ems Dollart Measurements 2018 / 19 (EDoM'18), Action Plan.

Mulder, H.P.J., 2013. Dredging volumes in the Ems-Dollard estuary for the period 1960-2011. Unpublished report, Dutch Ministry of Public Works (in Dutch).

Papenmeier S, Schrottke K, Bartholoma A, Flemming BW (2013) Sedimentological and rheological properties of the water–solid bed interface in the Weser and Ems estuaries, North Sea, Germany: implications for fluid mud classification. Journal of Coastal Research. doi:10.2112/JCOASTRES-D-11-00144.1

Pein, J.U., E. V. Stanev, and Y. S. Zhang, 2014. The tidal asymmetries and residual flows in Ems Estuary. Ocean Dynamics 64.12 (2014): 1719-1741.

Postma, H., 1967. Sediment transport and sedimentation in the marine environment. Estuaries, Special Publication 83, 158–179.

Schuttelaars, H.M., de Jonge, V.N., Chernetsky, A., 2013. Improving the predictive power when modelling physical effects of human interventions in estuarine systems, Ocean & Coastal Management, doi:10.1016/j.ocecoaman.2012.05.009

Simpson, J.H., Brown, J., Matthews, J.P., Allen, G., 1990. Tidal straining, density currents and stirring in the control of estuarine stratification. Estuaries 13 (2), 125–132.

Smits, B. & Van Maren, D.S. (2021). Sediment Concentrations in the Ems Estuary: Trend Analysis 1990-2020. Deltares rapport 11206835-000-ZKS-0001, 66 p.

Spingat, F. and Oumeraci, H., 2000. Schwebstoffdynamik in der Trubungszone des Ems-Astuars. Die Kuste, 62, pp. 159–219.

Talke, S.A., H.E. de Swart, and H.M. Schuttelaars. 2009. Feedback between residual circulations and sediment distribution in highly turbid estuaries: an analytical model. Continental Shelf Research 29: 119–135. doi:10.1016/j.csr.2007.09.002.

Uncles RJ, Stephens JA, Harris C (2006) Runoff and tidal influences on the estuarine turbidity maximum of a turbid system: the upper Humber and Ouse estuary, UK. Mar Geol 235: 213–228

Van de Kreeke J, Robaczewska K (1993) Tide-induced residual transport of coarse sediment: Application to the Ems estuary. Neth J. Sea Res 31(3):209–220

van Maren, D.S., van Kessel, T., Cronin, K., Sittoni, L. 2015a. The impact of channel deepening and dredging on estuarine sediment concentration. Continental Shelf Research 95, p. 1-14 http://dx.doi.org/10.1016/j.csr.2014.12.010.

van Maren, D.S., Winterwerp, J.C., Vroom, J., 2015b. Fine sediment transport into the hyperturbid lower Ems River: the role of channel deepening and sediment-induced drag reduction, Ocean Dynamics, DOI 10.1007/s10236-015-0821-2.

Vroom, J, de Vries, B., Dankers, PJT, van Maren, D.S. (2021). Cumulatieve effecten baggeren en verspreiden op habitattype H1130 in het Eems estuarium. Deltares rapport 11206835-000.

Winterwerp, J. C., Manning, A. J., Martens, C., de Mulder, T., & Vanlede, J. (2006). A heuristic formula for turbulence-induced flocculation of cohesive sediment. Estuarine, Coastal and Shelf Science, 68(1), 195-207. DOI: 10.1016/j.ecss.2006.02.003

Winterwerp, J.C., 2011. Fine sediment transport by tidal asymmetry in the high-concentrated Ems River: indications for a regime shift in response to channel deepening. Ocean Dynamics 61:203-215.

Winterwerp JC, Wang ZB (2013) Man-induced regime shifts in small estuaries – I: theory. Ocean Dyn 63(11–12):1279–1292

Winterwerp JC, Wang ZB, van Braeckel A, van Holland G, Kösters F (2013) Man-induced regime shifts in small estuaries – I: a comparison of rivers. Ocean Dyn 63 (11–12):1293–1306

Winterwerp, J. C., Vroom, J., Wang, Z. B., Krebs, M., Hendriks, E. C., van Maren, D. S., Schrottke, K, Borgsmuller, C., and Schöl, A. (2017). SPM response to tide and river flow in the hyper-turbid Ems River. Ocean Dynamics, 67(5), 559-583.

Winterwerp, J.C., T. Van Kessel, D.S. Van Maren, B.C. Van Prooijen (2021). Fine sediment in open water: from fundamentals to modeling. World Scientific Publishing, 600 p.

Wunsche, A. (2019). Short report on processing of mooring chain data EDoM'18. BAW report BAW-No.: B3955.01.34.10002, 8 p.

7 Annexes

More detailed information is provided in the Annexes.

Annex A Overview of measurements per station

Annex B A more detailed visualization and short description of the data, including

- Detailed timeseries of all data during the EDoM surveys (28 August 2018 and 24 January 2019)
- Asymmetry plots (relation between flow velocity, SSC and salinity)
- Bathymetric changes

Annex C Dredging information

Annex D Additional figures without description:

- Full timeseries of the moorings
- Subtidal flow velocities of the moorings
- Timestacks of the 13-hrs observations (flow velocity, SSC, and salinity as a function of time and depth)
- Sediment fluxes
- Cross-sectional flow velocities, fluxes, and SSC for the cross-sections
- SSC and salinity of the longitudinal surveys
- Flow over the Geise dam (2019 only)

Annex E Observations Geise dam

Annex F Settling velocity observations

A Overview of elaborated observations

List observations + link to annex in which they are shown

Permanent monitoring frames

- Discharge Versen
- Water level Knock
- SPM, vel, salinity at various frames

Fixed monitoring for EDoM (~one month of data per year)

Construction	Measuring organisation	locations	Instruments & parameters	period
Frame at bed	BAW	GAT, KNO (only 2018), GEI, EFW, DOL	ADCP (velocity, missing lower 2 m of water column) OBS (turbidity) CTD (salinity, temperature) Water level	8/9 Aug – 2/5 Sep 2018 and 9/10 Jan – 20 Jan (GAT) or 6/7 Feb 2019
	RWS	EFW, DOL	Upward and downward looking ADCP (velocity, temperature, pressure) OBS (turbidity) ADV (velocity, temperature, pressure) MPP (temperature, salinity, pressure, pH, turbidity, Chlorophyll, oxygen)	24 Aug – 12 Sep 2018 and 16 Jan – 7 Feb 2019
Frame at bed + chain to surface	BAW	KNO, EFW, DOL	Multiparameter instruments at 3 positions in the water column (velocity, salinity, temperature, turbidity, oxygen, pressure)	6 Aug – 3 Sep 2018 and 8 Jan – 5 Feb 2019

Sailing monitoring for EDoM (13 hours measurements)

- Cross-sections
- Fixed position ships (stationary boats)

Table A.2 Organizations with key participants of the EDoM campaigns

Organisation	***Persons involved***
BAW – DH	Christian Maushake, Anna Wunsch, Jens Jurges
RWS	Jan Willem Mol
RHDHV	Petra Dankers
Deltares	Bas van Maren
ICBM Uni Ol	Thomas Badewien
WSA Emden	Timo Rosendahl, Martin Krebs
NLWKN Norderney	Dennis Oberrecht
	Andreas Wurpts

NLWKN Aurich	Andreas Engels, Dirk Post
NIOZ	Theo Gerkema
Uni. Maine	Lauren Ross
IOW	Hans Burchard
Wageningen University	Ton Hoitink
HR Wallingford	Andy Manning
Antwerpen University	Dante Horemans
CAU Kiel (Marum)	Christian Winter
BfG	Christine Borgsmüller
Delft University	Henk Schuttelaars

B Sediment fluxes

B.1 Residual sediment fluxes over a spring neap cycle

In 2018 and 2019 (Figure 7-1) some clear patterns in the residual sediment fluxes can be observed: the fairway to Emden is for most frames exporting sediment, while the Dollard shows an import. In 2019, some of the frames in the fairway to Emden show a near-bed to mid-depth import and near surface export, which relates to the classical estuarine circulation mechanism which is stronger in 2019 due to the higher discharge from the Ems River.

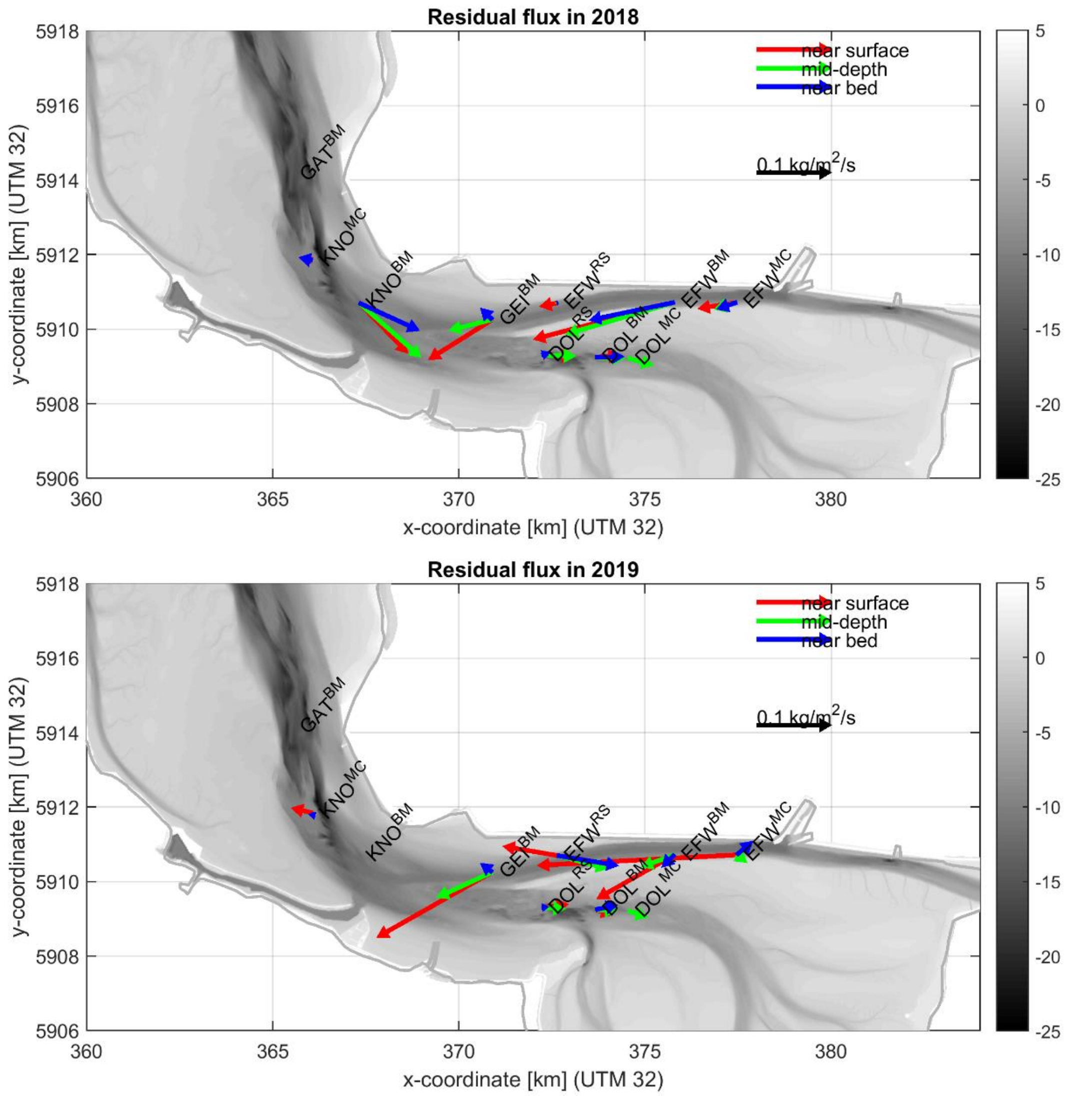

Figure 7-1 Residual sediment transports for a spring-neap cycle for all available locations. Time series should be cover at least one spring neap tidal cycle to be included in the figure and both current velocities and calibrated turbidity measurements (i.e. suspended sediment concentrations) should be available. At MC stations, velocities at 3 positions in the vertical are multiplied with SSC at the same position. At other locations velocity profiles, as collected by an ADCP are multiplied with near bed SSC.

The profiles of the sediment fluxes for the RS and BM frames have been computed by multiplying the velocity profile by the near-bed SSC measurements, as no SSC measurements higher in the water column are available at those stations. This will overestimate the mid-depth and surface sediment fluxes.

The export through the fairway to Emden in 2018 and some locations in 2019 is surprising, and we will zoom into the area to closely investigate the sediment transport at the various locations. In the Dollard the residual fluxes are similar in 2018 and 2019.

A converging point seems to be present between BM_GEI and BM_KNO in 2018 and possibly also 2019, which cannot be know because of lack of data to compute a spring-neap tidal residual flux at BM_KNO. The converging point seems to coincide with a local turbidity maximum from longitudinal transects (see Appendix D) and largest dredging volumes per kilometre of thalweg (Appendix C).

Due to estuarine circulation, a - more consistent in both place and time - near-bed landward sediment flux and a seaward near surface flux is expected in the fairway to Emden. The measurements in Figure 7-1 do not or only limitedly show estuarine circulation. Possibly, import of sediment is occurring at part of the channel that are not covered by the observations, i.e. the lowest part of the water column, centre of the channel and/or over the sides (Geiseleitdamm). Or, another mechanism is overruling the estuarine circulation, for example suspended sediment concentrations that are much higher during ebb than during flood.

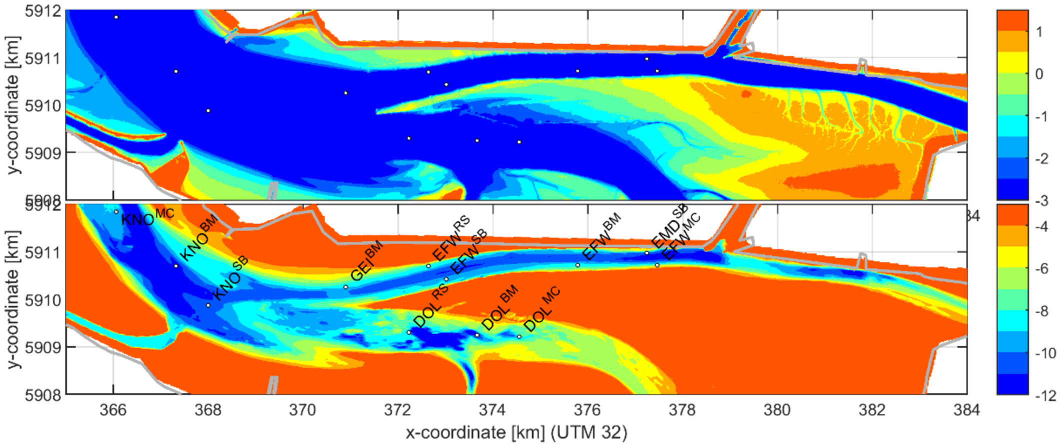

Figure 7-2 Bathymetry of the study area. Top panel shows height differences in the intertidal area and lower panel shows bathymetric features in the channels. Measurement locations are indicated with white dots and abbreviations in the lower panel. BM = Bottom Mooring, MC = Mooring Chain, RS = RWS frame, SB = Stationary boats that conducted measurements for 13 hours.

The lower panel of Figure 7-2 shows that all stations in the fairway to Emden are located on the flanks of the channel. Also, the measurements in Figure 7-1 do not cover the lowest part of the water column, except for the RS frames that were equipped with a downward looking ADCP (Table 7.1). However, at RS_EFW the near-bed sediment flux is negligible in 2018 and in seaward direction in 2019. Remarkably, the mid-depth sediment flux at RS_EFW is in landward direction in 2019.

Table 7.1 Vertical range or position of measurements

Location	Vertical range or position of measurements
MC_KNO	1.5 and 3.5 meter above the bed and 1.5 m below the water surface
BM_KNO	2018: 2.21 m above the bed and above
BM_GEI	2018: 2.20 m above the bed and above 2019: 2.3 m above the bed and above
RS_EFW	3.39 m above the bed and above, and downward looking ADCP (6.4 – 42.4 cm above the bed)
BM_EFW	2018: 2.20 m above the bed and above 2019: 1.7 m above the bed and above
MC_EFW	1.5 and 3.5 meter above the bed and 1.5 m below the water surface
RS_DOL	3.39 m above the bed and above, and downward looking ADCP (6.4 – 42.4 cm above the bed)
BM_DOL	2018: 2.21 m above the bed and above 2019: 1.7 m above the bed and above
MC_DOL	1.5 and 3.5 meter above the bed and 1.5 m below the water surface

B.2 Residual sediment fluxes over the 13-hour measurement period

A near-bed landward flux due to estuarine circulation could be more pronounced in the centre of channel, where the channel is deepest. This might be observed from the cross-sectional transects (13-hour measurements) as measured by ships, that measure the entire cross-section all the way to the bed. First, we compare the sediment fluxes over the spring neap tidal cycle with the sediment flux at the same locations for the period of the 13-hour measurements, to see if the patterns are consistent. Although magnitudes are different, directions are consistent for most of the locations (Figure 7-3), except for RS_DOL in 2018. Therefore, we assume that import or export in the sediment fluxes as measured by both the cross-sections and the stationary boat measurements are representative for a spring neap tidal cycle. Only for the stationary boat measurements we obtained a calibrated turbidity (SSC) signal, that can be used to compute sediment fluxes. For the cross-sections, we solely look at current velocities and ADCP backscatter, as a measure for high and low sediment concentrations.

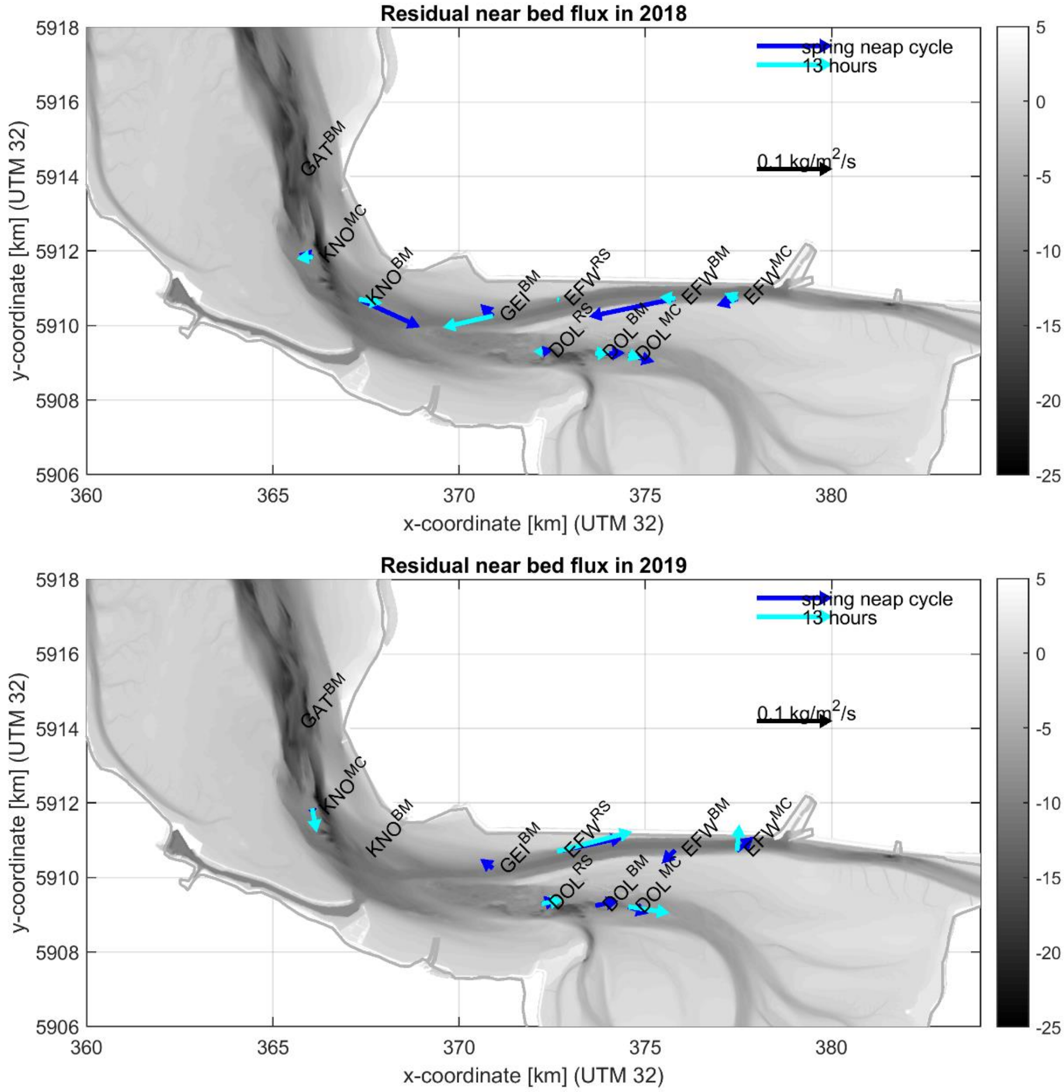

Figure 7-3 Comparison of near-bed sediment fluxes as derived from averaging over a spring neap tidal cycle (blue) and as derived from averaging over the period of the 13-hour measurements (cyan). For station DOL^{MC}, the mid-depth flux has been visualised in absence of near-bed calibrated turbidity measurements. In 2019 there are no SSC measurements at EFW^{BM} and DOL^{BM} during the 13-hour measurements.

The residual sediment fluxes for the 13-hour measurements obtained from the cross-sectional transects are shown in Figure 7-4 and Figure 7-5 and are compared with the stationary boots or frames data. Comparing the derived sediment fluxes allows to identify the quality of the ADCP converted sediment concentrations and derived sediment fluxes. But more important, it allows to investigate how well the sediment fluxes in the channel are captured by the stationary measurements at a single location.

Sediment in- and exporting channel sections are comparable for the Dollard cross-sectional transect between 2018 and 2019. The main channel (deepest section) imports sediment in the Dollard as well as the northern flank. The southern flank predominantly exports sediment, except from a region located between 550 and 650 m (see Figure 7-5). In 2019 the sediment importing regions are more pronounced in the figures. That the importing sections are more visible for 2019 is, however, likely not caused by estuarine circulation. Comparing the flood and ebb average variant of Figure 6.5 (data not shown), it is observed that sediment is mainly imported in the upper part of the column during the flood phase. If estuarine circulation would play a major role, sediment would mainly be imported trough the lower part of the water column. All measurement locations in the Dollard are in or at the edges of the main channel. In 2018 this RS_DOL is exporting sediment while BM_DOL, which is located at the edge of the main channel, is importing sediment. In 2019 RS_DOL is importing sediment in agreement with the cross-sectional transect.

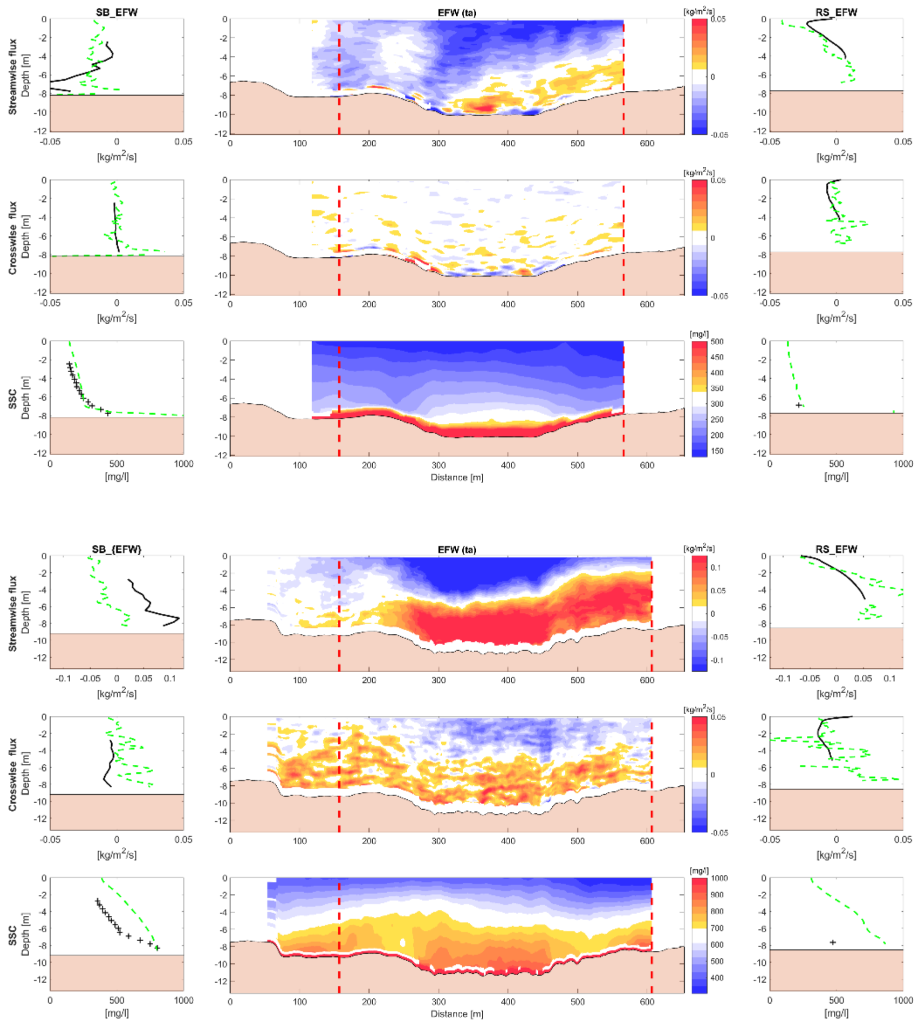

Figure 7-4 Comparison between the sediment fluxes derived from the cross-sectional transects and stationary boot or frame data for the years 2018 and 2019 at the EFW transect. The red dotted lines in the three middle panels indicate the (approximate) location in the channel of the stationary measurements. The side panels compare the data from the cross-sectional transects (dotted green) with the stationary boot or frame (solid black).

The EFW transect (in the fairway to Emden) shows different sediment in- and exporting sections for 2018 and 2019. But, before comparing data it is needed to state that the quality of the data for 2018 was poor, especially for the sediment concentration. Hence it was not possible to derive meaningful sediment fluxes for the cross-sectional transect. In 2019 sediment is imported through the lower water column in main channel and the northern bank. This contrasts with the upper part of the water column which exports sediment. Import near de bottom an export at the surface agrees well with the measurements at RS_EFW. Furthermore, it indicates that classical estuarine circulation is a dominant mechanism controlling sediment transport. Indeed, comparing the flood and ebb average variant of Figure 6.4 (data not shown) shows that during the flood sediment in imported near the bottom of the main channel. The southern bank is exporting according to the cross-sectional transect, however, this is not supported by the stationary boot data which shows an import of sediment. But a clear stratification caused by estuarine circulations is not visible at SB_EFW. Finally, in the cross-sectional transect of 2019 a counter clockwise lateral sediment transport is visible and is more dominant during the flood. This lateral transport seems to transport near bottom sediment towards the northern bank of the channel and surface water towards the southern bank. A counter clockwise lateral sediment transport can explain higher concentration at the northern bank.

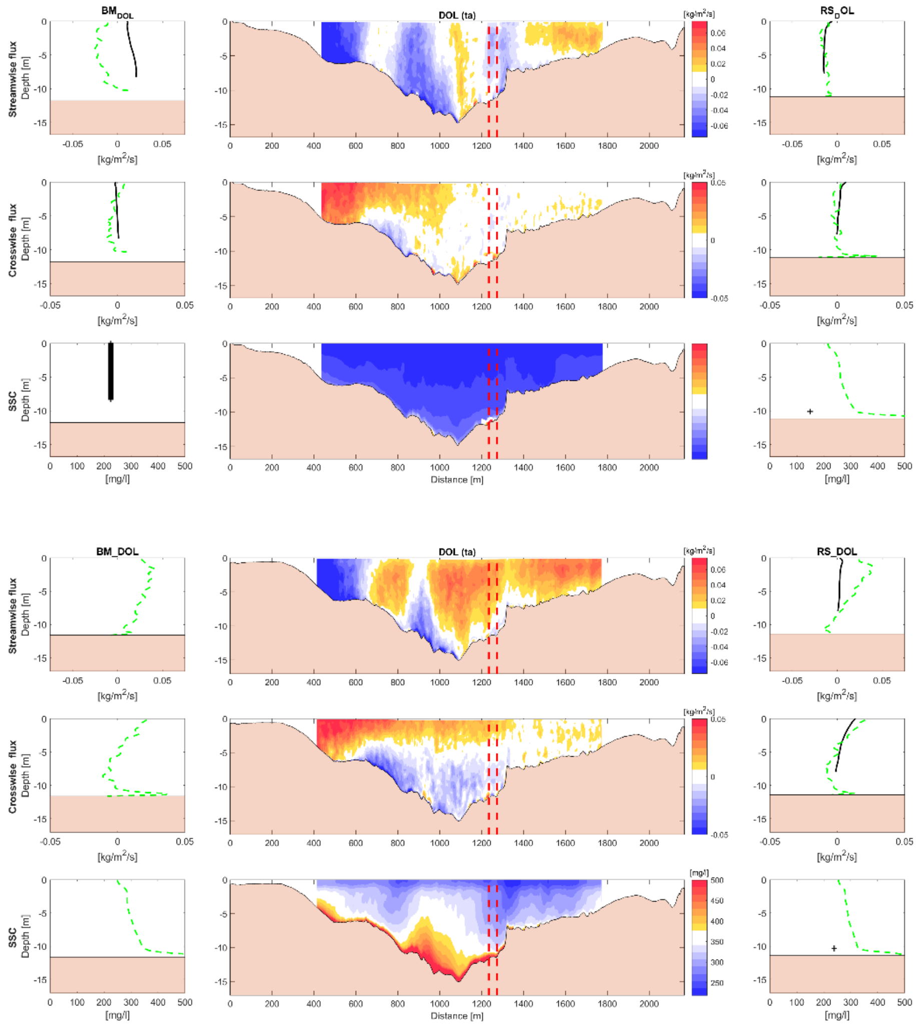

Figure 7-5 Comparison between the sediment fluxes derived from the cross-sectional transects and stationary boot or frame data for the years 2018 (top) and 2019 (bottom) at the Dollard transect. The red dotted lines in the three middle panels indicate the (approximate) location in the channel of the stationary measurements. The side panels compare the data from the cross-sectional transects (dotted green) with the stationary boot or frame (solid black).

The cross-sections indicated the variability in sediment fluxes over the cross-section. At the EFW, the behaviour at the northern bank of the channel is very different (i.e. mostly importing) than what was derived from the observations at the southern bank (exporting). Unfortunately, the 2018 measurements are of a poor quality, but the 2019 transect shows that the northern frames are probably more representative for the transports in the channel than the southern frames.

At the Dollard, all frames were at more or less the same part of the cross-section, which might give more consistency between the three frames (RS, BM and MC) although this is not representative for other positions along the cross-section. Also, the residual sediment flux at RS_DOL was different between the spring-neap cycle and the 13-hour period. However, it is clear that the import is much larger in 2019 than in 2018.

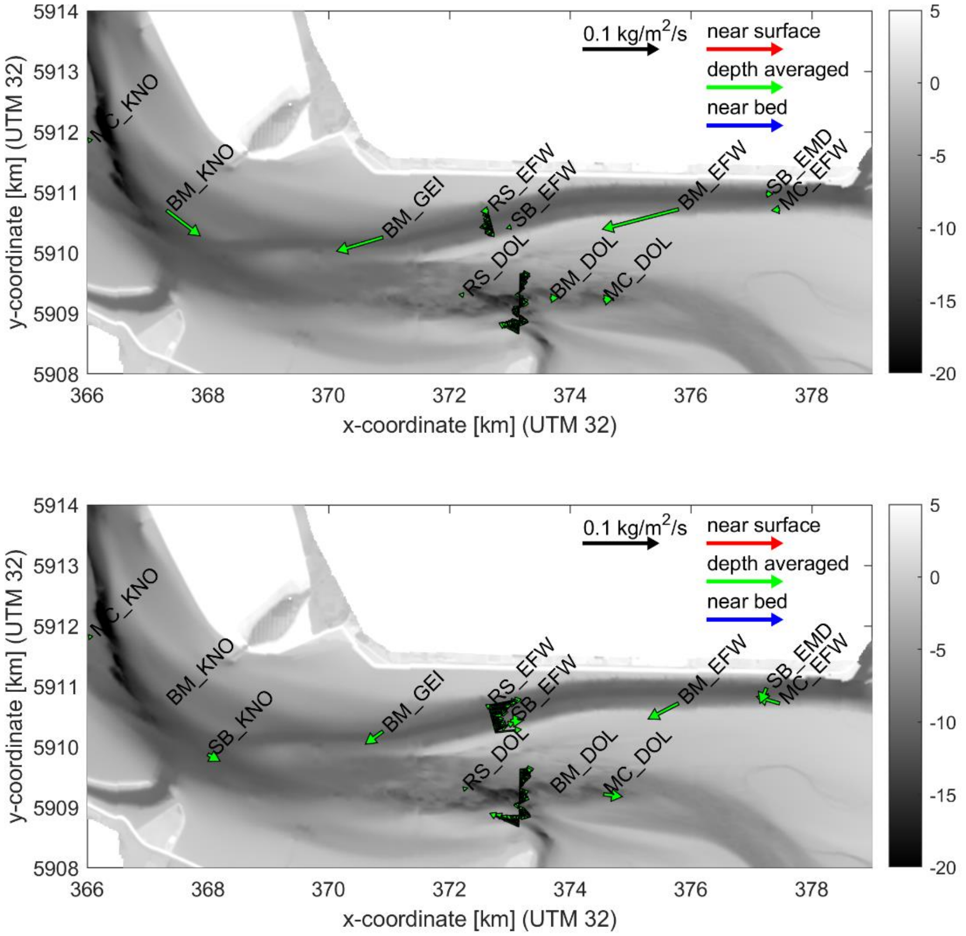

Figure 7-6 Depth averaged residual sediment transports for the 13 hours measurements for all available locations and cross-sectional measurements in 2018 (top) and 2019 (bottom). Note that the data quality between the locations greatly differ. Fluxes of the cross-sectional measurement derived 2018 contained several issues. The SSC quality of EFW was too poor to derive a residual flux. In addition, SSC derived from the backscatter is overestimated at the Dollar transect. Hence, the magnitudes of the fluxes are not suitable and should not be compared with nearby located station or compared with cross-sectional measurement of 2019.

B.3 Current velocities and SSC during 13-hour measurement periods

This section first describes the residual flow derived from the cross-sectional transect and compare them with stationary measurement. Hereafter, the 13-hour of the individual station will be described in detail.

In 2018 the Dollard show several distinct regions that import sediment (Figure 7-7). These regions become less distinct in 2019 when import predominates. In addition, there is not an unambiguously cause for the import at the individual sections which result both for asymmetry in the flow and SSC. The streamwise flood velocities are relatively homogeneous over the cross-sectional transects, with maximum velocities of ~0.8 m/s occurring near the surface. During ebb, more heterogeneity is observed. Maximum velocities of ~-1.0 m/s occur north of the main channel and at the most southern flank near the surface. In addition, low current velocities are observed in the main channel (near the bottom) and on the south flank of the main channel. Both these regions import sediment. The streamwise current of the cross-sectional transects agrees well with MC_DOL but less with RS_DOL. Crosswise velocities do not explain in- or export of sediment. However, from the crosswise velocities lateral divergence convergence during ebb is visible. Comparing the SSC, a degree of flood-ebb asymmetry is observed. During both flood and ebb highest SSC occur near the bottom of the main channel. At the northern bank, the flood concentrations are much higher which explains the import at this location. Overall, import of sediment results flood-ebb asymmetry in the velocities and SSC.

At the EFW transect (2019), import of sediment occurs near the bottom of the navigation channel and north bank (Figure 7-8). This while the rest of the channel shows export of sediment. Import or export is mainly determined by a flood-ebb asymmetry in the SSC. This is evaluated in more detail in section 3.3.2 of the main report.

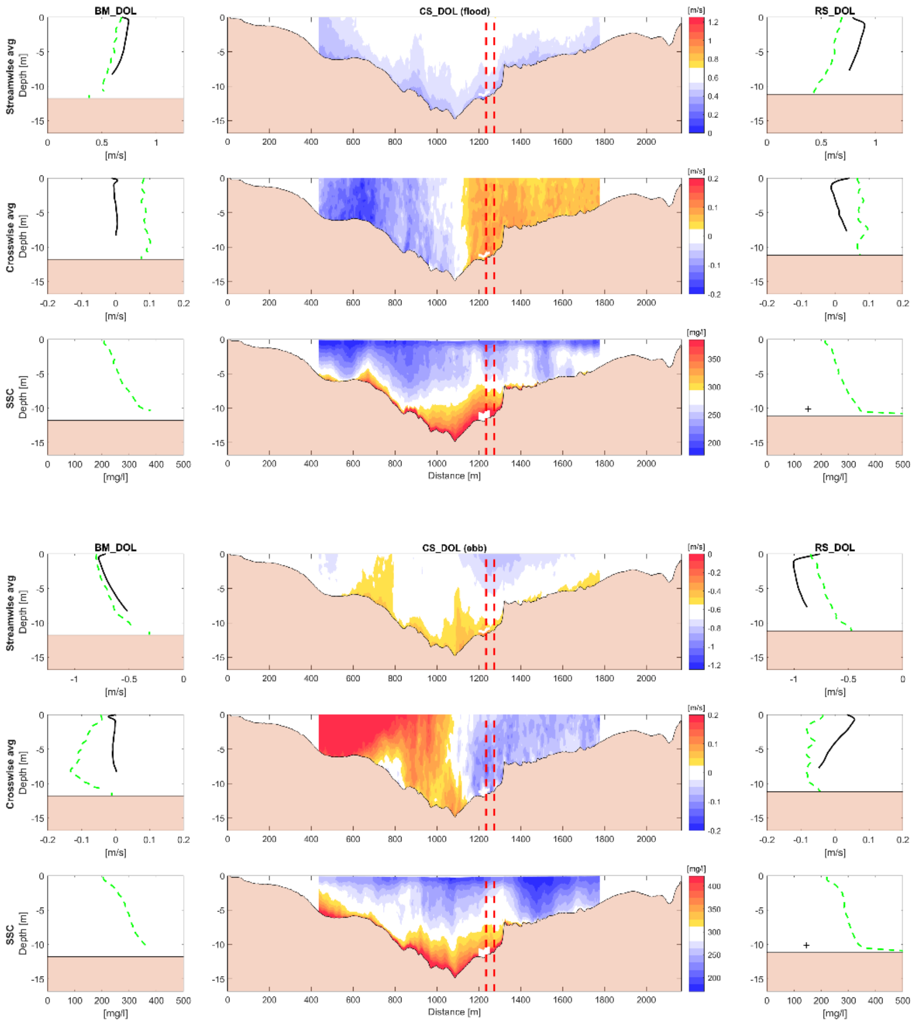

Figure 7-7 Comparison between residual velocities derived from the cross-sectional transects and stationary boot or frame data for the years 2018 and 2019 at the Dollard transect. The red dotted lines in the three middle panels indicate the (approximate) location in the channel of the stationary measurements. The side panels compare the data from the cross-sectional transects (dotted green) with the stationary boot or frame (solid black).

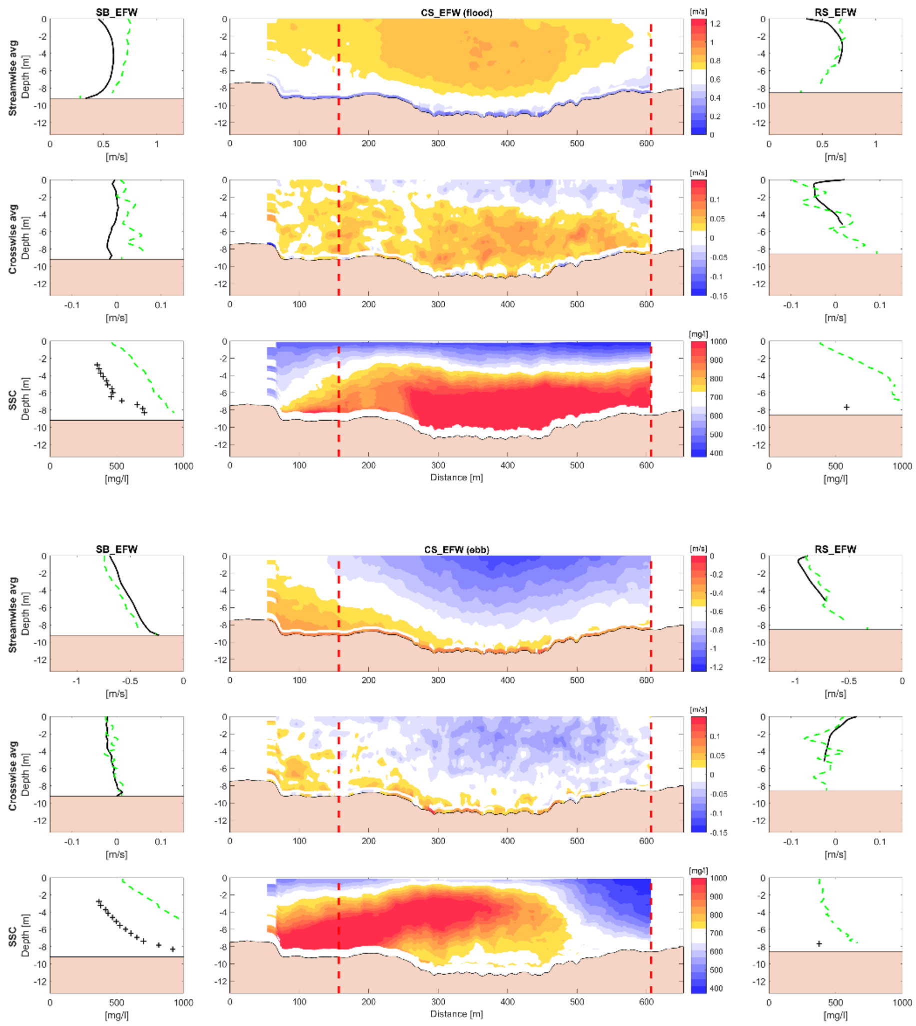

Figure 7-8 Comparison between the average flood and ebb velocities derived from the cross-sectional transects and stationary boot or frame data for the years 2019 at the Fairway to Emden transect. The red dotted lines in the three middle panels indicate the (approximate) location in the channel of the stationary measurements. The side panels compare the data from the cross-sectional transects (dotted green) with the stationary boot or frame (solid black).

Zooming in to the fairway to Emden, the export at BM_GEI just north of the navigational channel, is a result of larger ebb velocities than flood velocities in combination with similar SSC during ebb and flood of 1.5 g/l and elevated for almost the entire ebb and flood phase (section B.3.1 and B.3.2). The behaviour is similar at 2018 and 2019, although the SSC is lower in 2019 at the end of the flood phase and the start of the ebb. Further upstream, at RS_EFW also just north of the navigational channel, SSC is characterized by a flood peak occurring at mid-flood and moderate current velocities of ~0.8 m/s (remarkably they are lower near the surface!) followed by much larger ebb velocities up to 1.5 m/s in combination with a short SSC peak at the start of the ebb phase. The height of SSC is comparable at ebb and flood. The resulting residual sediment flux is negligible to slightly negative (exporting). In 2019, the same asymmetry in currents can be

observed, but a SSC peak at the start of the flood phase is present, resulting in a near-bed and mid-depth landward sediment flux.
The stationary boot SB_EFW is located on the opposite side of the navigation channel compared to RS_EFW. Here SSC is characterized by a (much) higher concentration during the ebb than flood phase, which is observed both in 2018 and 2019. Although, the difference is much more pronounced for 2018. During the ebb phase two peaks in the SSC are observed, with the second peak occurring just before slack tide being the highest. The magnitude of the peak ebb current (~0.8 m/s) is lower than the flood (~1.0 m/s), but the duration of the peak ebb current is more prolonged. However, this does not explain the high SSC during the ebb stage. The resulting residual sedimented fluxes cause an export of sediment in 2018 but import in 2019. Import during 2019 is mainly the result of higher SSC during the flood.

At BM_EFW, positioned just south of the navigational channel, ebb and flood velocities have similar magnitude, however, due to much higher SSC during ebb, a significant residual seaward sediment flux occurs. Further upstream and also at the south bank, at MC_EFW also a small seaward sediment flux is present, despite higher flood velocities than ebb velocities. SSC is elevated for a longer period during ebb, causing nett export. Note also that the current velocities at 1.5 m above the bed are quite low at this location. In 2019, ebb and flood velocities have similar magnitudes. However, the SSC show surprisingly at low water level higher SSC near the water surface than near the bed, at high water slack the SSC is low, hence sediment settles to the bed. The nett effect is seaward transport near the surface and a small import at mid-depth.

At SB_EMD, located north of the navigation channel, ebb and flood current velocities differ significantly between 2018 and 2019. In 2018, the magnitude of the ebb current (~1.5 m/s) was much higher than the flood (~1.0 m/s). Despite the lower flood current, SSC peaks during the flood phase. During the ebb phase SSC peaks shortly after the current peak, hereafter the SSC remain constant. In 2019, both the flood and ebb peaked at ~1.5 m/s. The concentration at which the SSC peaks during flood and ebb is comparable (~7 g/l). A distinct difference is that during the flood peak the SSC remain low near the surface (0.5 - 1 g/l). This while during the ebb a concentration of nearly 4 g/l is reached. In addition, SSC increases throughout the ebb phase and peaks just before low water slack when the current velocities are low. The net transport resulting from the residual fluxes indicate a net export in 2018 and 2019. However, in 2019 there import of sediment near the bottom.

In the Dollard, eastward stations BM_DOL and MC_DOL show that ebb and flood velocities are comparable and importing sediment flux is caused by high SSC at the start of the flood phase. At RS_DOL there is also a SSC peak at the start of the flood phase, although less pronounced, and also ebb velocities are higher than flood velocities. The nett effect is a negligible sediment flux for the tidal cycle considered. In 2019, observations at MC_DOL and RS_DOL show similar behaviour.

In the estuary, at BM_KNO, a current velocities peak at the start of the flood phase, and in combination with a peak in SSC, this results in a nett landward sediment flux. At the end of the ebb also a SSC peak is visible, but as current velocities are much lower, so is the sediment flux. In 2019, observations at BM_KNO are missing. However, at SB_KNO SSC data is available in 2019 and shows similar behaviour as BM_KNO. At the beginning of the flood, SSC peaks in combination with the peak current velocity. Moreover, during the ebb stage the SSC peak is observed near slack tide when the current velocities are ~0.25 m/s. This results in a net landward sediment transport (import).

B.3.1 13-hrs observations on 28 August 2018

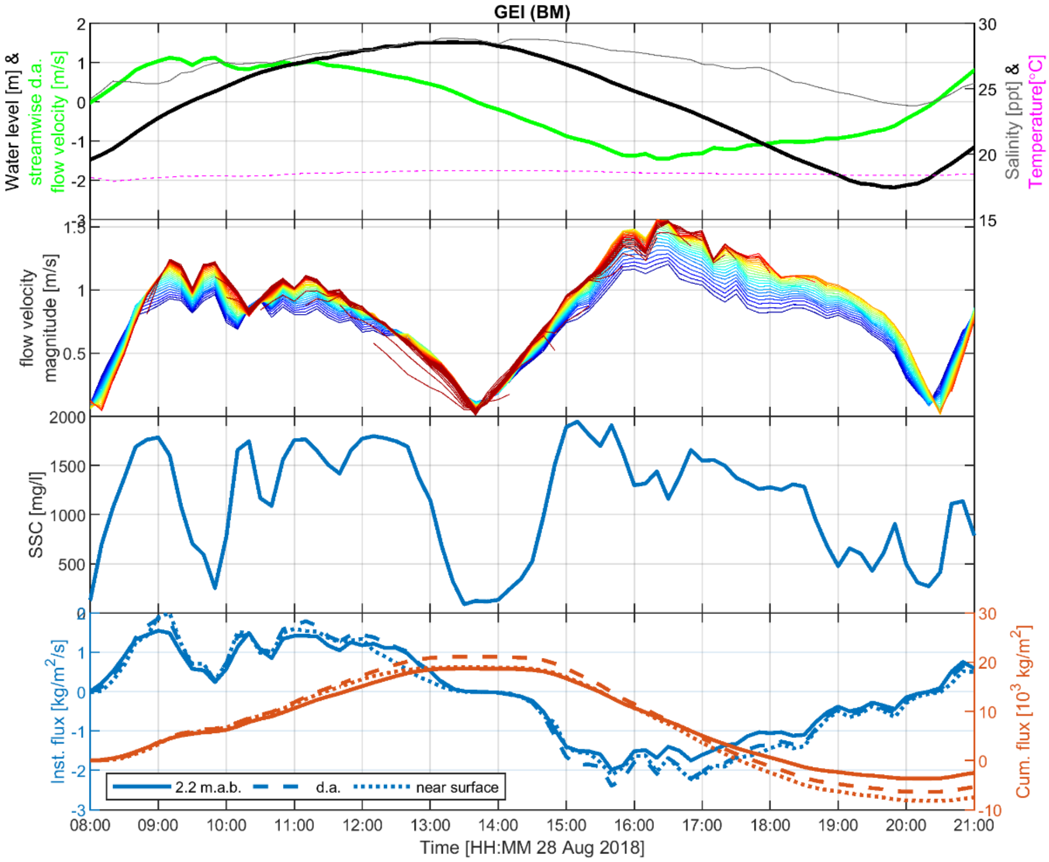

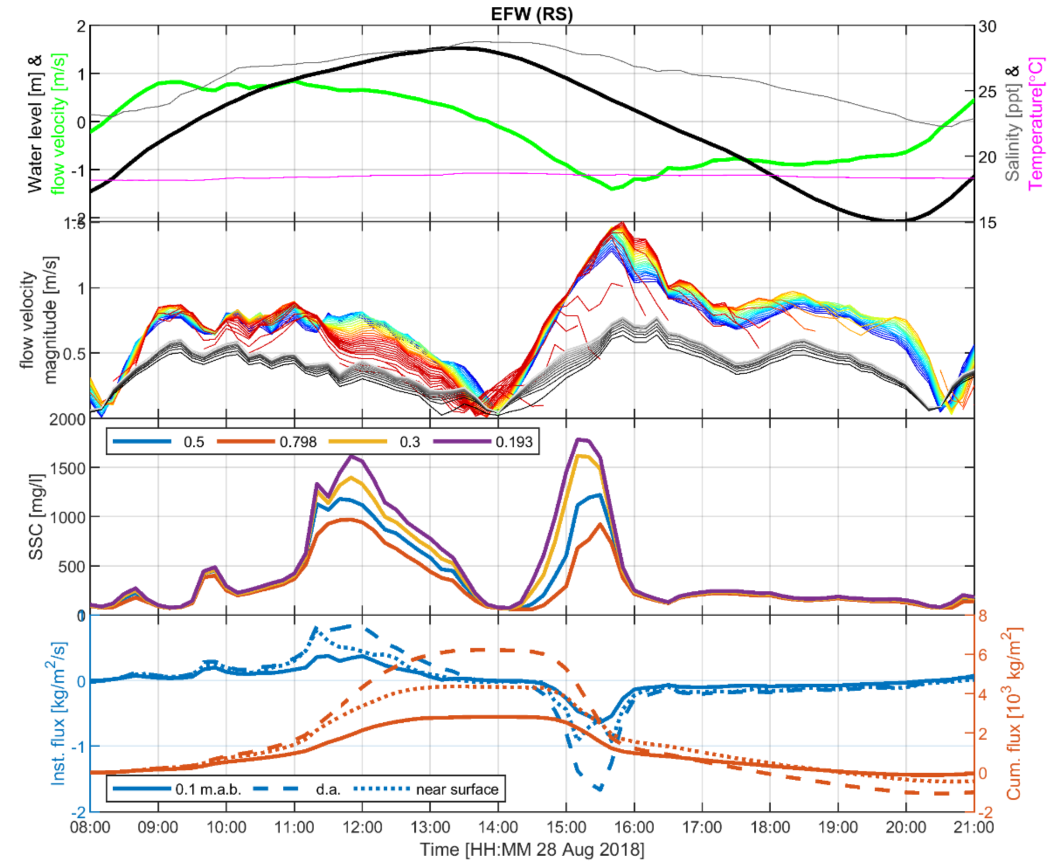

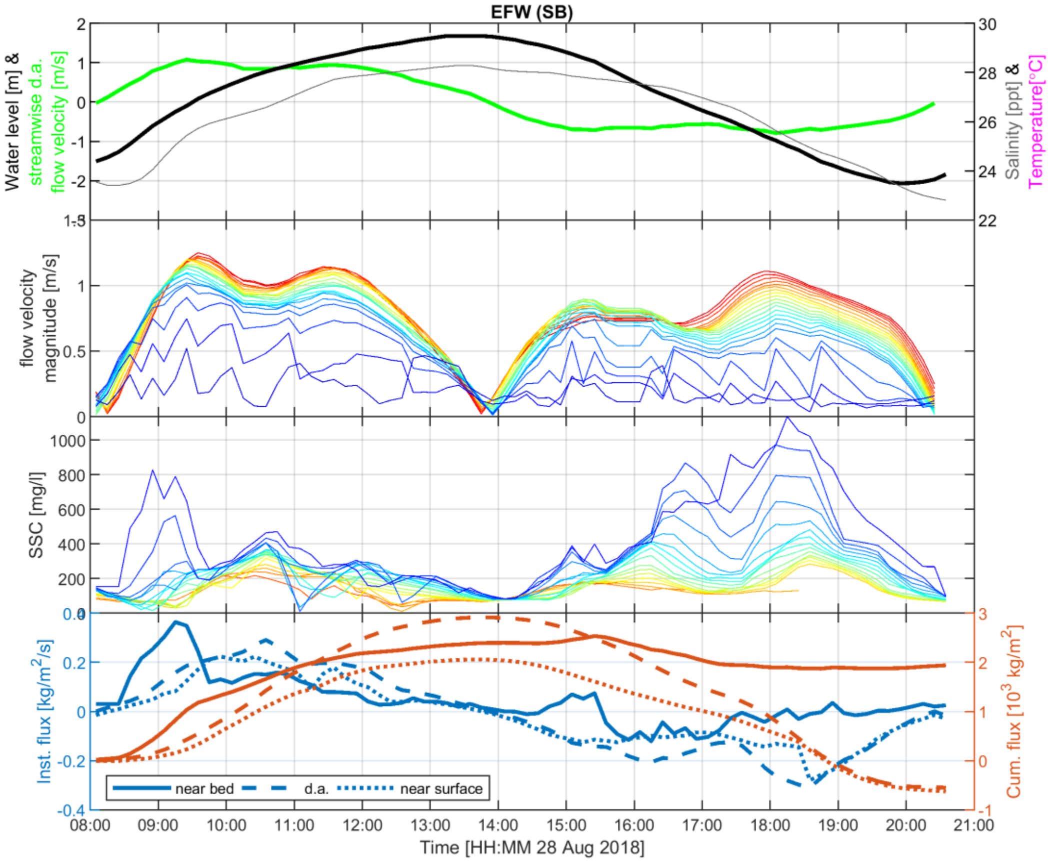
EFW (SB)
Water level [m] &
streamwise d.a.
flow velocity [m/s]
Salinity [ppt] &
Temperature[°C]
flow velocity
magnitude [m/s]
SSC [mg/l]
Inst. flux [kg/m²/s]
Cum. flux [10³ kg/m²]
near bed
d.a.
near surface
08:00
09:00
10:00
11:00
12:00
13:00
14:00
15:00
16:00
17:00
18:00
19:00
20:00
21:00
Time [HH:MM 28 Aug 2018]

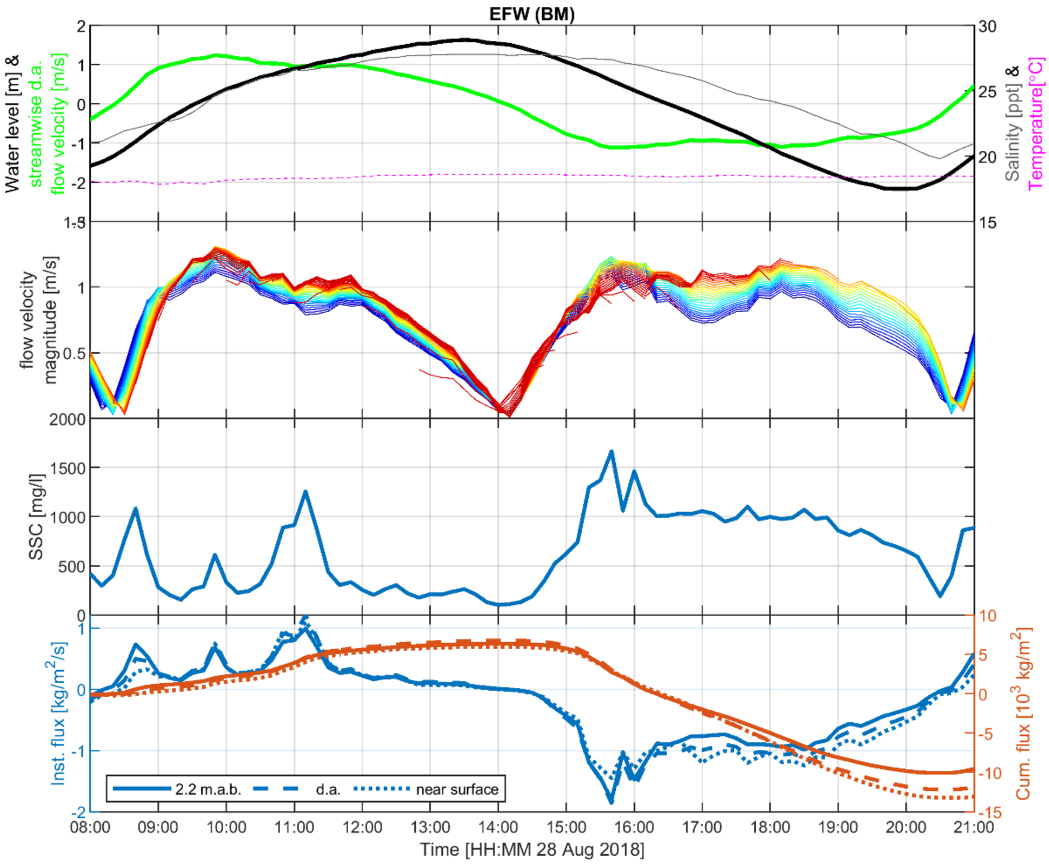
EFW (BM)
Water level [m] &
streamwise d.a.
flow velocity [m/s]
Salinity [ppt] &
Temperature[°C]
flow velocity
magnitude [m/s]
SSC [mg/l]
Inst. flux [kg/m²/s]
Cum. flux [10³ kg/m²]
2.2 m.a.b.
d.a.
near surface
08:00
09:00
10:00
11:00
12:00
13:00
14:00
15:00
16:00
17:00
18:00
19:00
20:00
21:00
Time [HH:MM 28 Aug 2018]

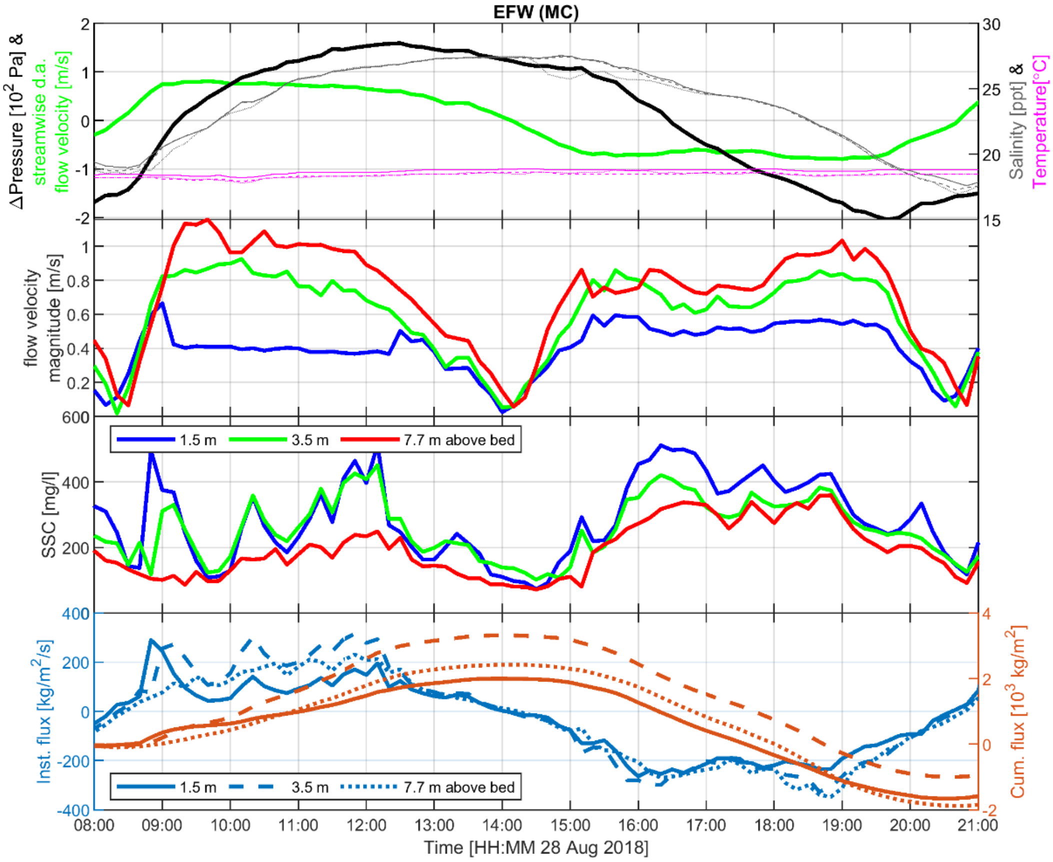
EFW (MC)
ΔPressure [10² Pa] &
streamwise d.a.
flow velocity [m/s]
Salinity [ppt] &
Temperature[°C]
flow velocity
magnitude [m/s]
1.5 m
3.5 m
7.7 m above bed
SSC [mg/l]
Inst. flux [kg/m²/s]
Cum. flux [10³ kg/m²]
1.5 m
3.5 m
7.7 m above bed
Time [HH:MM 28 Aug 2018]

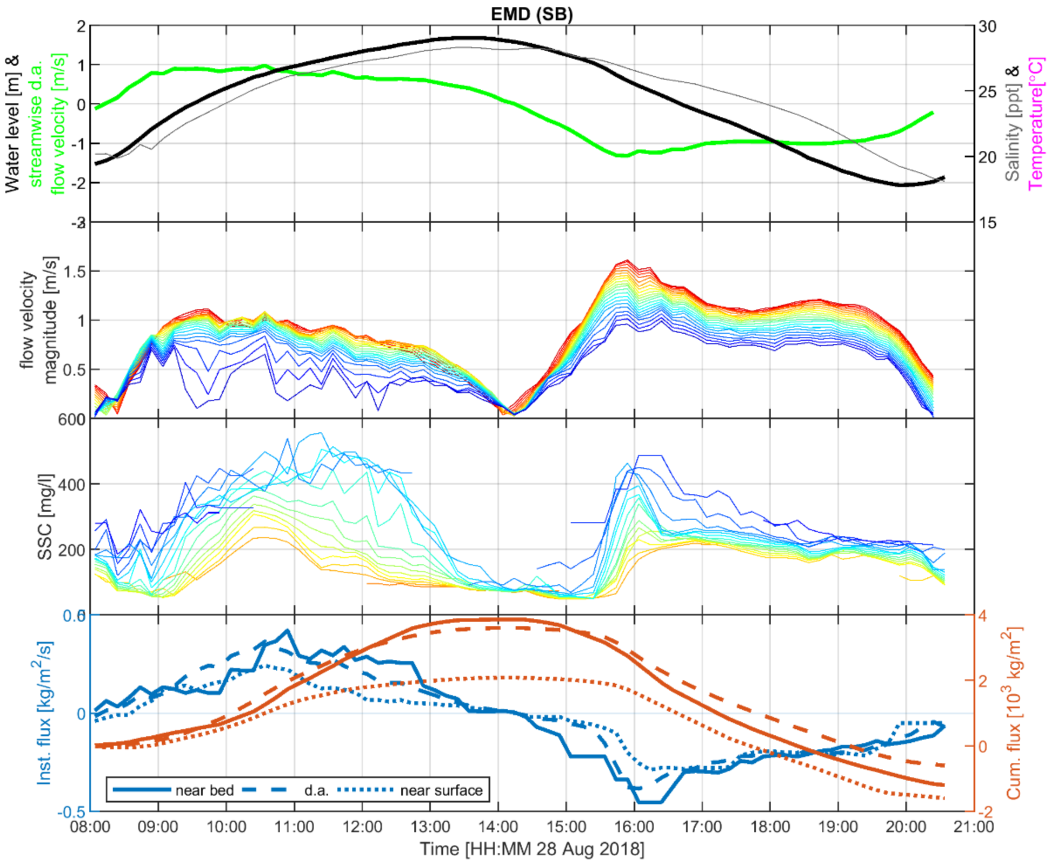
EMD (SB)
Water level [m] &
streamwise d.a.
flow velocity [m/s]
Salinity [ppt] &
Temperature[°C]
flow velocity
magnitude [m/s]
SSC [mg/l]
Inst. flux [kg/m²/s]
Cum. flux [10³ kg/m²]
near bed
d.a.
near surface
Time [HH:MM 28 Aug 2018]

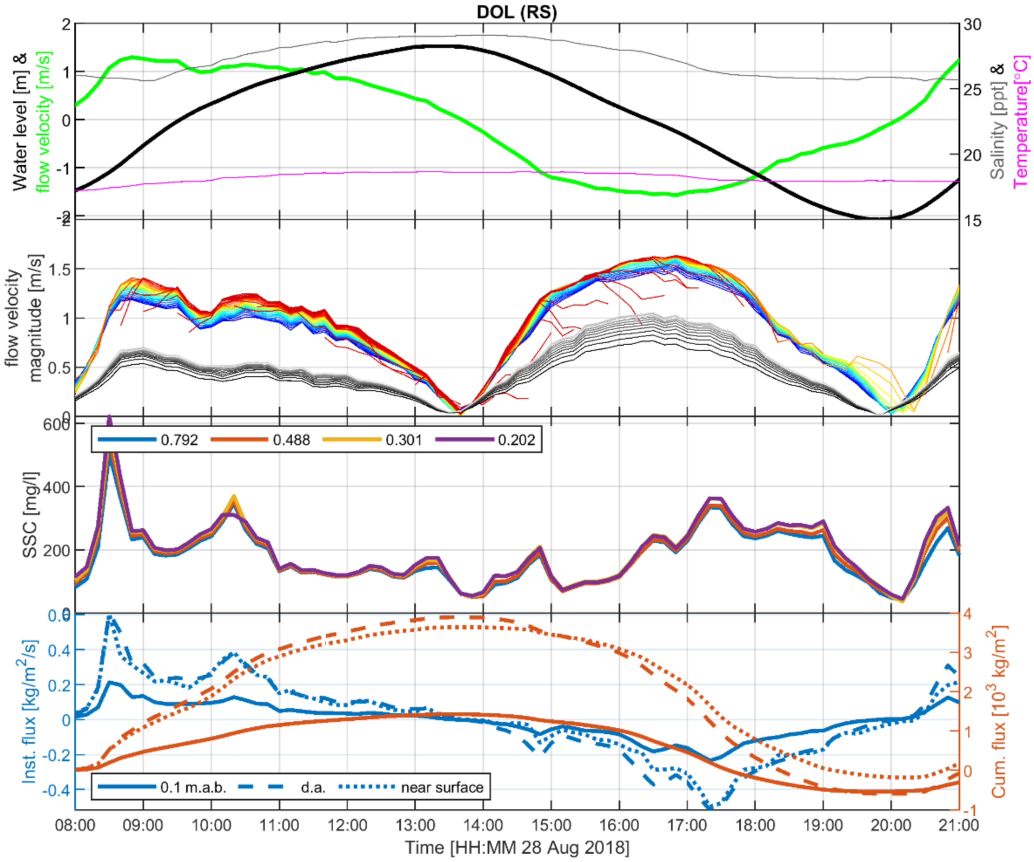
DOL (RS)
Water level [m] &
flow velocity [m/s]
Salinity [ppt] &
Temperature[°C]
flow velocity
magnitude [m/s]
0.792
0.488
0.301
0.202
SSC [mg/l]
Inst. flux [kg/m2/s]
Cum. flux [10³ kg/m²]
0.1 m.a.b.
d.a.
near surface
Time [HH:MM 28 Aug 2018]

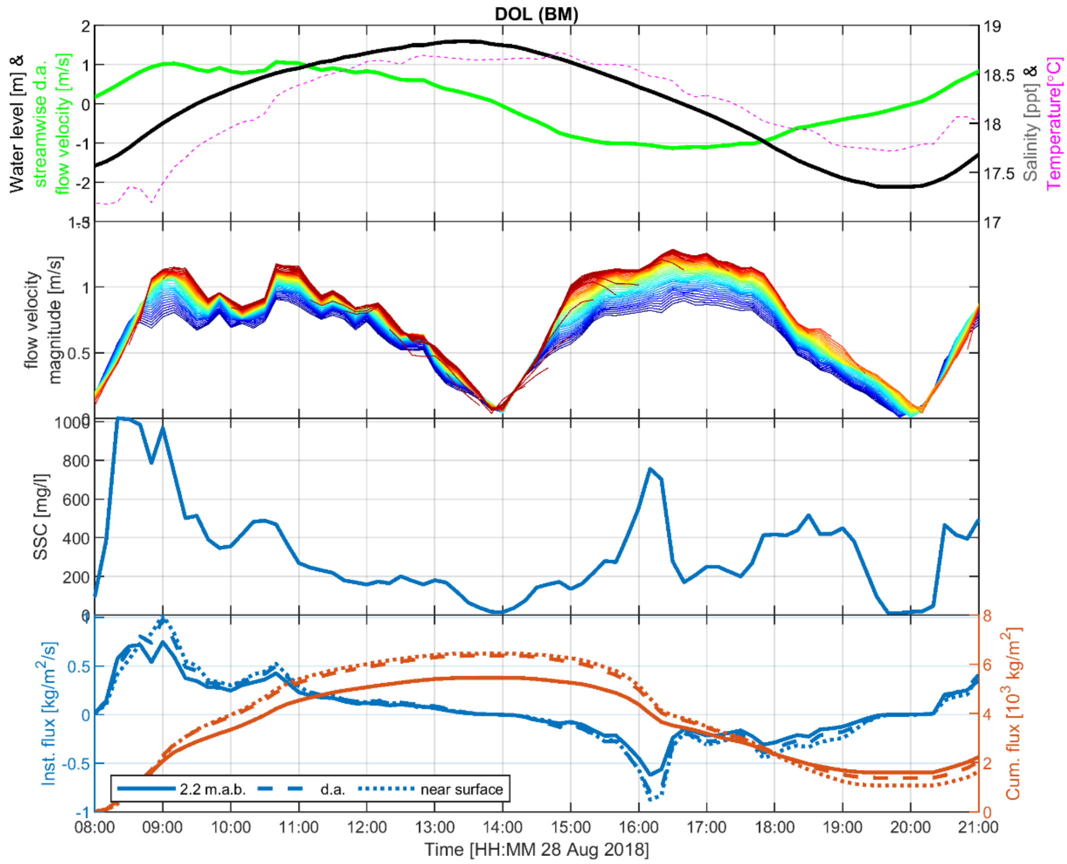
DOL (BM)
Water level [m] &
streamwise d.a.
flow velocity [m/s]
Salinity [ppt] &
Temperature[°C]
flow velocity
magnitude [m/s]
SSC [mg/l]
Inst. flux [kg/m2/s]
Cum. flux [10³ kg/m²]
2.2 m.a.b.
d.a.
near surface
Time [HH:MM 28 Aug 2018]

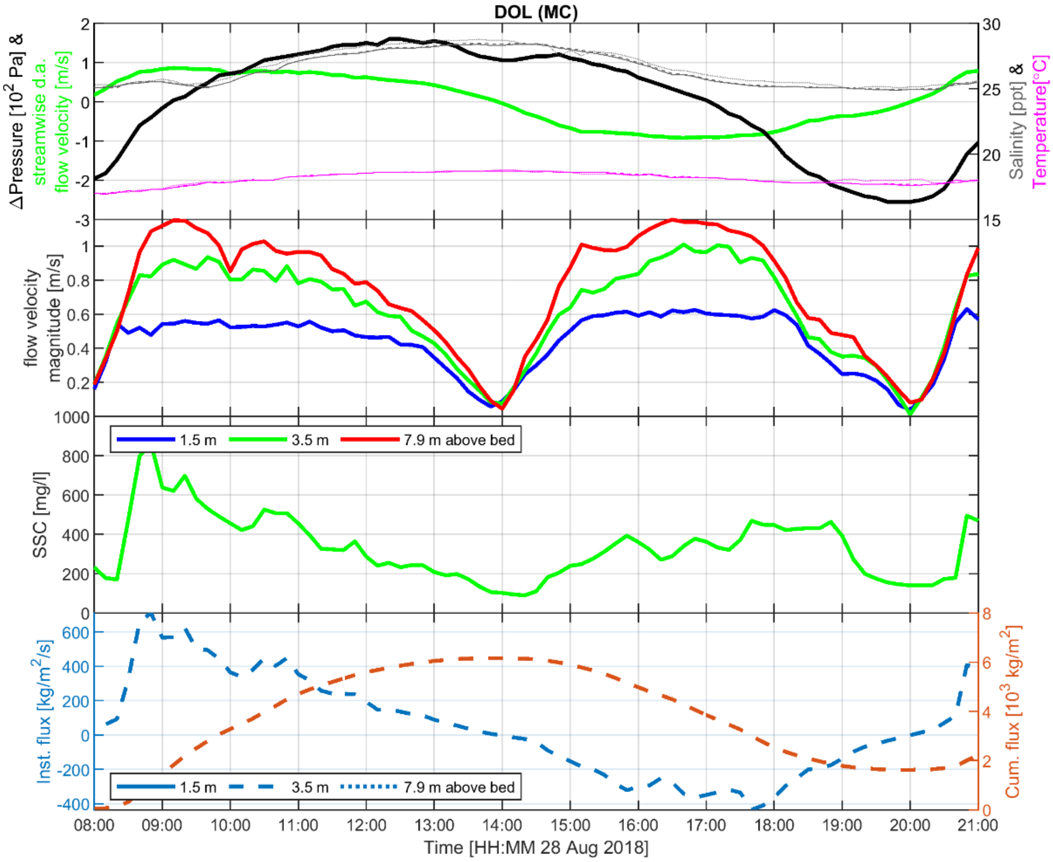
DOL (MC)
ΔPressure [10^2 Pa] &
streamwise d.a.
flow velocity [m/s]
Salinity [ppt] &
Temperature[°C]
flow velocity
magnitude [m/s]
1.5 m
3.5 m
7.9 m above bed
SSC [mg/l]
Inst. flux [kg/m^2/s]
Cum. flux [10^3 kg/m^2]
Time [HH:MM 28 Aug 2018]

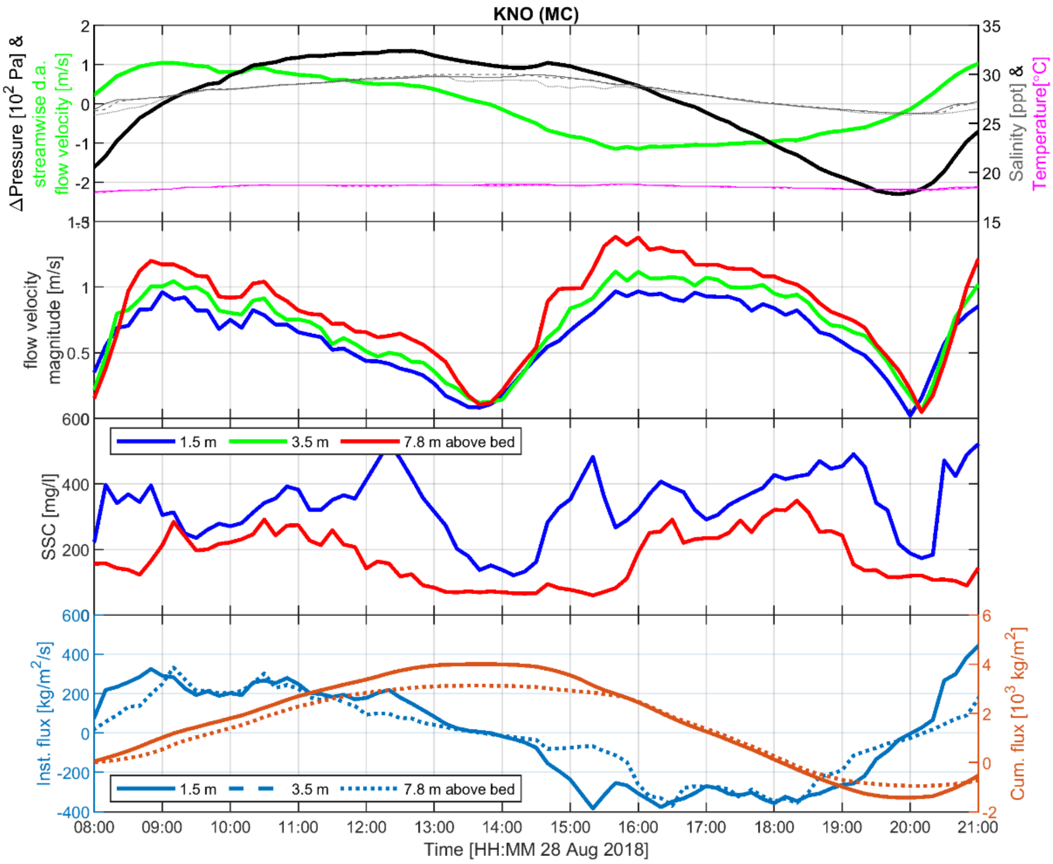
KNO (MC)
ΔPressure [10^2 Pa] &
streamwise d.a.
flow velocity [m/s]
Salinity [ppt] &
Temperature[°C]
flow velocity
magnitude [m/s]
1.5 m
3.5 m
7.8 m above bed
SSC [mg/l]
Inst. flux [kg/m^2/s]
Cum. flux [10^3 kg/m^2]
Time [HH:MM 28 Aug 2018]

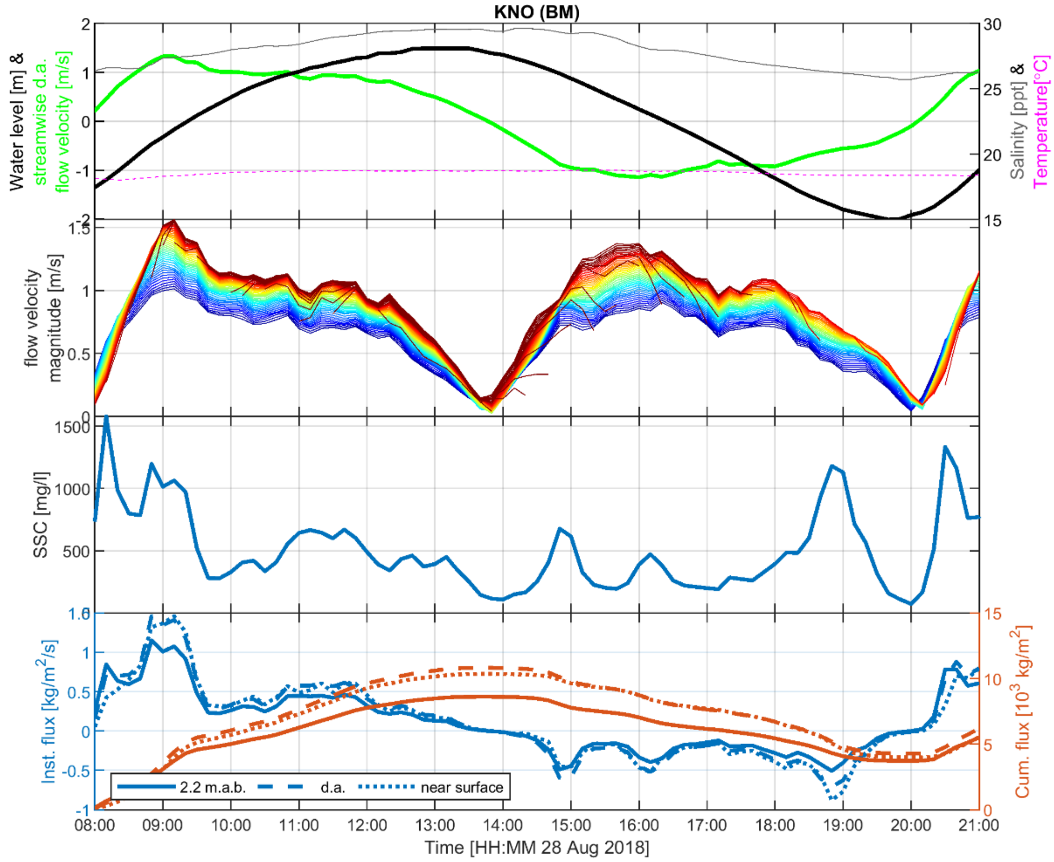
KNO (BM)
Water level [m] &
streamwise d.a.
flow velocity [m/s]
Salinity [ppt] &
Temperature[°C]
flow velocity
magnitude [m/s]
SSC [mg/l]
Inst. flux [kg/m²/s]
Cum. flux [10³ kg/m²]
2.2 m.a.b.
d.a.
near surface
Time [HH:MM 28 Aug 2018]

B.3.2 13-hrs observations on 24 january 2019

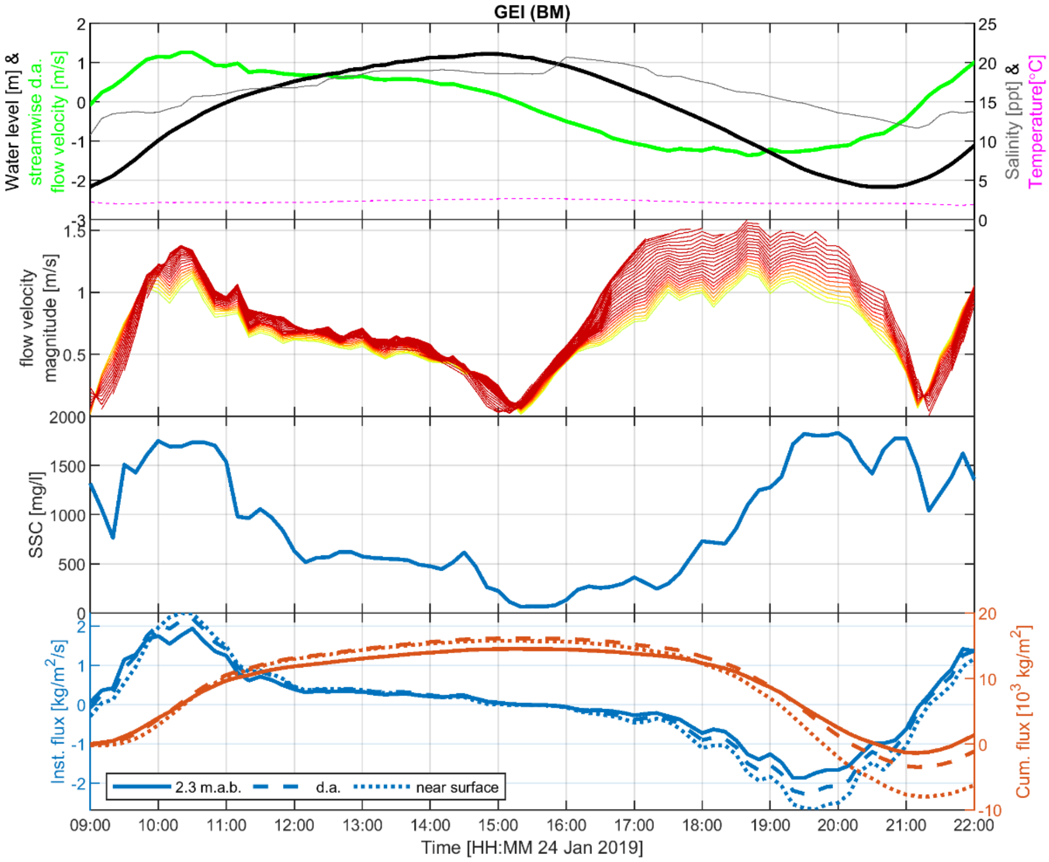

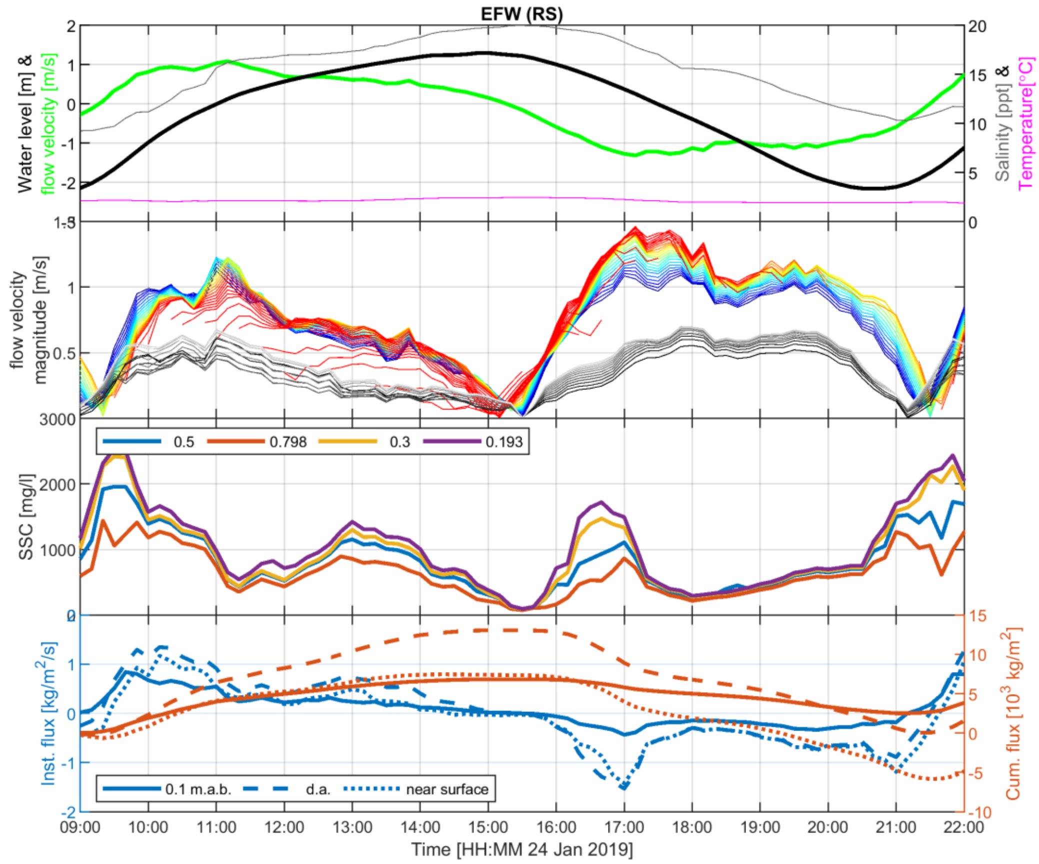

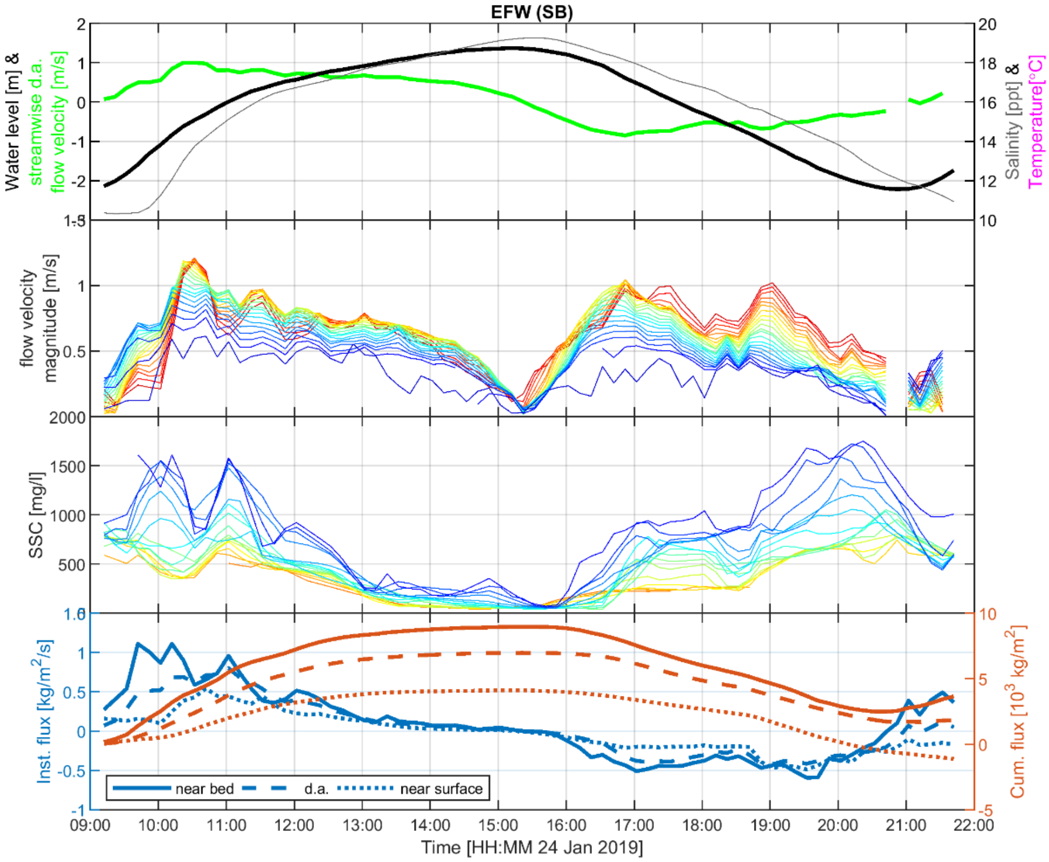
EFW (SB)
Water level [m] &
streamwise d.a.
flow velocity [m/s]
Salinity [ppt] &
Temperature[°C]
flow velocity
magnitude [m/s]
SSC [mg/l]
Inst. flux [kg/m²/s]
Cum. flux [10³ kg/m²]
near bed
d.a.
near surface
Time [HH:MM 24 Jan 2019]

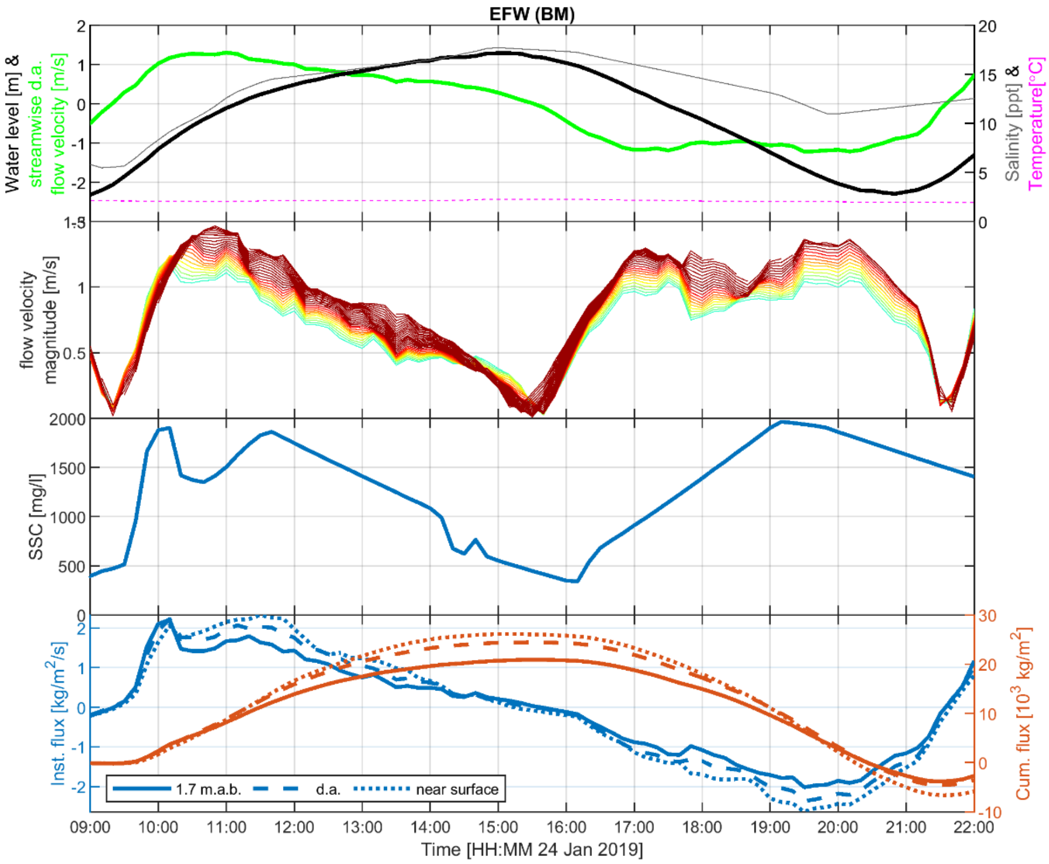
EFW (BM)
Water level [m] &
streamwise d.a.
flow velocity [m/s]
Salinity [ppt] &
Temperature[°C]
flow velocity
magnitude [m/s]
SSC [mg/l]
Inst. flux [kg/m²/s]
Cum. flux [10³ kg/m²]
1.7 m.a.b.
d.a.
near surface
Time [HH:MM 24 Jan 2019]

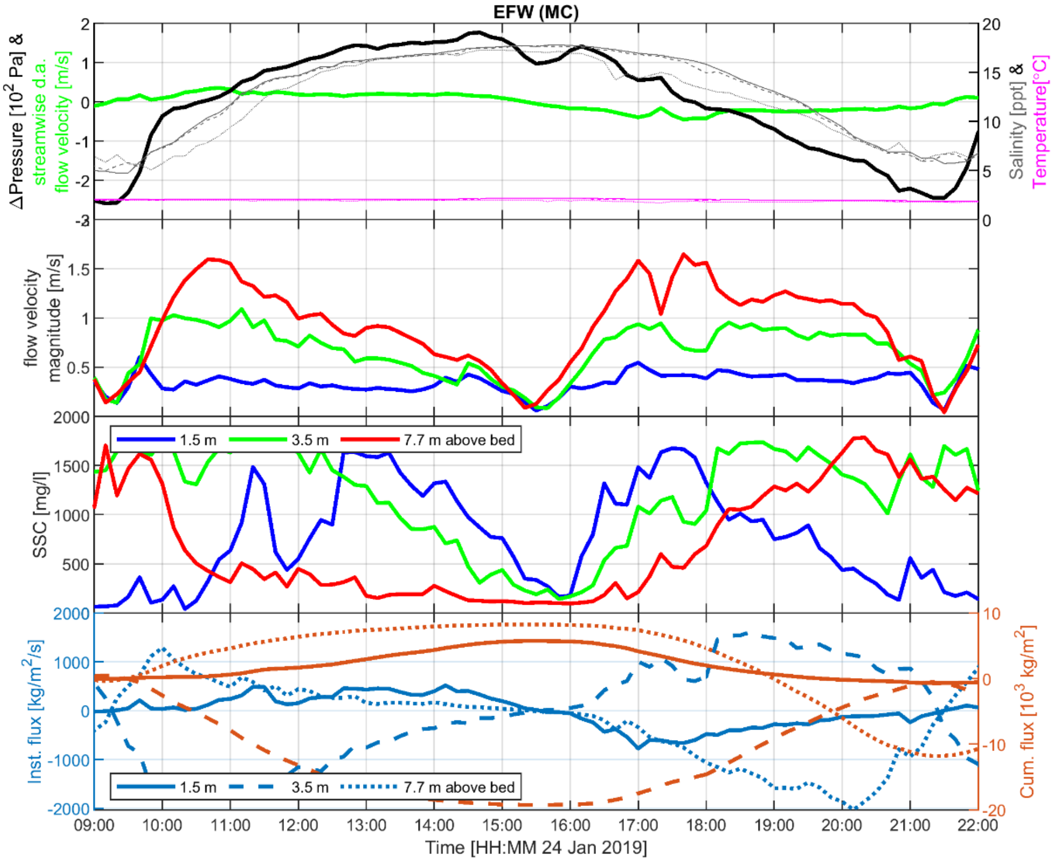
EFW (MC)
ΔPressure [10² Pa] & streamwise d.a. flow velocity [m/s]
Salinity [ppt] & Temperature[°C]
flow velocity magnitude [m/s]
SSC [mg/l]
1.5 m
3.5 m
7.7 m above bed
Inst. flux [kg/m²/s]
Cum. flux [10³ kg/m²]
Time [HH:MM 24 Jan 2019]

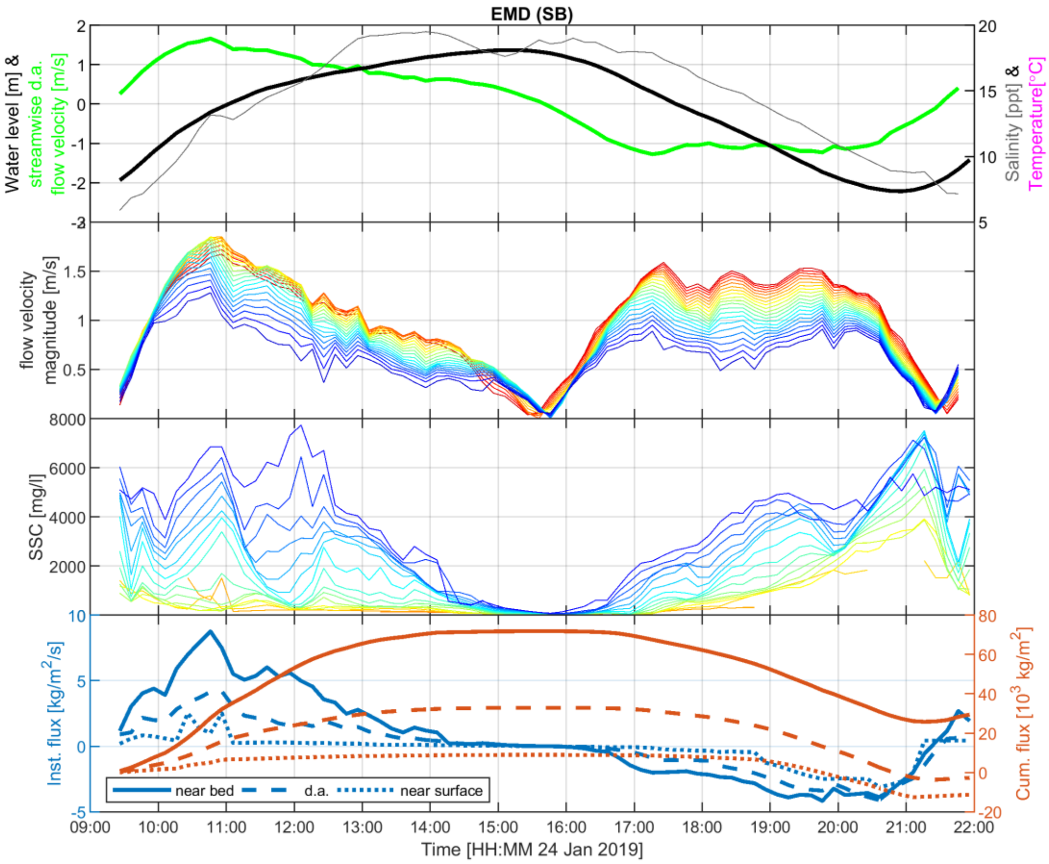
EMD (SB)
Water level [m] & streamwise d.a. flow velocity [m/s]
Salinity [ppt] & Temperature[°C]
flow velocity magnitude [m/s]
SSC [mg/l]
Inst. flux [kg/m²/s]
Cum. flux [10³ kg/m²]
near bed
d.a.
near surface
Time [HH:MM 24 Jan 2019]

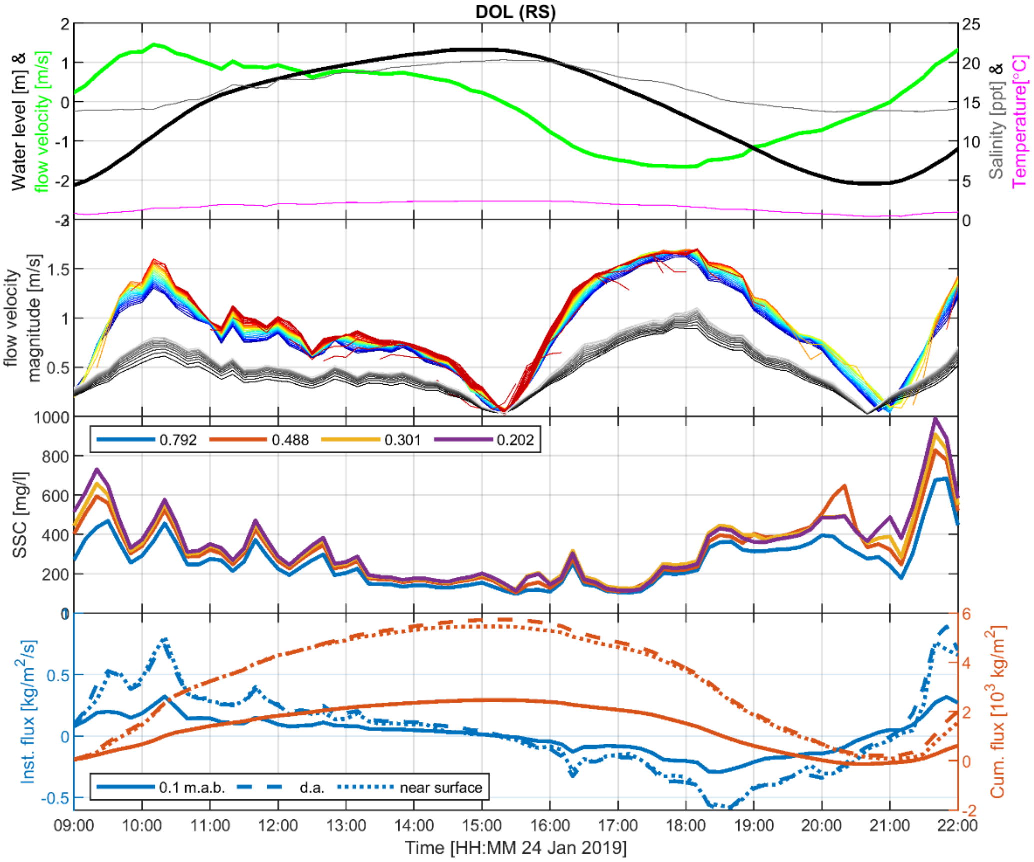
DOL (RS)
Water level [m] & flow velocity [m/s]
Salinity [ppt] & Temperature[°C]
flow velocity magnitude [m/s]
0.792
0.488
0.301
0.202
SSC [mg/l]
Inst. flux [kg/m^2/s]
Cum. flux [10^3 kg/m^2]
0.1 m.a.b.
d.a.
near surface
09:00
10:00
11:00
12:00
13:00
14:00
15:00
16:00
17:00
18:00
19:00
20:00
21:00
22:00
Time [HH:MM 24 Jan 2019]

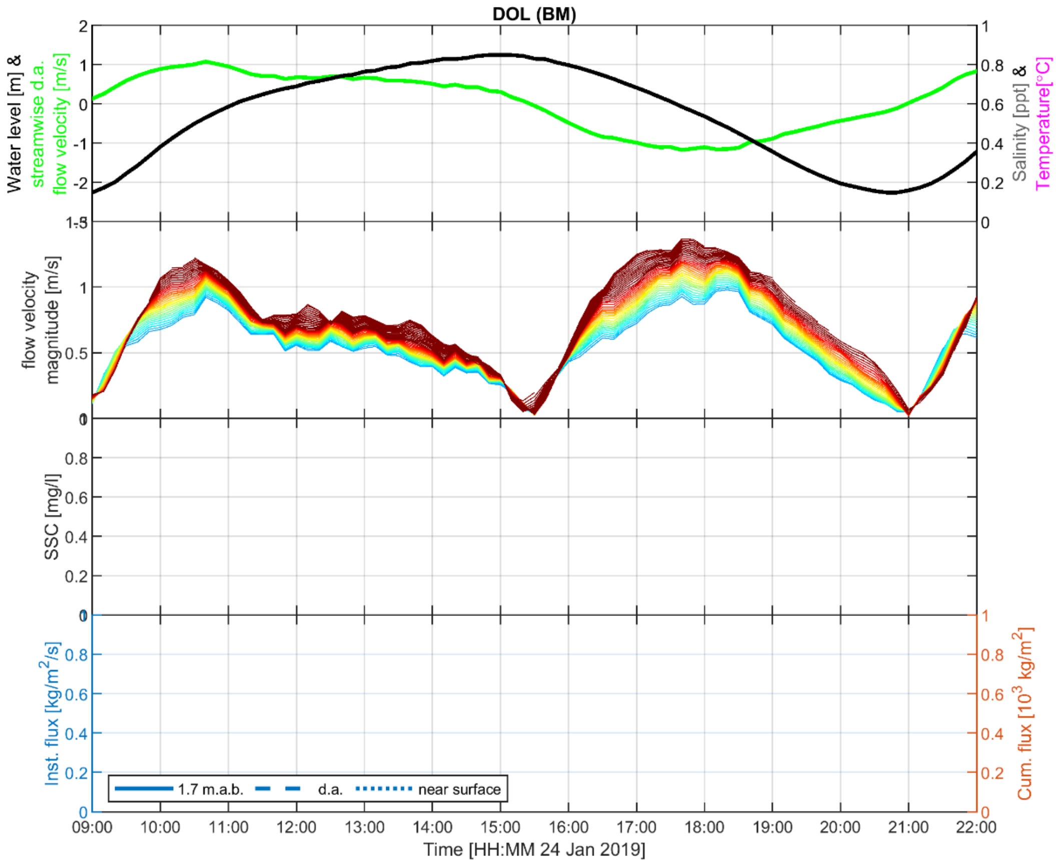
DOL (BM)
Water level [m] & streamwise d.a. flow velocity [m/s]
Salinity [ppt] & Temperature[°C]
flow velocity magnitude [m/s]
SSC [mg/l]
Inst. flux [kg/m^2/s]
Cum. flux [10^3 kg/m^2]
1.7 m.a.b.
d.a.
near surface
09:00
10:00
11:00
12:00
13:00
14:00
15:00
16:00
17:00
18:00
19:00
20:00
21:00
22:00
Time [HH:MM 24 Jan 2019]

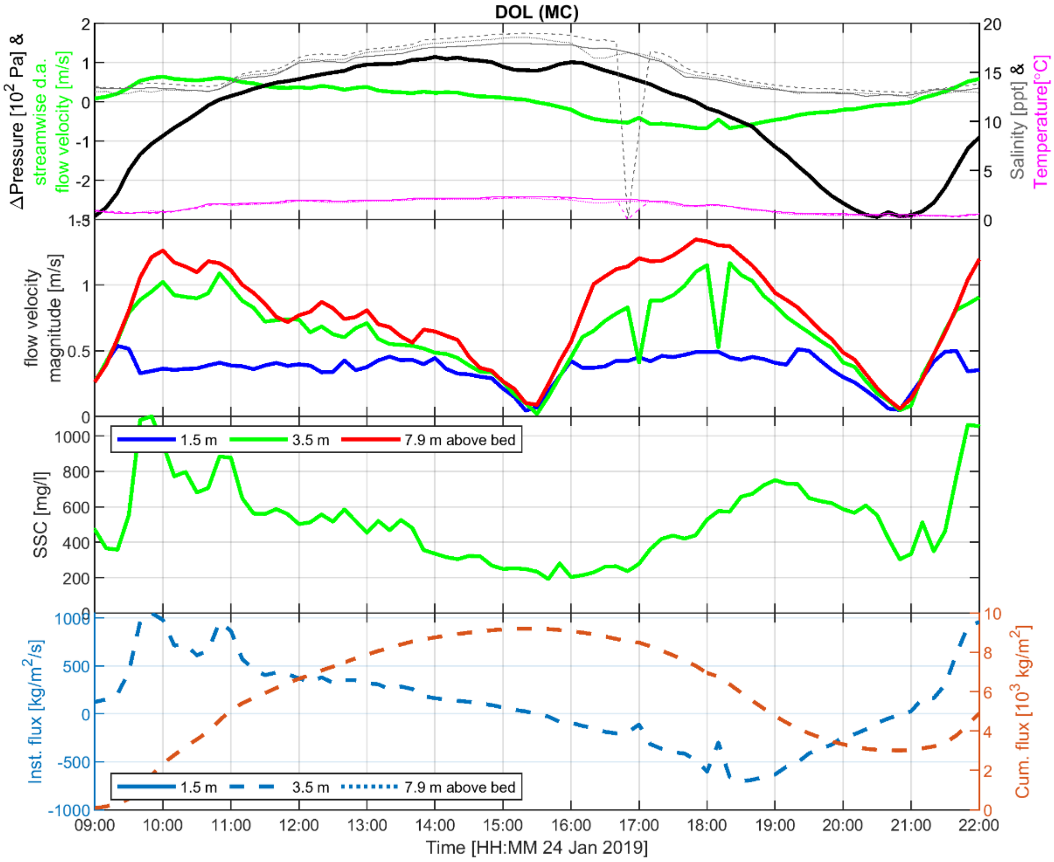

DOL (MC)
ΔPressure [10^2 Pa] &
streamwise d.a.
flow velocity [m/s]
Salinity [ppt] &
Temperature[°C]
flow velocity
magnitude [m/s]
1.5 m
3.5 m
7.9 m above bed
SSC [mg/l]
Inst. flux [kg/m²/s]
Cum. flux [10^3 kg/m²]
Time [HH:MM 24 Jan 2019]

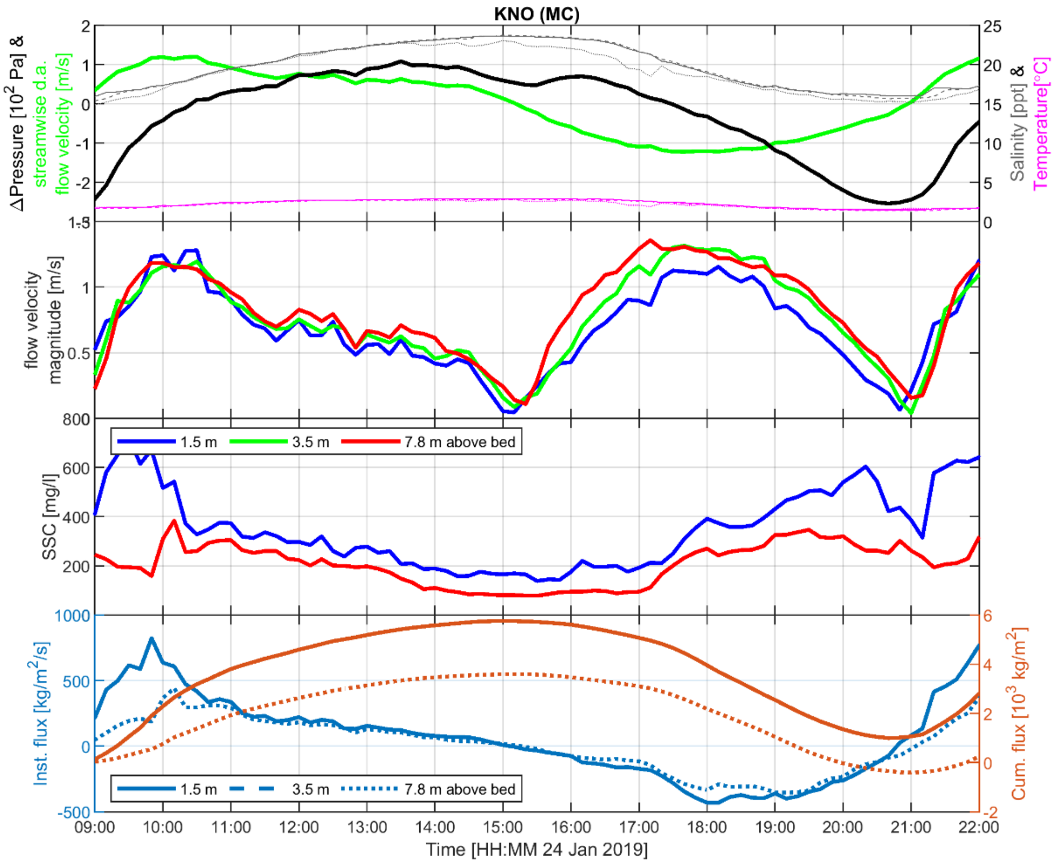

KNO (MC)
ΔPressure [10^2 Pa] &
streamwise d.a.
flow velocity [m/s]
Salinity [ppt] &
Temperature[°C]
flow velocity
magnitude [m/s]
1.5 m
3.5 m
7.8 m above bed
SSC [mg/l]
Inst. flux [kg/m²/s]
Cum. flux [10^3 kg/m²]
Time [HH:MM 24 Jan 2019]

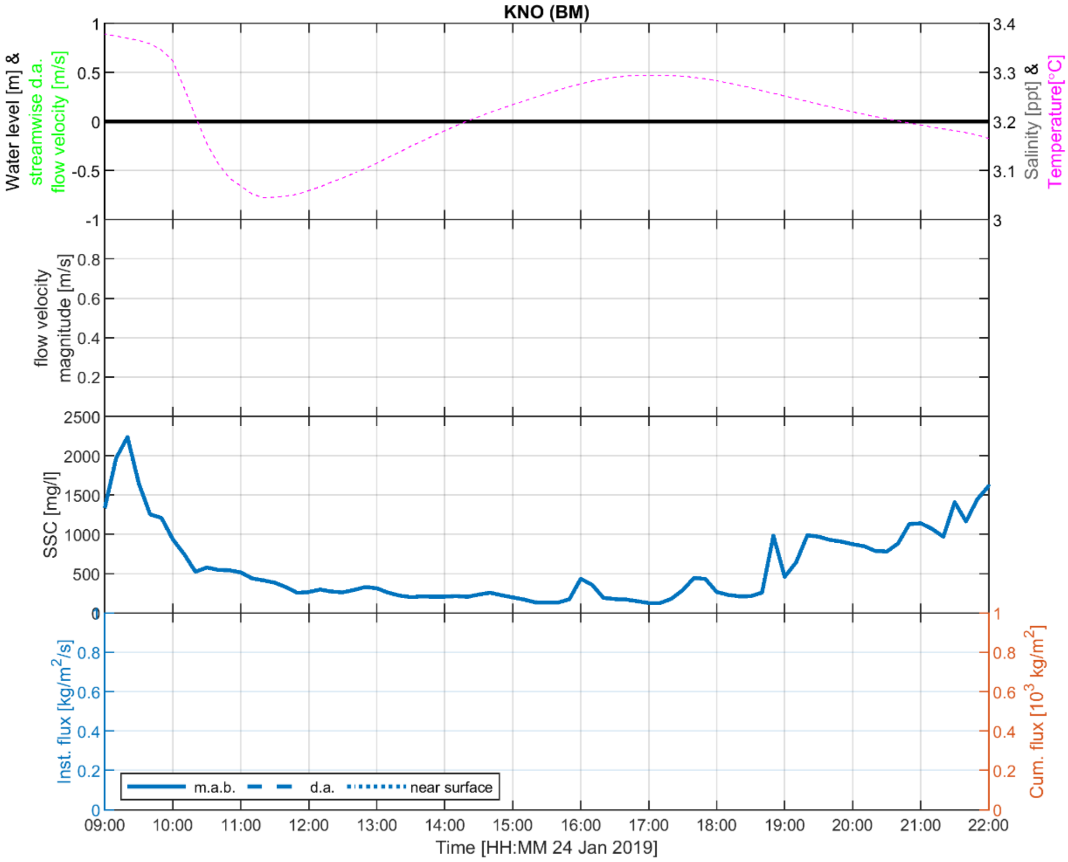
KNO (BM)
Water level [m] &
streamwise d.a.
flow velocity [m/s]
Salinity [ppt] &
Temperature[°C]
flow velocity
magnitude [m/s]
SSC [mg/l]
Inst. flux [kg/m2/s]
Cum. flux [10^3 kg/m2]
m.a.b.
d.a.
near surface
Time [HH:MM 24 Jan 2019]

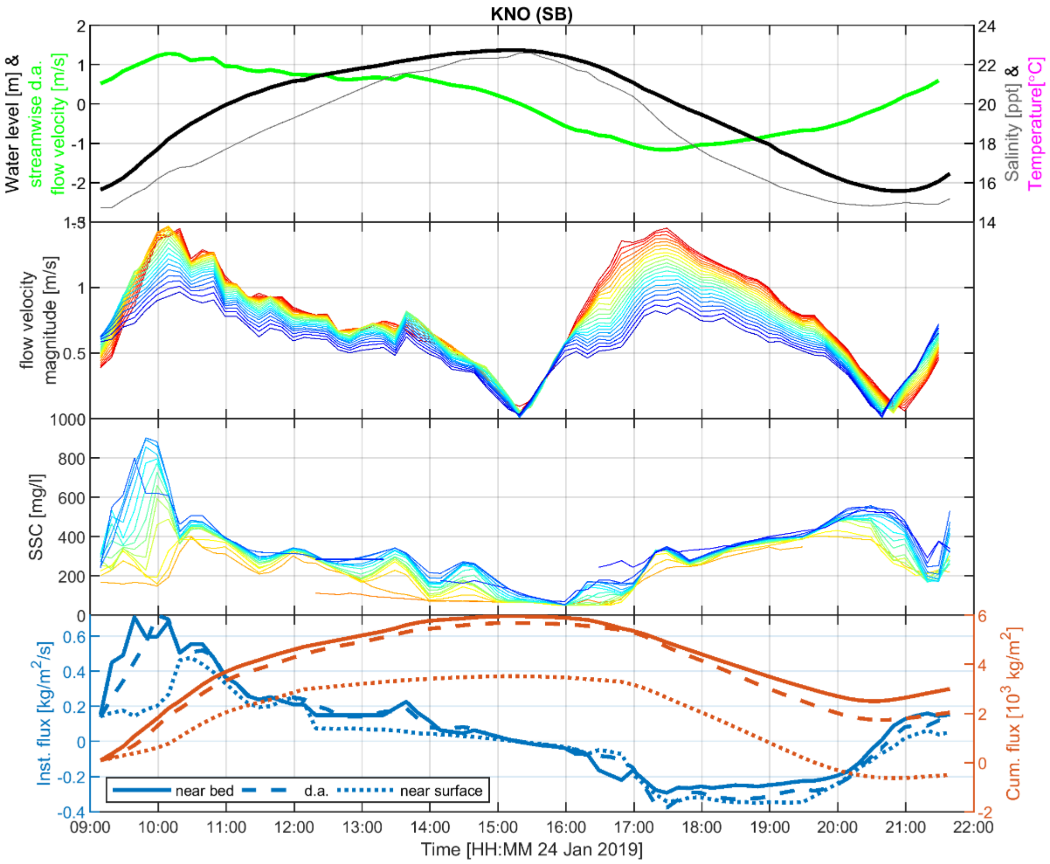
KNO (SB)
Water level [m] &
streamwise d.a.
flow velocity [m/s]
Salinity [ppt] &
Temperature[°C]
flow velocity
magnitude [m/s]
SSC [mg/l]
Inst. flux [kg/m2/s]
Cum. flux [10^3 kg/m2]
near bed
d.a.
near surface
Time [HH:MM 24 Jan 2019]

B.4 Characterization of tidal asymmetries over longer periods

Explain what observations from above are consistent for longer periods and differences and similarities 2018/2019.

In the previous section, timeseries of current velocities and SSC were described for the period of the 13-hour measurements. It is important to know whether the descriptions are also representative for longer periods. To condense the information of the timeseries, velocity-salinity-SSC plots have been created for 2018 and 2019. These plots average the SSC for specific current velocity and salinity values, like a more elaborated version of well-known butterfly plots (streamwise velocity vs. SSC). Adding salinity allows us to differentiate between different phases of the tidal cycle, like HW and LW slack and a closer analysis of the current velocities over the tidal cycle. Averaging better indicates at which current velocities highest SSC values occur.

Observations Dollard in 2018

At RS_DOL SSC is highest during the flood phase and remains around the same level for the entire flood phase. At the beginning of flood, current velocities quickly increase and slowly decrease afterwards. Ebb velocities are larger than flood velocities, which is not or hardly the case at BM and MC locations. At the end of ebb also higher SSC is observed at RS_DOL, but not as high as during flood. Both at BM_DOL and MC_DOL SSC peaks at the beginning of flood, when sometimes current velocities also peak. At both stations we also observe quite high SSC at the end of ebb, with comparable values as during flood, which is higher than at RS_DOL.

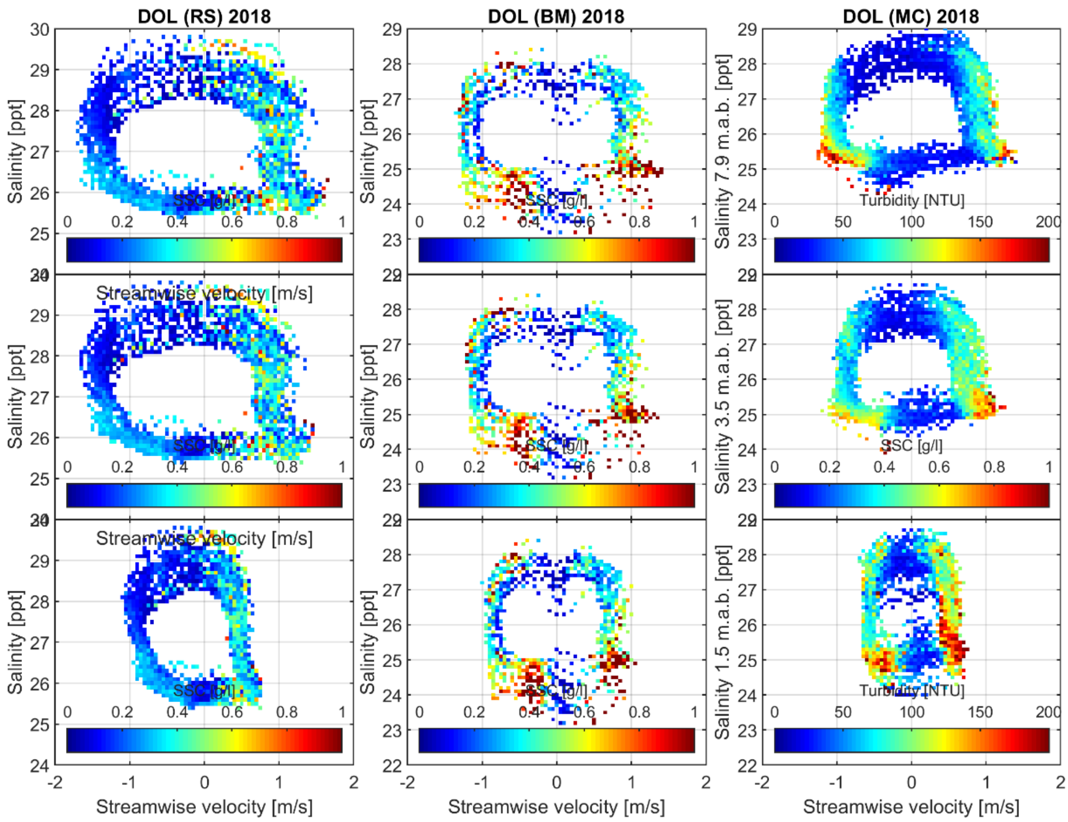

Figure 7-9 Current velocity-salinity-SSC plot for three frames/chains in the Dollard in 2018. For RS and BM near bed SSC and salinity observations have been used for current velocities at three positions in the vertical from ADCPs. The MC measurements use the parameters all measured at the height indicated in the y-axis.

Also, comparable SSC values at the end of ebb occur at a lower current velocity as during flood. High SSC values at the end of the ebb phase, when the current velocities are already high for a while and also at lower velocities than the SSC peak at the beginning of flood indicate that for transport at the end of the ebb phase advection is more important than resuspension. Sediment that has been transported out of the Dollard at the end of the ebb phase, will be transport in landward direction (into the Dollard or the fairway to Emden) during the subsequent flood phase.

At BM_DOL a remarkable drop in salinity occurs at HW slack, that is not present at the other two Dollard locations. Also at this location, the sediment flux during ebb peaks earlier than at RS_DOL and MC_DOL as a result of a peak in SSC (Figure 7-11). As this location lies in between RS_DOL and MC_DOL, this sediment may have another origin.

Observations Dollard in 2019
In 2019, we see a much larger spread in the salinity values. Other characteristics are similar to 2018. However, most remarkable is that for all three locations, the SSC during LW slack is much higher than during HW slack. This inequality favours sediment import. Possibly the lower SSC during HW slack is the result of the lower current velocities at the second half of the flood phase (Figure 7-12).

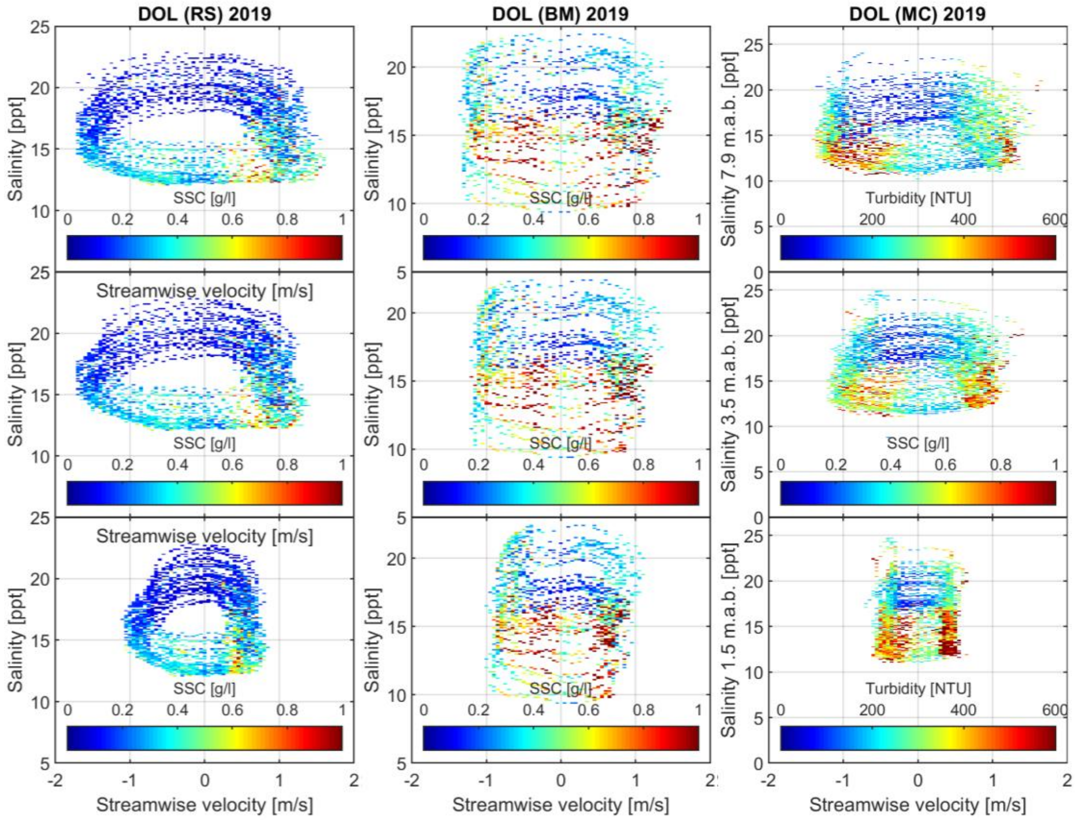

Figure 7-10 Current velocity-salinity-SSC plot for three frames/chains in the Dollard in 2019. For RS and BM near bed SSC and salinity observations have been used for current velocities at three positions in the vertical from ADCPs. The MC measurements use the parameters all measured at the height indicated in the y-axis.

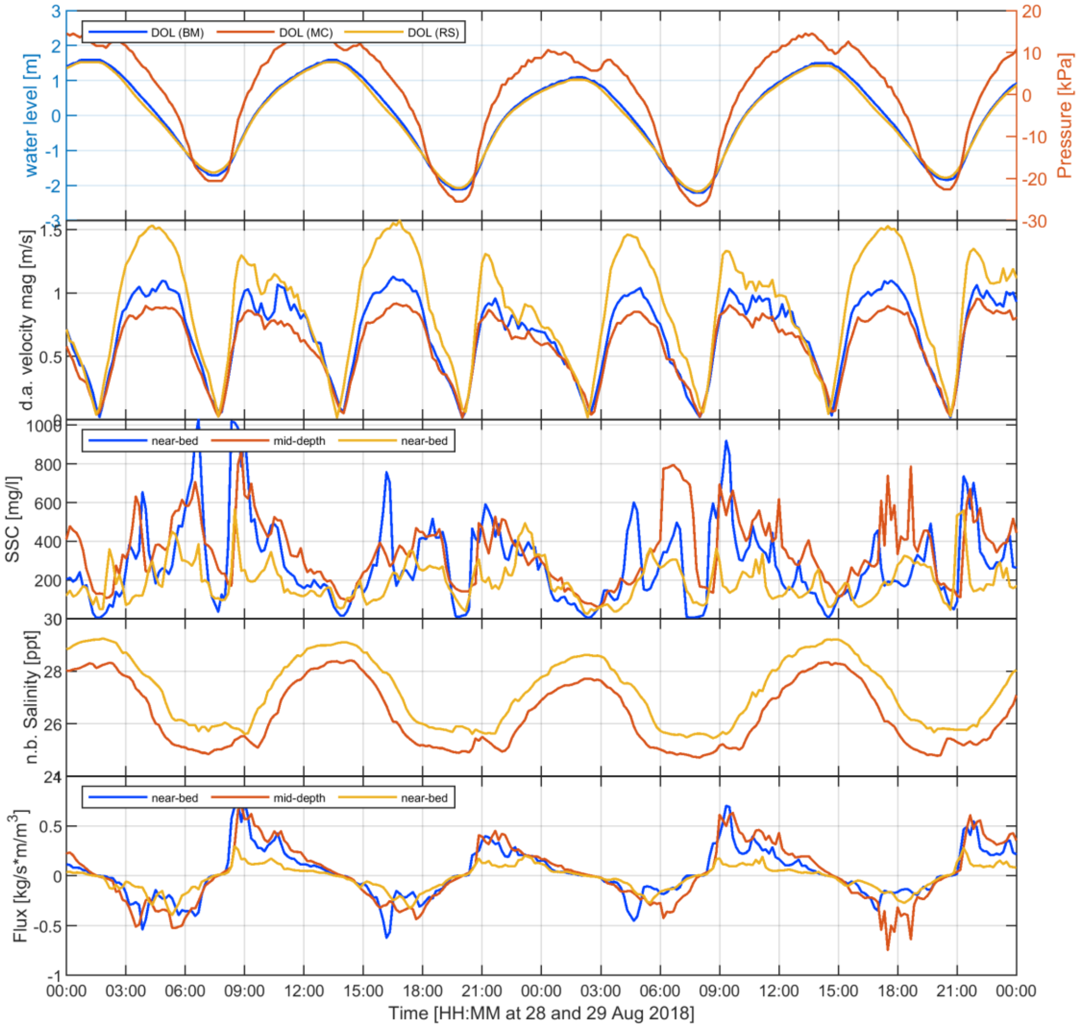

Figure 7-11 Timeseries of the three observation locations in the Dollard in 2018. From top to bottom: water level (proxy), depth averaged flow velocity for part of the water column (RS: above 3.3 m above the bed, BM: above 2.2 m above the bed, MC at 1.5, 3.5 m above the bed and 1.5 m below the surface), SSC, salinity (no data available at these dates for BM) and sediment fluxes.

Observations the fairway to Emden in 2018

For the EFW, the velocity-salinity-SSC plots show that the larger peak ebb velocities at BM_GEI are present, implying that this is typical for current velocities at this location. Also, SSC is high throughout almost the entire ebb and flood phase. Further upstream at RS_EFW, SSC mostly peaks at the end of flood and beginning of ebb. The beforementioned mid-flood peak is not very distinct in the plots. Other characteristics (high ebb velocities) are also visible from the plots. Reported high ebb SSC at BM_EFW is consistent for the longer period. HW slack coincides with lower SSC than LW slack, favouring landward sediment transport. Similar behaviour occurs at MC_EFW, but at much lower SSC. Figure 7-15 shows additionally that there is a large salinity gradient over the fairway to Emden of ~5 ppt and a variation of ~8 ppt over the tidal cycle. In 2019, variations become even larger, over 15 ppt over the tidal cycle and ~7 ppt between the frames.

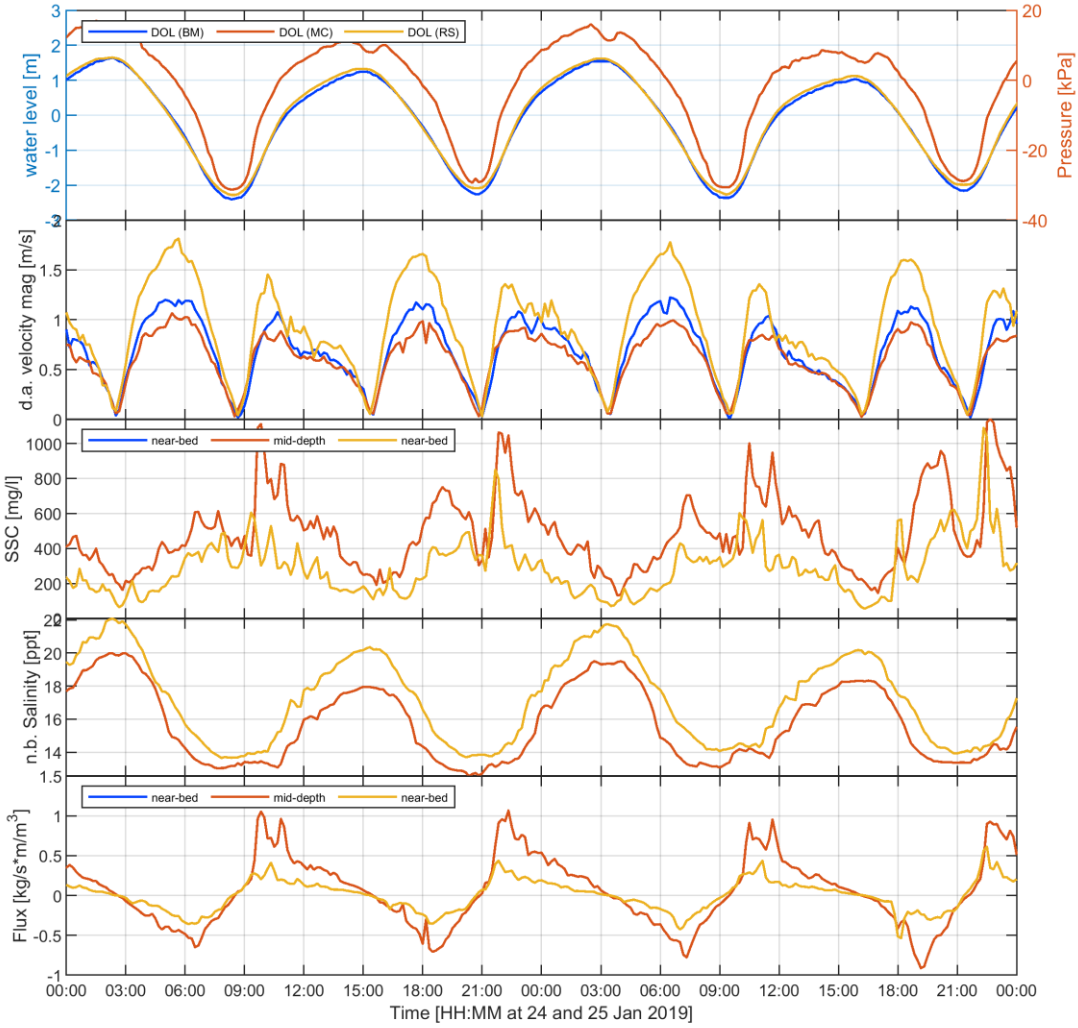

Figure 7-12 Timeseries of the three observation locations in the Dollard in 2019. From top to bottom: water level (proxy), depth averaged flow velocity for part of the water column (RS: above 3.3 m above the bed, BM: above 2.2 m above the bed, MC at 1.5, 3.5 m above the bed and 1.5 m below the surface), SSC (no data available at these dates for BM), salinity (no data available at these dates for BM) and sediment fluxes (no data available at these dates for BM).

Observations fairway to Emden in 2019

In 2019, SSC are different from 2018. At BM_GEI, SSC is lower in 2019 especially at the end of flood and the beginning of ebb, as is confirmed by Figure 7-15 and Figure 7-16. At RS_EFW, SSC is in 2019 also high at the end of ebb, during LW slack and at the beginning of flood. At BM_EFW, higher SSC in 2019 compared to 2018 during flood is visible. This may be the cause of the reduced residual seaward sediment transport in 2019. Also at MC_EFW, we see in 2019 a higher flood SSC than in 2018 in the lower half of the water column. Ebb and flood SSC have similar magnitude in 2019, in combination with larger flood velocities this results in a nett import. Near the surface only at the end of the ebb phase high SSC occur, resulting in export.

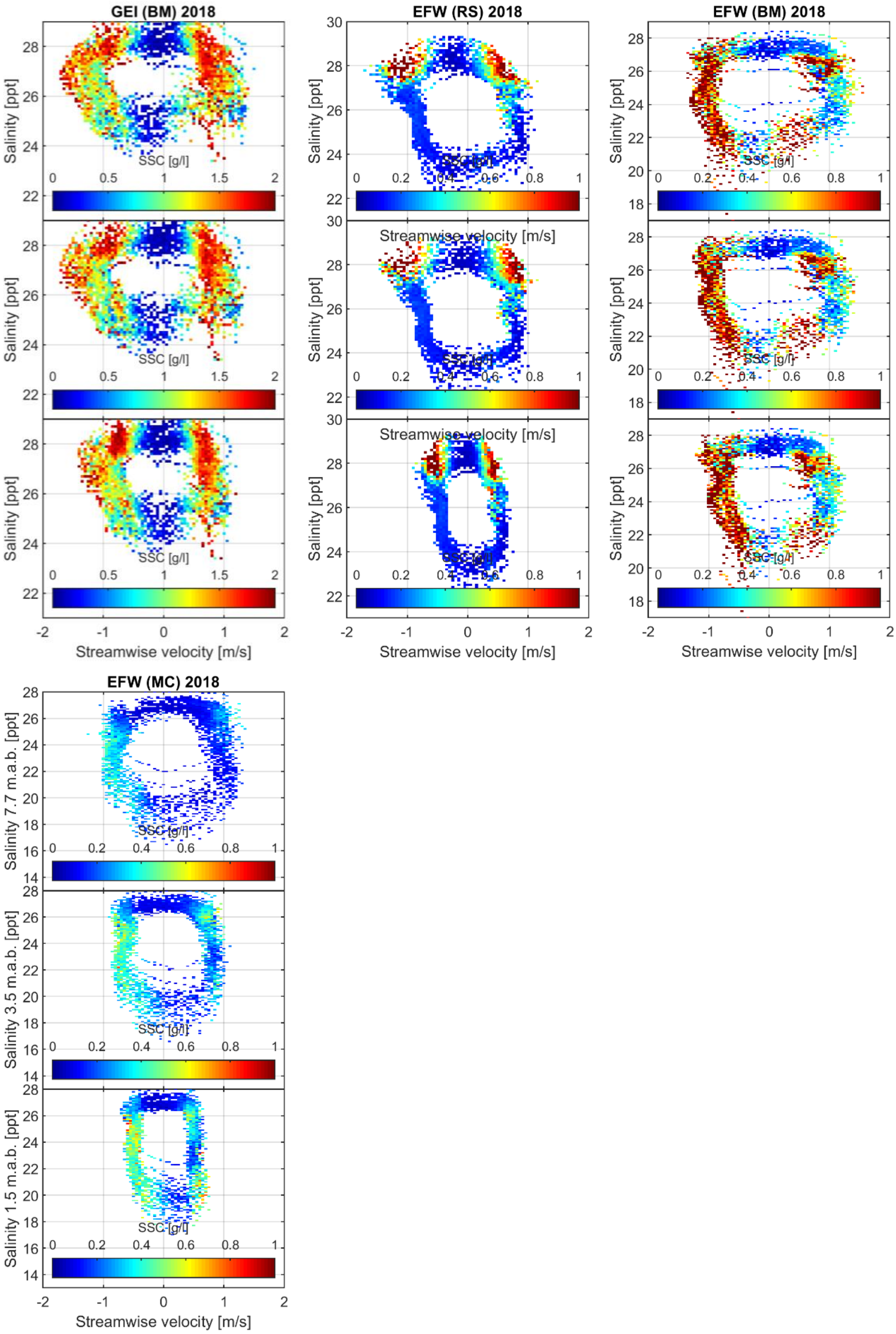

Figure 7-13 Current velocity-salinity-SSC plot for three frames/chains in the Fairway to Emden in 2018. For RS and BM near bed SSC and salinity observations have been used for current velocities at three positions in the vertical from ADCPs. The MC measurements use the parameters all measured at the height indicated in the y-axis.

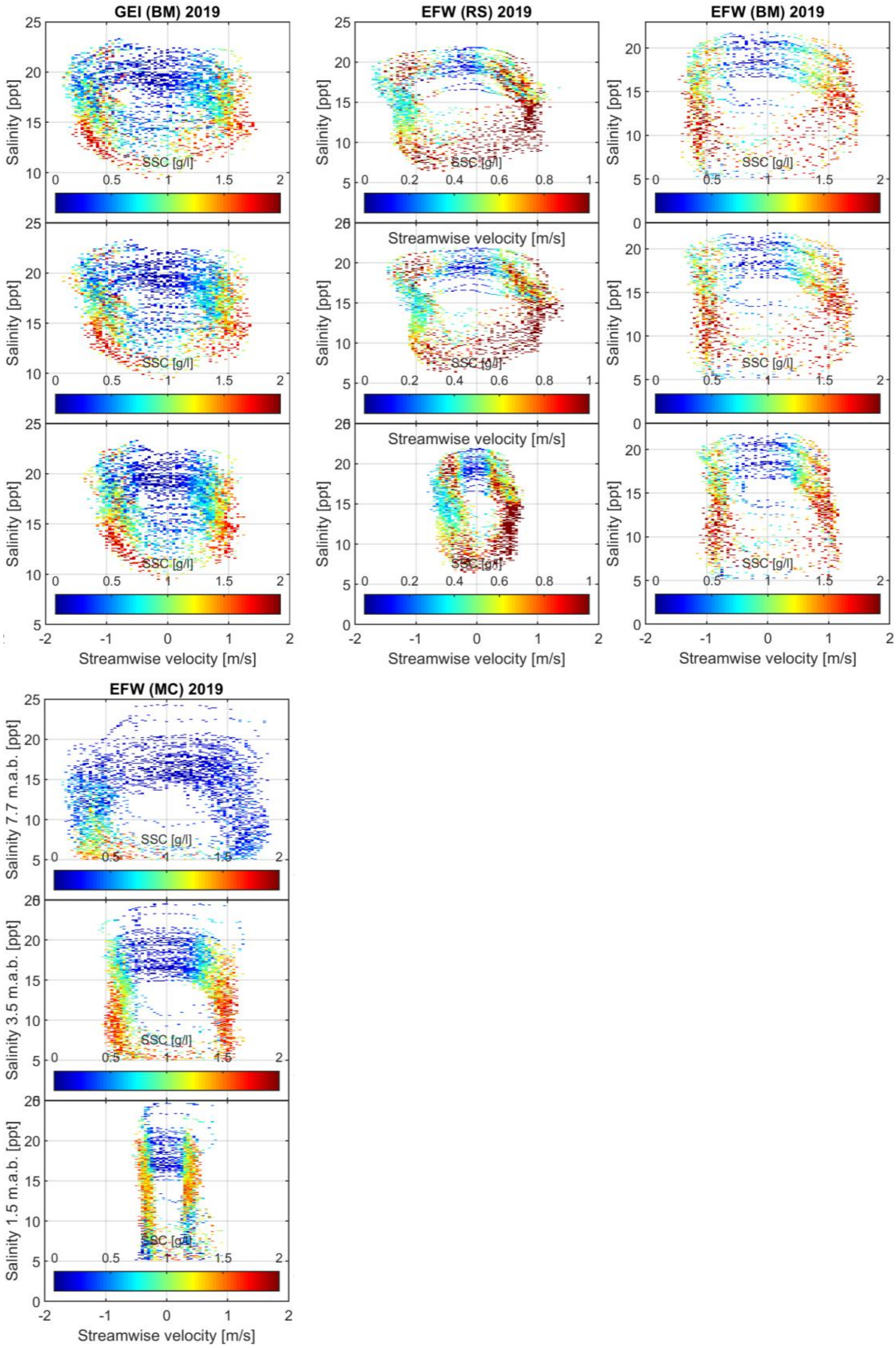

Figure 7-14 Current velocity-salinity-SSC plot for three frames/chains in the Fairway to Emden in 2019. For RS and BM near bed SSC and salinity observations have been used for current velocities at three positions in the vertical from ADCPs. The MC measurements use the parameters all measured at the height indicated in the y-axis.

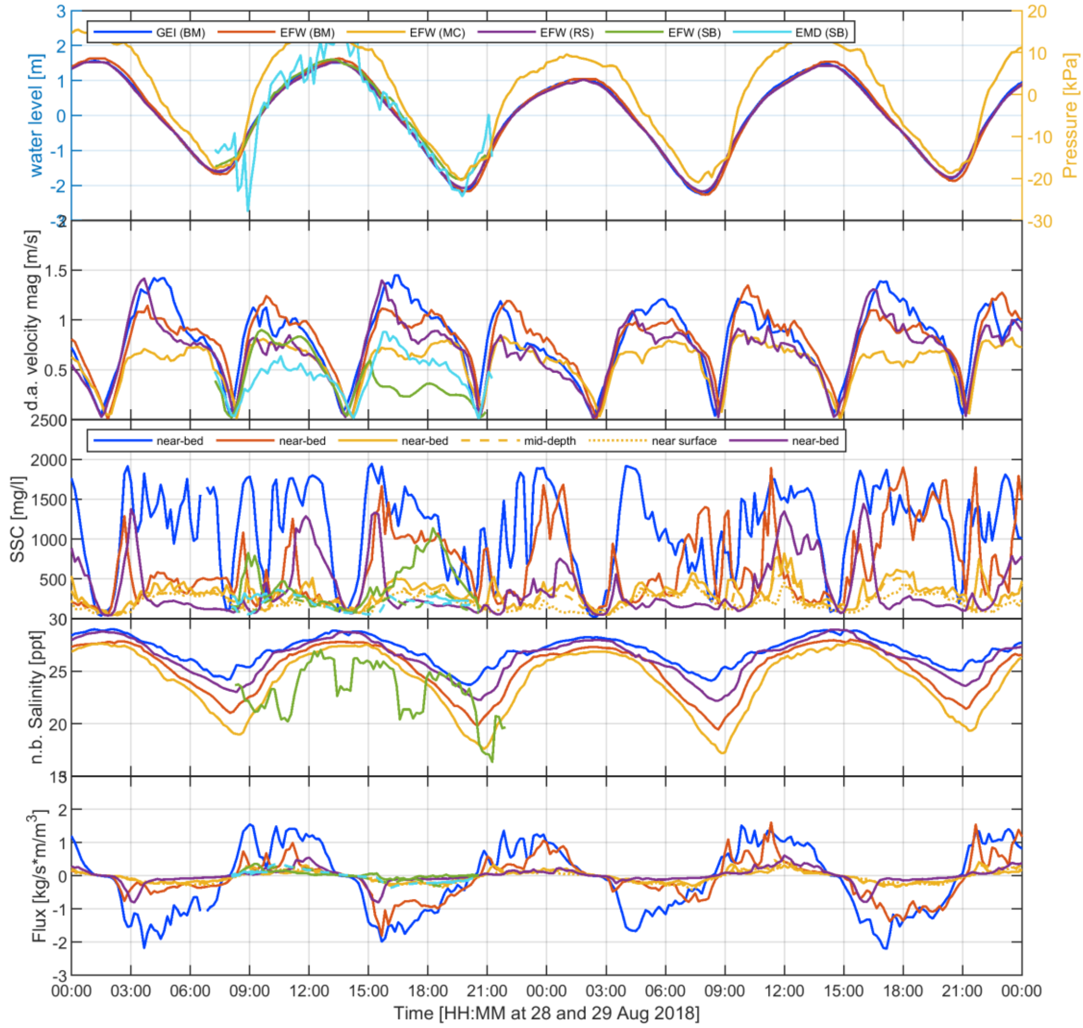

Figure 7-15 Timeseries of the three observation locations in the Fairway to Emden in 2018. From top to bottom: water level (proxy), depth averaged flow velocity for part of the water column (RS: above 3.3 m above the bed, BM: above 2.2 m above the bed, MC at 1.5, 3.5 m above the bed and 1.5 m below the surface), SSC, salinity and sediment fluxes.

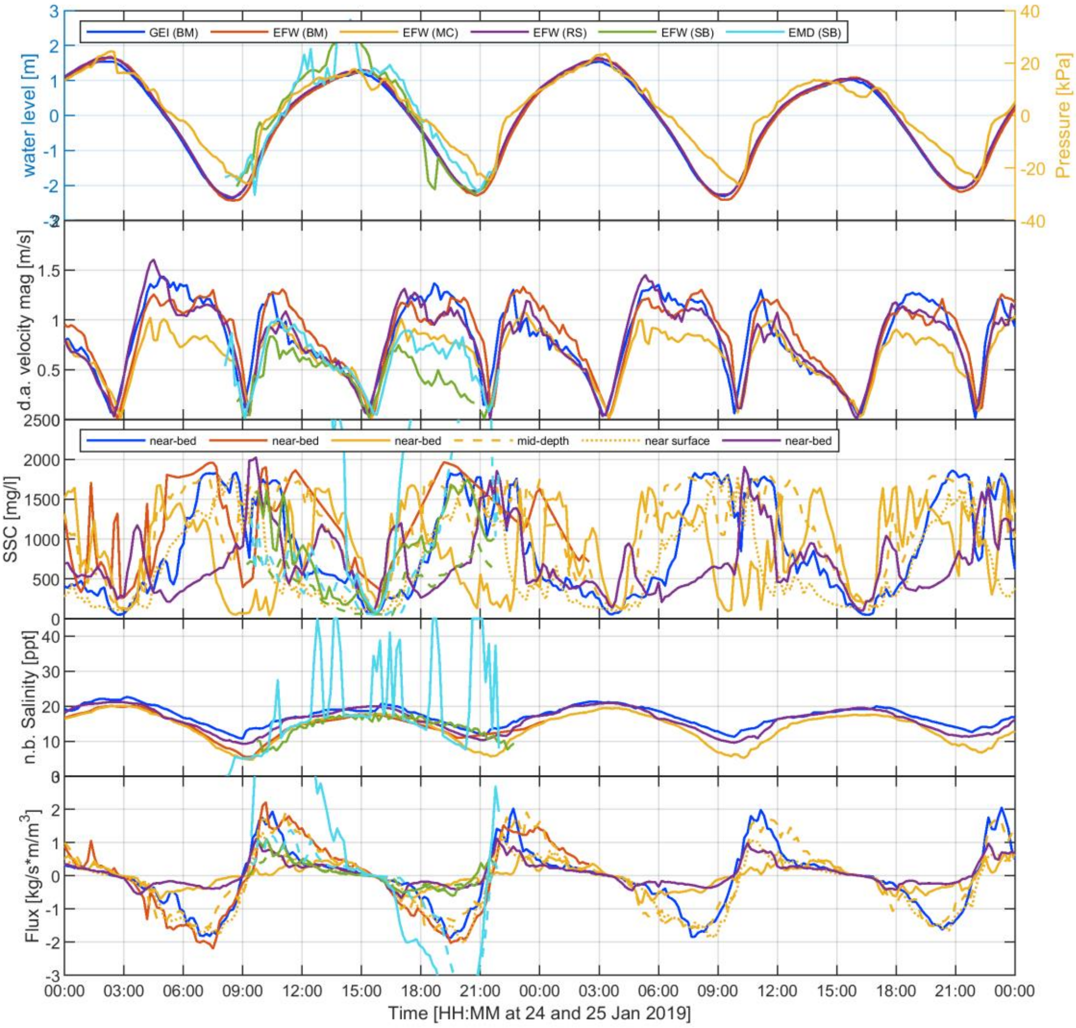

Figure 7-16 Timeseries of the three observation locations in the Fairway to Emden in 2019. From top to bottom: water level (proxy), depth averaged flow velocity for part of the water column (RS: above 3.3 m above the bed, BM: above 2.2 m above the bed, MC at 1.5, 3.5 m above the bed and 1.5 m below the surface), SSC, salinity and sediment fluxes.

Figure 7-15 and Figure 7-16 also include the measurements by stationary boats. The depth-averaged current velocity magnitude shows a large variation over the Fairway to Emden, especially during the ebb phase. Generally, current velocities are larger at the westside (i.e. GEI^{BM}) of the Fairway to Emden than at the east side (i.e. EMD^{SB}). In 2018, also gross sediment fluxes are larger at the west side than the east side. In 2019 however, high SSC at EMD^{SB} cause very large gross fluxes near the bed.

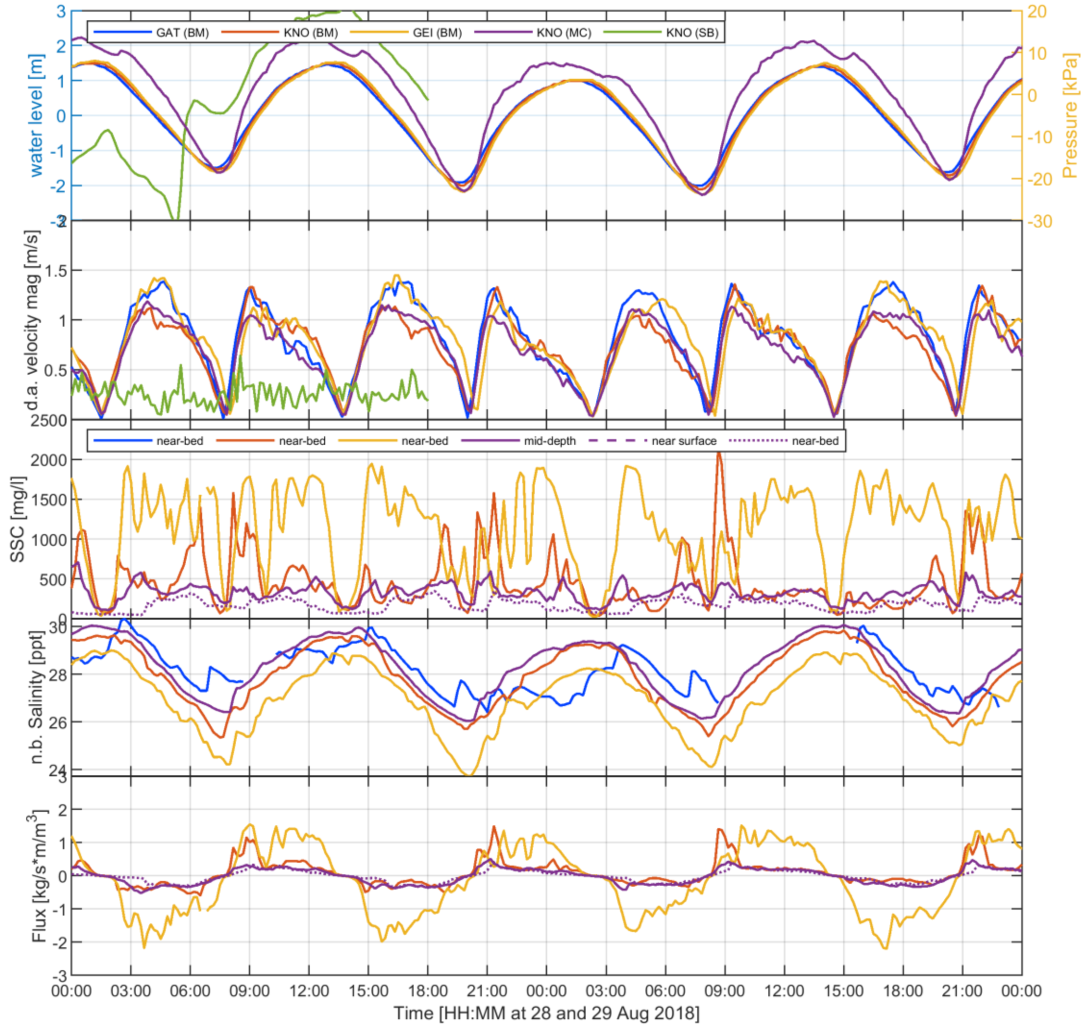

Figure 7-17 Timeseries of the three observation locations in the Gatjebogen in 2018. From top to bottom: water level (proxy), depth averaged flow velocity for part of the water column (BM: above 2.2 m above the bed, MC at 1.5, 3.5 m above the bed and 1.5 m below the surface), SSC, salinity and sediment fluxes.

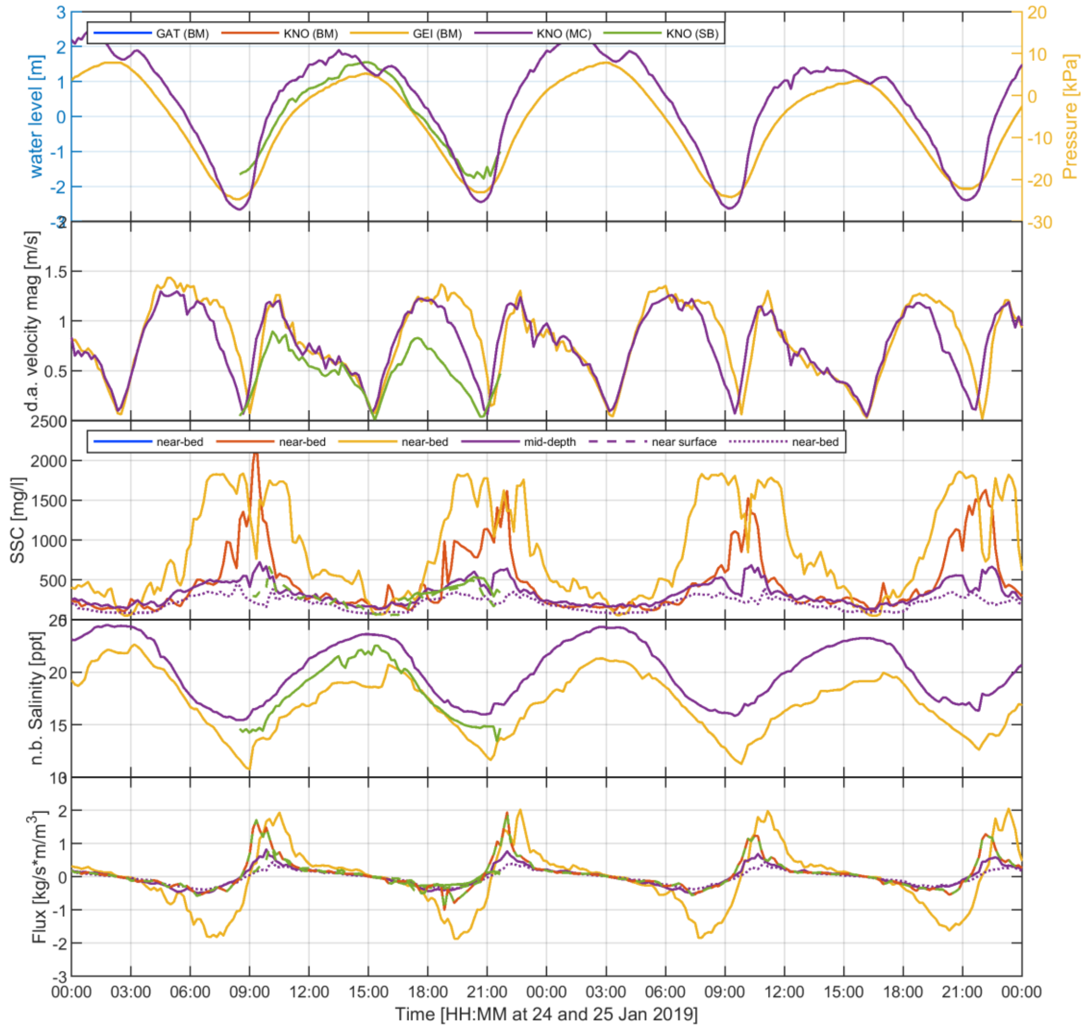

Figure 7-18 Timeseries of the three observation locations in the Gatjebogen in 2019. From top to bottom: water level (proxy), depth averaged flow velocity for part of the water column (BM: above 2.2 m above the bed, MC at 1.5, 3.5 m above the bed and 1.5 m below the surface), SSC, salinity and sediment fluxes. The sediment flux at KNO^{BM} has been computed by combining near bed streamwise velocity of KNO^{MC} and SSC at KNO^{BM} as velocities at KNO^{BM} are missing.

B.5 Bathymetry and morphological changes

The bathymetry of the intertidal area shows that the intertidal flats at the east side of the fairway to Emden (east of Emden) are higher and have pronounced small channels that drain the flats into the fairway to Emden (Figure 7-2). Water and sediment transport from the Dollard into the fairway to Emden seem likely here. At the west side of the intertidal area, the elevation of the flats is lower, and the flat area is more confined. The hydrodynamic energy is apparently too high to allow for further sedimentation. This is also supported by erosion/sedimentation maps (Figure 7-19).

The deeper parts of the study area also show some remarkable features. At station BM_GEI the channel is slightly shallower and also the entrance into the Dollard Bay is shallower and is bordered by a sill. Just east of the Port of Emden, there is a sudden step in bed level of approximately 3 m. Eastwards, the bed is lower again.

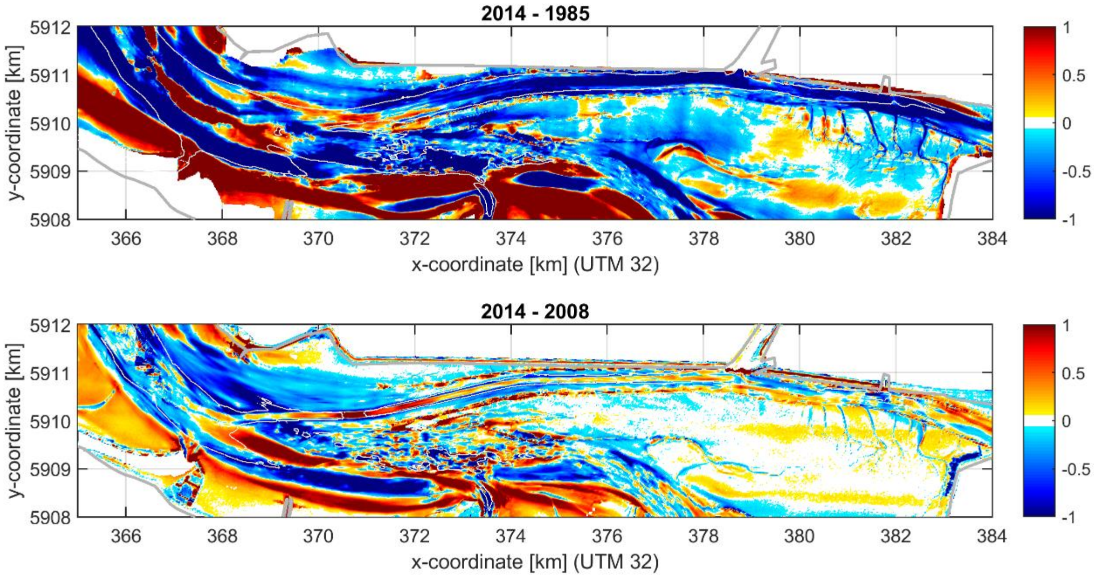

Figure 7-19 Erosion (blue) and sedimentation (red/yellow) over 30 years (top panel) and recently (lower panel). There is no clear and consistent accretional trend at the flats around the Geiseleitdamm west of Emden.

C Dredging

Dredging data was available for the years in which the EDoM campaigns were executed. The data revealed that the largest dredging volumes are removed in the channel sections just west of the Geisesteert (Figure 7-20), which becomes even more clear when we divide by the length of the section (Figure 7-21). When we compute summer and winter volumes, it is remarkable that in the Fairway to Emden largest volumes are dredged in summer, while just west of the Geisesteert summer and winter volumes are comparable (Figure 7-22). We also noticed that during the August 2018 campaign, significant amounts of sediments were dredged (not shown here), which might influence SSC observations.

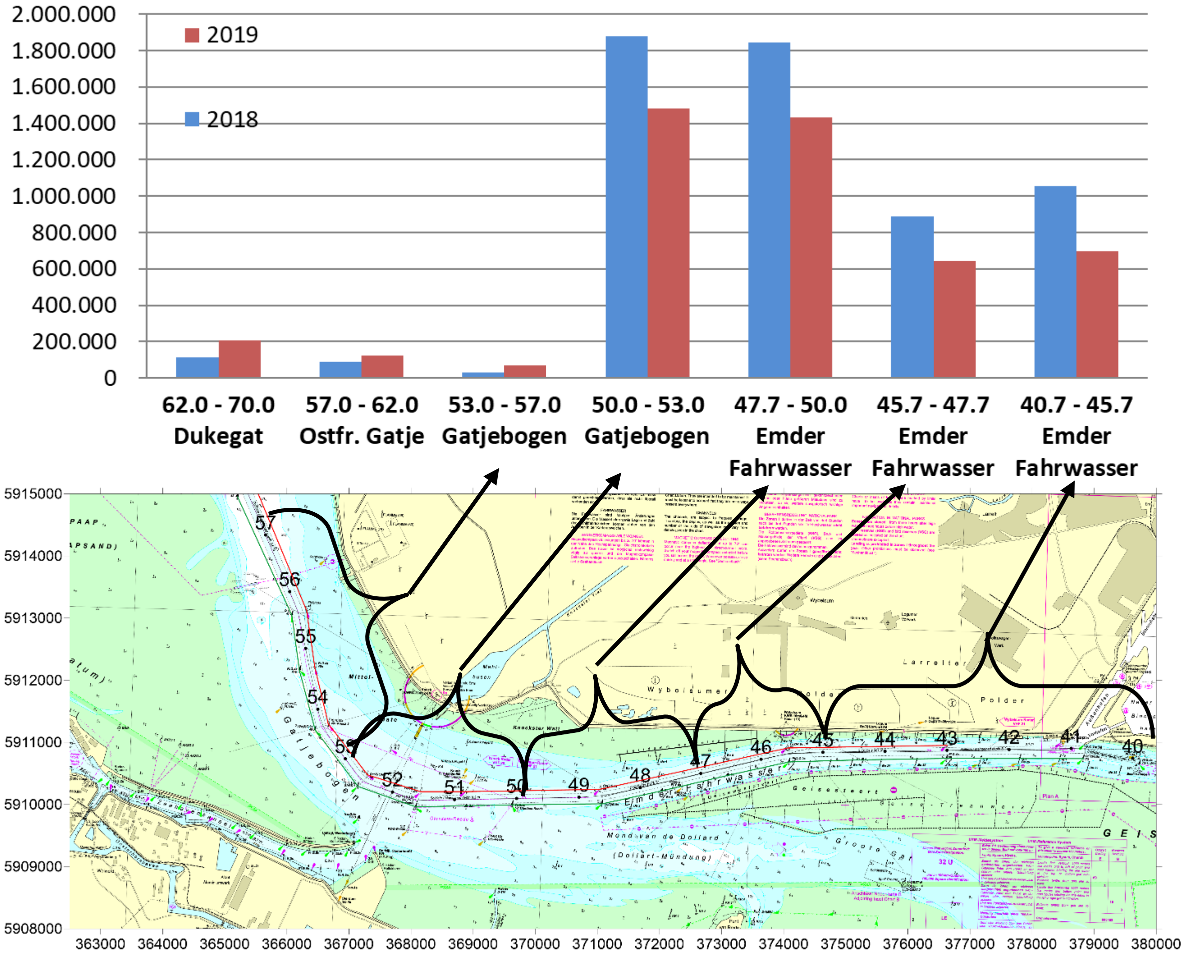

Figure 7-20 Dredging volumes [m³] per section of navigational channel per year. Blue = 2018, red = 2019.

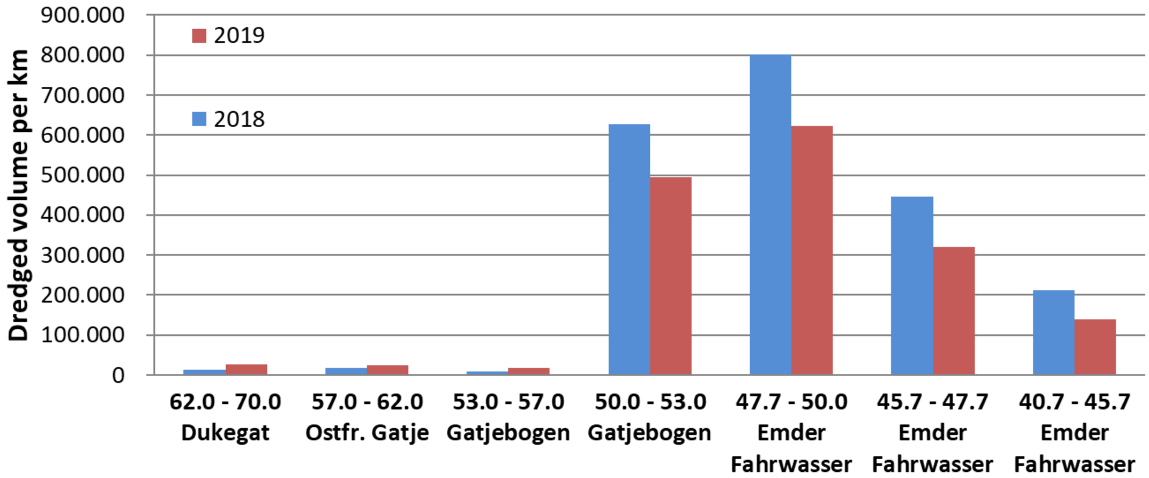

Figure 7-21 Dredging volumes divided per length of the section [m³/km], per section of navigational channel per year. Blue = 2018, red = 2019.

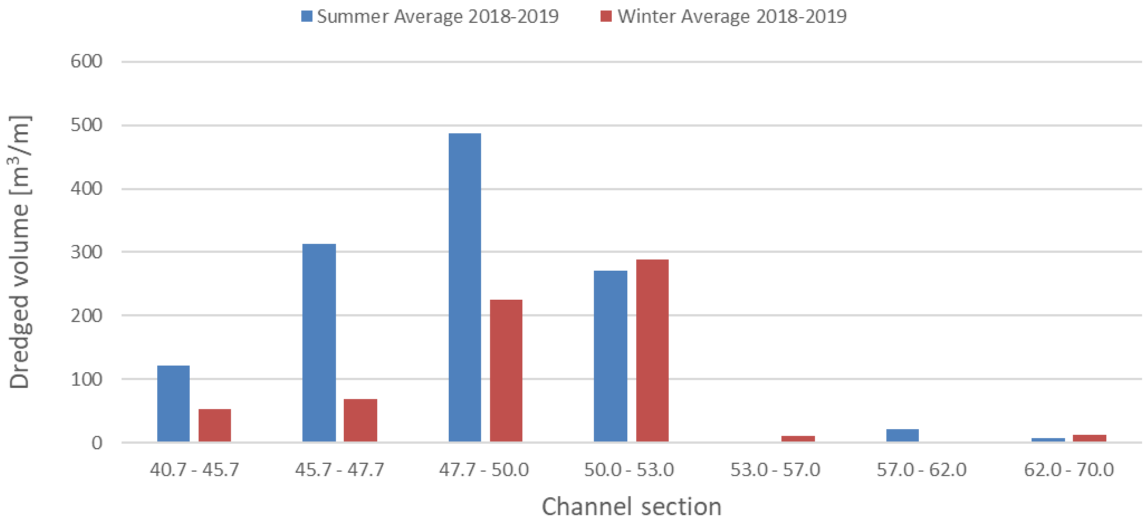

Figure 7-22 Dredging volumes divided per length of the section [m³/m], per section of navigational channel per season, based on the average between 2018 and 2019. Blue = summer, red = winter.

D Detailed figures (timeseries, etc)

D.1 August 2018

D.1.1 Postprocessing and visualisations

The high-frequency velocity data from the various frames and mooring chains have all been averaged to 10-minute data.

Subsequently, the 10-min velocity data have been decomposed into a streamwise and streamcross component: in the direction of the main flow direction (determined by fitting a least-square error linear line through the depth-averaged data) and the direction perpendicular to the main direction, respectively.

Finally, the data have been adjusted by making the vertical coordinate dimensionless, for easy computation of residual velocities and sediment fluxes. To this end, the lowest cell got z-coordinate 0 and the highest cell z-coordinate 1. And interpolation has been made to have 100 cells over the vertical for each location.

Residual velocities have been computed over a period of a tidal cycle, to compare with 13-hour measurements, and over a spring-neap tidal cycle to show variations over a longer period. A Godin filter (averaging 2 times over 24 hours and once over 25 hours) has been applied to filter low frequency signals, although weather events are still visible and even attenuated in the data (Walters & Heston, 1981).

In this appendix all observations and the results of the post-processing are shown.

D.1.1.1. Streamwise velocities

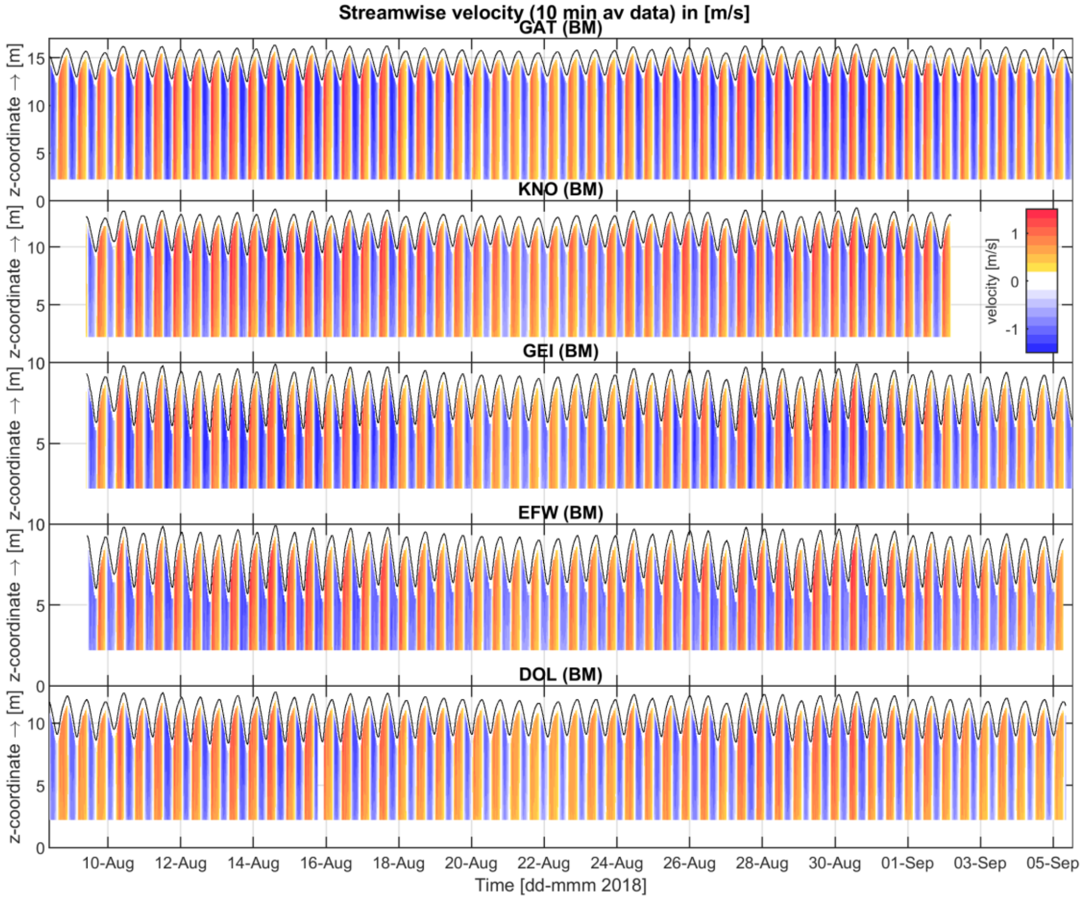
Streamwise velocity (10 min av data) in [m/s]
GAT (BM)
KNO (BM)
GEI (BM)
EFW (BM)
DOL (BM)
z-coordinate → [m]
velocity [m/s]
10-Aug
12-Aug
14-Aug
16-Aug
18-Aug
20-Aug
22-Aug
24-Aug
26-Aug
28-Aug
30-Aug
01-Sep
03-Sep
05-Sep
Time [dd-mmm 2018]

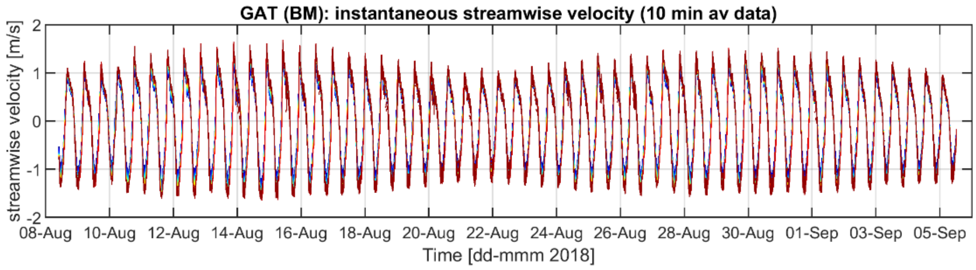
GAT (BM): instantaneous streamwise velocity (10 min av data)
streamwise velocity [m/s]
08-Aug
10-Aug
12-Aug
14-Aug
16-Aug
18-Aug
20-Aug
22-Aug
24-Aug
26-Aug
28-Aug
30-Aug
01-Sep
03-Sep
05-Sep
Time [dd-mmm 2018]

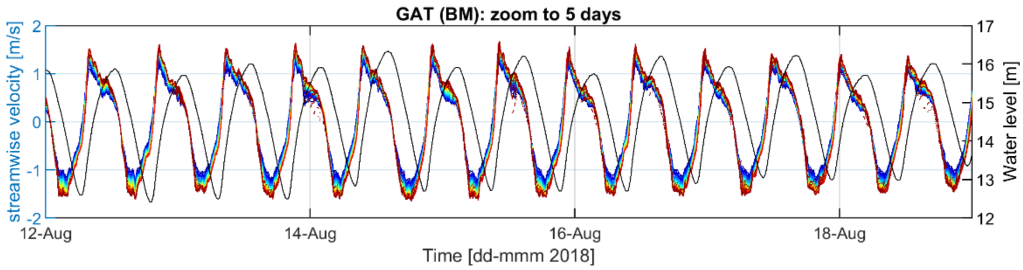
GAT (BM): zoom to 5 days
streamwise velocity [m/s]
Water level [m]
12-Aug
14-Aug
16-Aug
18-Aug
Time [dd-mmm 2018]

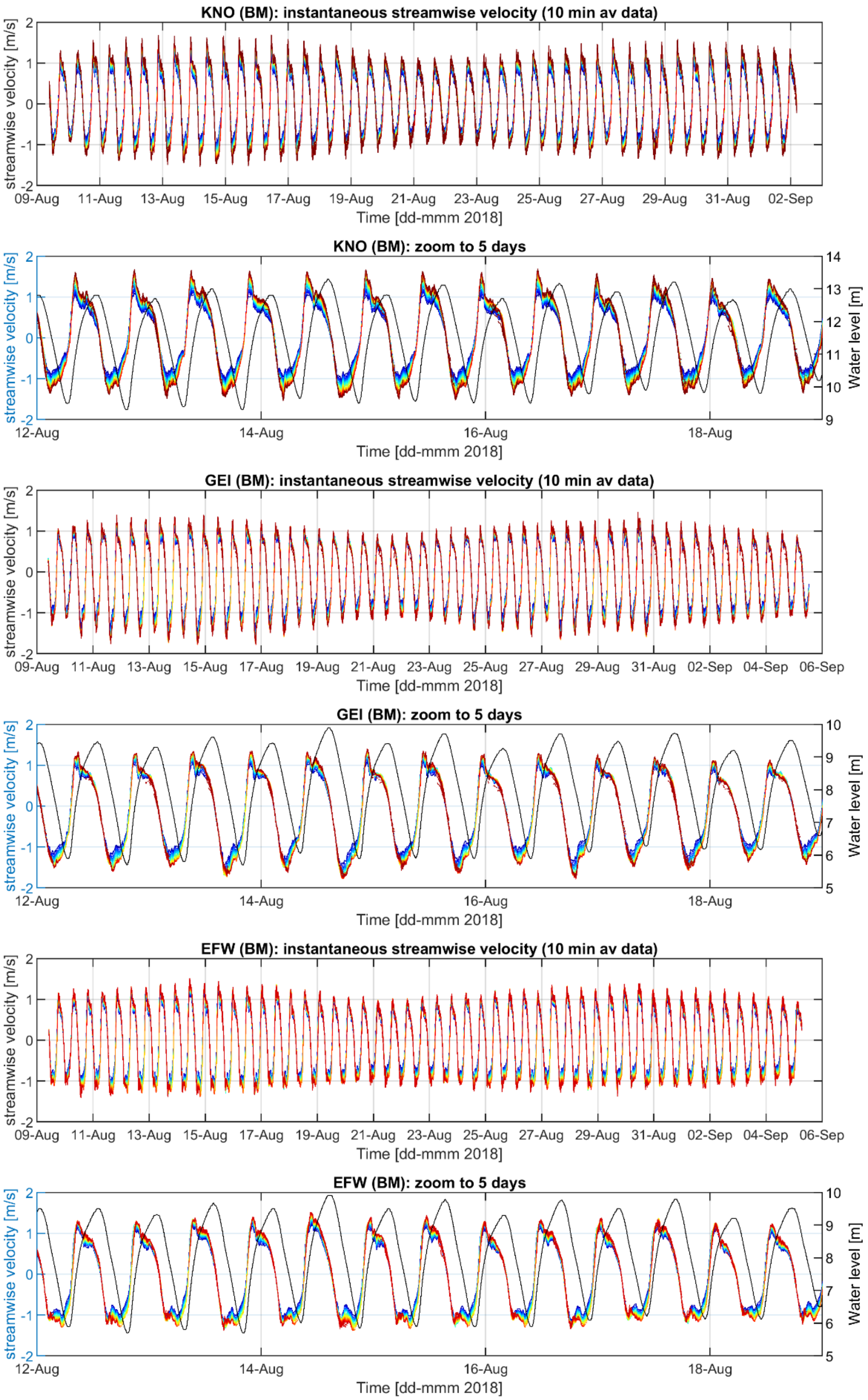
KNO (BM): instantaneous streamwise velocity (10 min av data)
streamwise velocity [m/s]
Time [dd-mmm 2018]
KNO (BM): zoom to 5 days
streamwise velocity [m/s]
Water level [m]
Time [dd-mmm 2018]
GEI (BM): instantaneous streamwise velocity (10 min av data)
streamwise velocity [m/s]
Time [dd-mmm 2018]
GEI (BM): zoom to 5 days
streamwise velocity [m/s]
Water level [m]
Time [dd-mmm 2018]
EFW (BM): instantaneous streamwise velocity (10 min av data)
streamwise velocity [m/s]
Time [dd-mmm 2018]
EFW (BM): zoom to 5 days
streamwise velocity [m/s]
Water level [m]
Time [dd-mmm 2018]

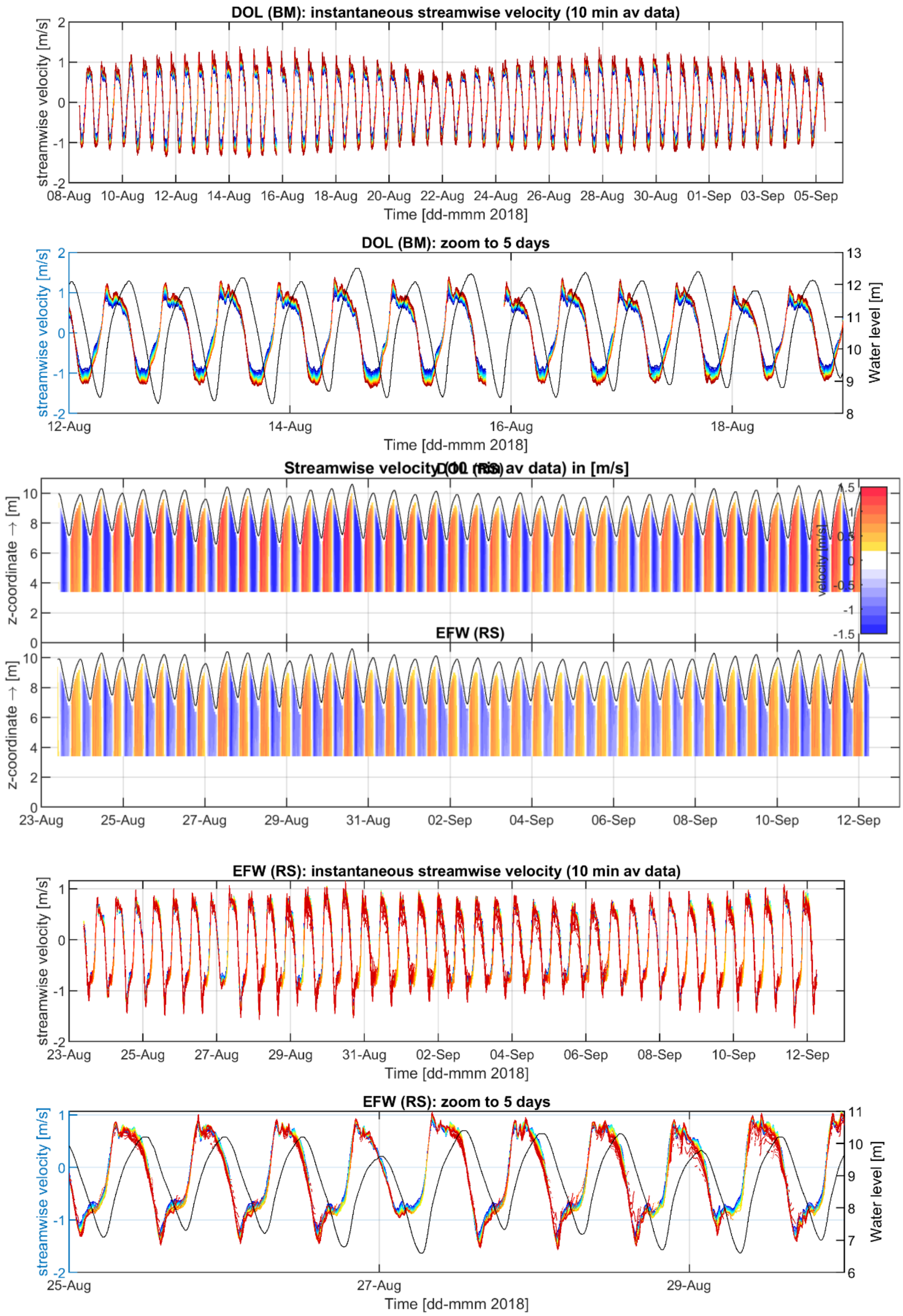
DOL (BM): instantaneous streamwise velocity (10 min av data)
streamwise velocity [m/s]
Time [dd-mmm 2018]
DOL (BM): zoom to 5 days
Water level [m]
Streamwise velocity (10 min av data) in [m/s]
DOL (RS)
EFW (RS)
z-coordinate → [m]
velocity [m/s]
EFW (RS): instantaneous streamwise velocity (10 min av data)
EFW (RS): zoom to 5 days

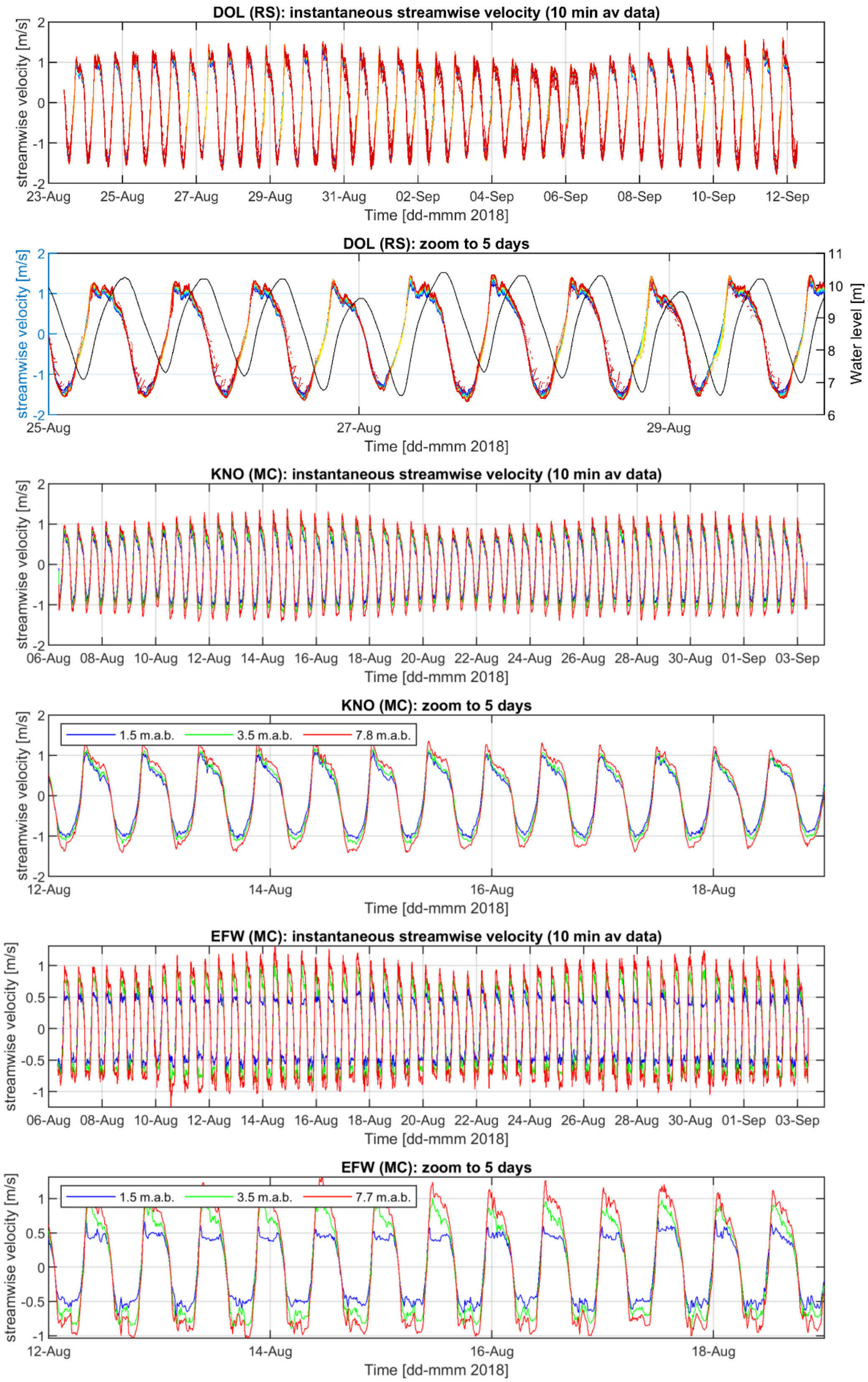

DOL (RS): instantaneous streamwise velocity (10 min av data)
streamwise velocity [m/s]
Time [dd-mmm 2018]
DOL (RS): zoom to 5 days
streamwise velocity [m/s]
Water level [m]
Time [dd-mmm 2018]
KNO (MC): instantaneous streamwise velocity (10 min av data)
streamwise velocity [m/s]
Time [dd-mmm 2018]
KNO (MC): zoom to 5 days
1.5 m.a.b.
3.5 m.a.b.
7.8 m.a.b.
streamwise velocity [m/s]
Time [dd-mmm 2018]
EFW (MC): instantaneous streamwise velocity (10 min av data)
streamwise velocity [m/s]
Time [dd-mmm 2018]
EFW (MC): zoom to 5 days
1.5 m.a.b.
3.5 m.a.b.
7.7 m.a.b.
streamwise velocity [m/s]
Time [dd-mmm 2018]

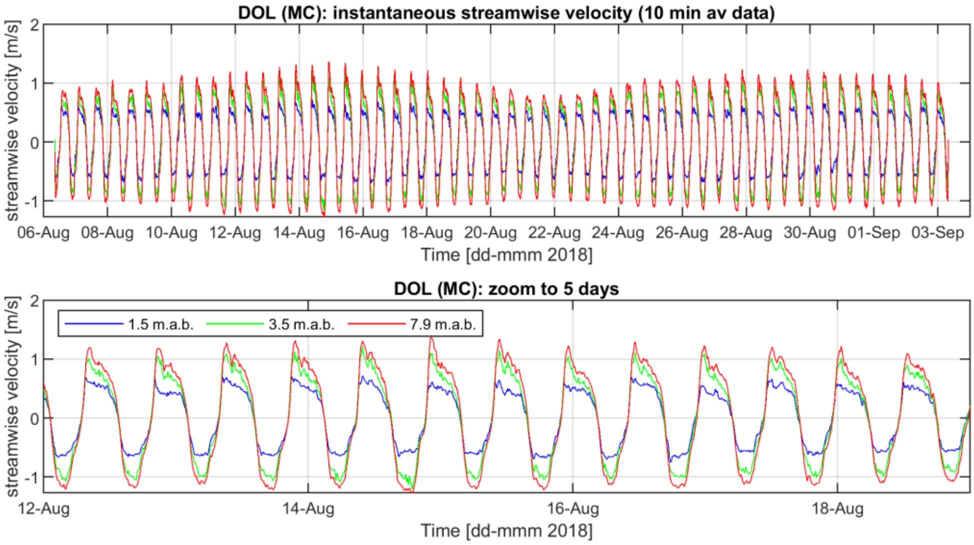

D.1.1.2. Streamcross velocities

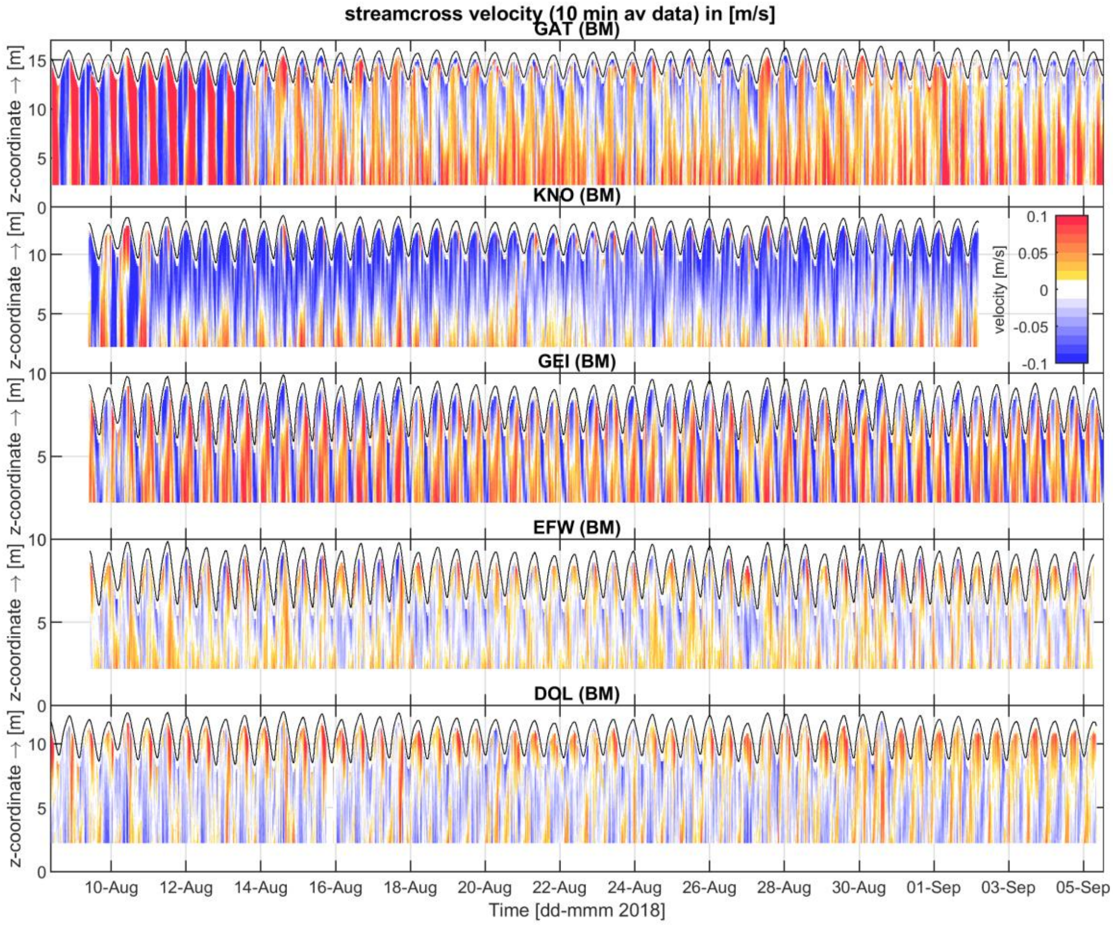

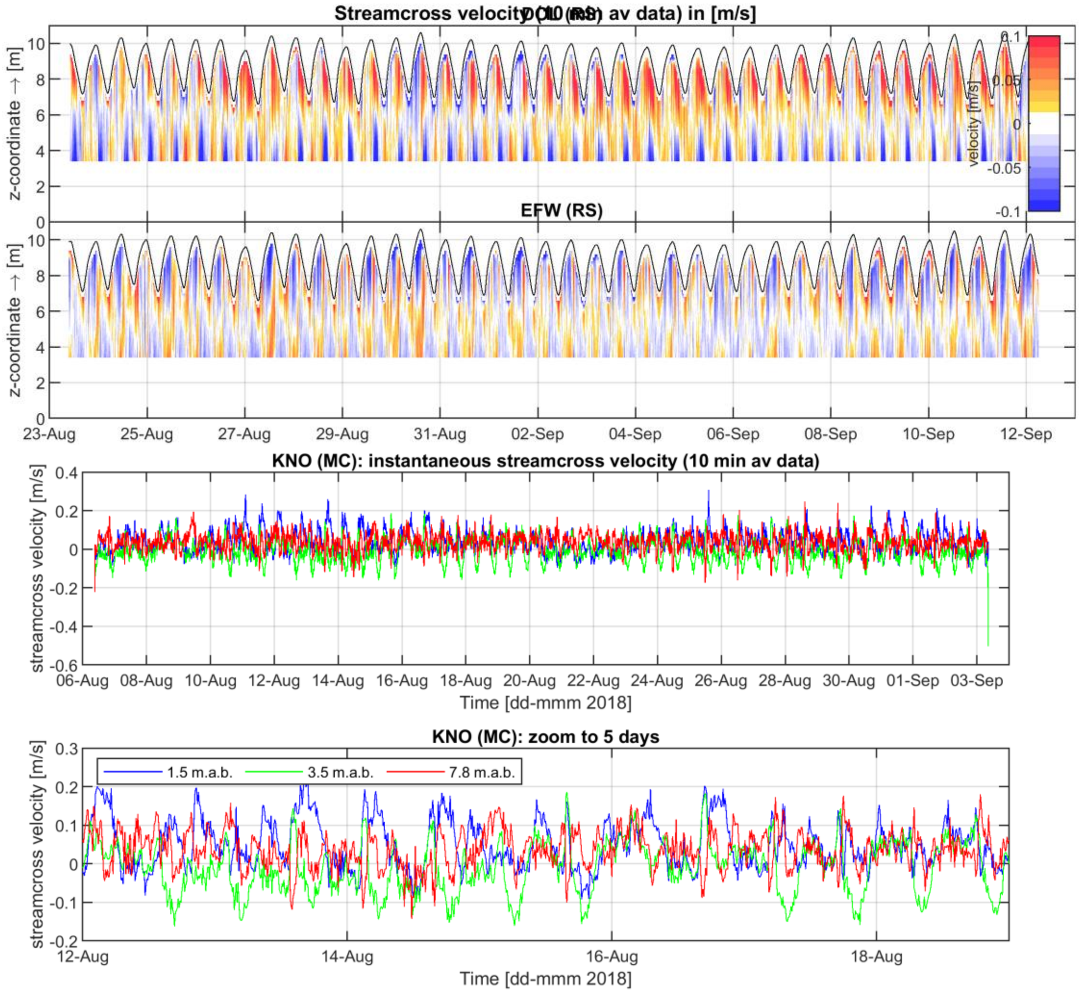

Streamcross velocity (10 min av data) in [m/s]
DOLL (RS)
EFW (RS)
z-coordinate → [m]
velocity [m/s]
23-Aug
25-Aug
27-Aug
29-Aug
31-Aug
02-Sep
04-Sep
06-Sep
08-Sep
10-Sep
12-Sep
KNO (MC): instantaneous streamcross velocity (10 min av data)
streamcross velocity [m/s]
06-Aug
08-Aug
10-Aug
12-Aug
14-Aug
16-Aug
18-Aug
20-Aug
22-Aug
24-Aug
26-Aug
28-Aug
30-Aug
01-Sep
03-Sep
Time [dd-mmm 2018]
KNO (MC): zoom to 5 days
1.5 m.a.b.
3.5 m.a.b.
7.8 m.a.b.
12-Aug
14-Aug
16-Aug
18-Aug
Time [dd-mmm 2018]

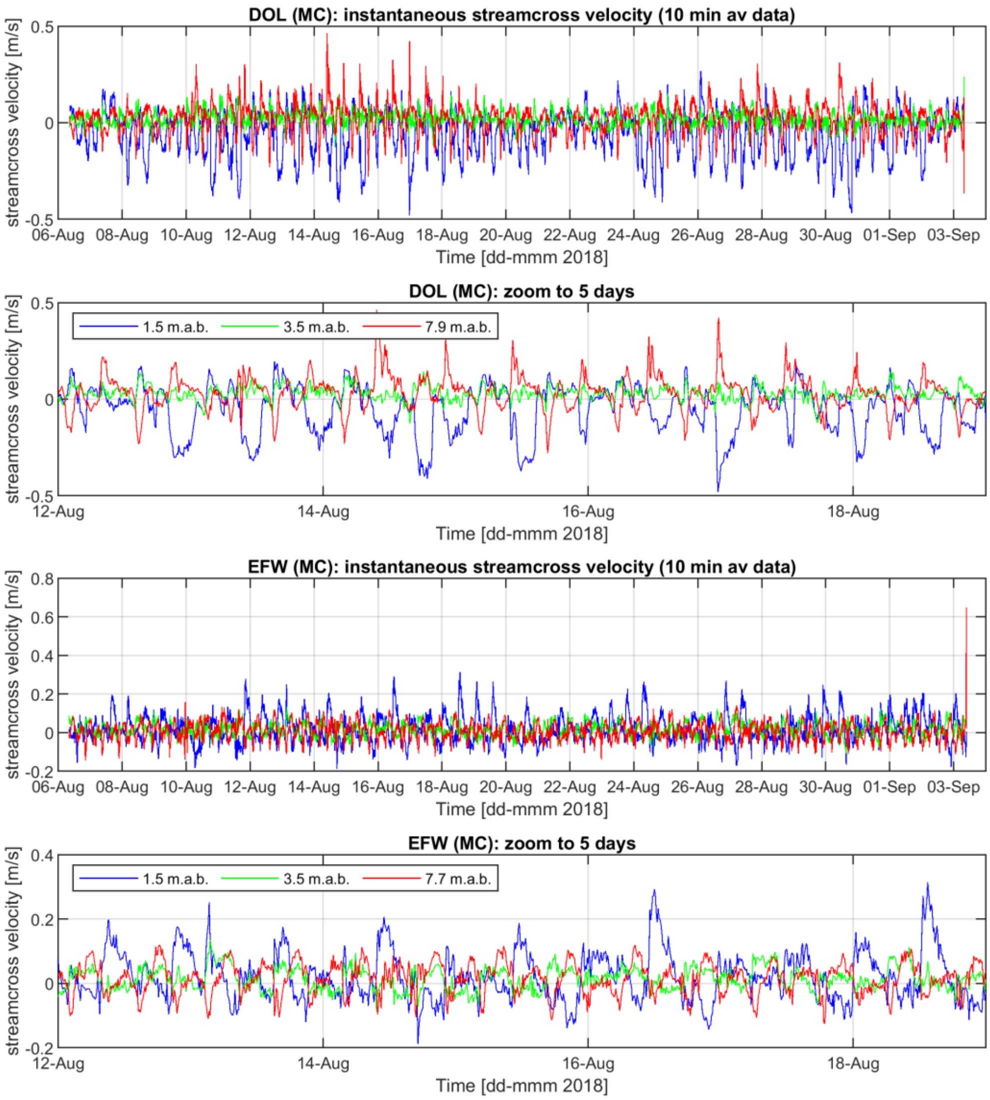

D.1.1.3. Sub-tidal flows

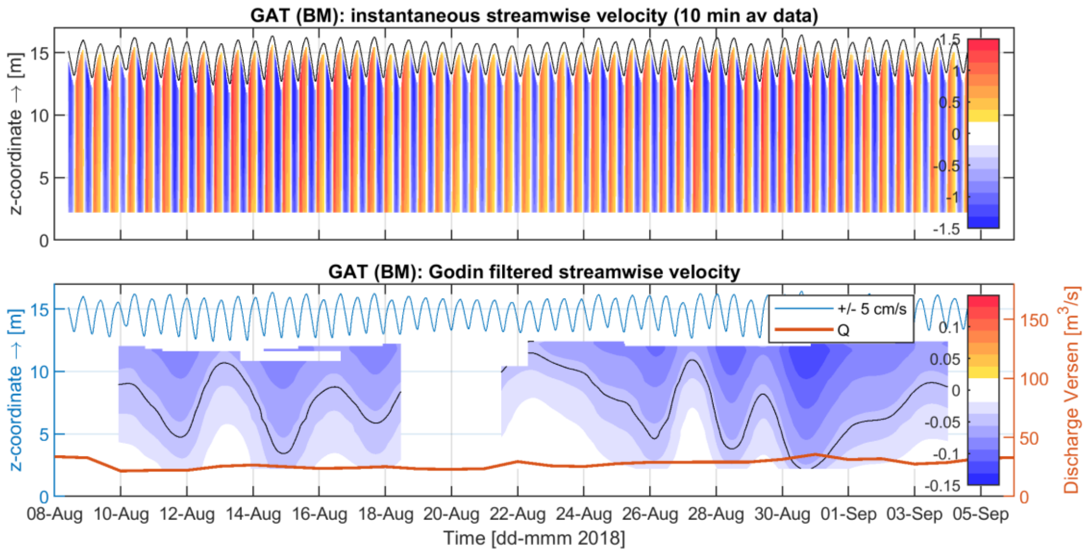

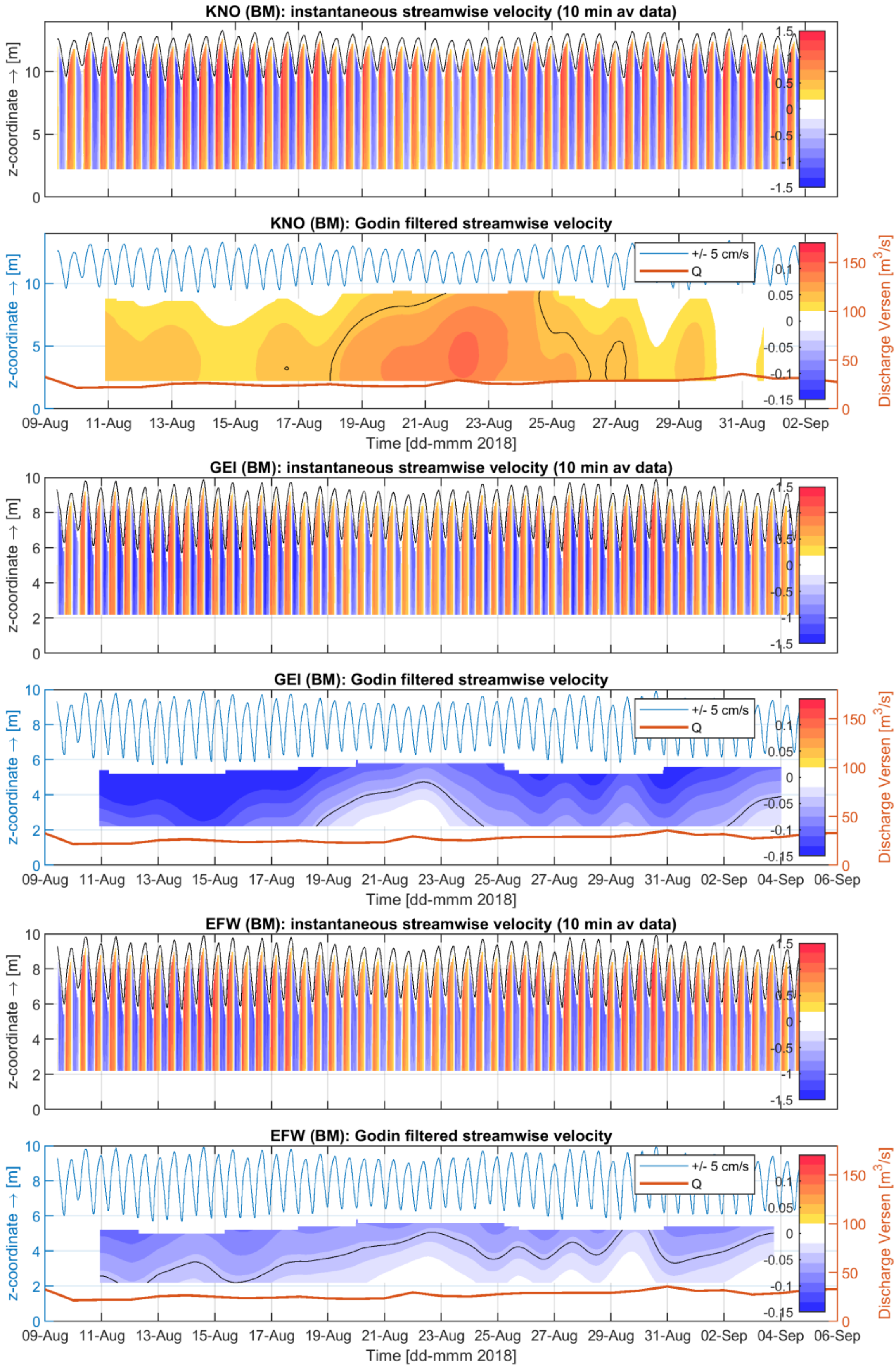
KNO (BM): instantaneous streamwise velocity (10 min av data)
z-coordinate → [m]
KNO (BM): Godin filtered streamwise velocity
+/- 5 cm/s
Q
Discharge Versen [m³/s]
09-Aug 11-Aug 13-Aug 15-Aug 17-Aug 19-Aug 21-Aug 23-Aug 25-Aug 27-Aug 29-Aug 31-Aug 02-Sep
Time [dd-mmm 2018]
GEI (BM): instantaneous streamwise velocity (10 min av data)
GEI (BM): Godin filtered streamwise velocity
09-Aug 11-Aug 13-Aug 15-Aug 17-Aug 19-Aug 21-Aug 23-Aug 25-Aug 27-Aug 29-Aug 31-Aug 02-Sep 04-Sep 06-Sep
Time [dd-mmm 2018]
EFW (BM): instantaneous streamwise velocity (10 min av data)
EFW (BM): Godin filtered streamwise velocity
Time [dd-mmm 2018]

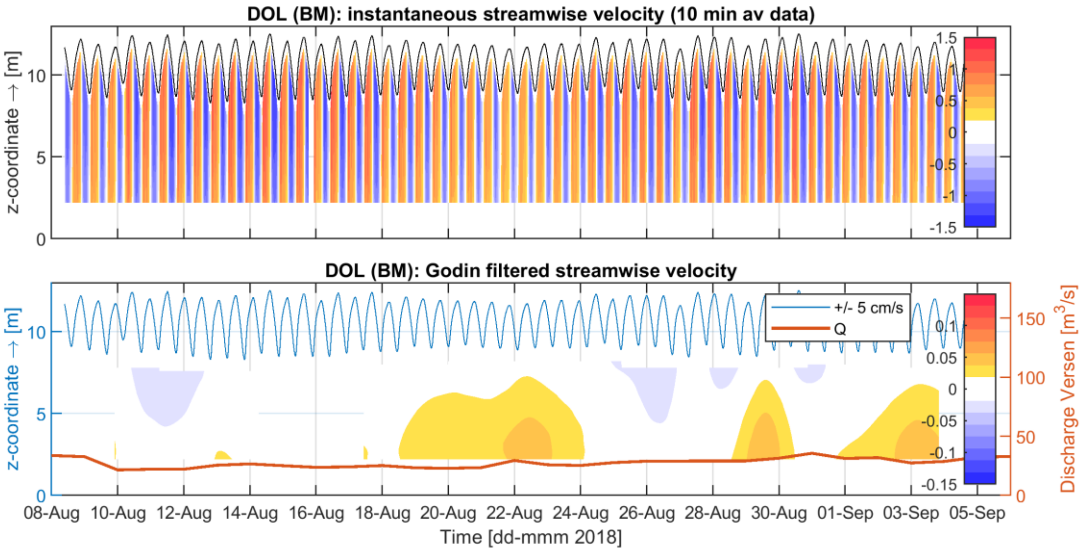
DOL (BM): instantaneous streamwise velocity (10 min av data)
z-coordinate → [m]
DOL (BM): Godin filtered streamwise velocity
+/- 5 cm/s
Q
Discharge Versen [m^3/s]
08-Aug 10-Aug 12-Aug 14-Aug 16-Aug 18-Aug 20-Aug 22-Aug 24-Aug 26-Aug 28-Aug 30-Aug 01-Sep 03-Sep 05-Sep
Time [dd-mmm 2018]

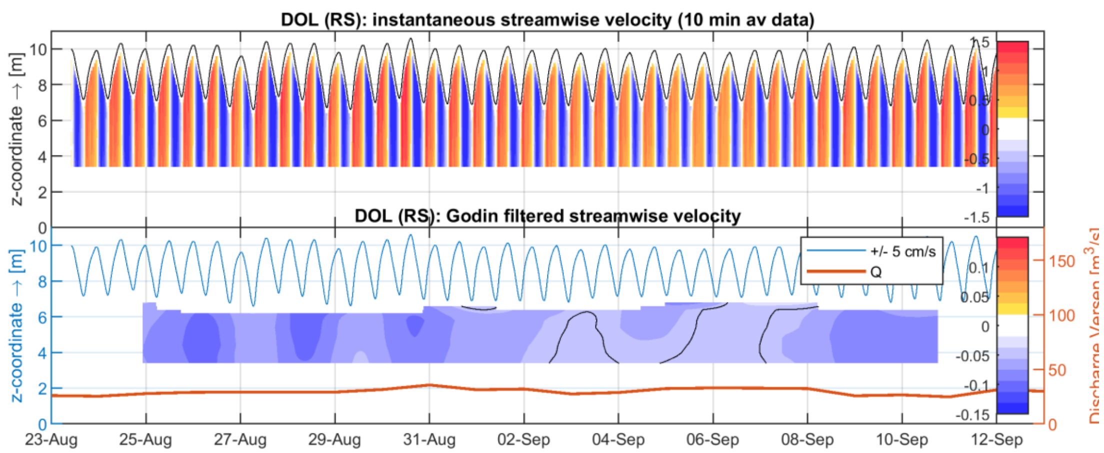
DOL (RS): instantaneous streamwise velocity (10 min av data)
z-coordinate → [m]
DOL (RS): Godin filtered streamwise velocity
+/- 5 cm/s
Q
23-Aug 25-Aug 27-Aug 29-Aug 31-Aug 02-Sep 04-Sep 06-Sep 08-Sep 10-Sep 12-Sep

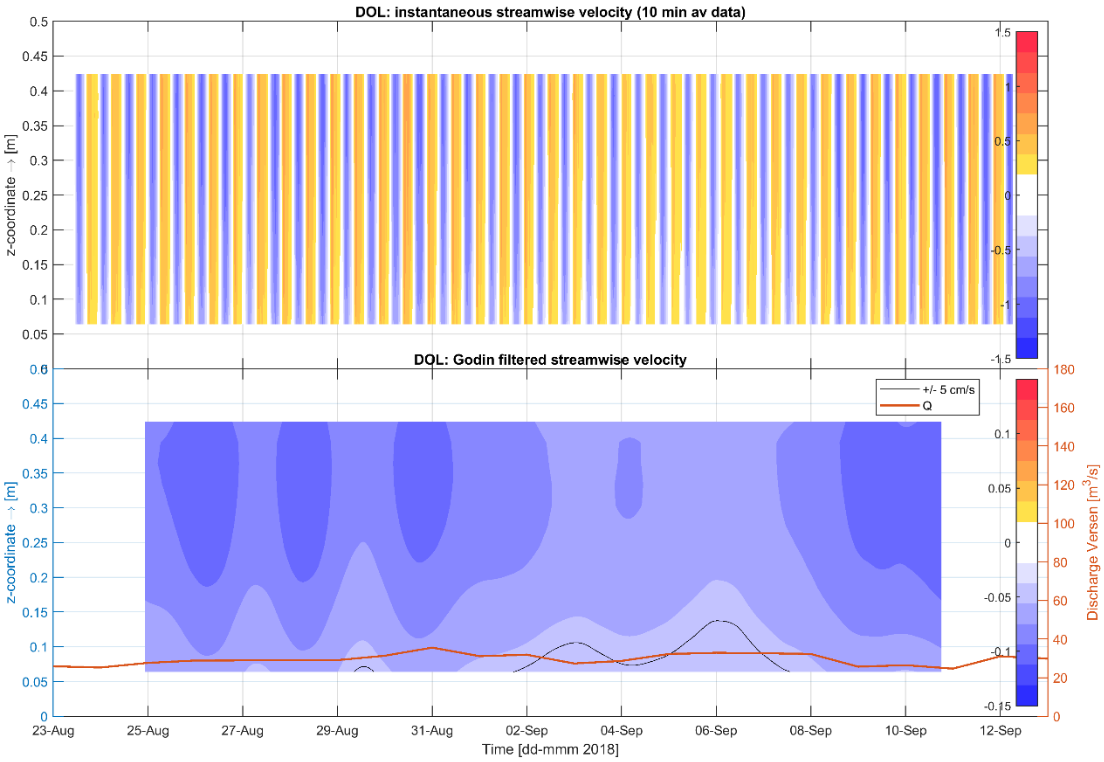
DOL: instantaneous streamwise velocity (10 min av data)
z-coordinate → [m]
DOL: Godin filtered streamwise velocity
+/- 5 cm/s
Q
Discharge Versen [m^3/s]
23-Aug 25-Aug 27-Aug 29-Aug 31-Aug 02-Sep 04-Sep 06-Sep 08-Sep 10-Sep 12-Sep
Time [dd-mmm 2018]

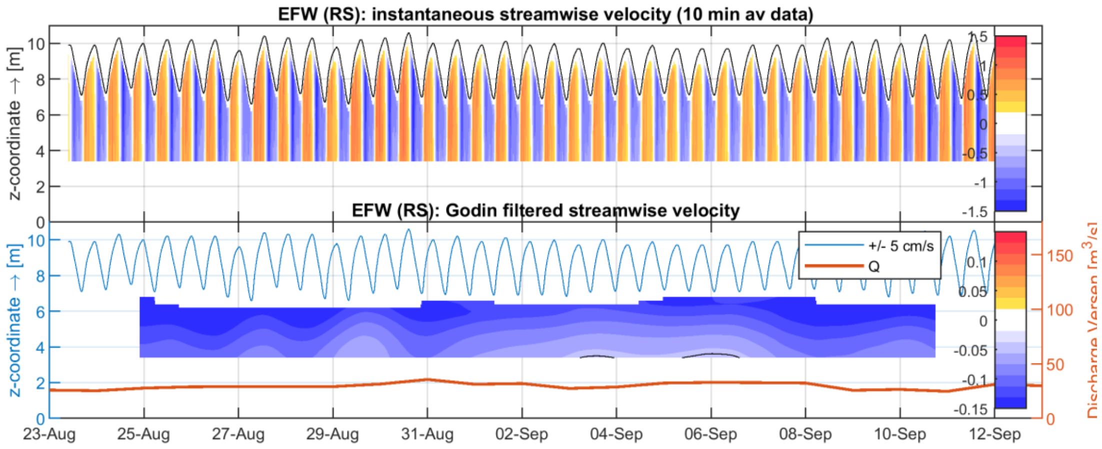
EFW (RS): instantaneous streamwise velocity (10 min av data)
z-coordinate → [m]
EFW (RS): Godin filtered streamwise velocity
+/- 5 cm/s
Q
Discharge Versen [m^3/s]
23-Aug
25-Aug
27-Aug
29-Aug
31-Aug
02-Sep
04-Sep
06-Sep
08-Sep
10-Sep
12-Sep

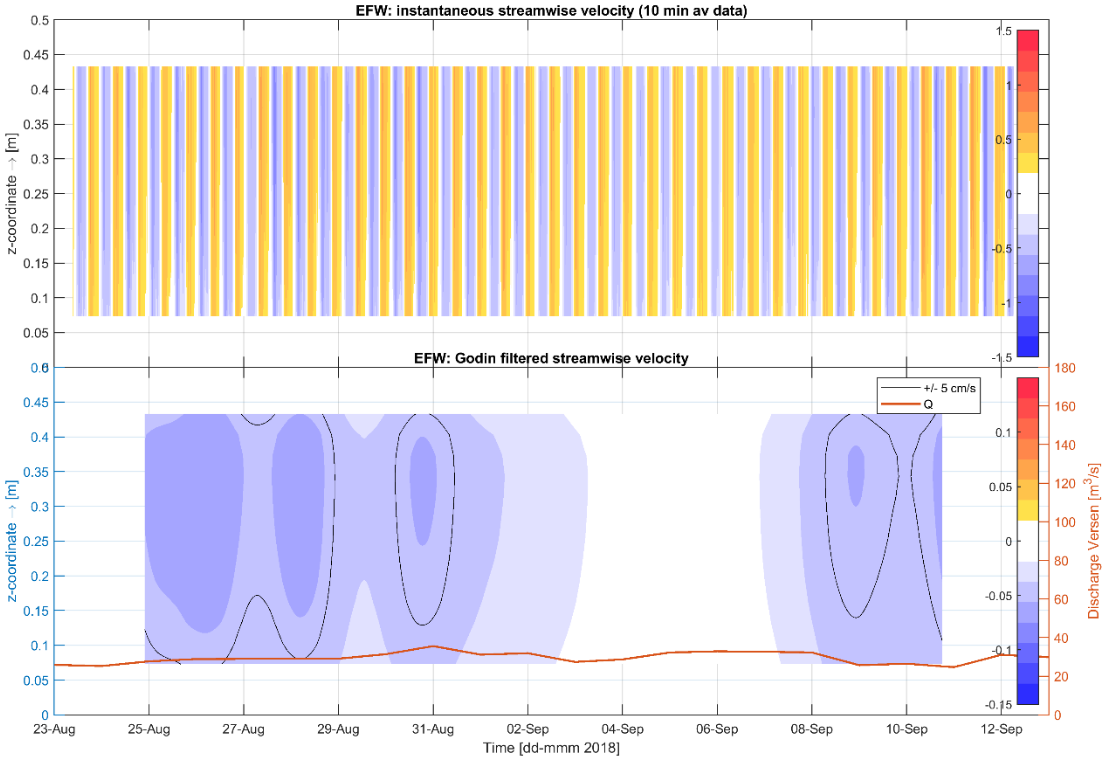
EFW: instantaneous streamwise velocity (10 min av data)
z-coordinate → [m]
EFW: Godin filtered streamwise velocity
+/- 5 cm/s
Q
Discharge Versen [m^3/s]
Time [dd-mmm 2018]

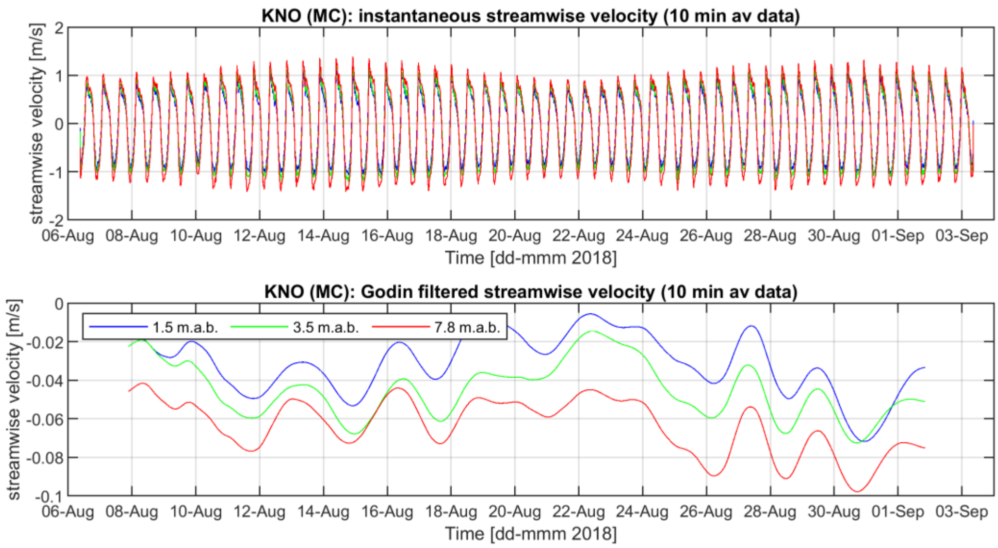
KNO (MC): instantaneous streamwise velocity (10 min av data)
streamwise velocity [m/s]
Time [dd-mmm 2018]
KNO (MC): Godin filtered streamwise velocity (10 min av data)
1.5 m.a.b.
3.5 m.a.b.
7.8 m.a.b.
06-Aug
08-Aug
10-Aug
12-Aug
14-Aug
16-Aug
18-Aug
20-Aug
22-Aug
24-Aug
26-Aug
28-Aug
30-Aug
01-Sep
03-Sep

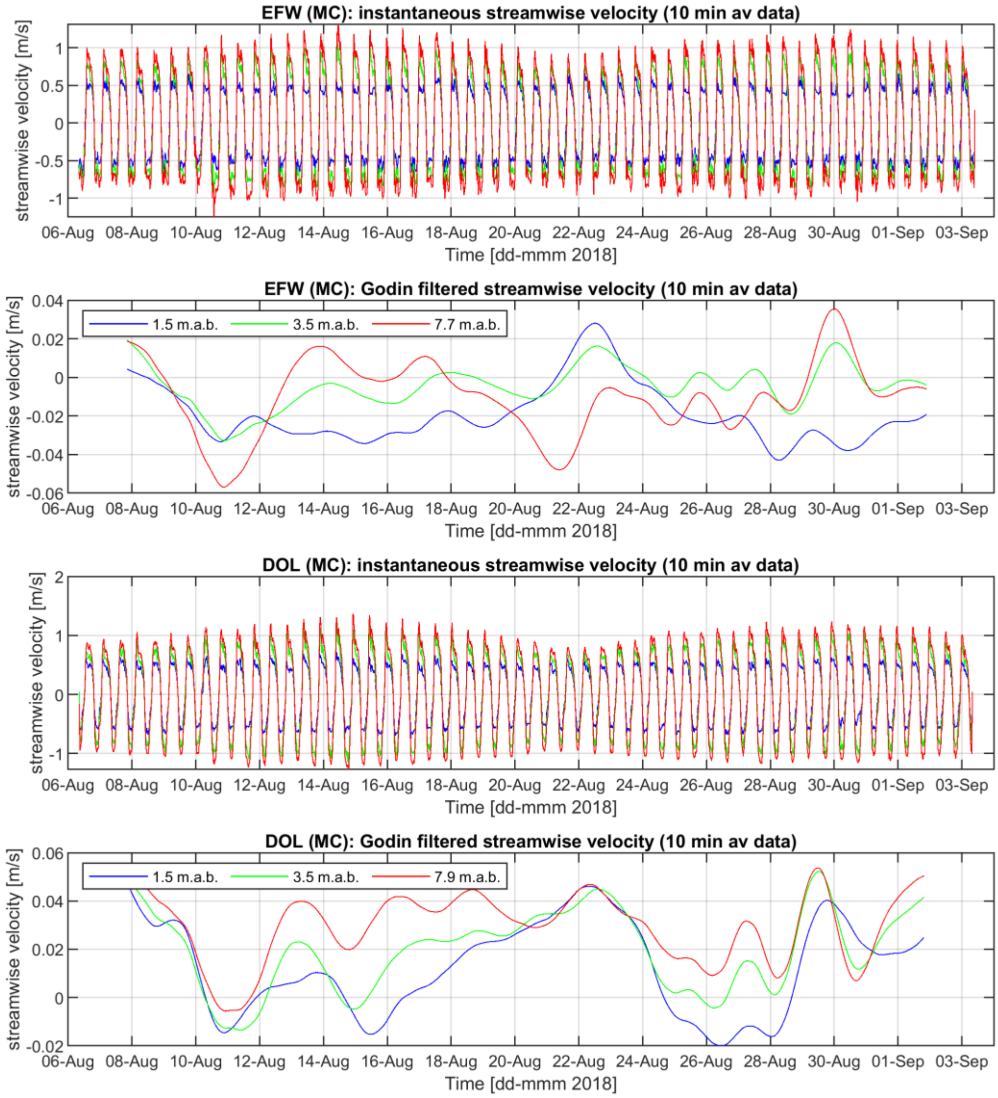

EFW (MC): instantaneous streamwise velocity (10 min av data)
streamwise velocity [m/s]
Time [dd-mmm 2018]
EFW (MC): Godin filtered streamwise velocity (10 min av data)
1.5 m.a.b.
3.5 m.a.b.
7.7 m.a.b.
DOL (MC): instantaneous streamwise velocity (10 min av data)
DOL (MC): Godin filtered streamwise velocity (10 min av data)
7.9 m.a.b.
06-Aug 08-Aug 10-Aug 12-Aug 14-Aug 16-Aug 18-Aug 20-Aug 22-Aug 24-Aug 26-Aug 28-Aug 30-Aug 01-Sep 03-Sep

D.1.1.4. Residual flow over a spring-neap tidal cycle

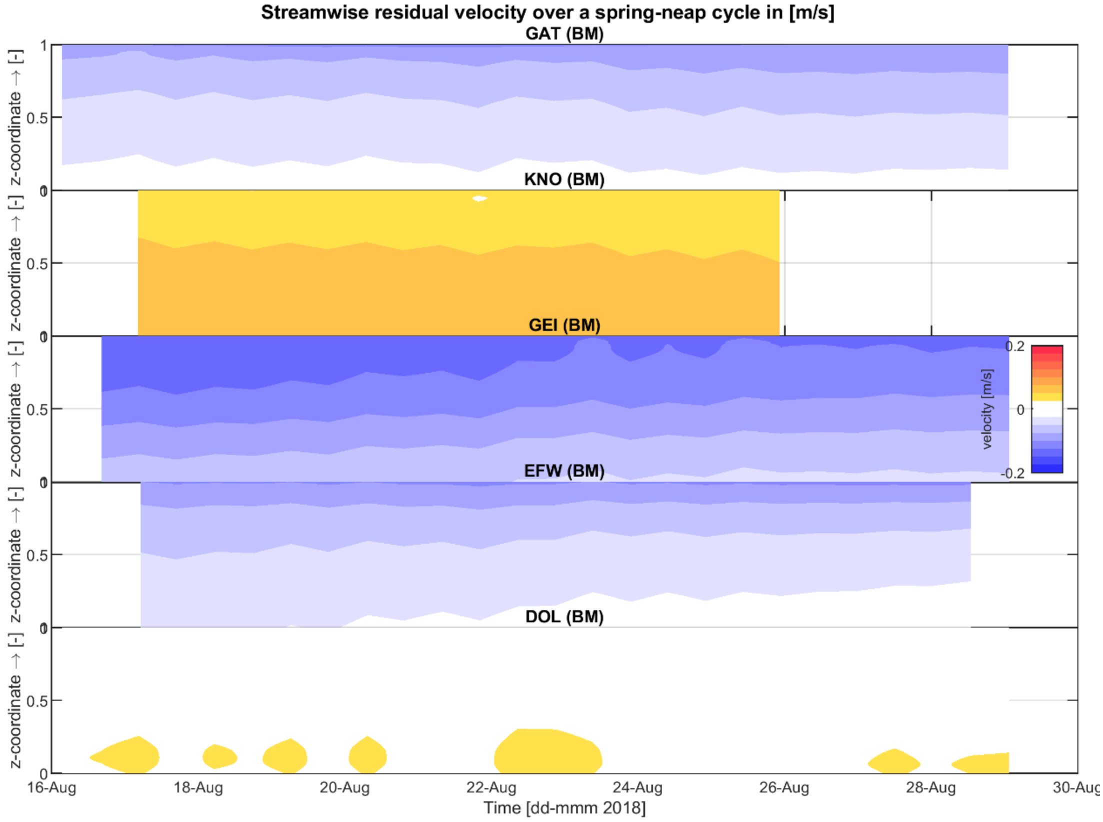

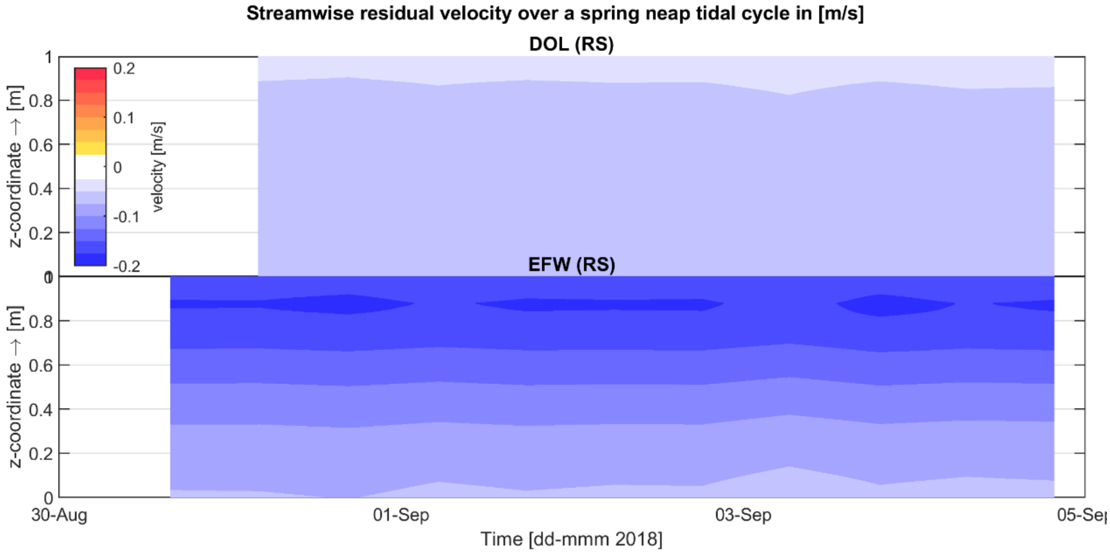

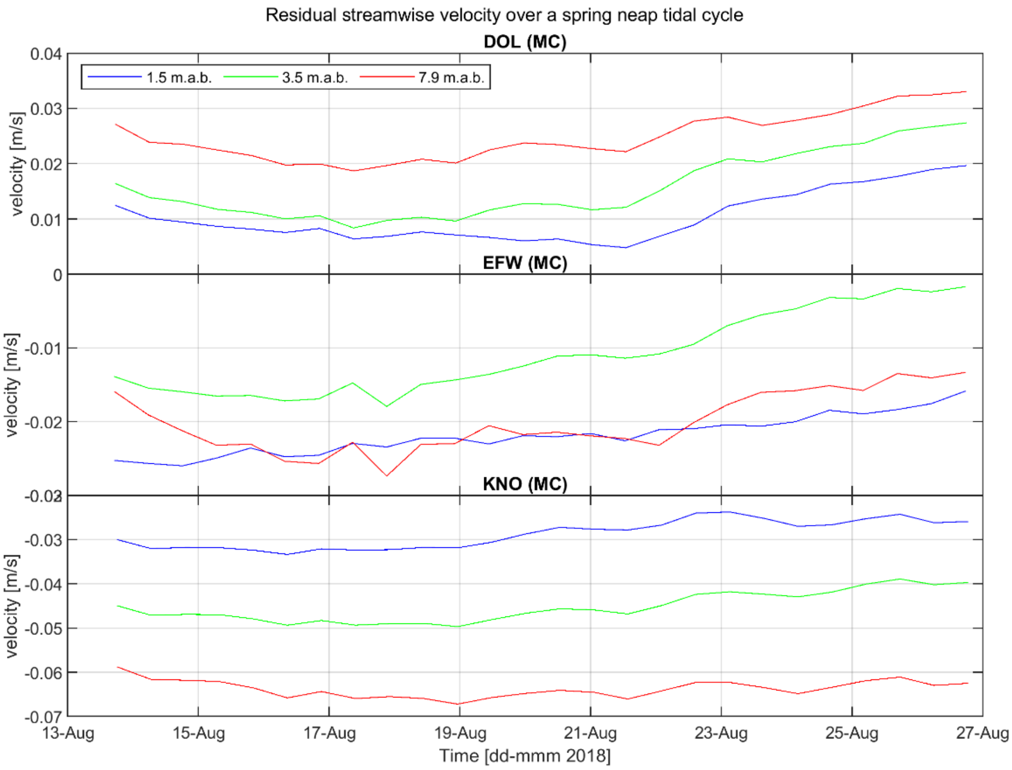
Residual streamwise velocity over a spring neap tidal cycle
DOL (MC)
1.5 m.a.b.
3.5 m.a.b.
7.9 m.a.b.
velocity [m/s]
EFW (MC)
KNO (MC)
13-Aug
15-Aug
17-Aug
19-Aug
21-Aug
23-Aug
25-Aug
27-Aug
Time [dd-mmm 2018]

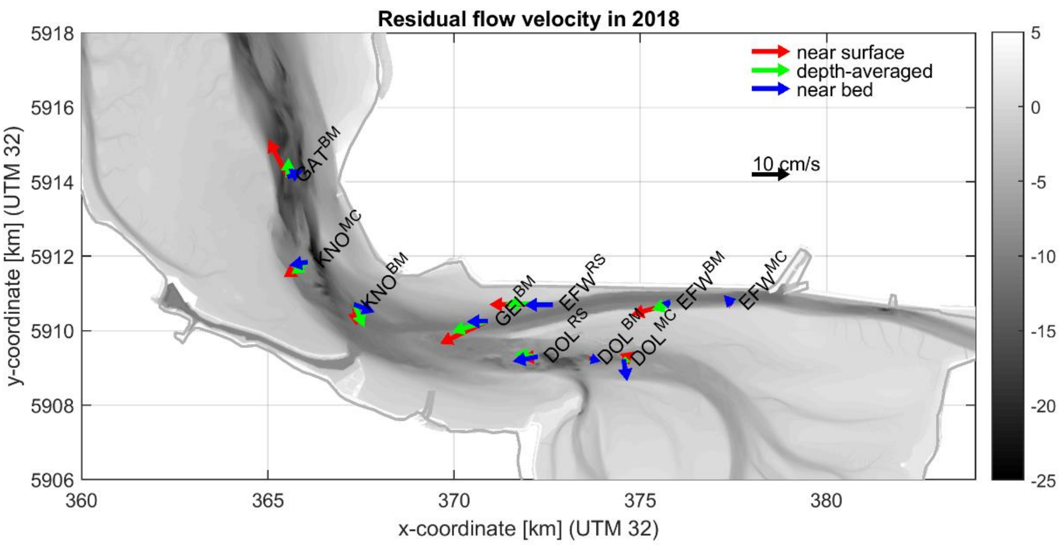
Residual flow velocity in 2018
near surface
depth-averaged
near bed
10 cm/s
y-coordinate [km] (UTM 32)
x-coordinate [km] (UTM 32)

Deltares

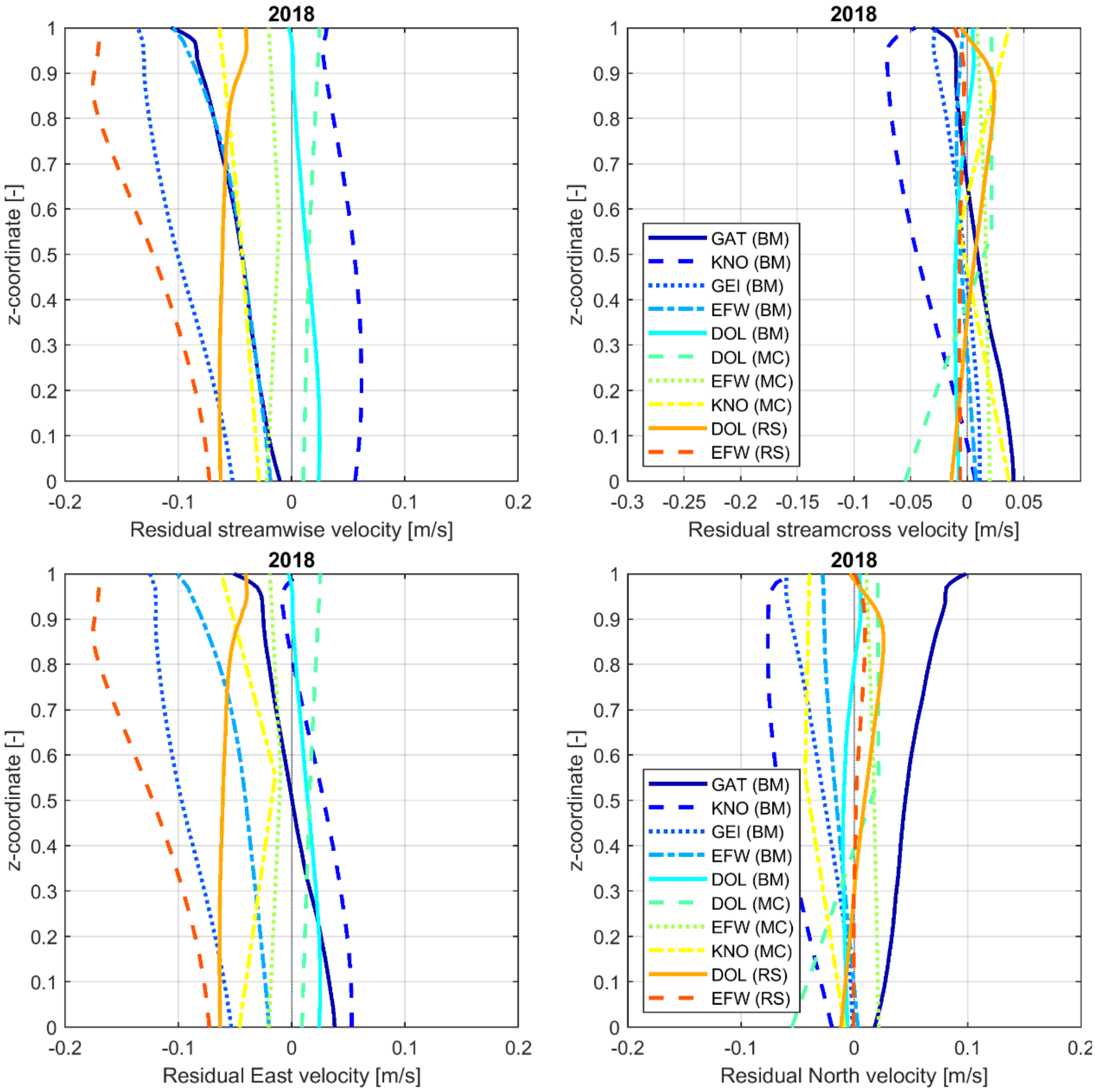
2018
z-coordinate [-]
Residual streamwise velocity [m/s]
2018
z-coordinate [-]
Residual streamcross velocity [m/s]
GAT (BM)
KNO (BM)
GEI (BM)
EFW (BM)
DOL (BM)
DOL (MC)
EFW (MC)
KNO (MC)
DOL (RS)
EFW (RS)
2018
z-coordinate [-]
Residual East velocity [m/s]
2018
z-coordinate [-]
Residual North velocity [m/s]

D.1.1.5. Suspended sediment concentration and additional parameters

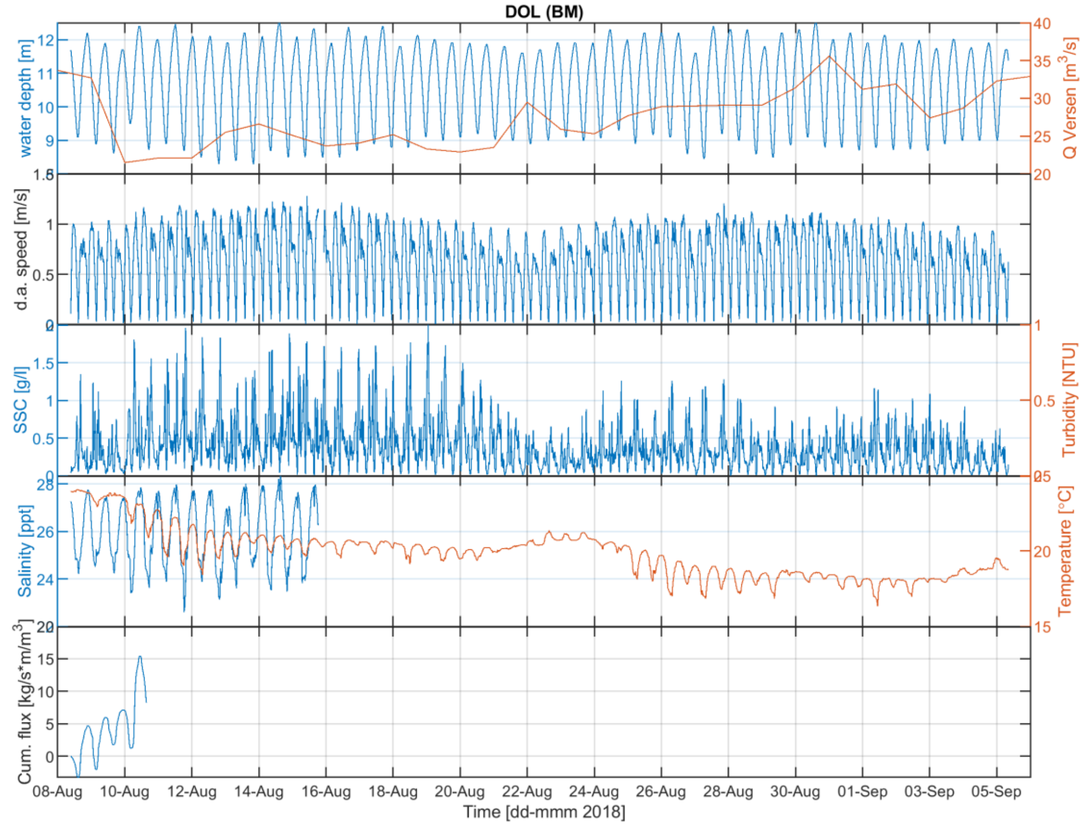

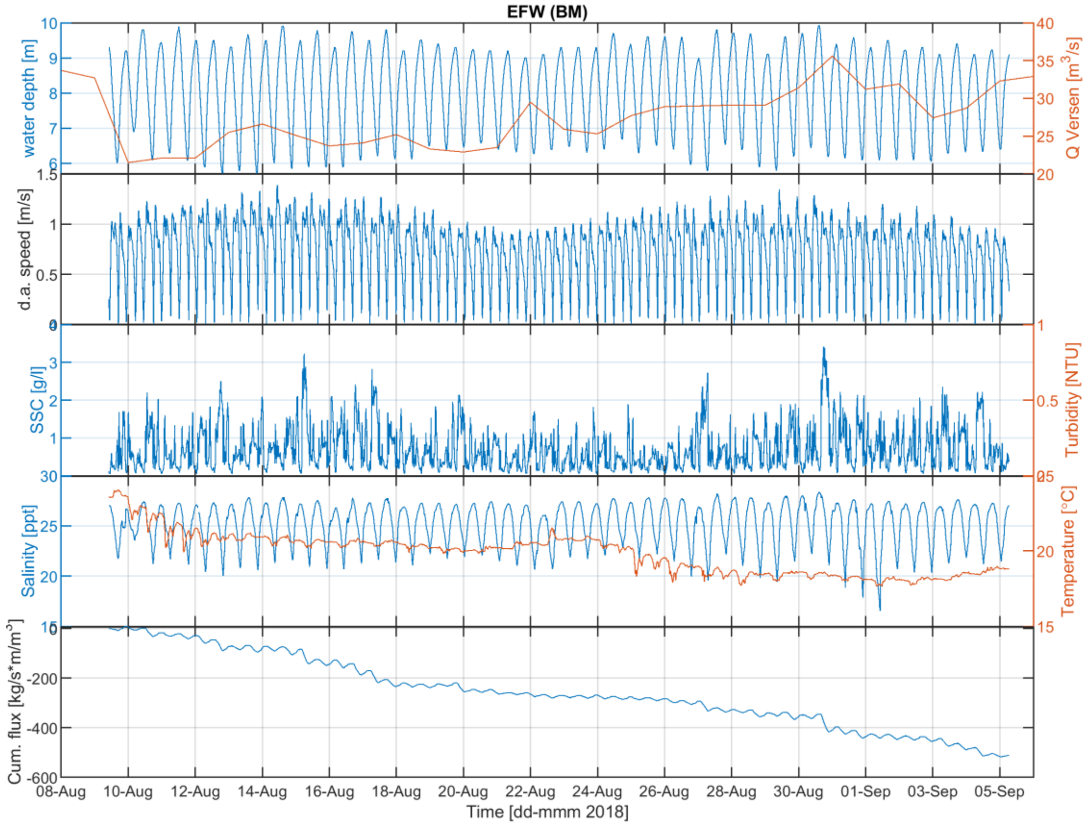

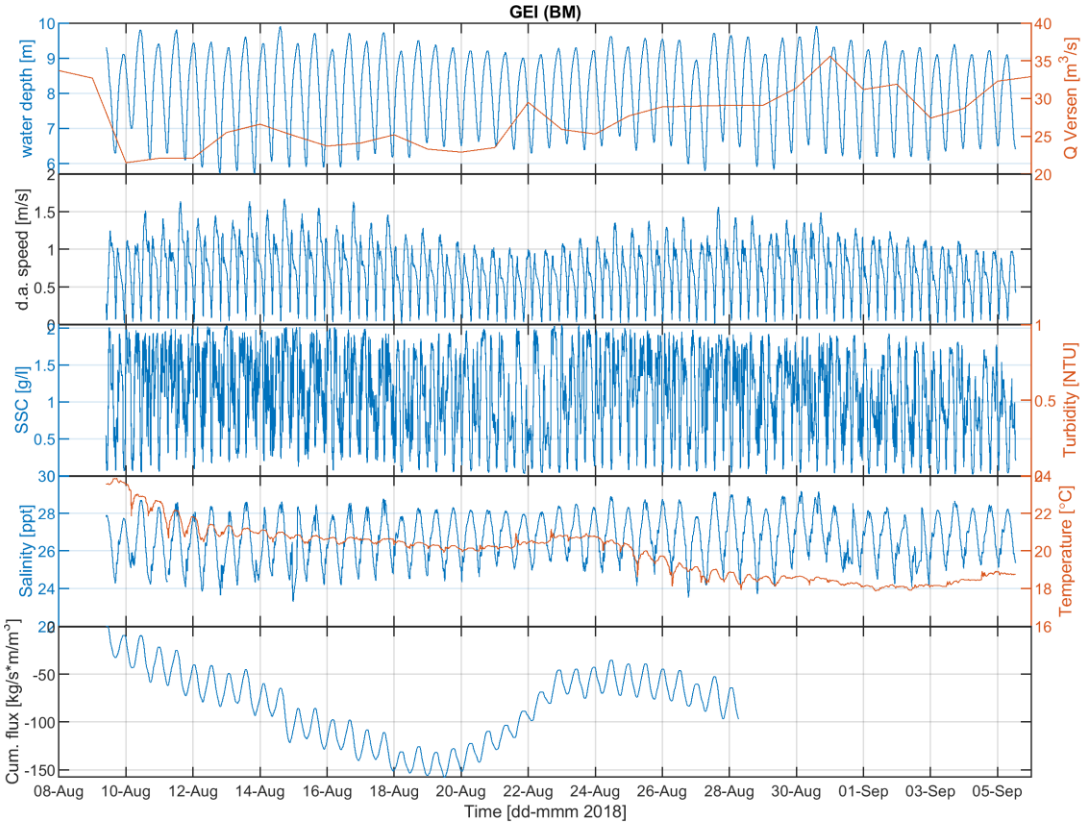
GEI (BM)
water depth [m]
Q Versen [m^3/s]
d.a. speed [m/s]
SSC [g/l]
Turbidity [NTU]
Salinity [ppt]
Temperature [°C]
Cum. flux [kg/s*m/m^3]
08-Aug 10-Aug 12-Aug 14-Aug 16-Aug 18-Aug 20-Aug 22-Aug 24-Aug 26-Aug 28-Aug 30-Aug 01-Sep 03-Sep 05-Sep
Time [dd-mmm 2018]

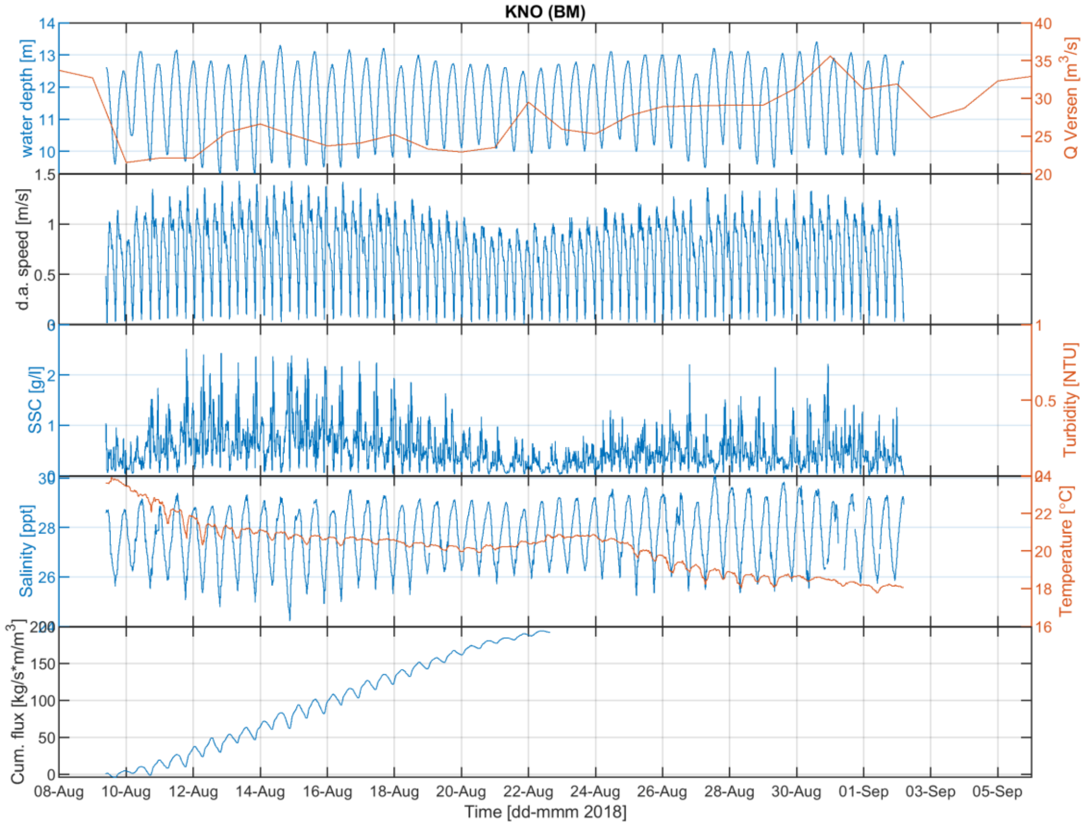
KNO (BM)
water depth [m]
Q Versen [m^3/s]
d.a. speed [m/s]
SSC [g/l]
Turbidity [NTU]
Salinity [ppt]
Temperature [°C]
Cum. flux [kg/s*m/m^3]
08-Aug 10-Aug 12-Aug 14-Aug 16-Aug 18-Aug 20-Aug 22-Aug 24-Aug 26-Aug 28-Aug 30-Aug 01-Sep 03-Sep 05-Sep
Time [dd-mmm 2018]

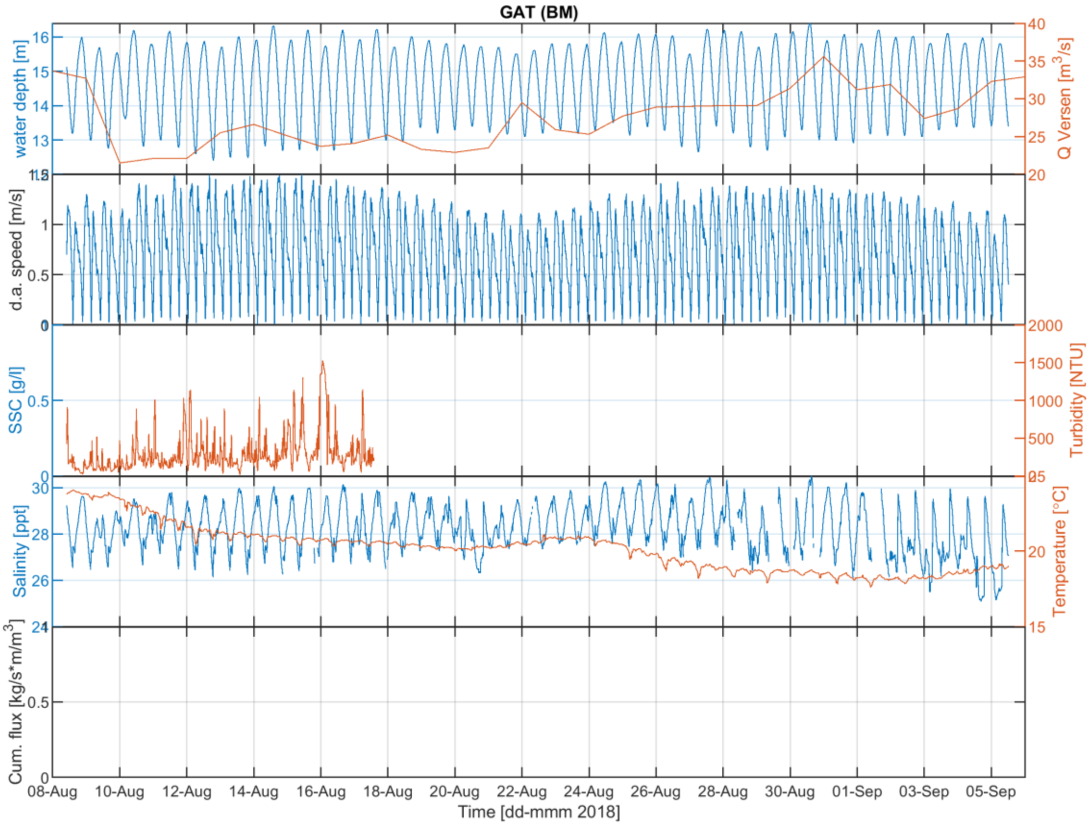
GAT (BM)
water depth [m]
Q Versen [m³/s]
d.a. speed [m/s]
SSC [g/l]
Turbidity [NTU]
Salinity [ppt]
Temperature [°C]
Cum. flux [kg/s*m/m³]
08-Aug 10-Aug 12-Aug 14-Aug 16-Aug 18-Aug 20-Aug 22-Aug 24-Aug 26-Aug 28-Aug 30-Aug 01-Sep 03-Sep 05-Sep
Time [dd-mmm 2018]

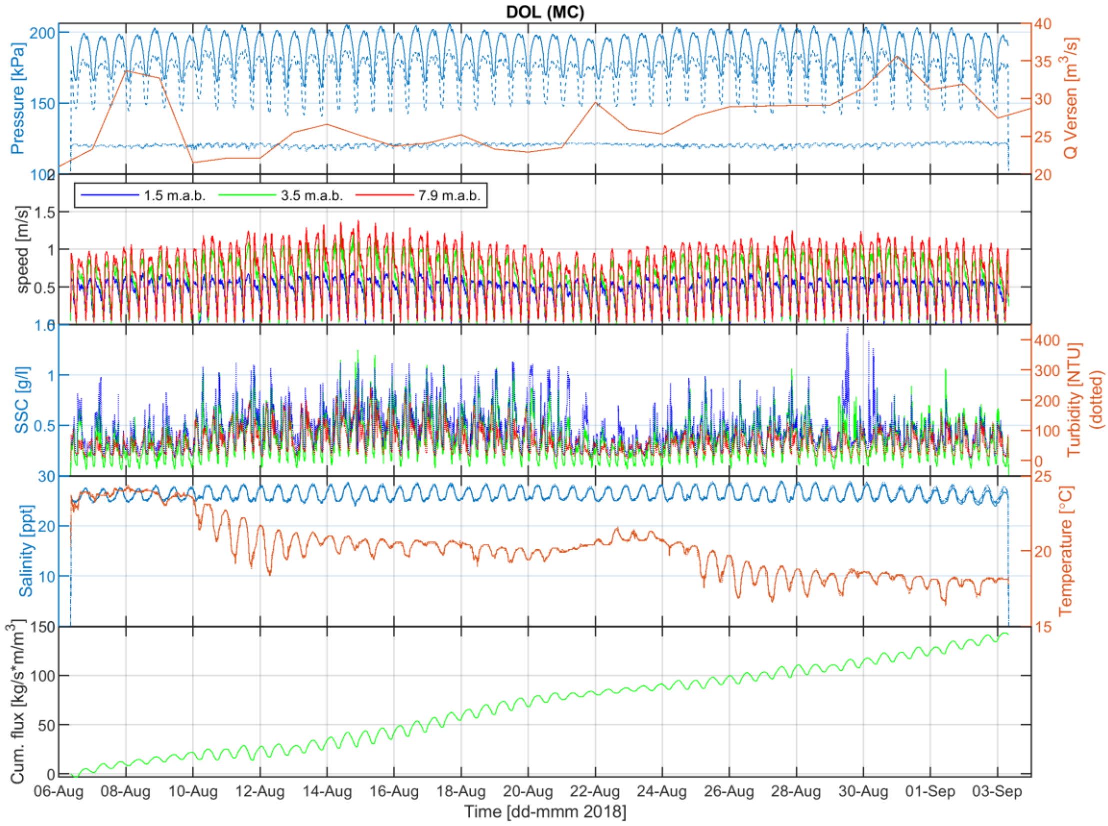
DOL (MC)
Pressure [kPa]
Q Versen [m^3/s]
1.5 m.a.b.
3.5 m.a.b.
7.9 m.a.b.
speed [m/s]
SSC [g/l]
Turbidity [NTU] (dotted)
Salinity [ppt]
Temperature [°C]
Cum. flux [kg/s*m/m^3]
06-Aug 08-Aug 10-Aug 12-Aug 14-Aug 16-Aug 18-Aug 20-Aug 22-Aug 24-Aug 26-Aug 28-Aug 30-Aug 01-Sep 03-Sep
Time [dd-mmm 2018]

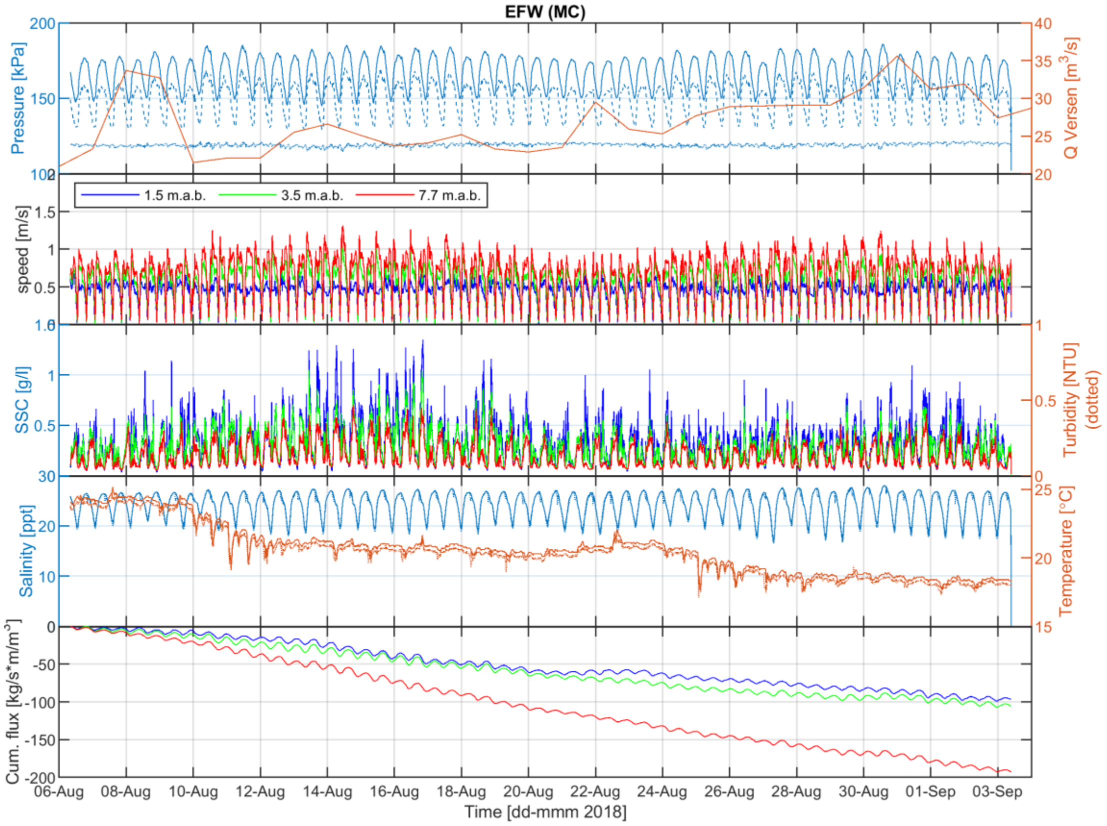
EFW (MC)
Pressure [kPa]
Q Versen [m^3/s]
1.5 m.a.b.
3.5 m.a.b.
7.7 m.a.b.
speed [m/s]
SSC [g/l]
Turbidity [NTU] (dotted)
Salinity [ppt]
Temperature [°C]
Cum. flux [kg/s*m/m^3]
06-Aug 08-Aug 10-Aug 12-Aug 14-Aug 16-Aug 18-Aug 20-Aug 22-Aug 24-Aug 26-Aug 28-Aug 30-Aug 01-Sep 03-Sep
Time [dd-mmm 2018]

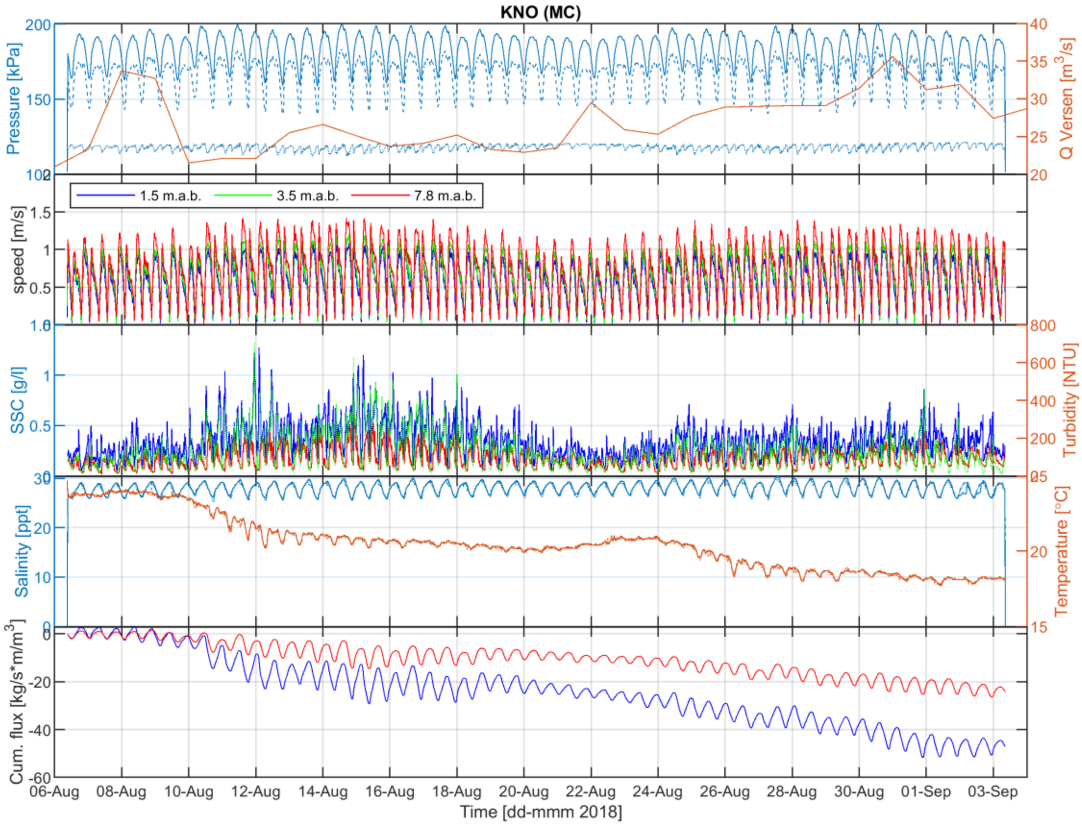

KNO (MC)
Pressure [kPa]
Q Versen [m^3/s]
1.5 m.a.b.
3.5 m.a.b.
7.8 m.a.b.
speed [m/s]
SSC [g/l]
Turbidity [NTU] (dotted)
Salinity [ppt]
Temperature [°C]
Cum. flux [kg/s*m/m^3]
Time [dd-mmm 2018]

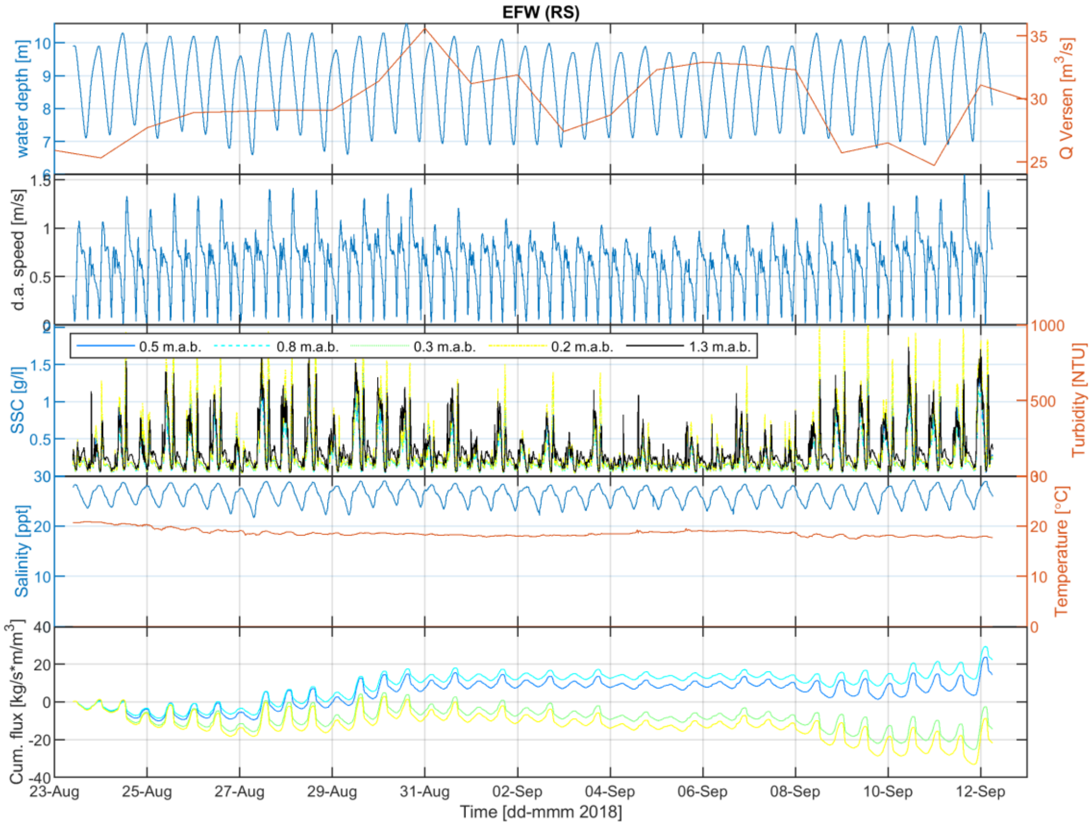
EFW (RS)
water depth [m]
Q Versen [m3/s]
d.a. speed [m/s]
0.5 m.a.b.
0.8 m.a.b.
0.3 m.a.b.
0.2 m.a.b.
1.3 m.a.b.
SSC [g/l]
Turbidity [NTU]
Salinity [ppt]
Temperature [°C]
Cum. flux [kg/s*m/m3]
Time [dd-mmm 2018]

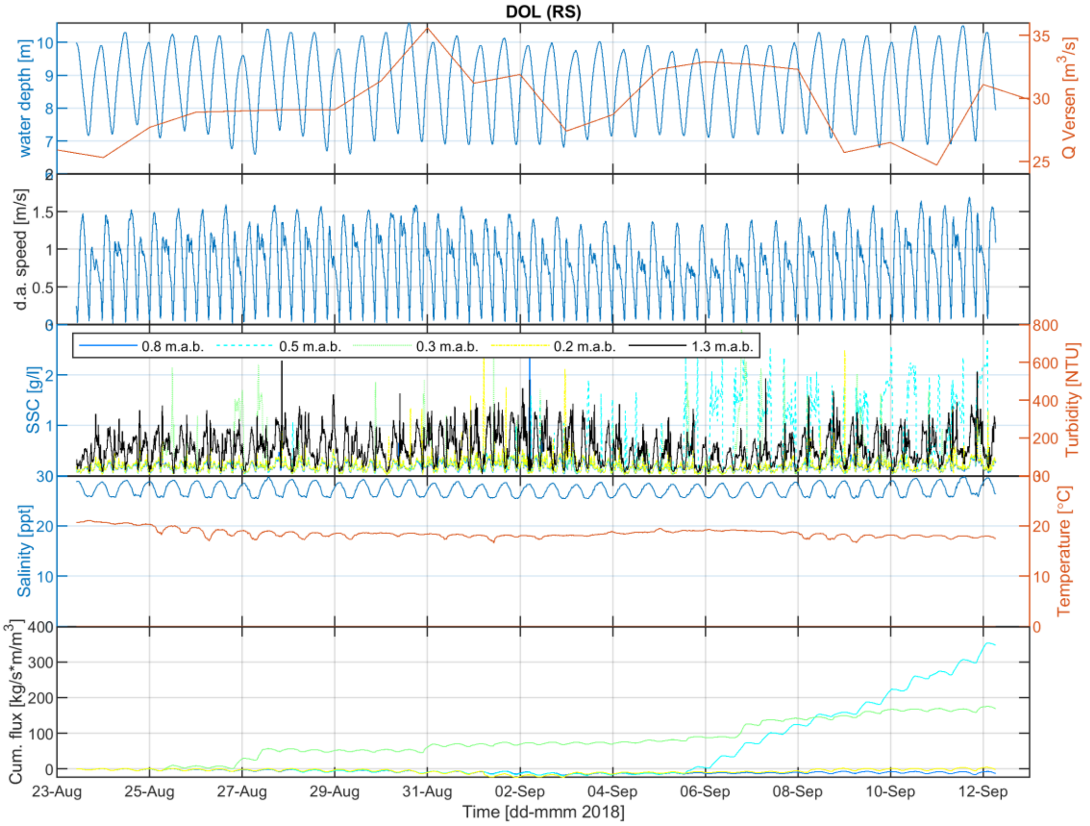
DOL (RS)
water depth [m]
Q Versen [m3/s]
d.a. speed [m/s]
0.8 m.a.b.
0.5 m.a.b.
0.3 m.a.b.
0.2 m.a.b.
1.3 m.a.b.
SSC [g/l]
Turbidity [NTU]
Salinity [ppt]
Temperature [°C]
Cum. flux [kg/s*m/m3]
Time [dd-mmm 2018]

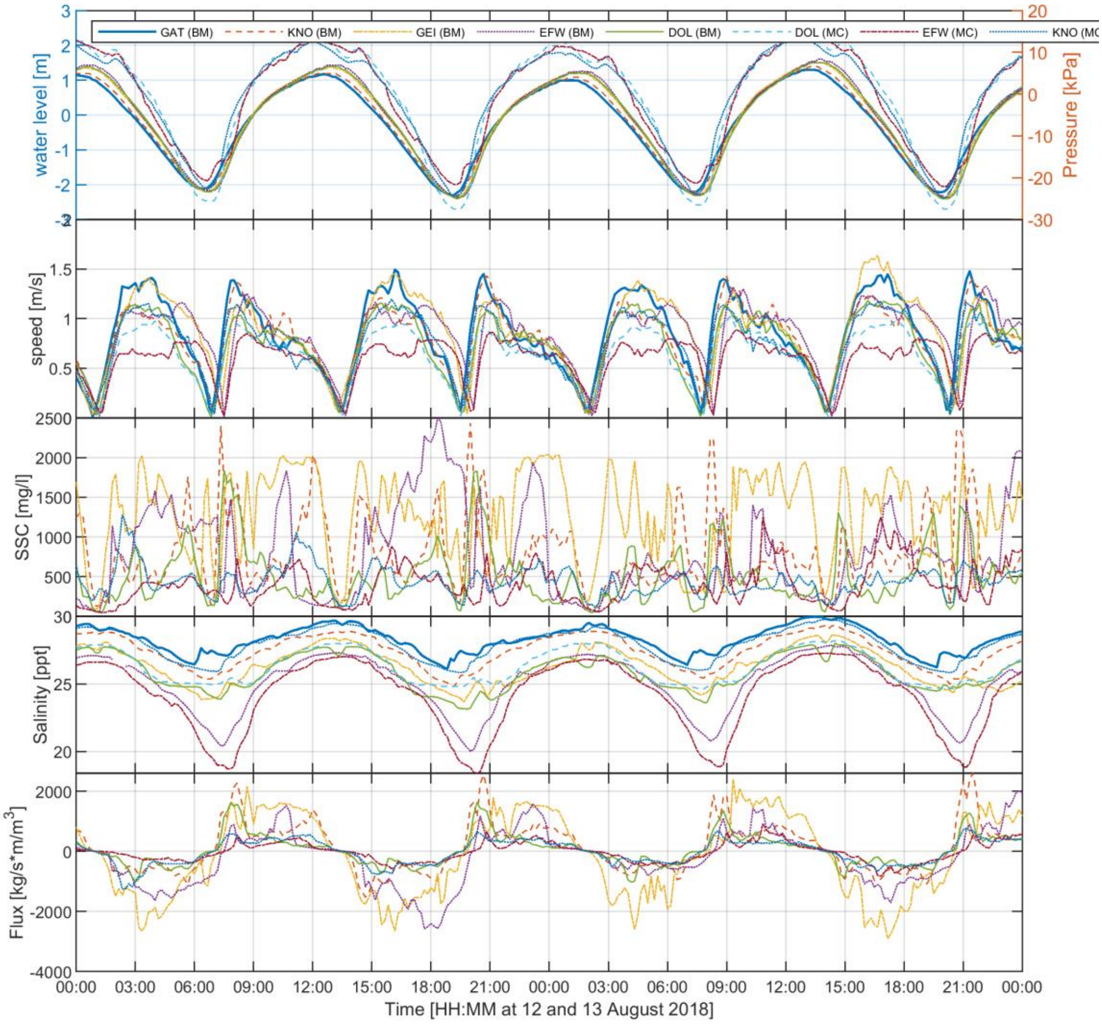

High-frequency data (not averaged to 10-mins)

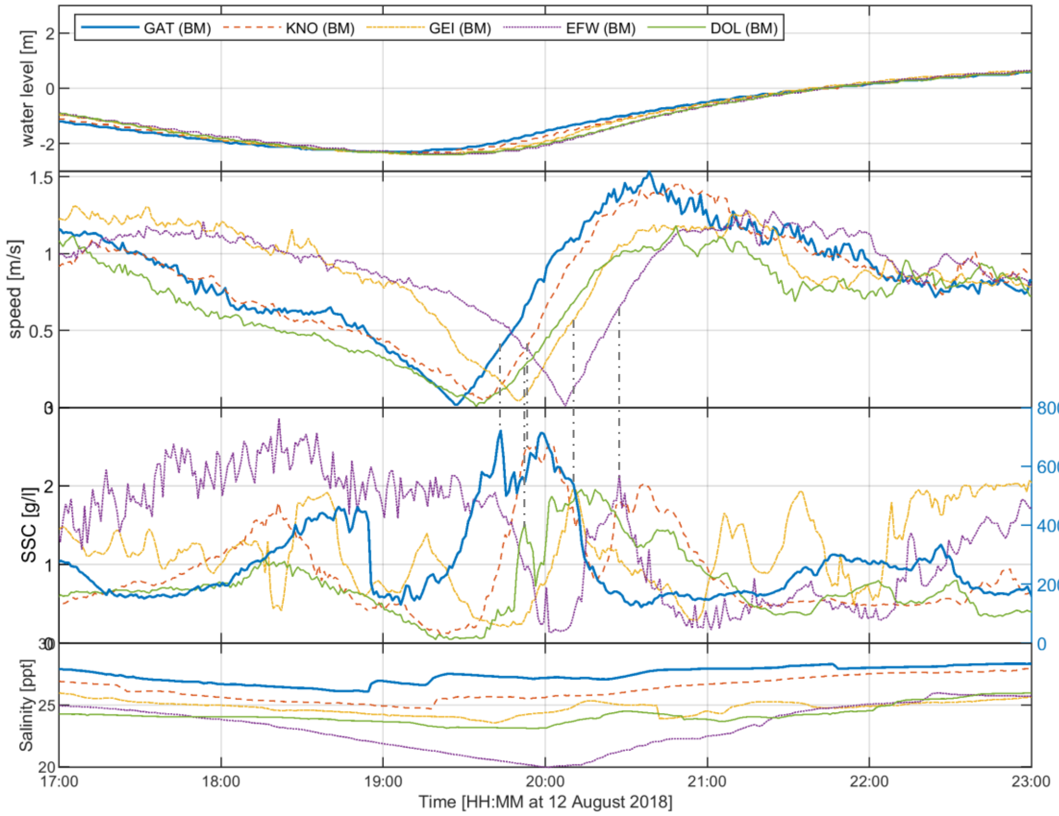

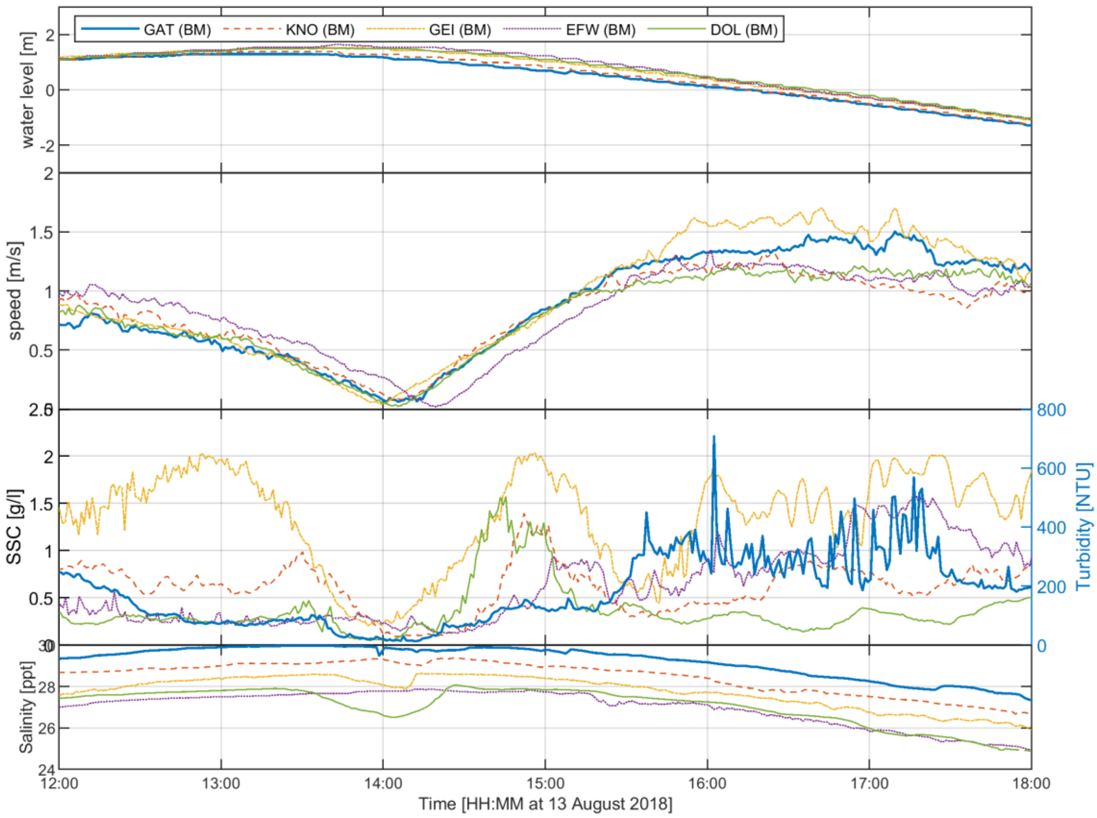

D.1.1.6. Sediment fluxes

At GAT (BM), the turbidity time series is too short (due to malfunctioning of the sensor) to compute a residual flux over a spring-neap tidal cycle.

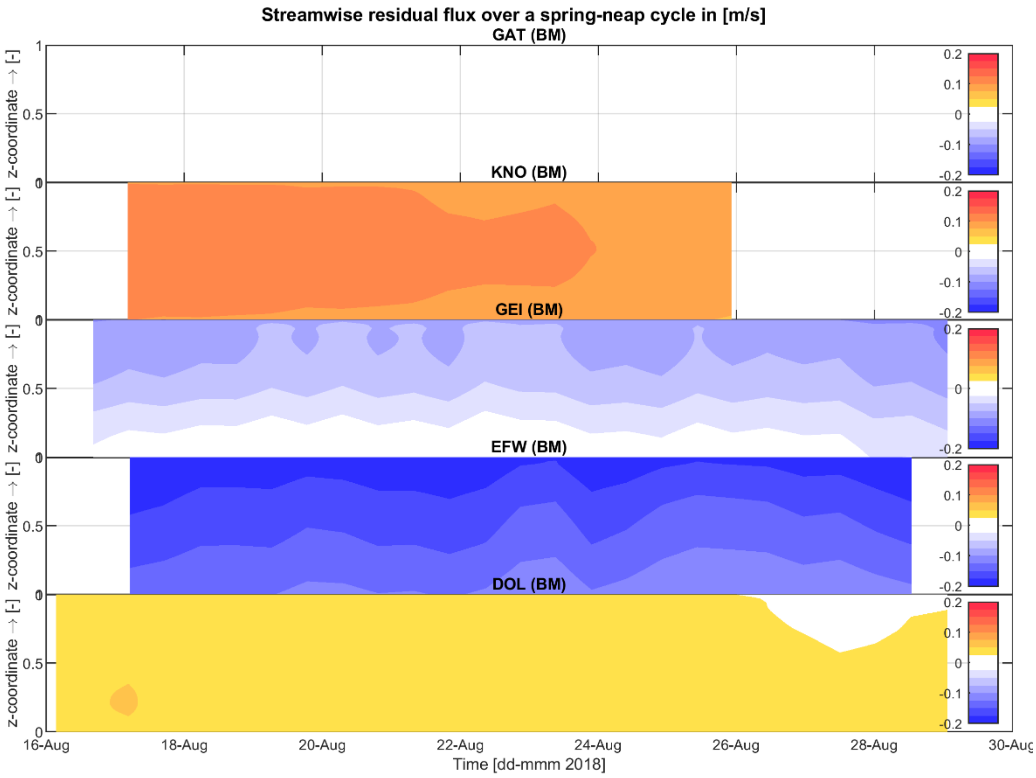
Streamwise residual flux over a spring-neap cycle in [m/s]
GAT (BM)
KNO (BM)
GEI (BM)
EFW (BM)
DOL (BM)
z-coordinate → [-]
0.2
0.1
0
-0.1
-0.2
16-Aug
18-Aug
20-Aug
22-Aug
24-Aug
26-Aug
28-Aug
30-Aug
Time [dd-mmm 2018]

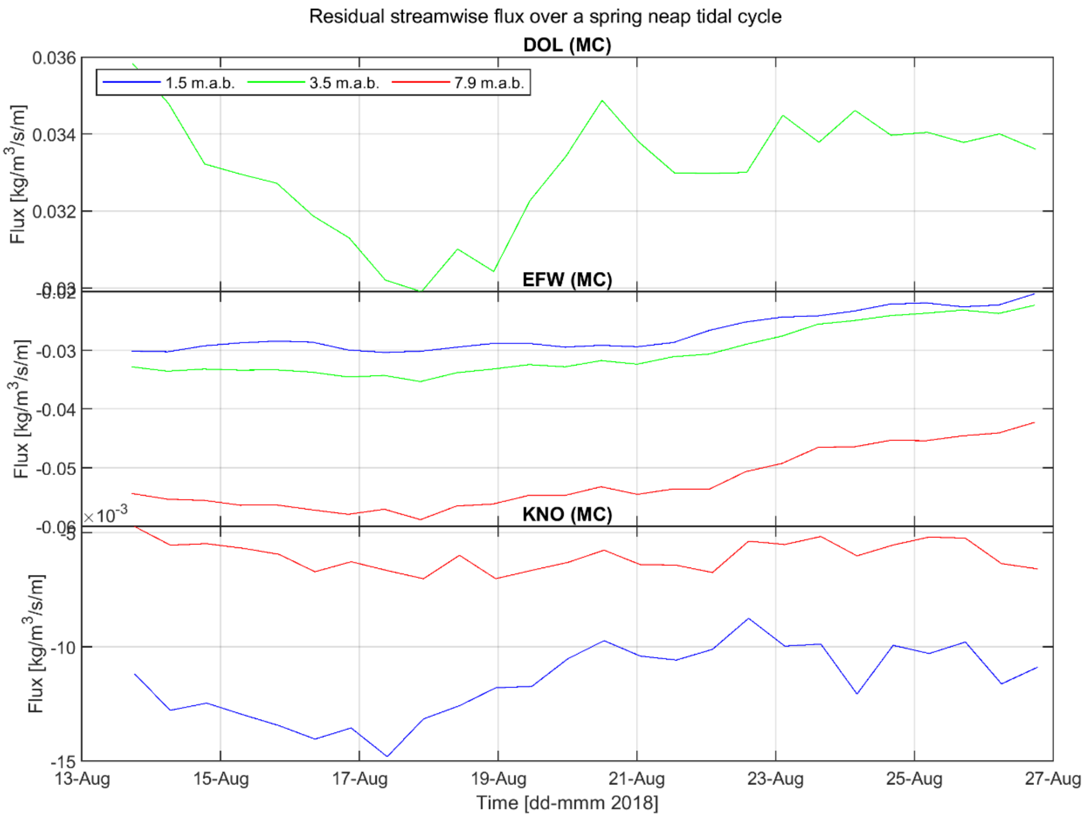
Residual streamwise flux over a spring neap tidal cycle
DOL (MC)
1.5 m.a.b.
3.5 m.a.b.
7.9 m.a.b.
EFW (MC)
KNO (MC)
Flux [kg/m^3/s/m]
×10^-3
13-Aug
15-Aug
17-Aug
19-Aug
21-Aug
23-Aug
25-Aug
27-Aug
Time [dd-mmm 2018]

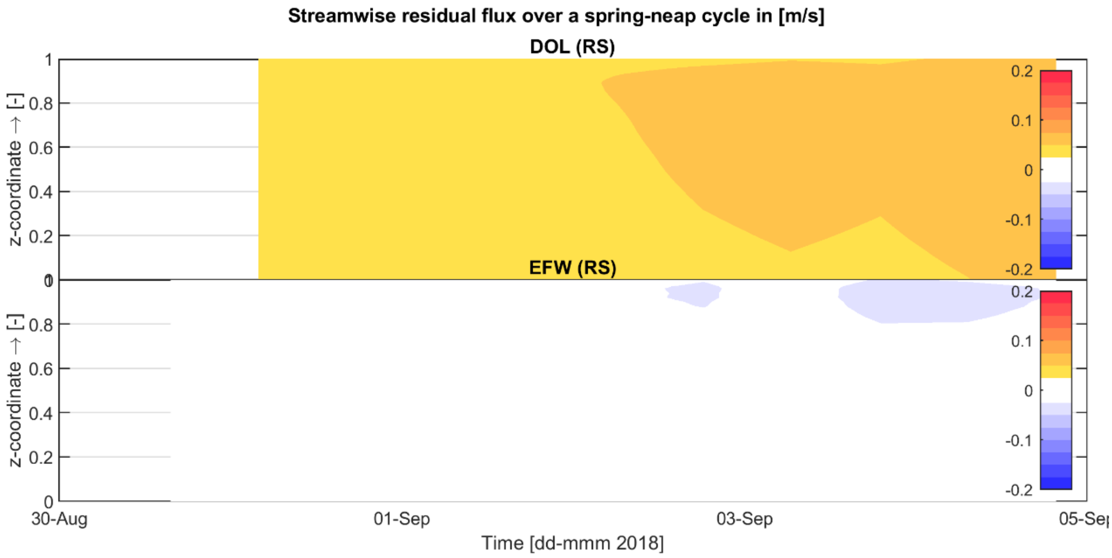

D.1.1.7. Time stack plots stream-, crosswise and upward velocities (13-hour measurements)

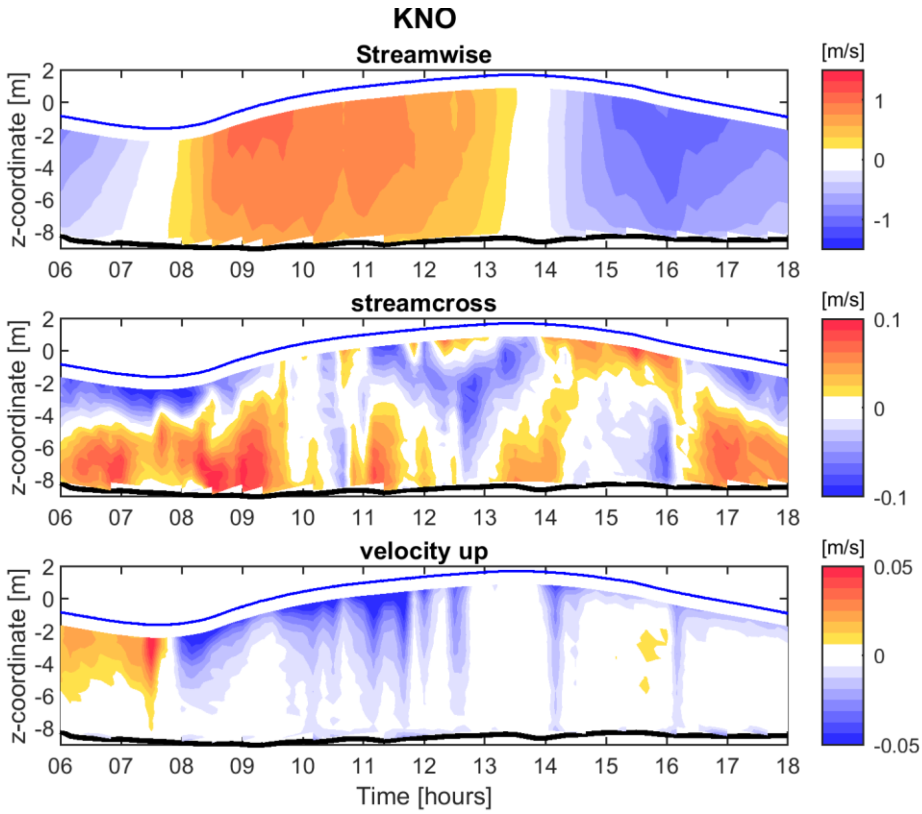

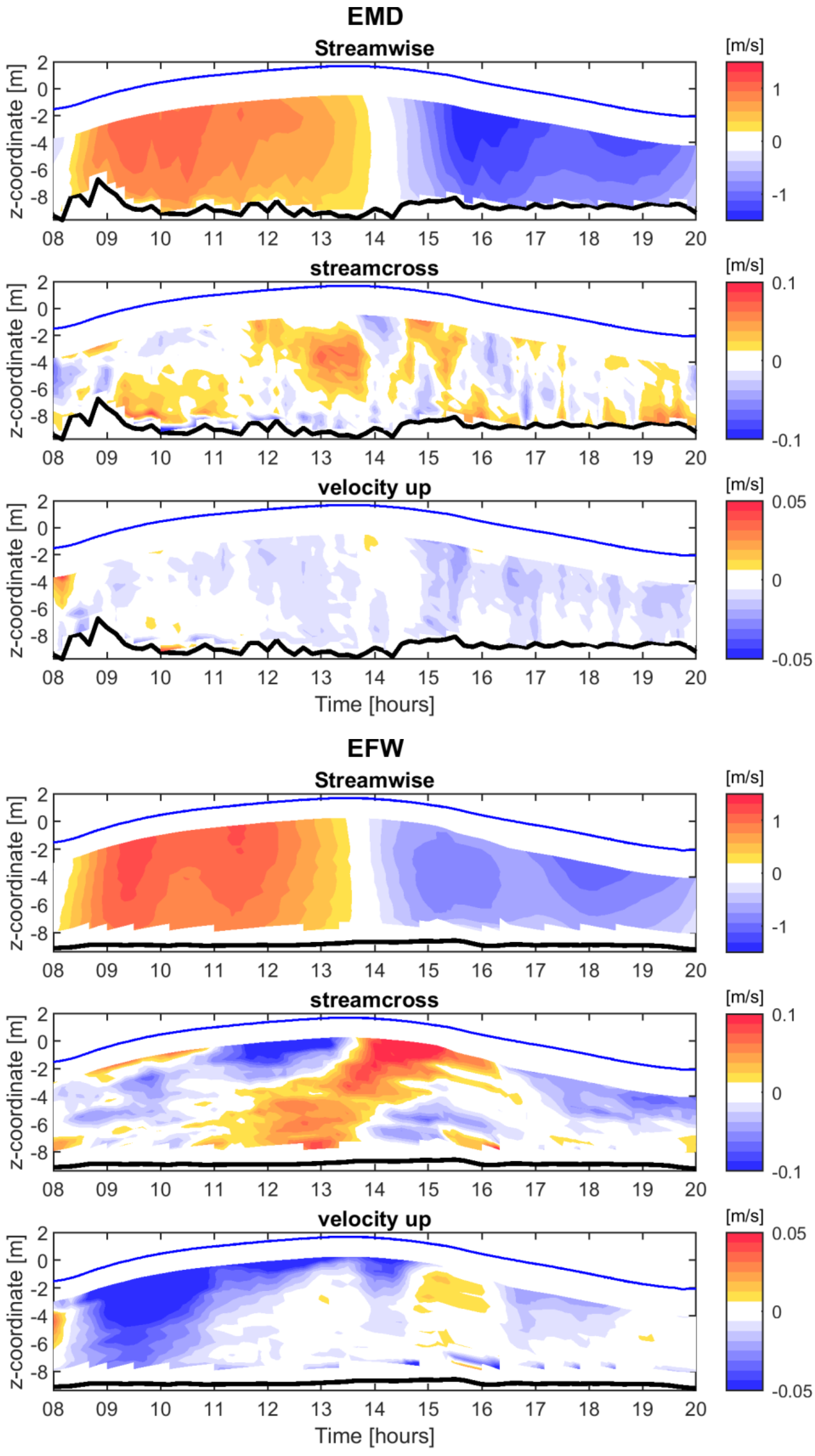
EMD
Streamwise
streamcross
velocity up
z-coordinate [m]
Time [hours]
[m/s]
EFW
Streamwise
streamcross
velocity up

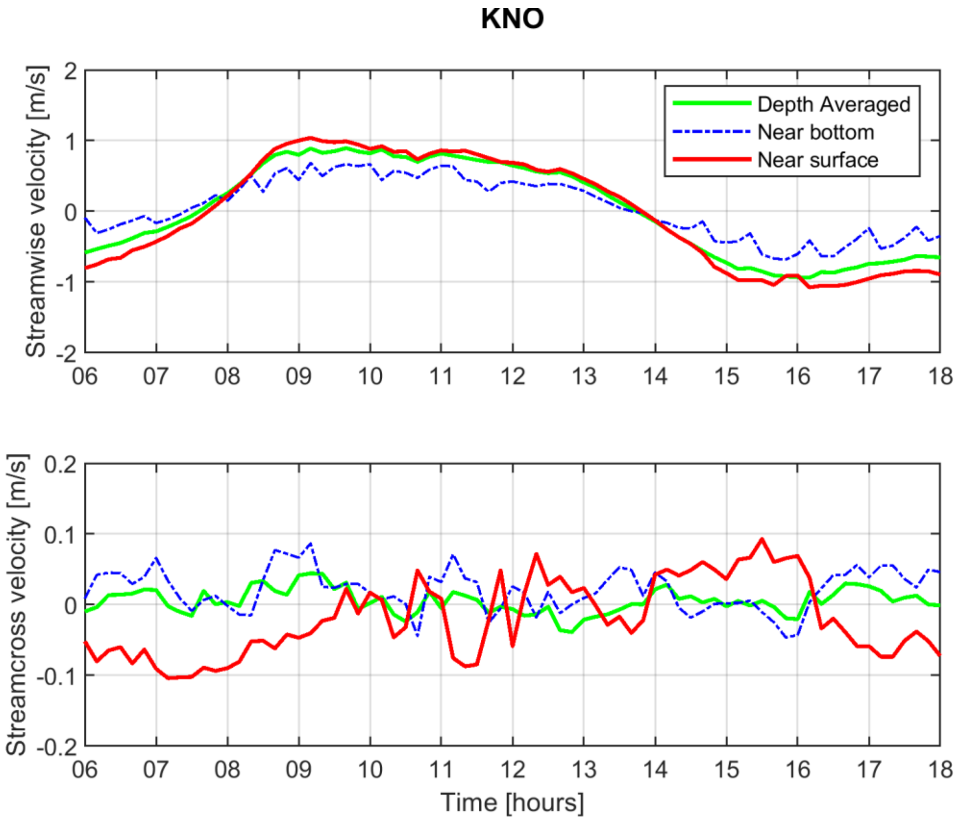
KNO
Streamwise velocity [m/s]
Depth Averaged
Near bottom
Near surface
Streamcross velocity [m/s]
Time [hours]

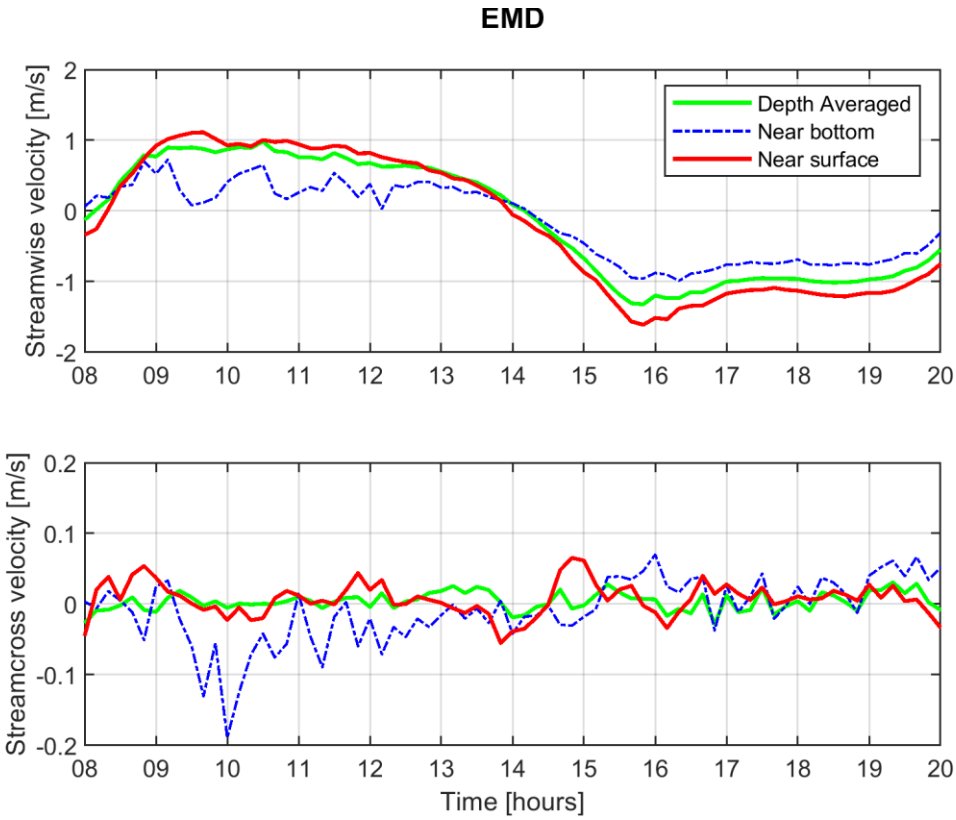
EMD
Streamwise velocity [m/s]
Depth Averaged
Near bottom
Near surface
Streamcross velocity [m/s]
Time [hours]

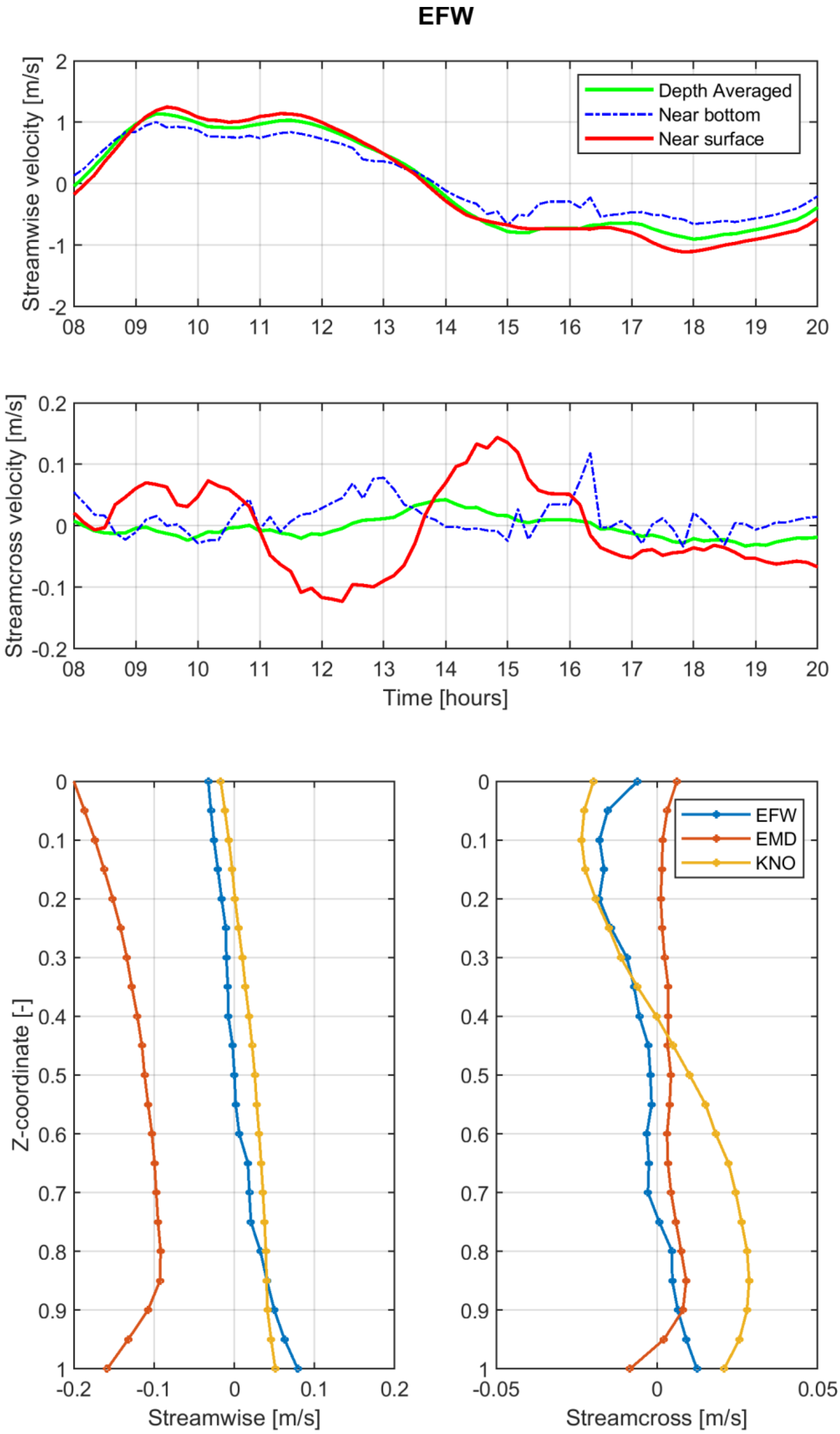

D.1.1.8. Time stack plots sediment concentrations and sediment flux (OBS)

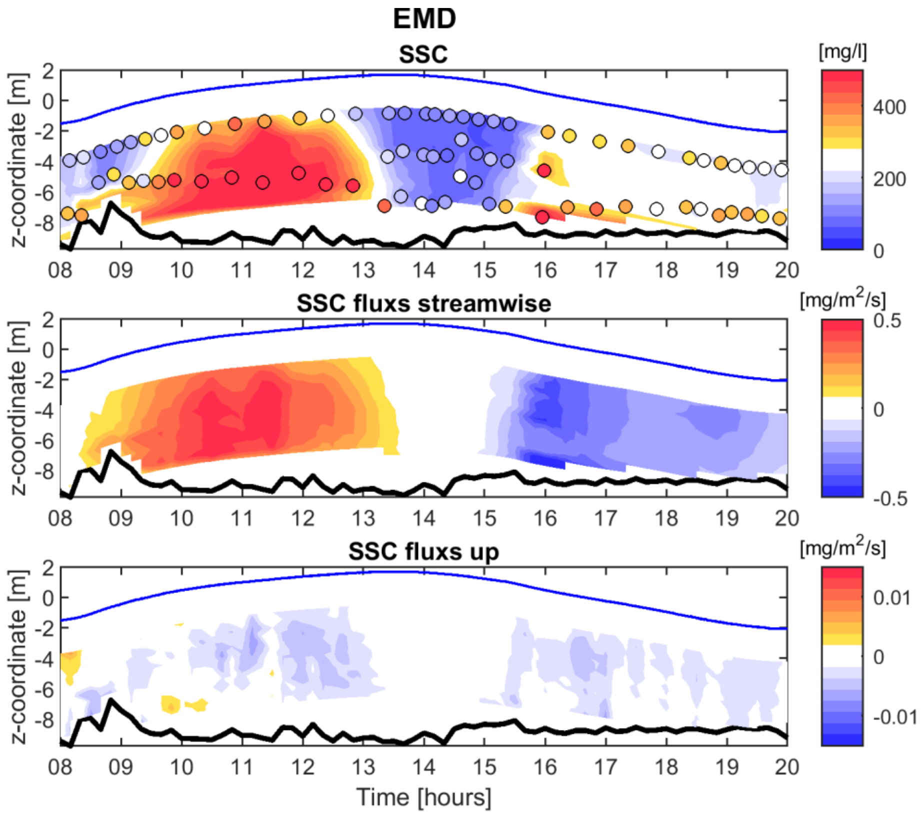

EMD
SSC
[mg/l]
SSC fluxs streamwise
[mg/m2/s]
SSC fluxs up
z-coordinate [m]
Time [hours]

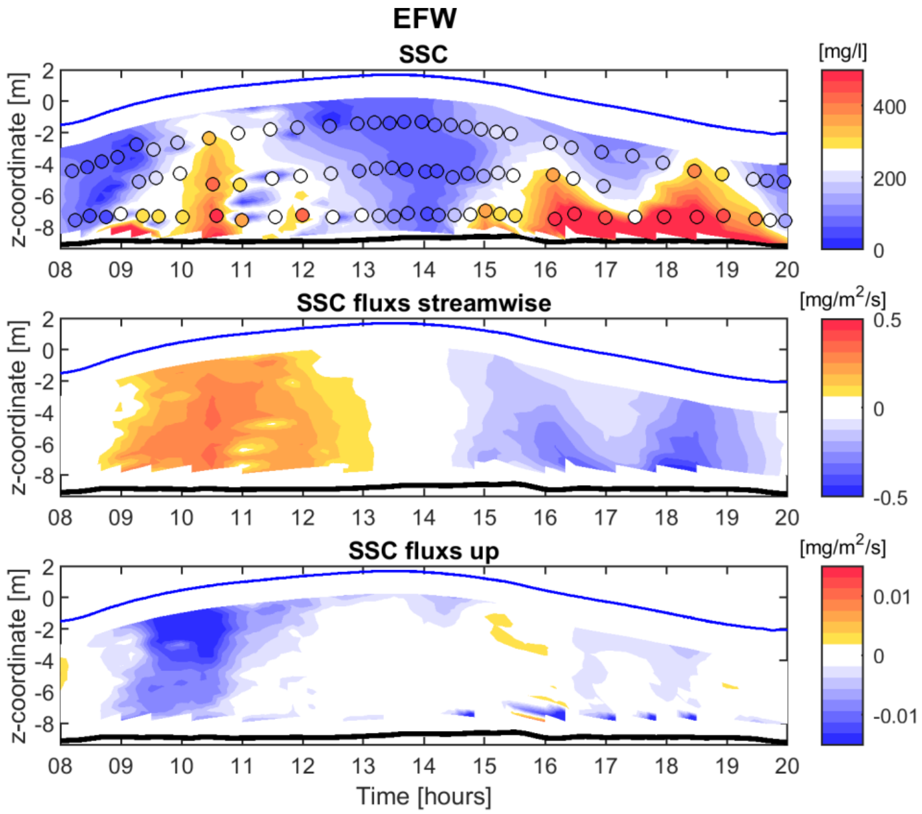

EFW
SSC
[mg/l]
SSC fluxs streamwise
[mg/m2/s]
SSC fluxs up
z-coordinate [m]
Time [hours]

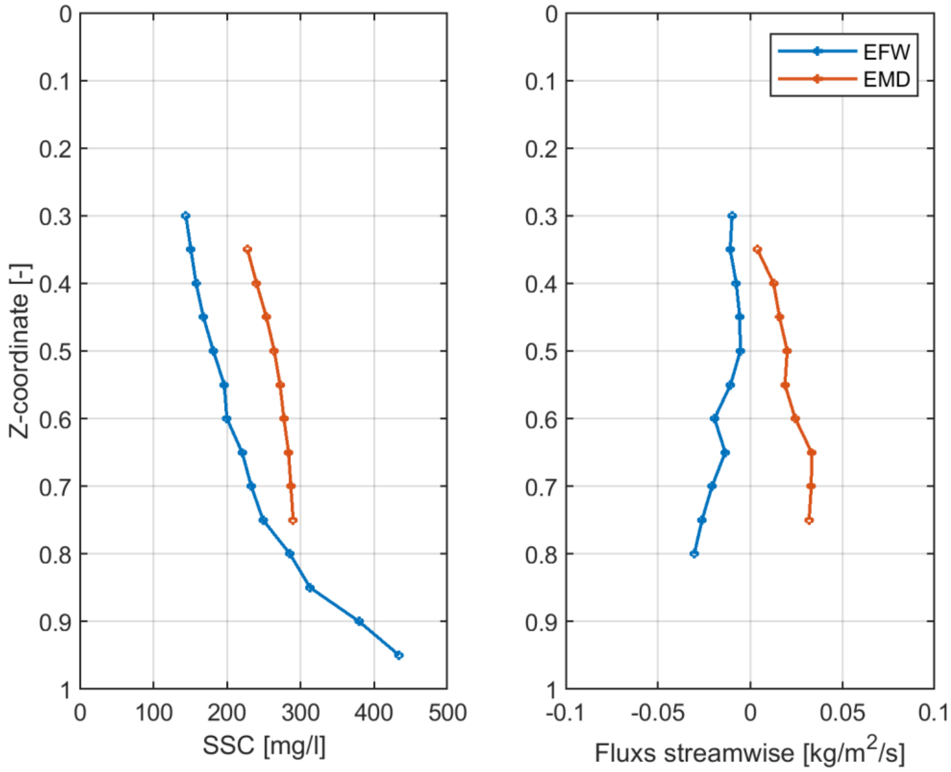

D.1.1.9. Time stack plots sediment concentrations and sediment flux (ADCP, echo intensity)

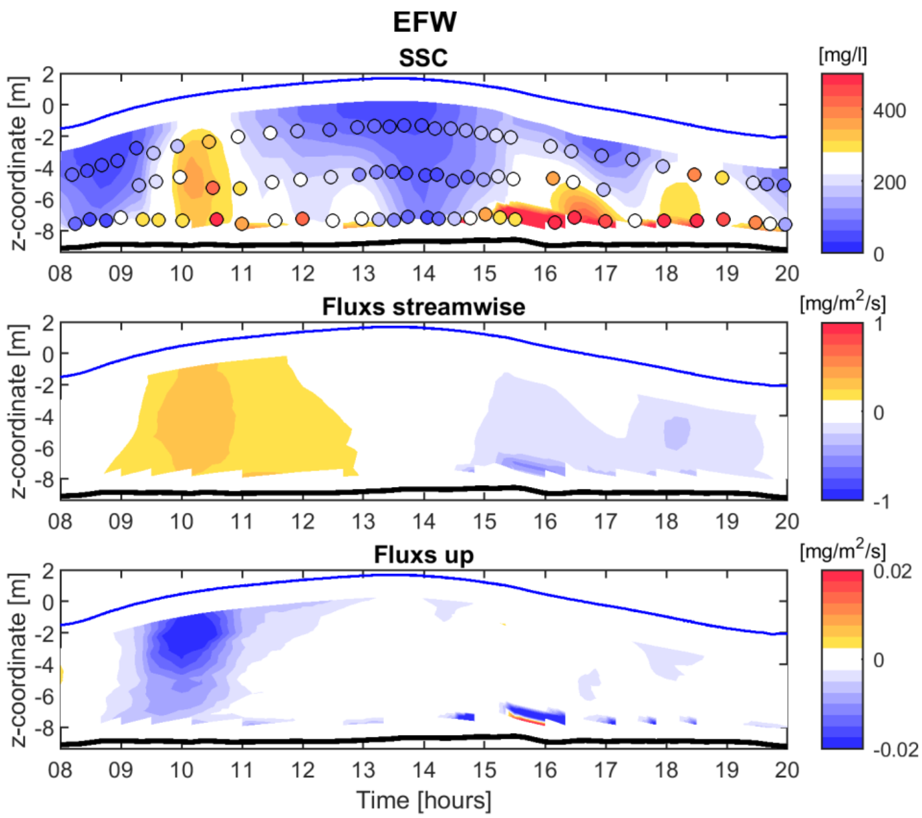

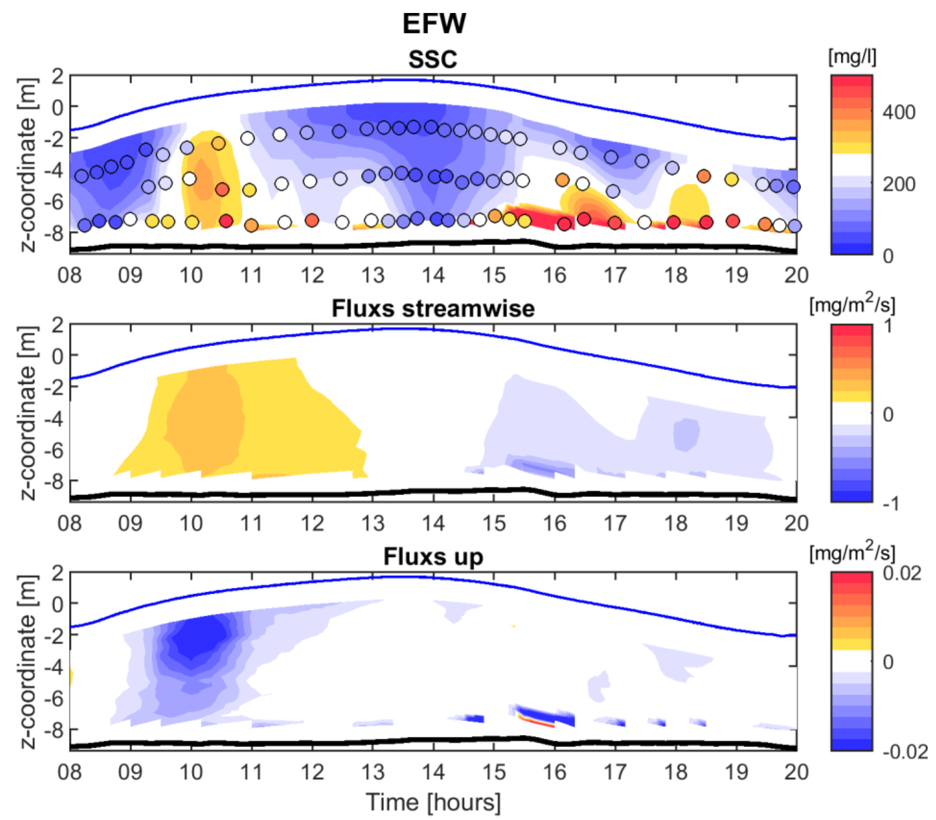
EFW
SSC
[mg/l]
Fluxs streamwise
[mg/m^2/s]
Fluxs up
[mg/m^2/s]
z-coordinate [m]
Time [hours]

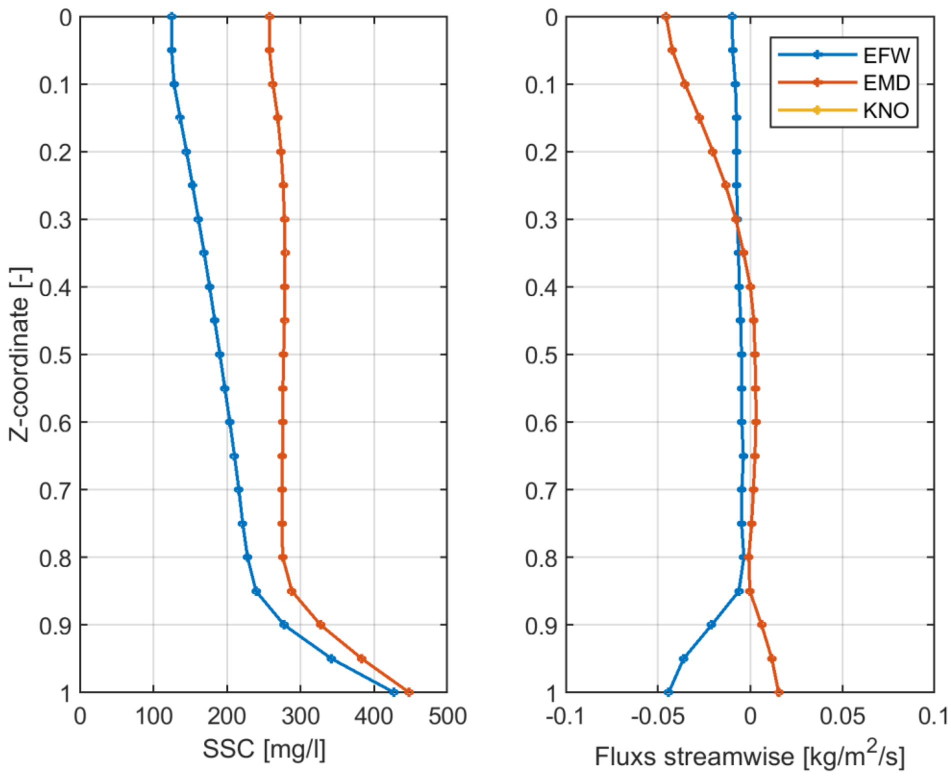
Z-coordinate [-]
SSC [mg/l]
Fluxs streamwise [kg/m^2/s]
EFW
EMD
KNO

D.1.1.10. Time stack plots salinity measurement (CTD data)

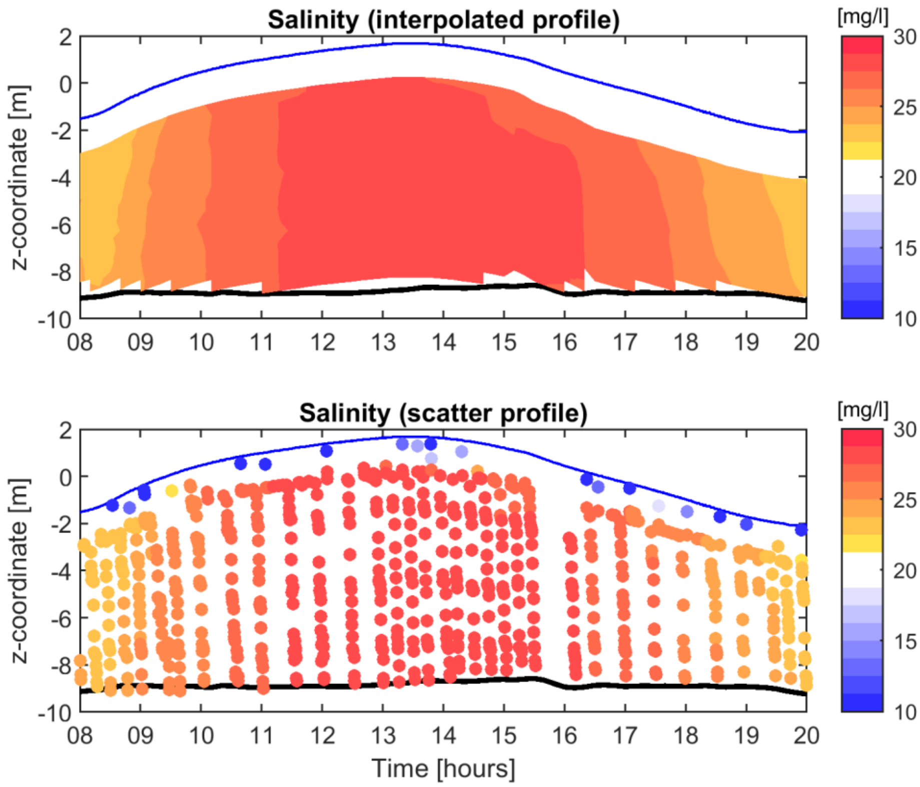

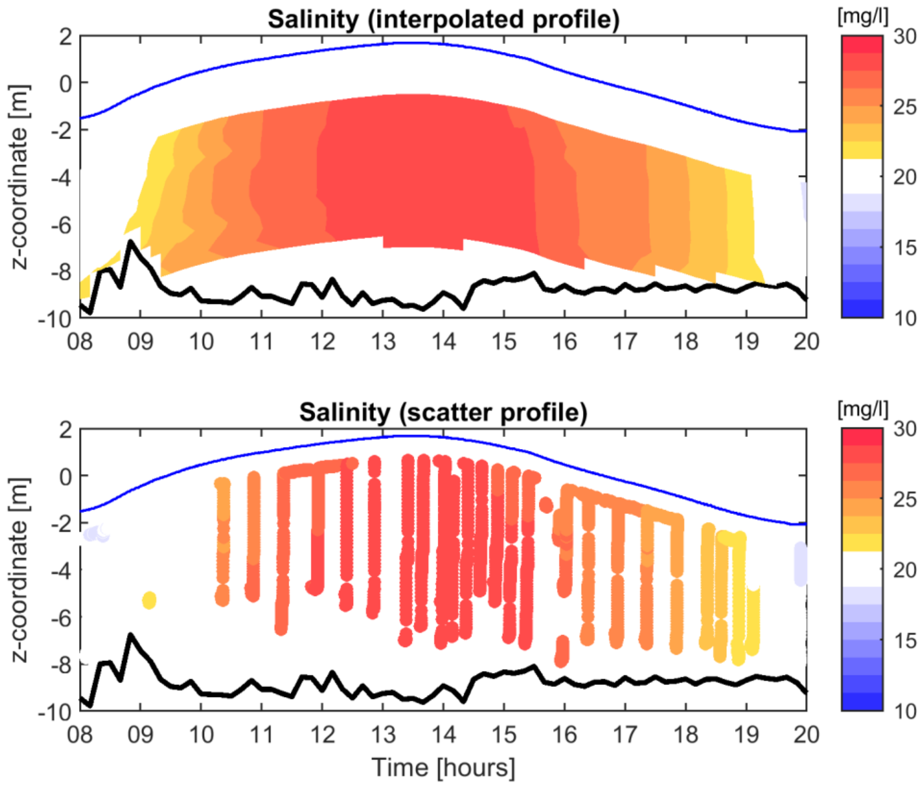

D.1.1.11. Stack plots cross-sectional measurement velocities and spatial suspended sediment variability

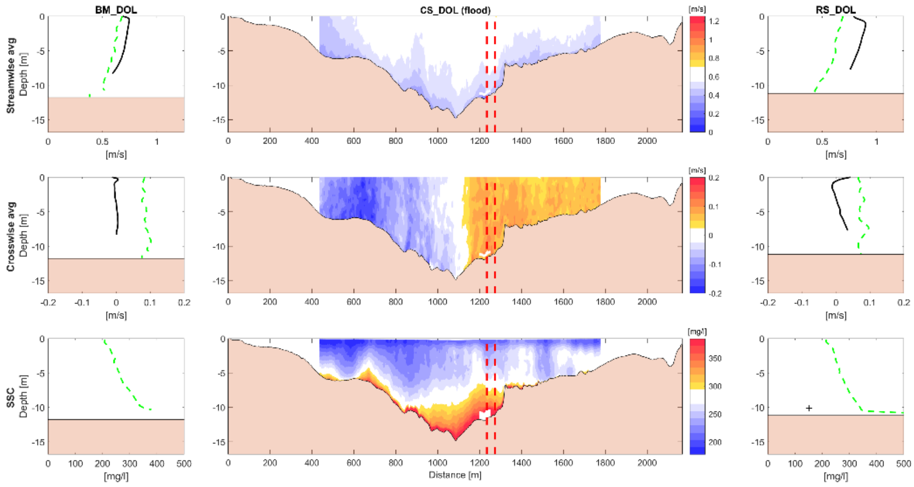

Longitudinal flow velocity (top), cross-sectional velocity (2nd panel) and SSC (based on echo intensity) (3rd panel), averaged over the flood period in the Dollard cross-section

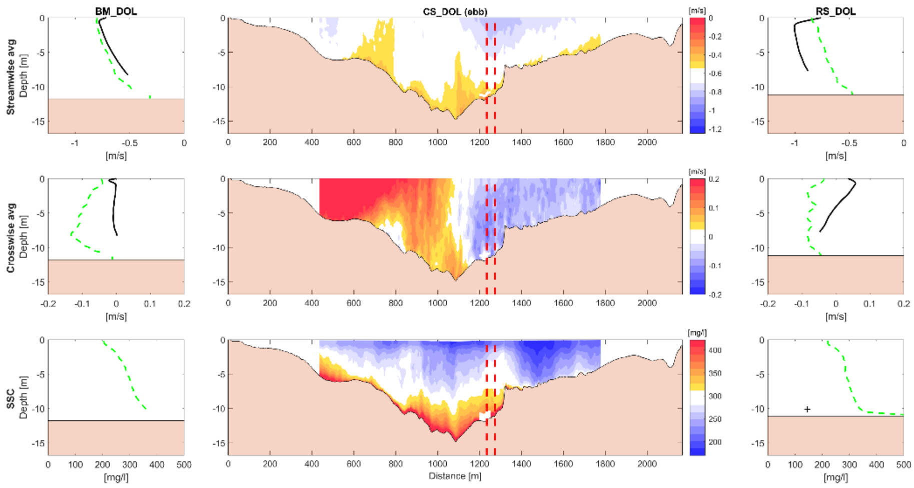

Longitudinal flow velocity (top), cross-sectional velocity (2nd panel) and SSC (based on echo intensity) (3rd panel), averaged over the ebb period in the Dollard cross-section

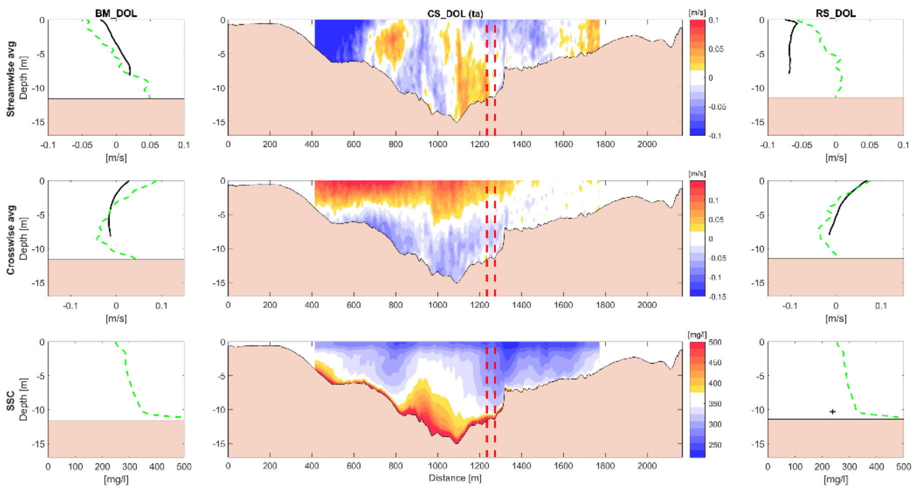

Longitudinal flow velocity (top), cross-sectional velocity (2nd panel) and SSC (based on echo intensity) (3rd panel), averaged over the full tidal period in the Dollard cross-section

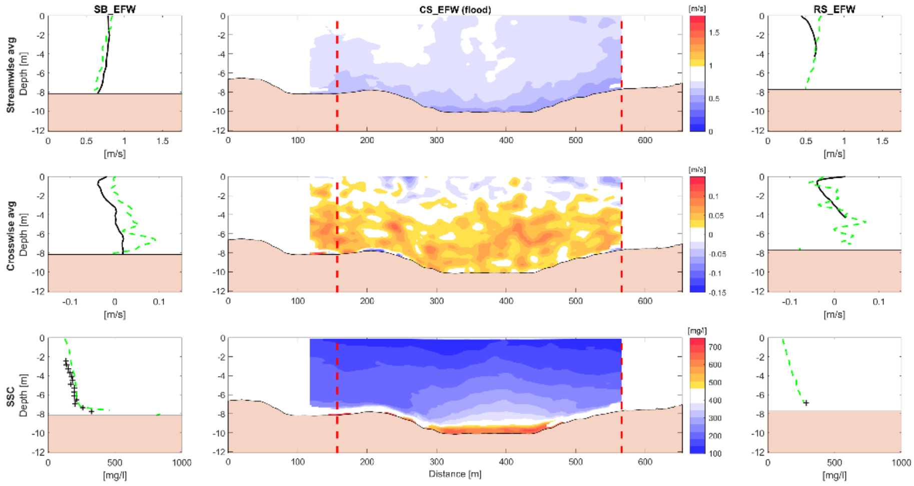

Longitudinal flow velocity (top), cross-sectional velocity (2nd panel) and SSC (based on echo intensity) (3rd panel), averaged over the flood period in the Emden Fairway cross-section

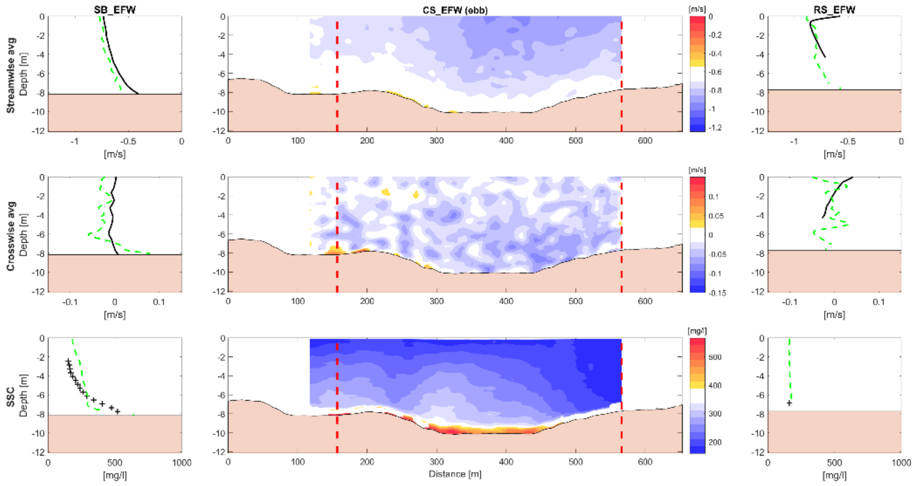

Longitudinal flow velocity (top), cross-sectional velocity (2nd panel) and SSC (based on echo intensity) (3rd panel), averaged over the ebb period in the Emden Fairway cross-section

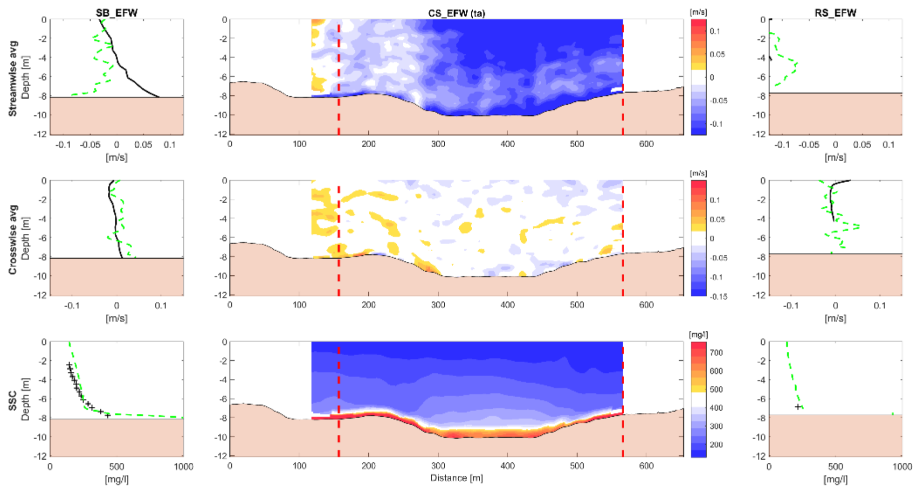

Longitudinal flow velocity (top), cross-sectional velocity (2nd panel) and SSC (based on echo intensity) (3rd panel), averaged over the full tidal period in the Emden Fairway cross-section

D.1.1.12. Stack plots cross-sectional measurement sediment fluxes and spatial suspended sediment variability.

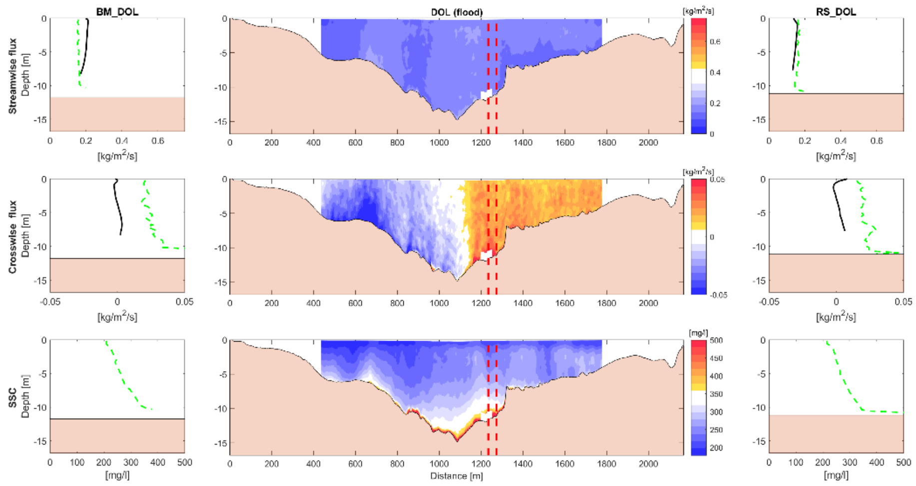

Longitudinal sediment flux (top), cross-sectional sediment flux (2nd panel) and SSC (based on echo intensity) (3rd panel), averaged over the flood period in the Dollard cross-section

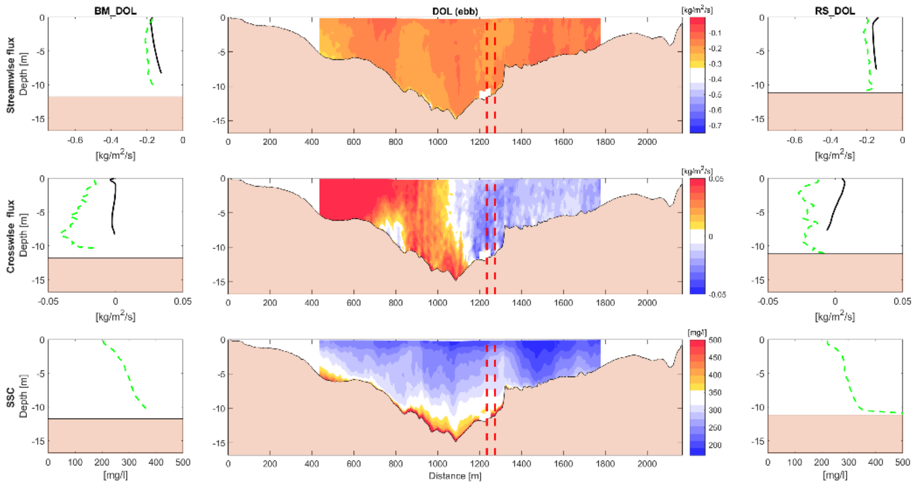

Longitudinal sediment flux (top), cross-sectional sediment flux (2nd panel) and SSC (based on echo intensity) (3rd panel), averaged over the ebb period in the Dollard cross-section

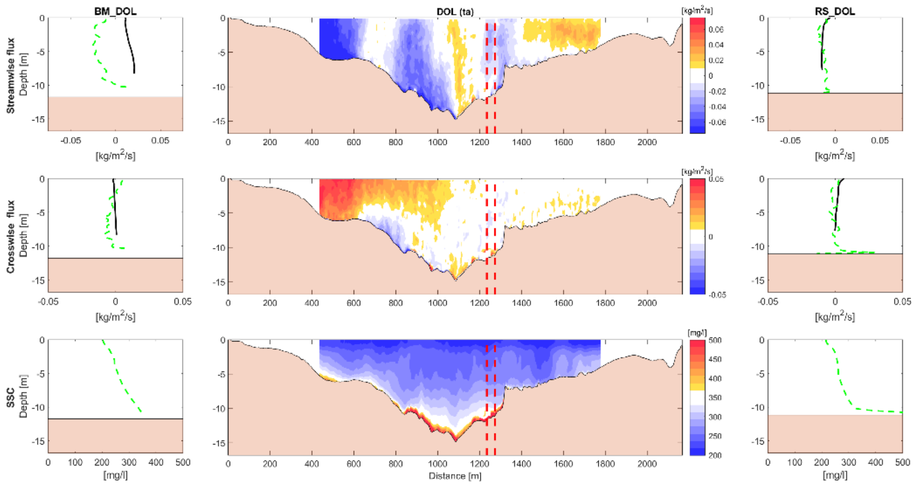

Longitudinal sediment flux (top), cross-sectional sediment flux (2nd panel) and SSC (based on echo intensity) (3rd panel), averaged over the full tidal period in the Dollard cross-section

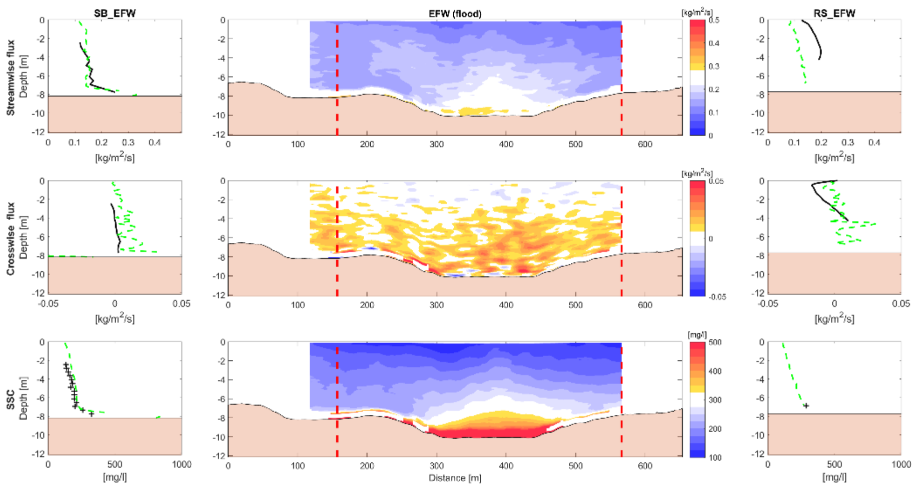

Longitudinal sediment flux (top), cross-sectional sediment flux (2nd panel) and SSC (based on echo intensity) (3rd panel), averaged over the flood period in the Emden Fairway cross-section

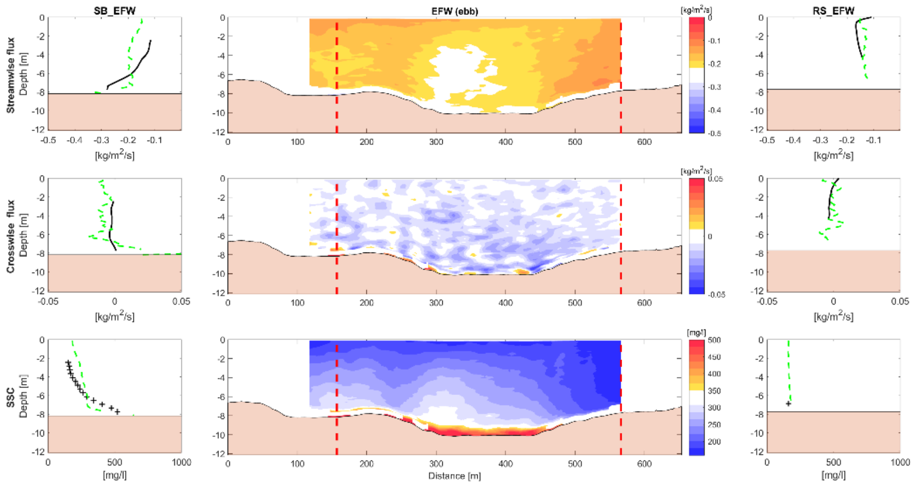

Longitudinal sediment flux (top), cross-sectional sediment flux (2nd panel) and SSC (based on echo intensity) (3rd panel), averaged over the ebb period in the Emden Fairway cross-section

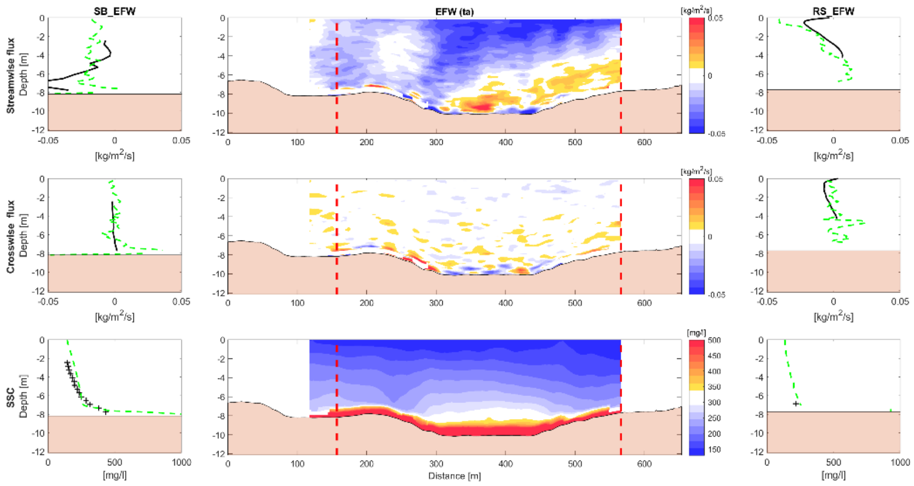

Longitudinal sediment flux (top), cross-sectional sediment flux (2nd panel) and SSC (based on echo intensity) (3rd panel), averaged over the full tidal period in the Emden Fairway cross-section

D.1.1.13. Longitudinal survey of turbidity and salinity

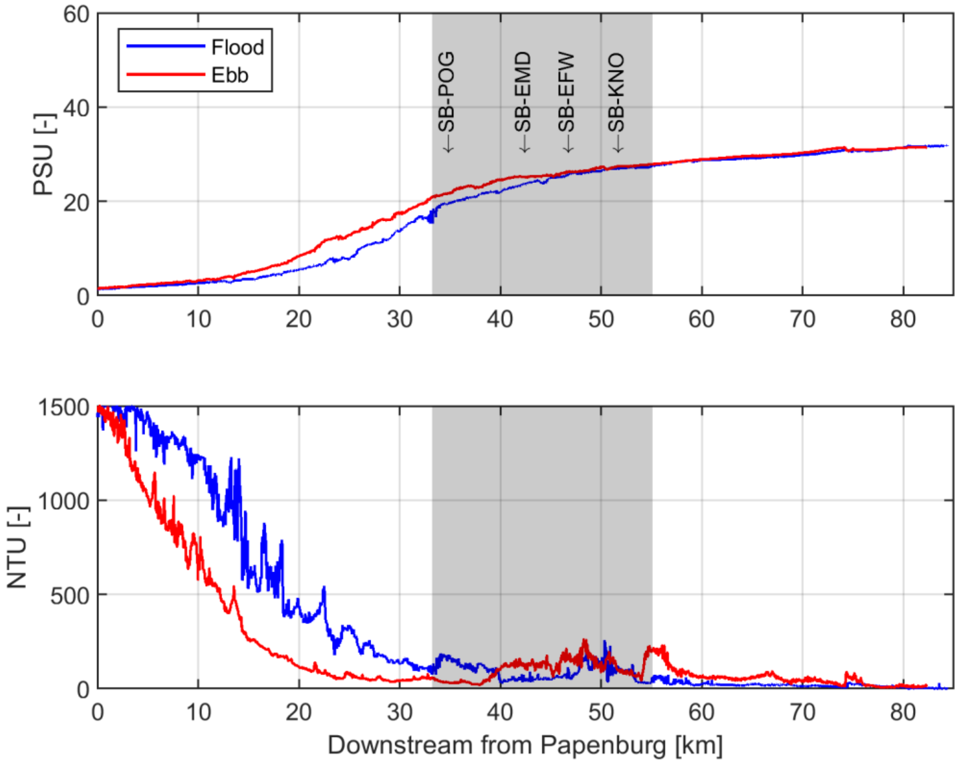

Salinity (in psu) and turbidity (in ntu) measured near-surface during the longitudinal cross-section between Papenburg and Borkum, measured on 28 August 2018

D.2 January 2019

D.2.1.1. Streamwise velocities

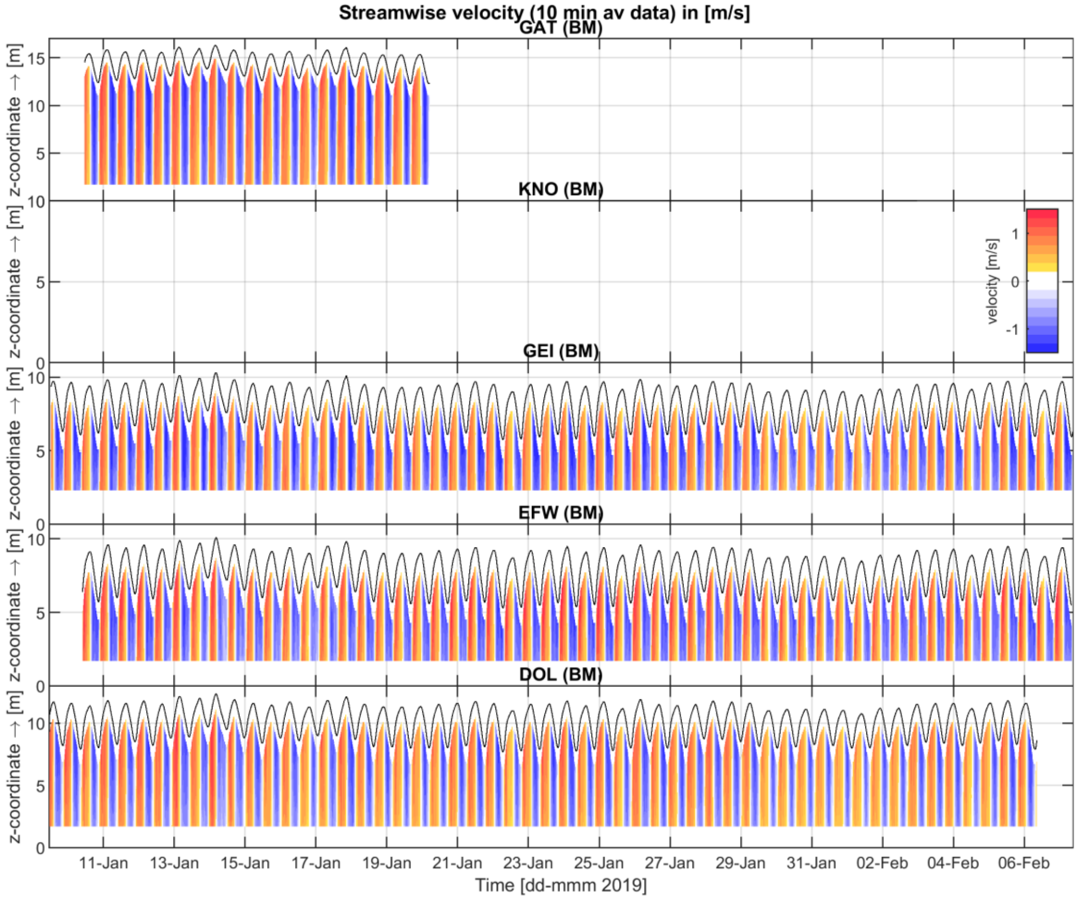
Streamwise velocity (10 min av data) in [m/s]
GAT (BM)
KNO (BM)
GEI (BM)
EFW (BM)
DOL (BM)
z-coordinate → [m]
velocity [m/s]
11-Jan
13-Jan
15-Jan
17-Jan
19-Jan
21-Jan
23-Jan
25-Jan
27-Jan
29-Jan
31-Jan
02-Feb
04-Feb
06-Feb
Time [dd-mmm 2019]

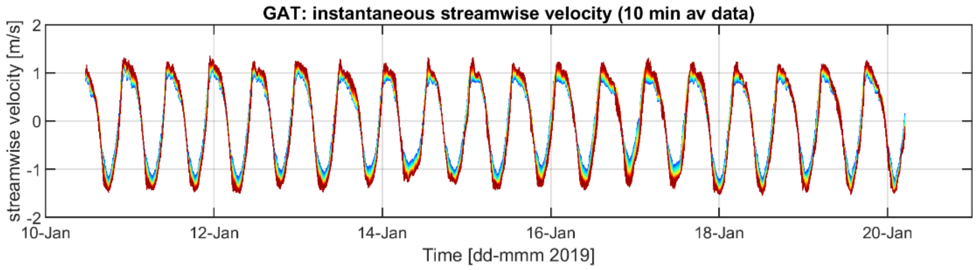
GAT: instantaneous streamwise velocity (10 min av data)
streamwise velocity [m/s]
10-Jan
12-Jan
14-Jan
16-Jan
18-Jan
20-Jan
Time [dd-mmm 2019]

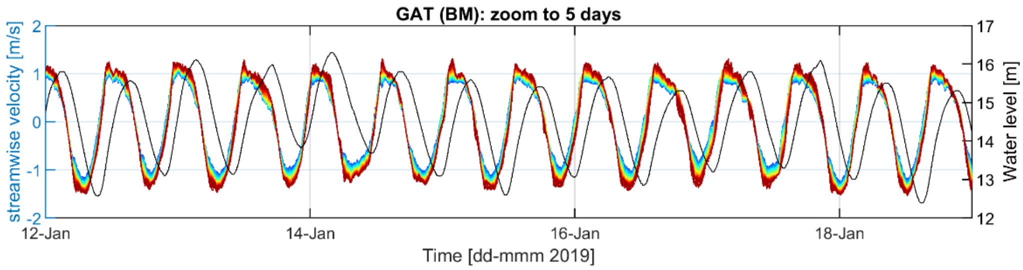
GAT (BM): zoom to 5 days
streamwise velocity [m/s]
Water level [m]
12-Jan
14-Jan
16-Jan
18-Jan
Time [dd-mmm 2019]

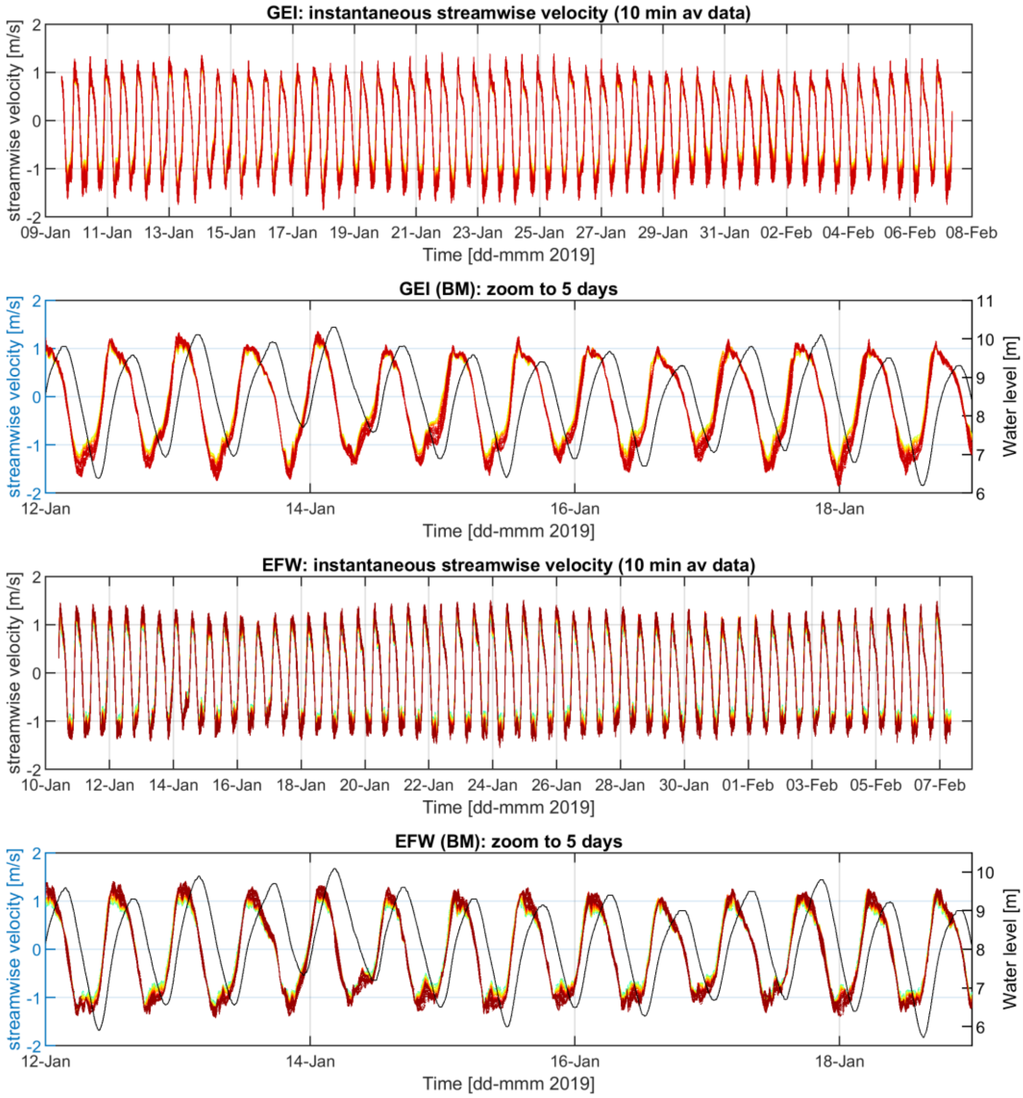
GEI: instantaneous streamwise velocity (10 min av data)
streamwise velocity [m/s]
Time [dd-mmm 2019]
GEI (BM): zoom to 5 days
streamwise velocity [m/s]
Water level [m]
Time [dd-mmm 2019]
EFW: instantaneous streamwise velocity (10 min av data)
streamwise velocity [m/s]
Time [dd-mmm 2019]
EFW (BM): zoom to 5 days
streamwise velocity [m/s]
Water level [m]
Time [dd-mmm 2019]

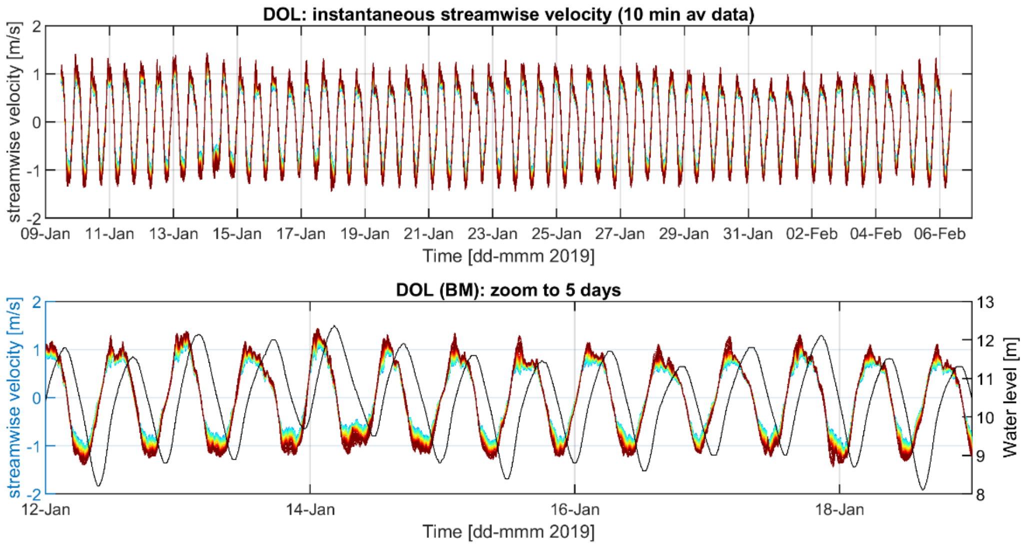
DOL: instantaneous streamwise velocity (10 min av data)
streamwise velocity [m/s]
Time [dd-mmm 2019]
DOL (BM): zoom to 5 days
streamwise velocity [m/s]
Water level [m]
Time [dd-mmm 2019]

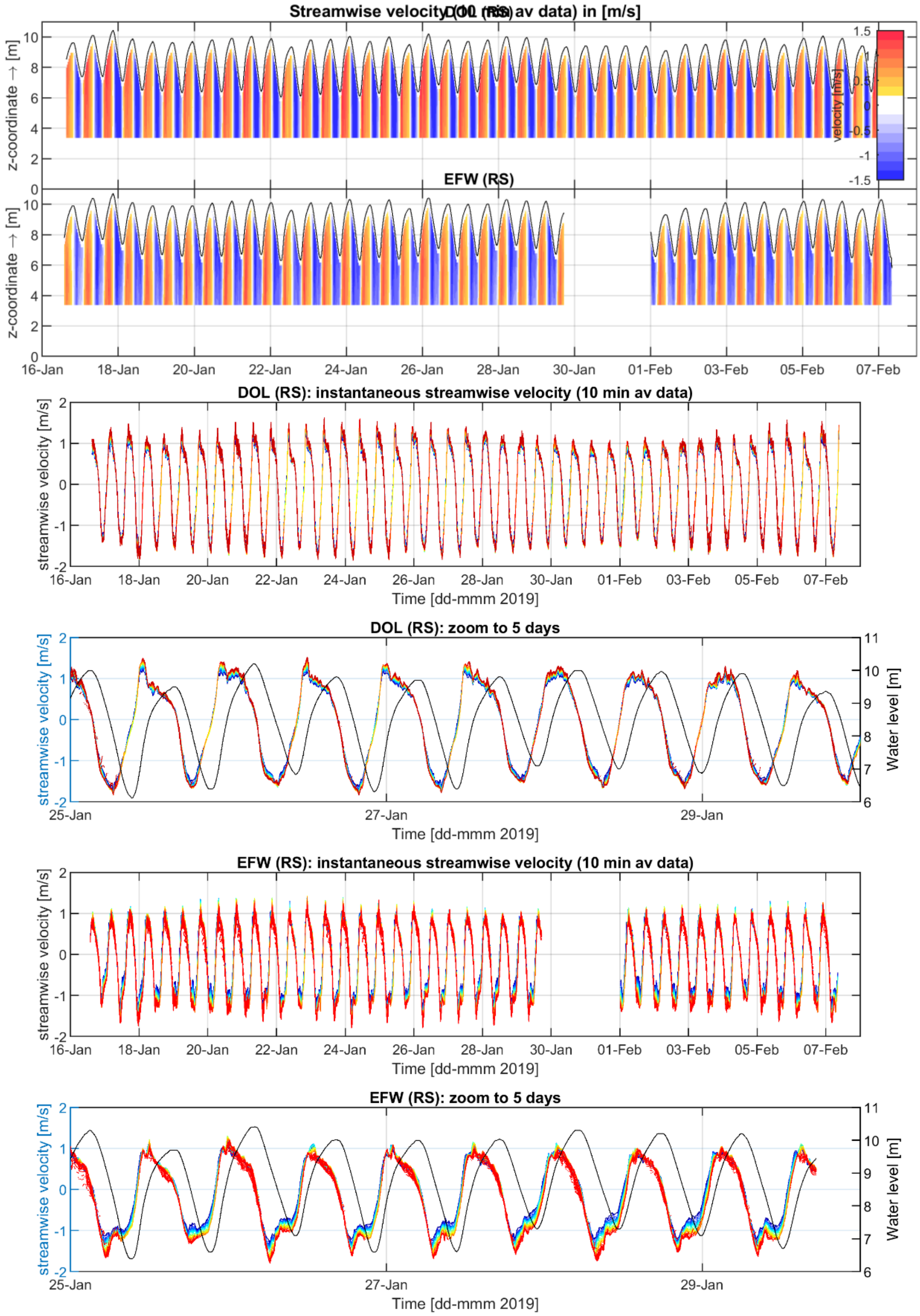
Streamwise velocity (10 min av data) in [m/s]
DOL (RS)
z-coordinate → [m]
velocity [m/s]
EFW (RS)
16-Jan 18-Jan 20-Jan 22-Jan 24-Jan 26-Jan 28-Jan 30-Jan 01-Feb 03-Feb 05-Feb 07-Feb
DOL (RS): instantaneous streamwise velocity (10 min av data)
streamwise velocity [m/s]
Time [dd-mmm 2019]
DOL (RS): zoom to 5 days
Water level [m]
25-Jan 27-Jan 29-Jan
EFW (RS): instantaneous streamwise velocity (10 min av data)
EFW (RS): zoom to 5 days

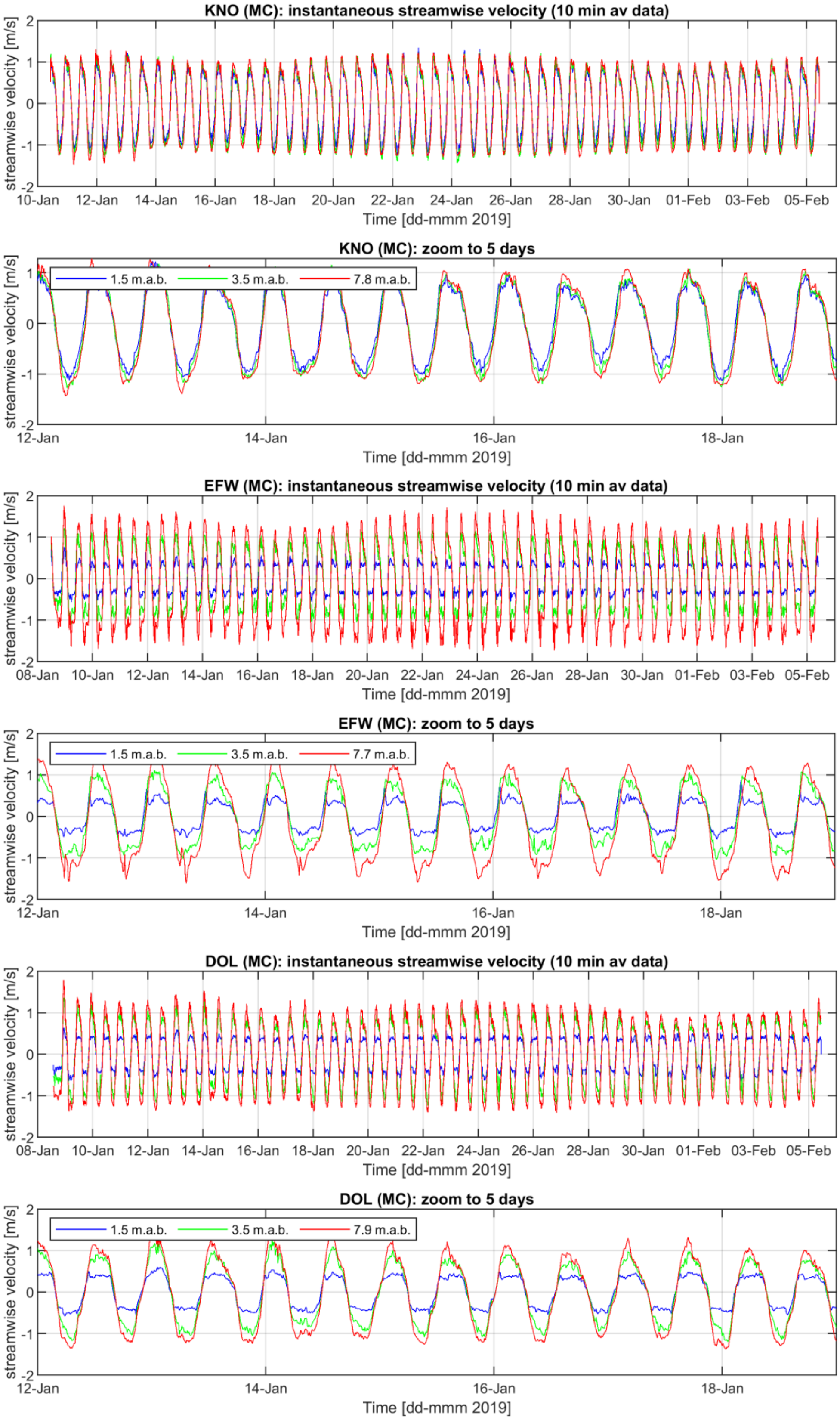
KNO (MC): instantaneous streamwise velocity (10 min av data)
streamwise velocity [m/s]
Time [dd-mmm 2019]
10-Jan 12-Jan 14-Jan 16-Jan 18-Jan 20-Jan 22-Jan 24-Jan 26-Jan 28-Jan 30-Jan 01-Feb 03-Feb 05-Feb
KNO (MC): zoom to 5 days
1.5 m.a.b.
3.5 m.a.b.
7.8 m.a.b.
12-Jan 14-Jan 16-Jan 18-Jan
EFW (MC): instantaneous streamwise velocity (10 min av data)
08-Jan 10-Jan 12-Jan 14-Jan 16-Jan 18-Jan 20-Jan 22-Jan 24-Jan 26-Jan 28-Jan 30-Jan 01-Feb 03-Feb 05-Feb
EFW (MC): zoom to 5 days
1.5 m.a.b.
3.5 m.a.b.
7.7 m.a.b.
DOL (MC): instantaneous streamwise velocity (10 min av data)
DOL (MC): zoom to 5 days
1.5 m.a.b.
3.5 m.a.b.
7.9 m.a.b.

D.2.1.2. Streamcross velocities

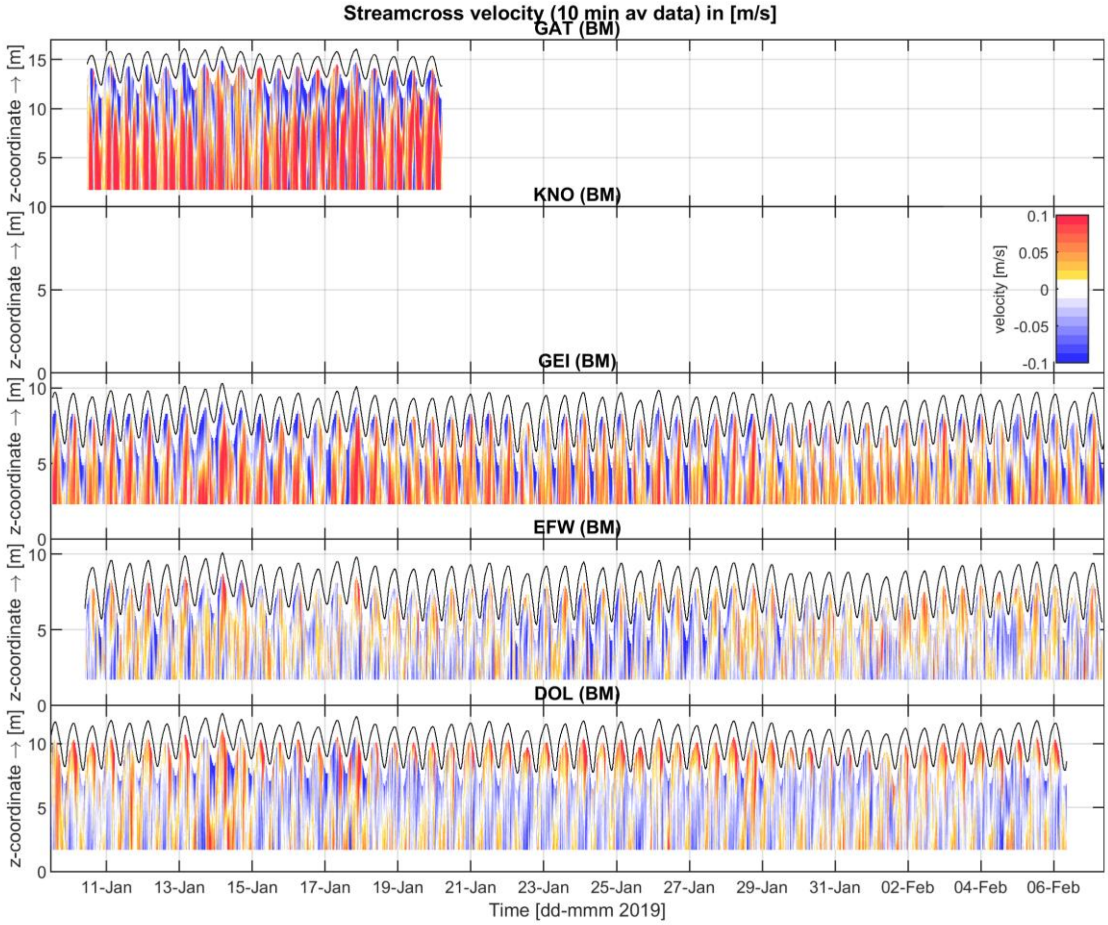

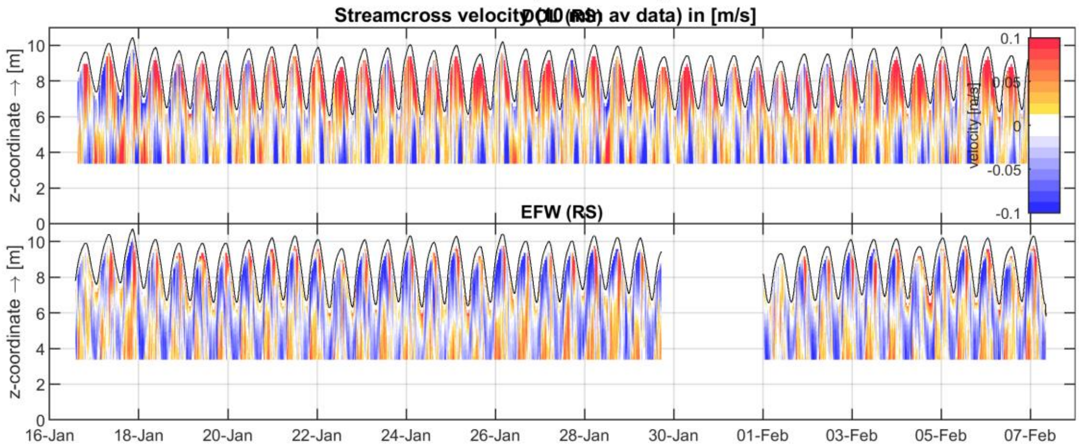

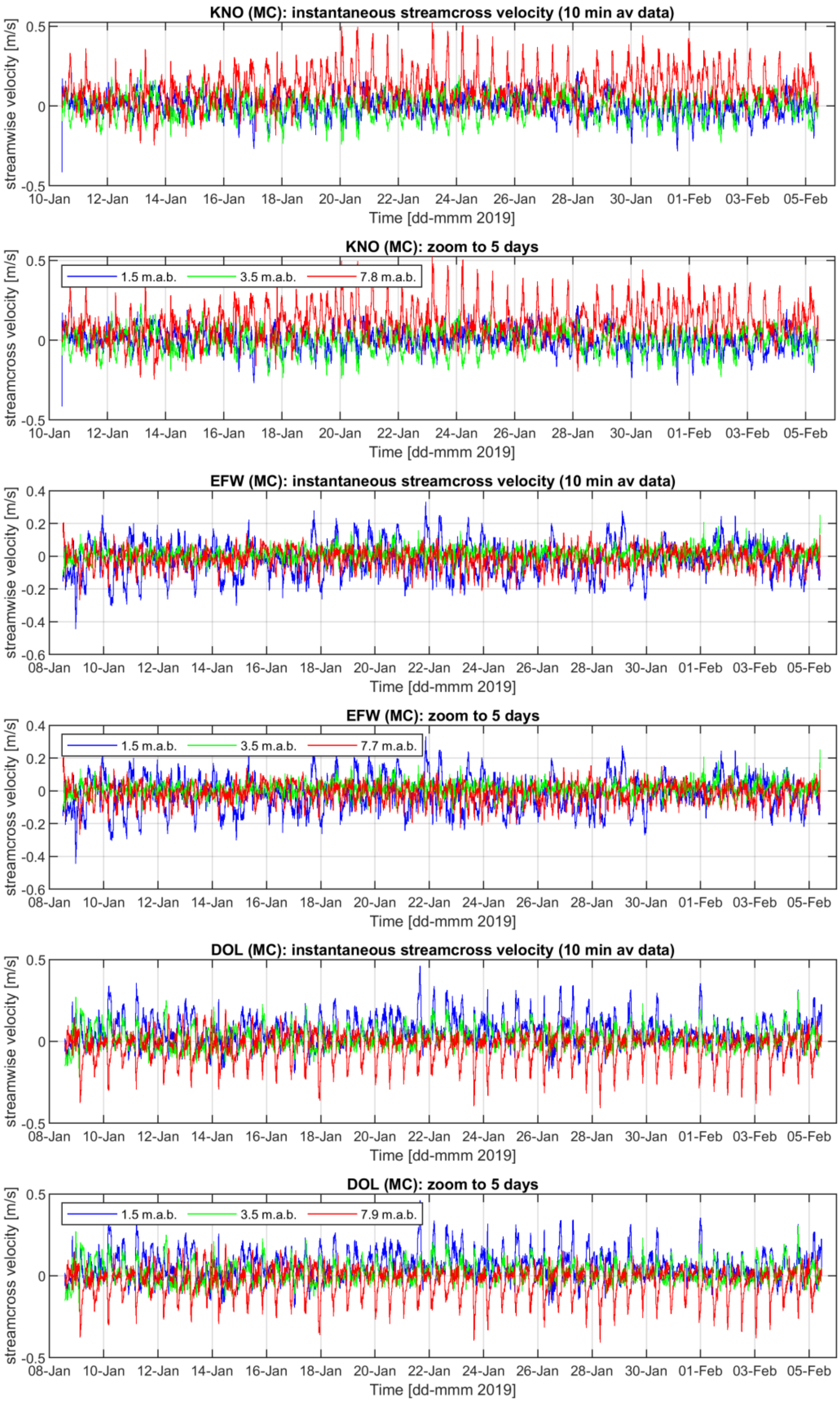
KNO (MC): instantaneous streamcross velocity (10 min av data)
streamwise velocity [m/s]
Time [dd-mmm 2019]
KNO (MC): zoom to 5 days
1.5 m.a.b.
3.5 m.a.b.
7.8 m.a.b.
streamcross velocity [m/s]
Time [dd-mmm 2019]
EFW (MC): instantaneous streamcross velocity (10 min av data)
streamwise velocity [m/s]
Time [dd-mmm 2019]
EFW (MC): zoom to 5 days
1.5 m.a.b.
3.5 m.a.b.
7.7 m.a.b.
streamcross velocity [m/s]
Time [dd-mmm 2019]
DOL (MC): instantaneous streamcross velocity (10 min av data)
streamwise velocity [m/s]
Time [dd-mmm 2019]
DOL (MC): zoom to 5 days
1.5 m.a.b.
3.5 m.a.b.
7.9 m.a.b.
streamcross velocity [m/s]
Time [dd-mmm 2019]

D.2.1.3. Sub-tidal flows

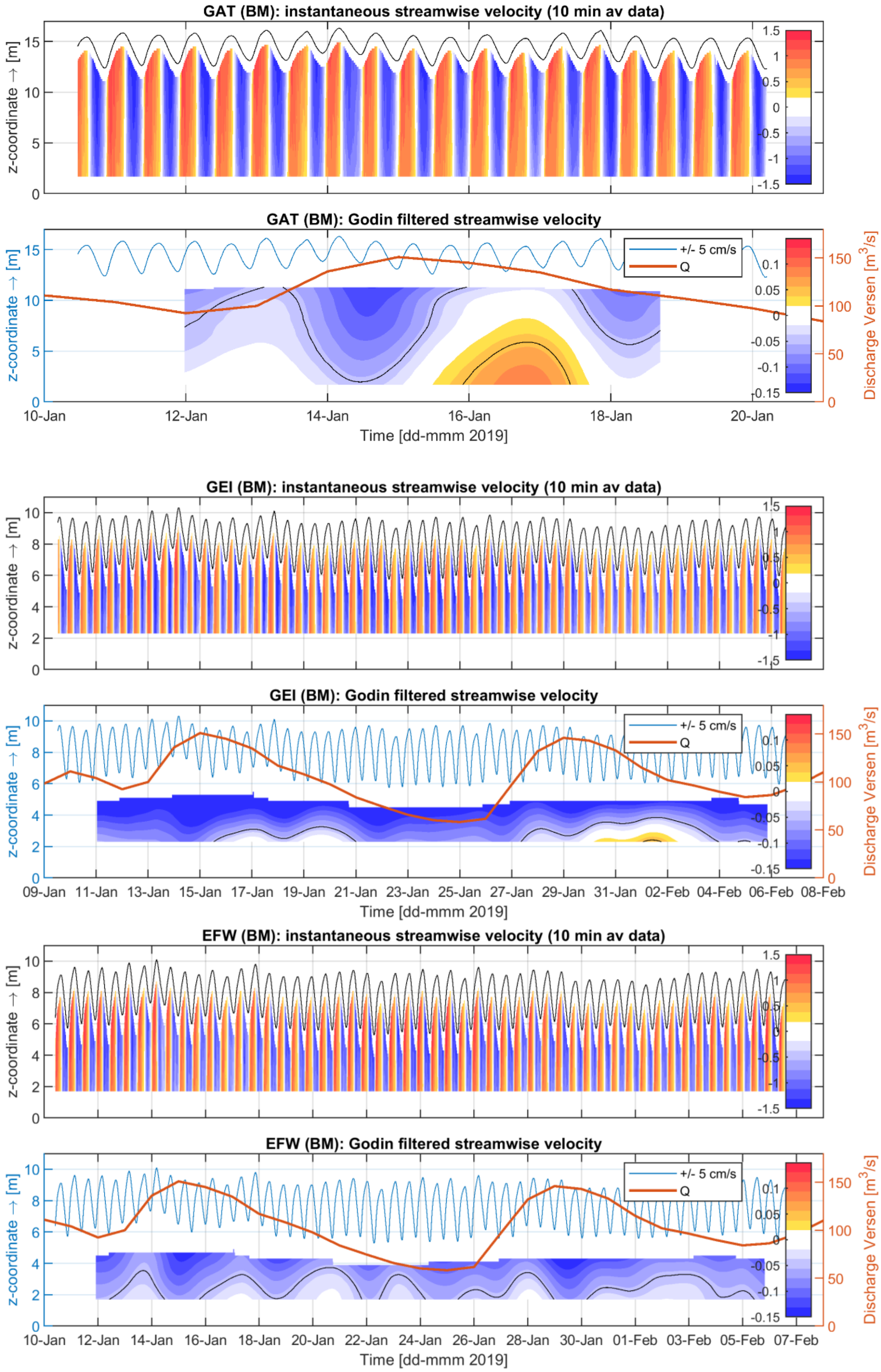

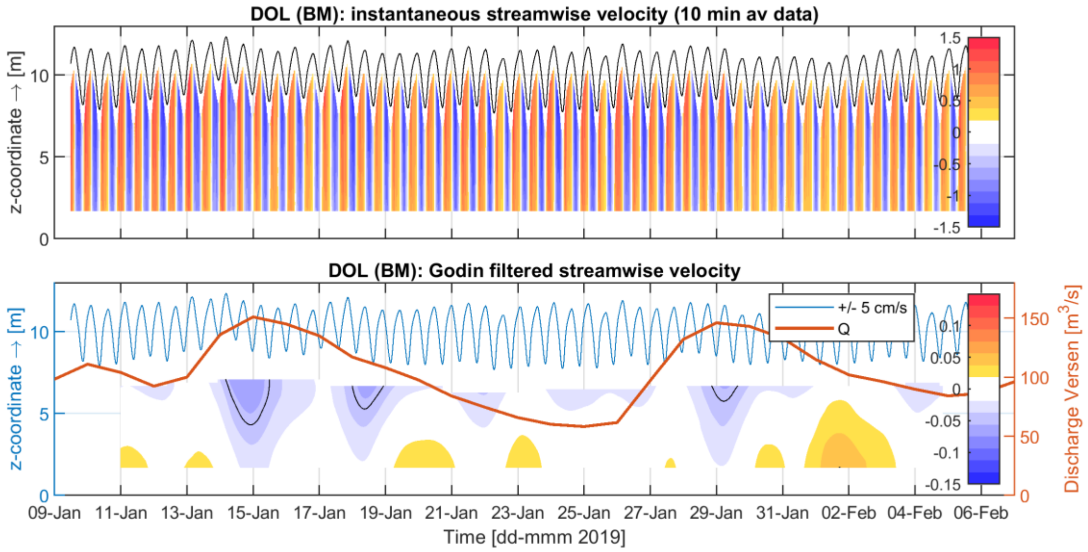
DOL (BM): instantaneous streamwise velocity (10 min av data)
z-coordinate → [m]
DOL (BM): Godin filtered streamwise velocity
+/- 5 cm/s
Q
Discharge Versen [m^3/s]
Time [dd-mmm 2019]

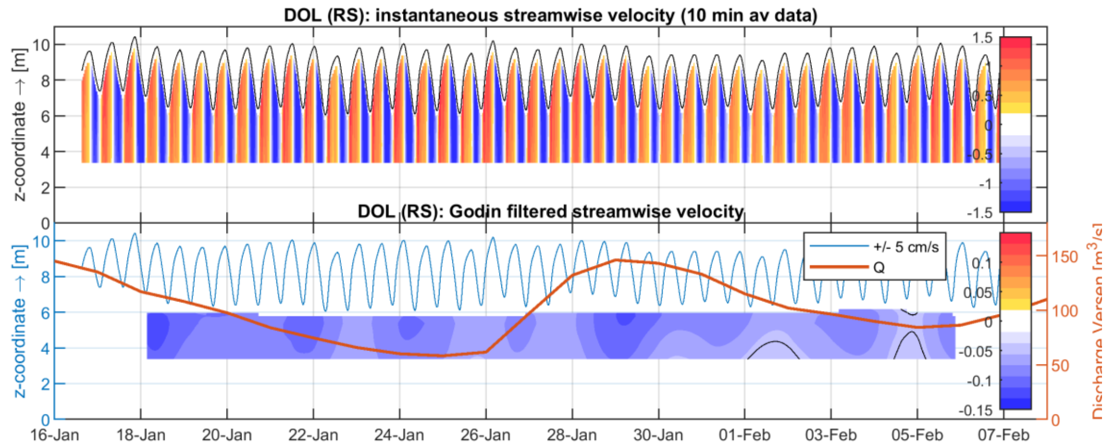
DOL (RS): instantaneous streamwise velocity (10 min av data)
z-coordinate → [m]
DOL (RS): Godin filtered streamwise velocity
+/- 5 cm/s
Q

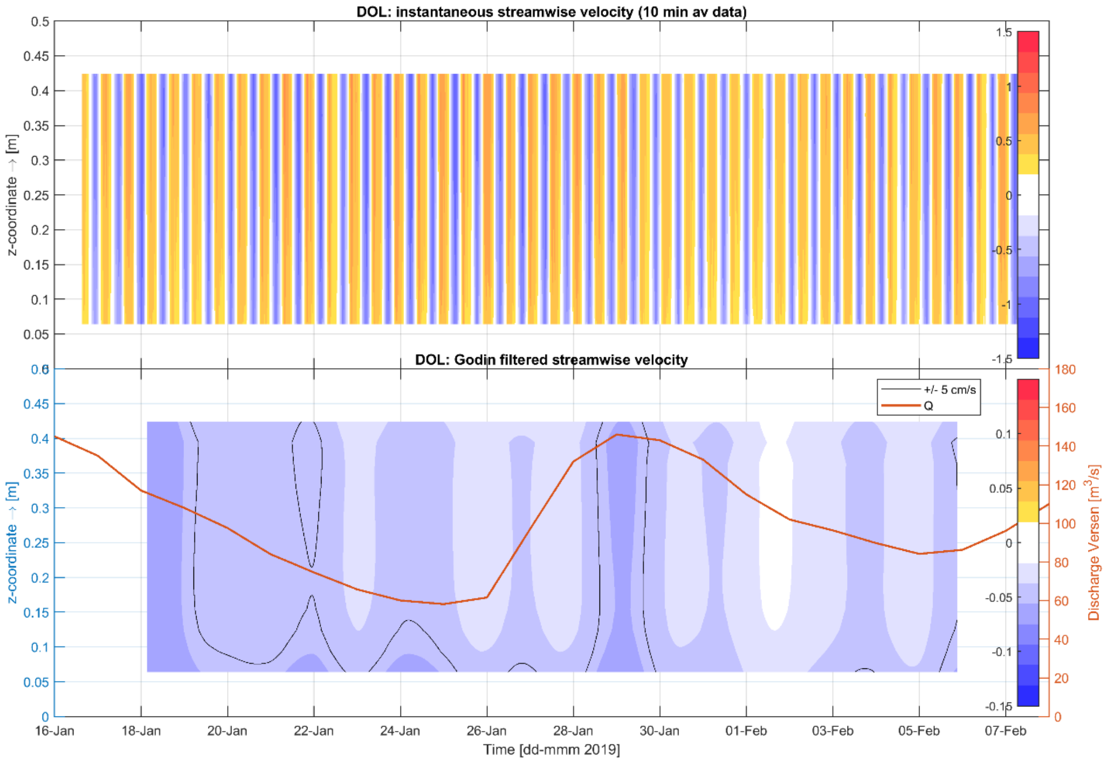
DOL: instantaneous streamwise velocity (10 min av data)
z-coordinate → [m]
DOL: Godin filtered streamwise velocity
+/- 5 cm/s
Q
Discharge Versen [m^3/s]
Time [dd-mmm 2019]

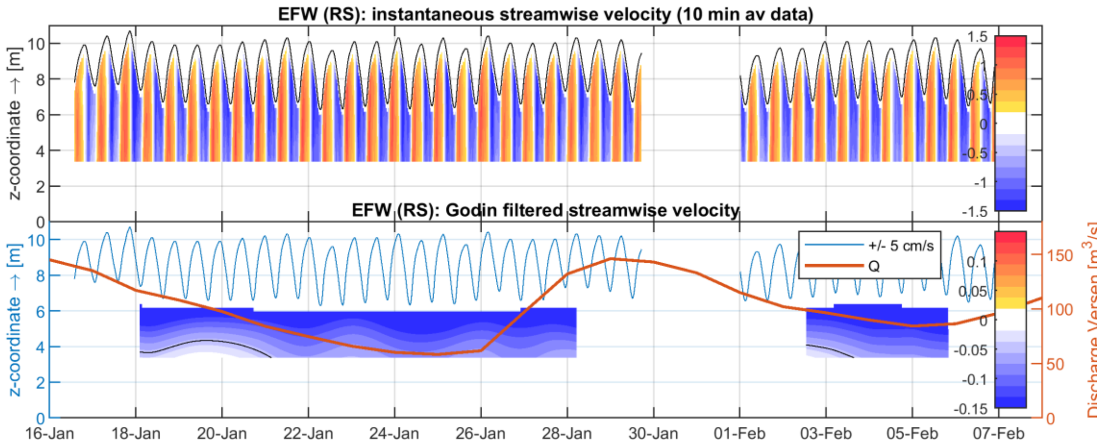
EFW (RS): instantaneous streamwise velocity (10 min av data)
z-coordinate → [m]
EFW (RS): Godin filtered streamwise velocity
+/- 5 cm/s
Q
Discharge Versen [m^3/s]
16-Jan 18-Jan 20-Jan 22-Jan 24-Jan 26-Jan 28-Jan 30-Jan 01-Feb 03-Feb 05-Feb 07-Feb

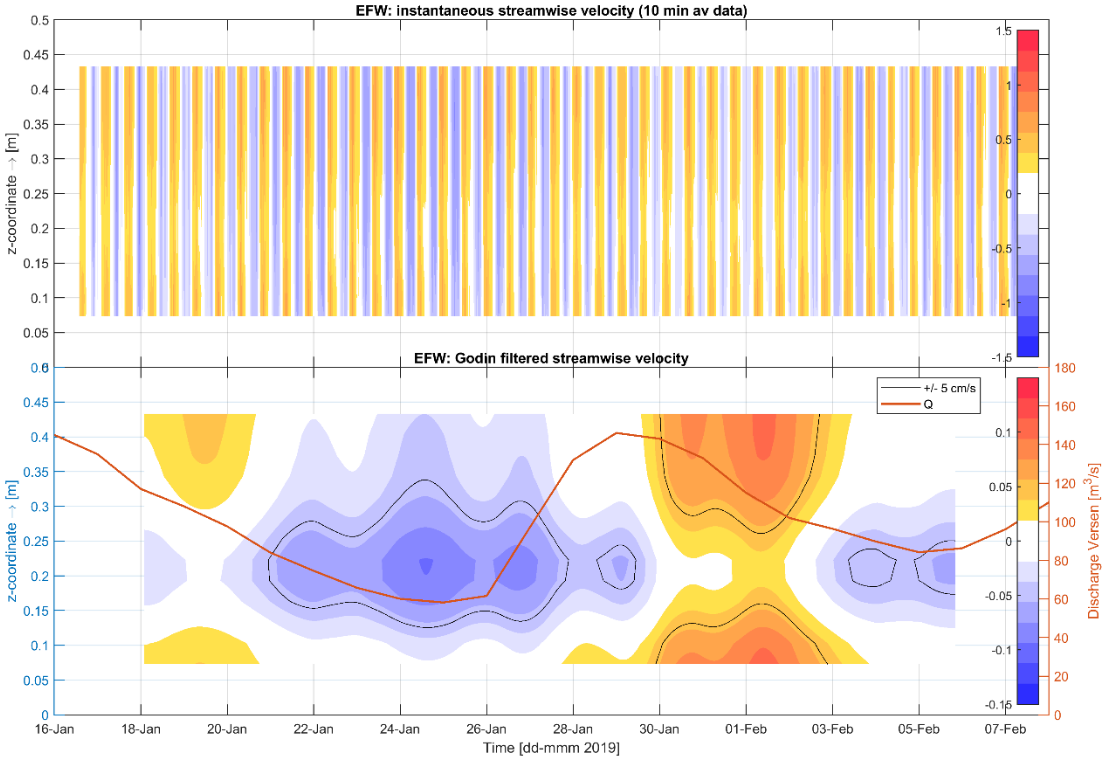
EFW: instantaneous streamwise velocity (10 min av data)
z-coordinate → [m]
EFW: Godin filtered streamwise velocity
+/- 5 cm/s
Q
Discharge Versen [m^3/s]
16-Jan 18-Jan 20-Jan 22-Jan 24-Jan 26-Jan 28-Jan 30-Jan 01-Feb 03-Feb 05-Feb 07-Feb
Time [dd-mmm 2019]

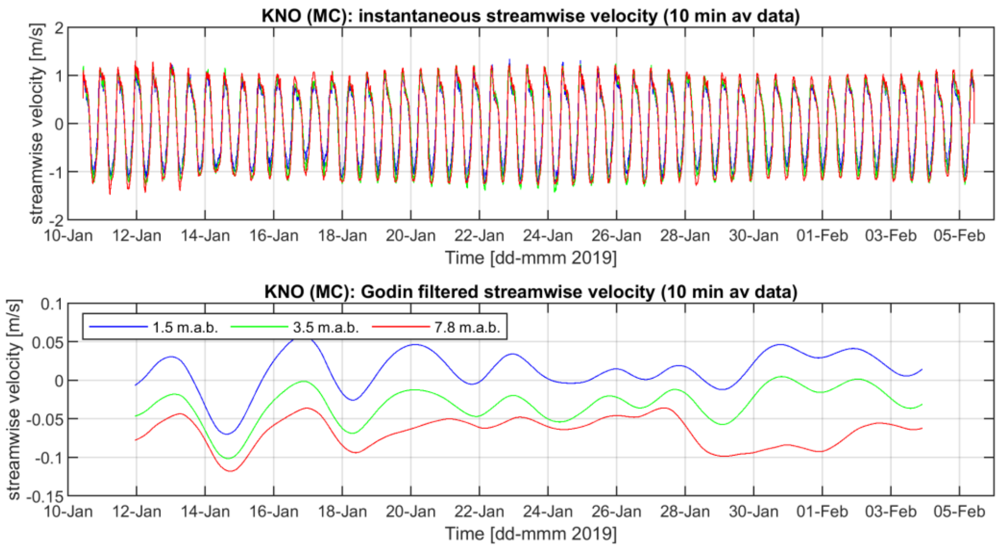
KNO (MC): instantaneous streamwise velocity (10 min av data)
streamwise velocity [m/s]
10-Jan 12-Jan 14-Jan 16-Jan 18-Jan 20-Jan 22-Jan 24-Jan 26-Jan 28-Jan 30-Jan 01-Feb 03-Feb 05-Feb
Time [dd-mmm 2019]
KNO (MC): Godin filtered streamwise velocity (10 min av data)
1.5 m.a.b.
3.5 m.a.b.
7.8 m.a.b.
streamwise velocity [m/s]
10-Jan 12-Jan 14-Jan 16-Jan 18-Jan 20-Jan 22-Jan 24-Jan 26-Jan 28-Jan 30-Jan 01-Feb 03-Feb 05-Feb
Time [dd-mmm 2019]

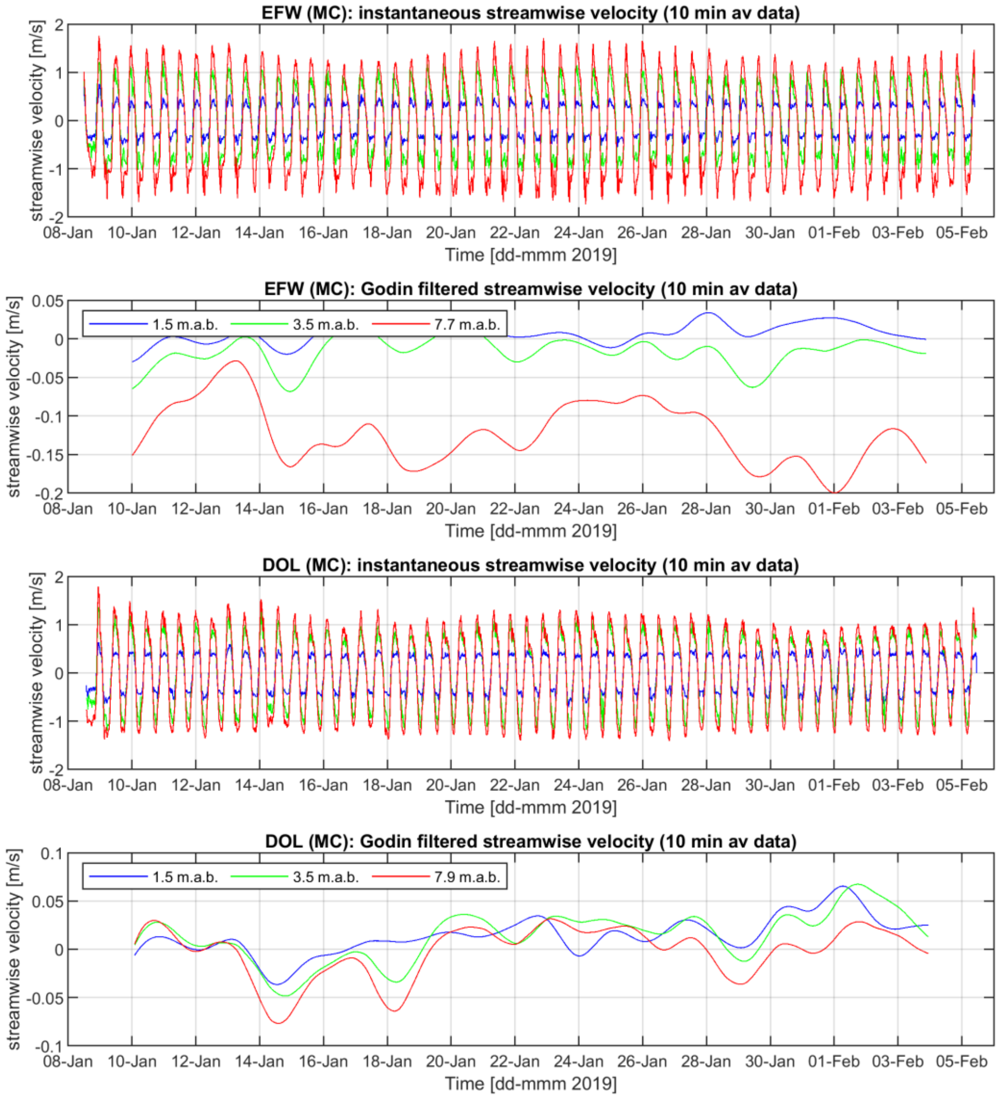

EFW (MC): instantaneous streamwise velocity (10 min av data)
streamwise velocity [m/s]
Time [dd-mmm 2019]
EFW (MC): Godin filtered streamwise velocity (10 min av data)
1.5 m.a.b.
3.5 m.a.b.
7.7 m.a.b.
streamwise velocity [m/s]
Time [dd-mmm 2019]
DOL (MC): instantaneous streamwise velocity (10 min av data)
streamwise velocity [m/s]
Time [dd-mmm 2019]
DOL (MC): Godin filtered streamwise velocity (10 min av data)
1.5 m.a.b.
3.5 m.a.b.
7.9 m.a.b.
streamwise velocity [m/s]
Time [dd-mmm 2019]

D.2.1.4. Residual flow over a spring-neap tidal cycle

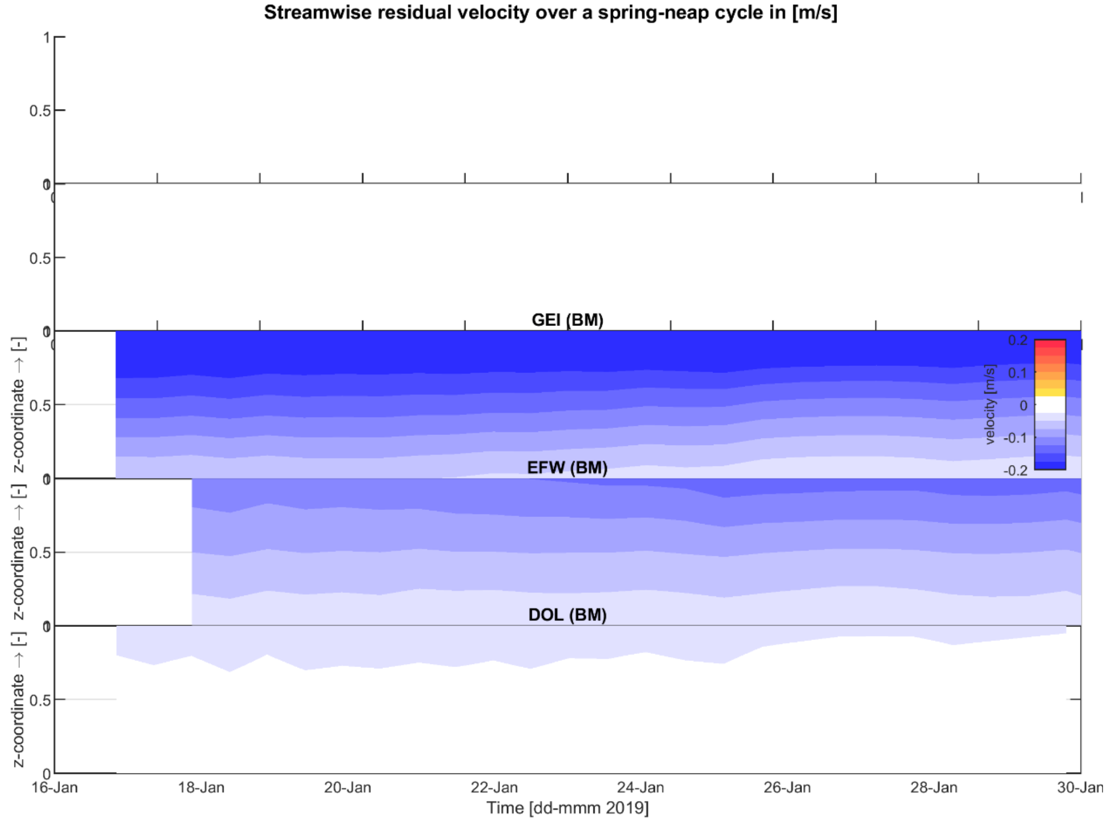

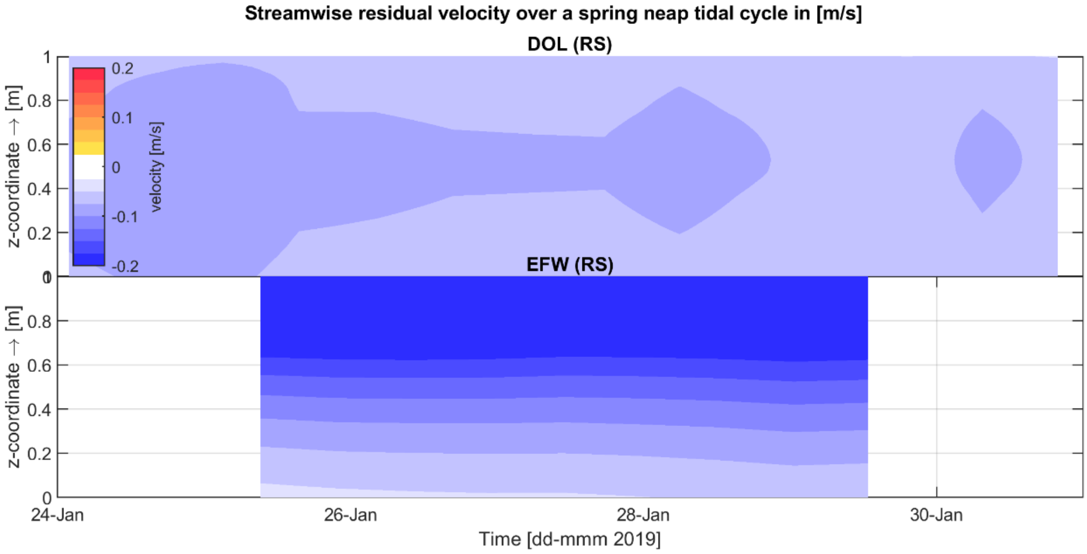

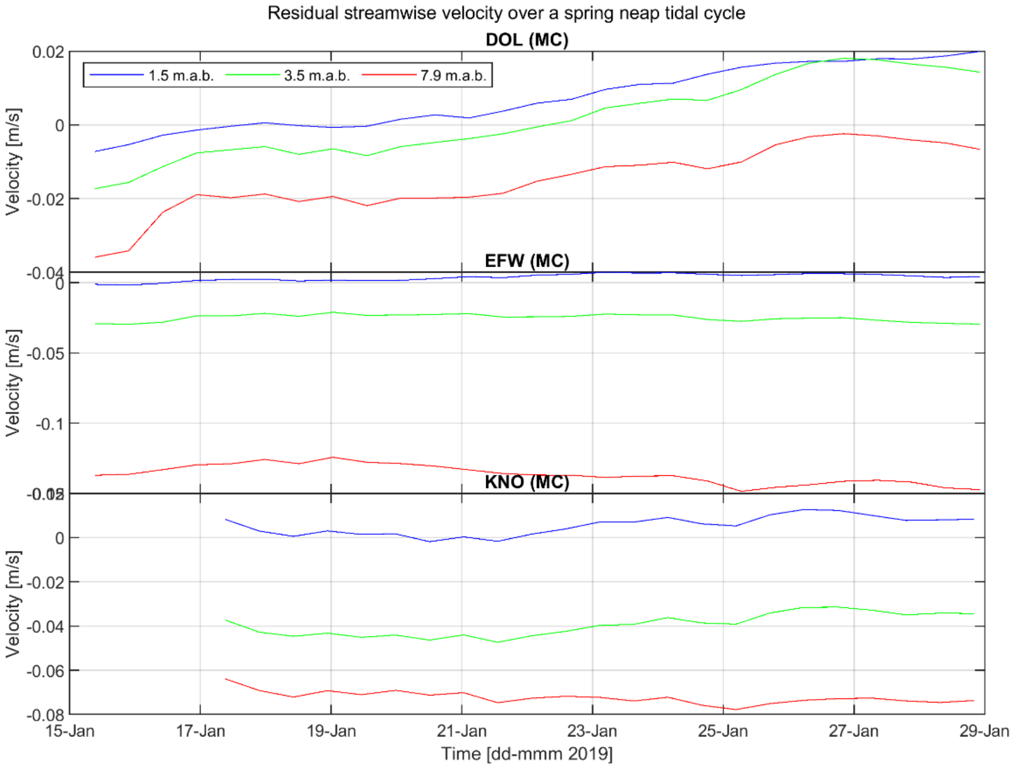
Residual streamwise velocity over a spring neap tidal cycle
DOL (MC)
EFW (MC)
KNO (MC)
1.5 m.a.b.
3.5 m.a.b.
7.9 m.a.b.
Velocity [m/s]
Time [dd-mmm 2019]
15-Jan
17-Jan
19-Jan
21-Jan
23-Jan
25-Jan
27-Jan
29-Jan

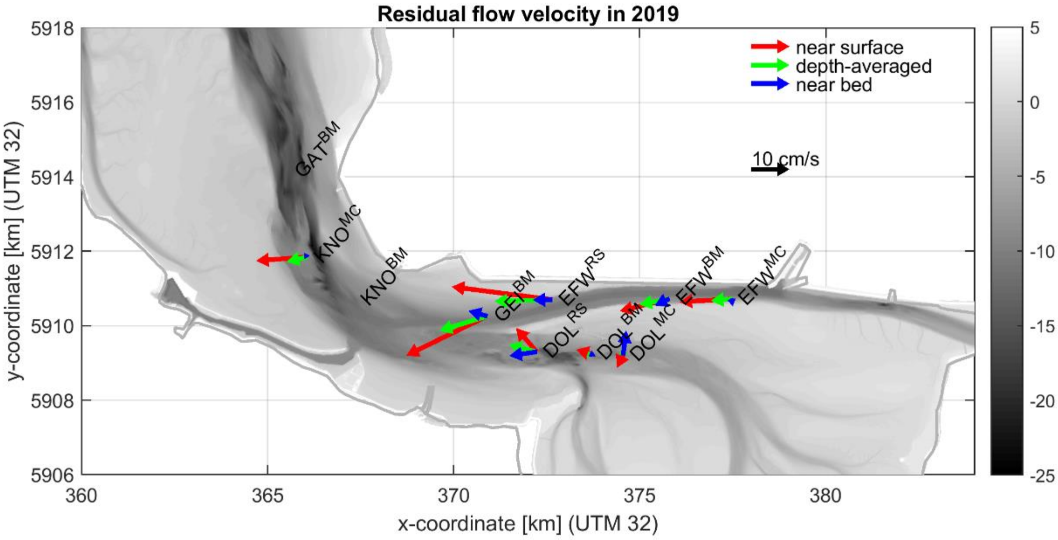
Residual flow velocity in 2019
near surface
depth-averaged
near bed
10 cm/s
GAT^BM
KNO^MC
KNO^BM
GE^BM
EFW^RS
DOL^RS
DOL^BM
DOL^MC
EFW^BM
EFW^MC
y-coordinate [km] (UTM 32)
x-coordinate [km] (UTM 32)

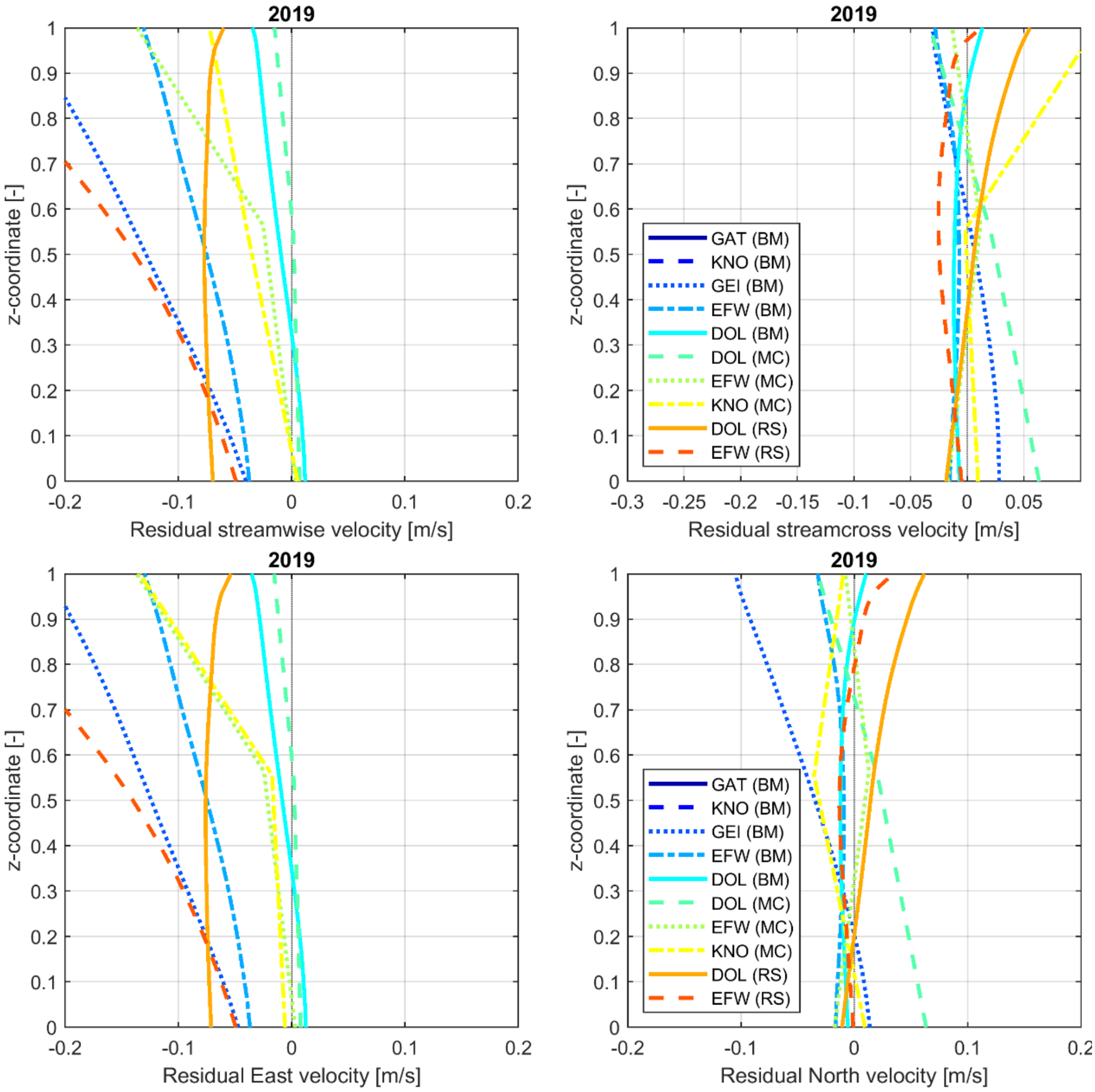
2019
z-coordinate [-]
Residual streamwise velocity [m/s]
2019
z-coordinate [-]
Residual streamcross velocity [m/s]
GAT (BM)
KNO (BM)
GEI (BM)
EFW (BM)
DOL (BM)
DOL (MC)
EFW (MC)
KNO (MC)
DOL (RS)
EFW (RS)
2019
z-coordinate [-]
Residual East velocity [m/s]
2019
z-coordinate [-]
Residual North velocity [m/s]
GAT (BM)
KNO (BM)
GEI (BM)
EFW (BM)
DOL (BM)
DOL (MC)
EFW (MC)
KNO (MC)
DOL (RS)
EFW (RS)

D.2.1.5. Suspended sediment concentration and additional parameters

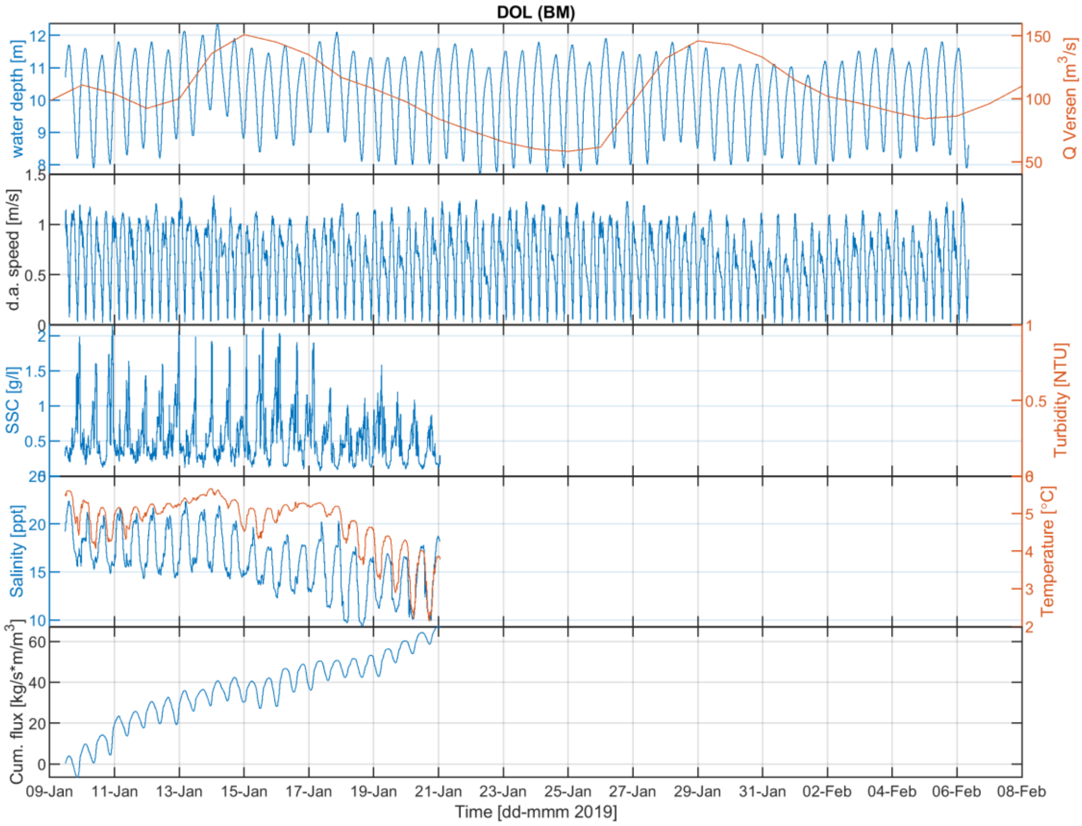

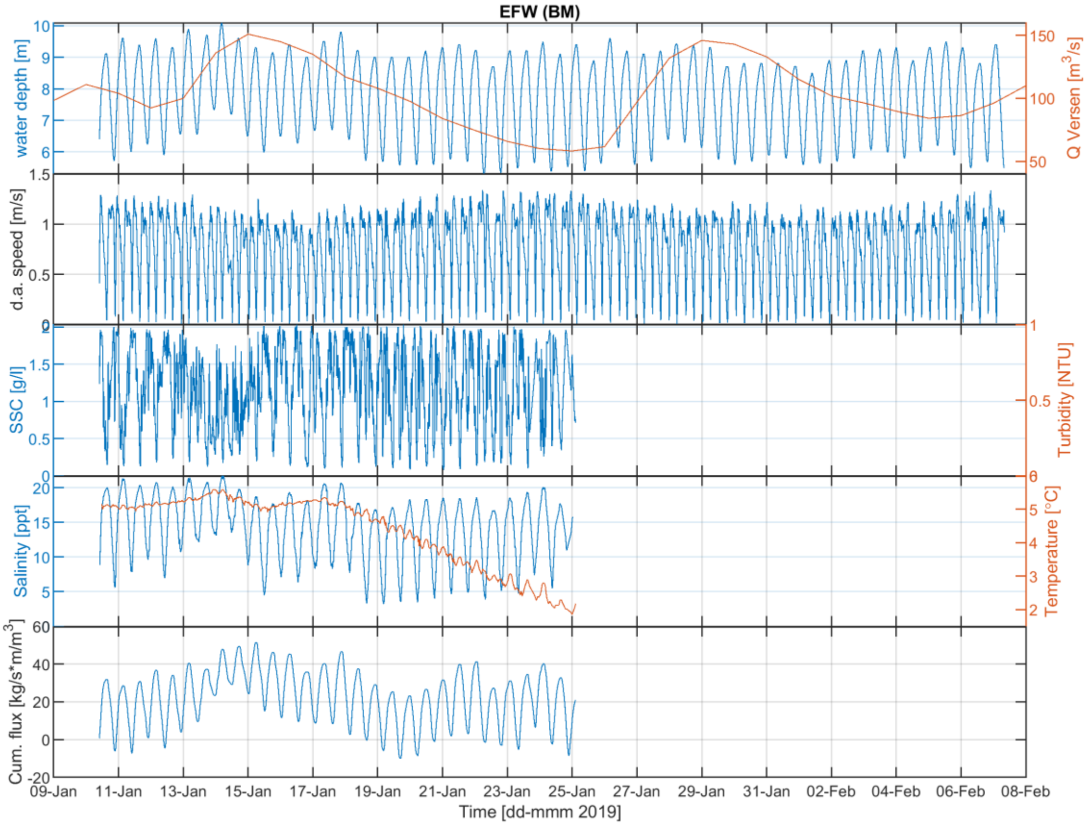

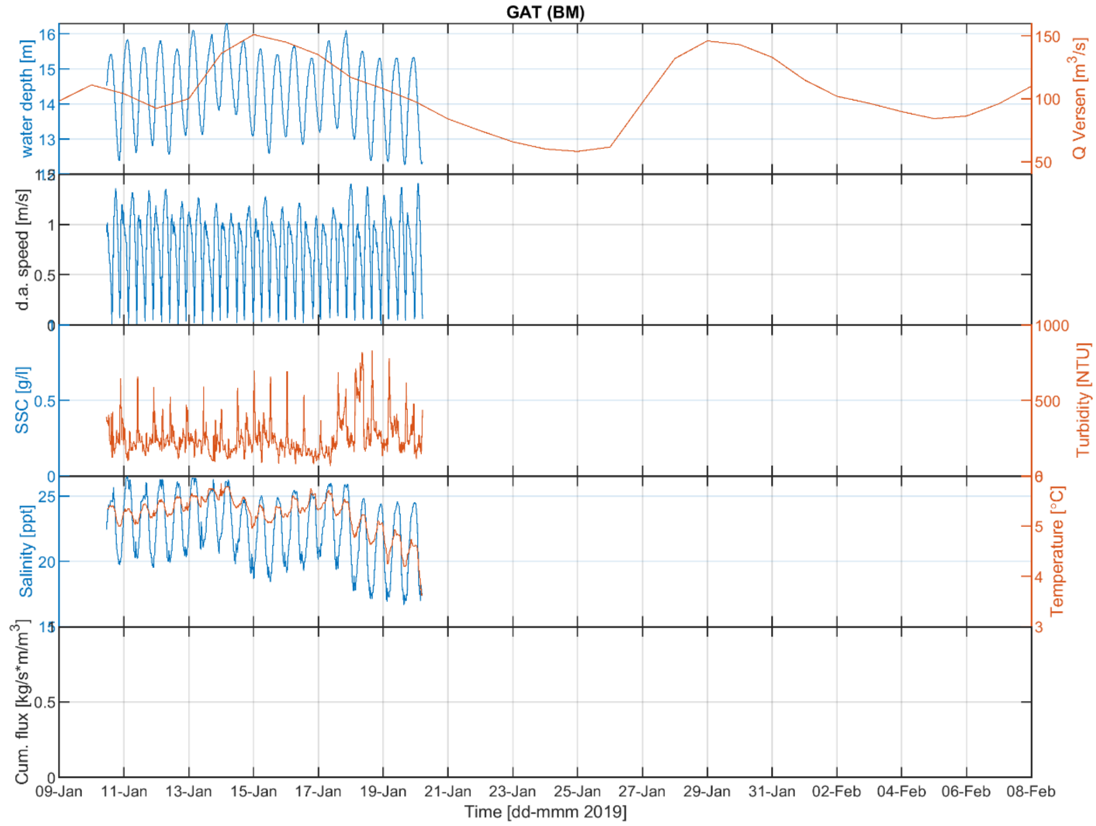
GAT (BM)
water depth [m]
Q Versen [m^3/s]
d.a. speed [m/s]
SSC [g/l]
Turbidity [NTU]
Salinity [ppt]
Temperature [°C]
Cum. flux [kg/s*m/m^3]
09-Jan 11-Jan 13-Jan 15-Jan 17-Jan 19-Jan 21-Jan 23-Jan 25-Jan 27-Jan 29-Jan 31-Jan 02-Feb 04-Feb 06-Feb 08-Feb
Time [dd-mmm 2019]

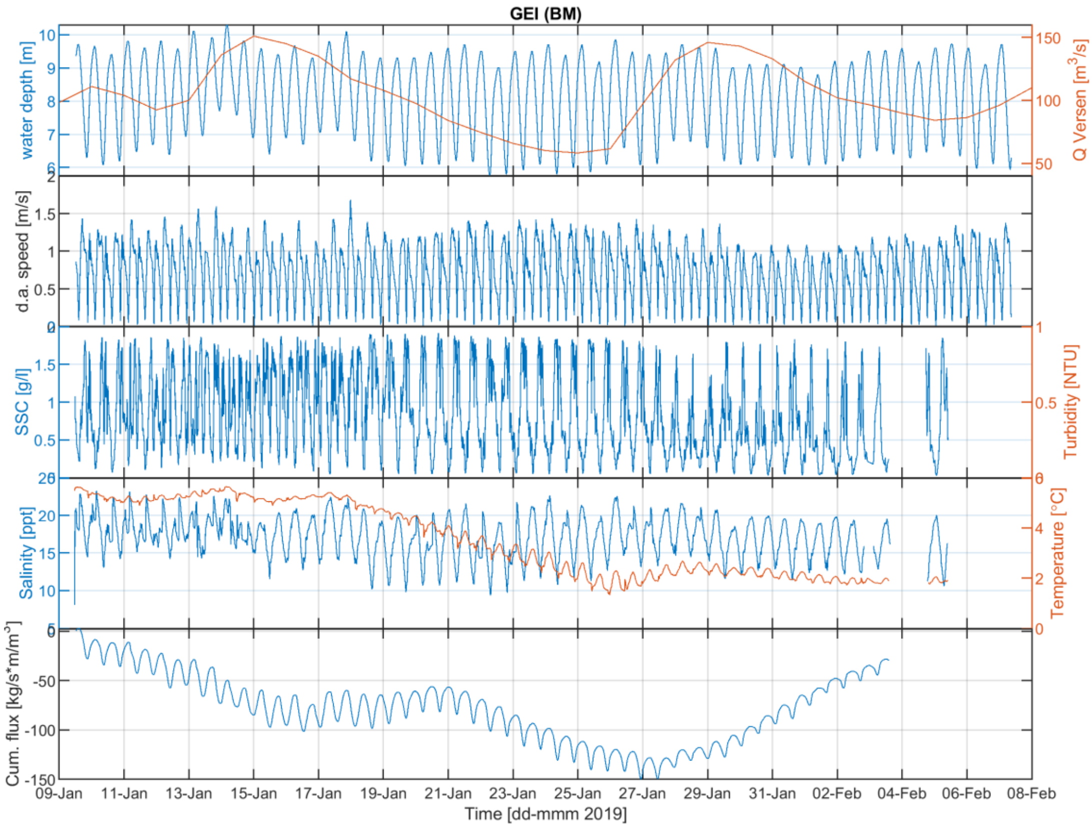
GEI (BM)
water depth [m]
Q Versen [m^3/s]
d.a. speed [m/s]
SSC [g/l]
Turbidity [NTU]
Salinity [ppt]
Temperature [°C]
Cum. flux [kg/s*m/m^3]
09-Jan 11-Jan 13-Jan 15-Jan 17-Jan 19-Jan 21-Jan 23-Jan 25-Jan 27-Jan 29-Jan 31-Jan 02-Feb 04-Feb 06-Feb 08-Feb
Time [dd-mmm 2019]

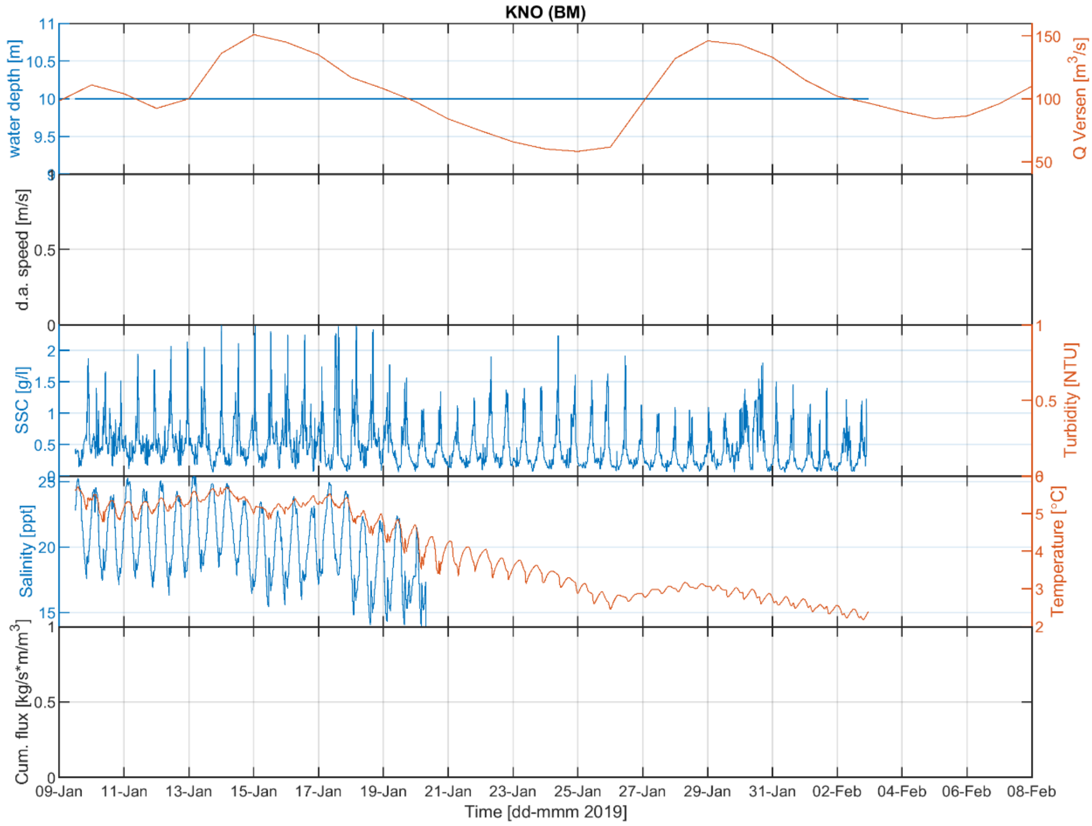
KNO (BM)
water depth [m]
Q Versen [m3/s]
d.a. speed [m/s]
SSC [g/l]
Turbidity [NTU]
Salinity [ppt]
Temperature [°C]
Cum. flux [kg/s*m/m3]
09-Jan 11-Jan 13-Jan 15-Jan 17-Jan 19-Jan 21-Jan 23-Jan 25-Jan 27-Jan 29-Jan 31-Jan 02-Feb 04-Feb 06-Feb 08-Feb
Time [dd-mmm 2019]

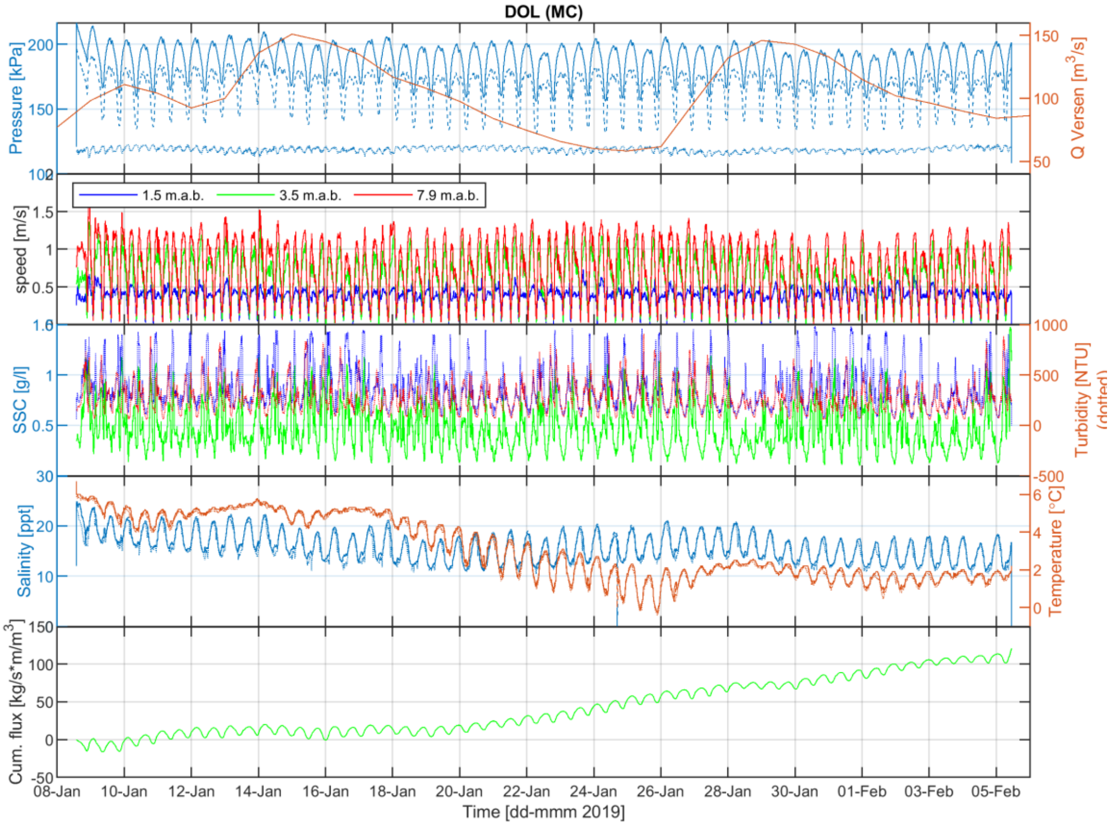
DOL (MC)
Pressure [kPa]
Q Versen [m^3/s]
speed [m/s]
1.5 m.a.b.
3.5 m.a.b.
7.9 m.a.b.
SSC [g/l]
Turbidity [NTU] (dotted)
Salinity [ppt]
Temperature [°C]
Cum. flux [kg/s*m/m^3]
08-Jan 10-Jan 12-Jan 14-Jan 16-Jan 18-Jan 20-Jan 22-Jan 24-Jan 26-Jan 28-Jan 30-Jan 01-Feb 03-Feb 05-Feb
Time [dd-mmm 2019]

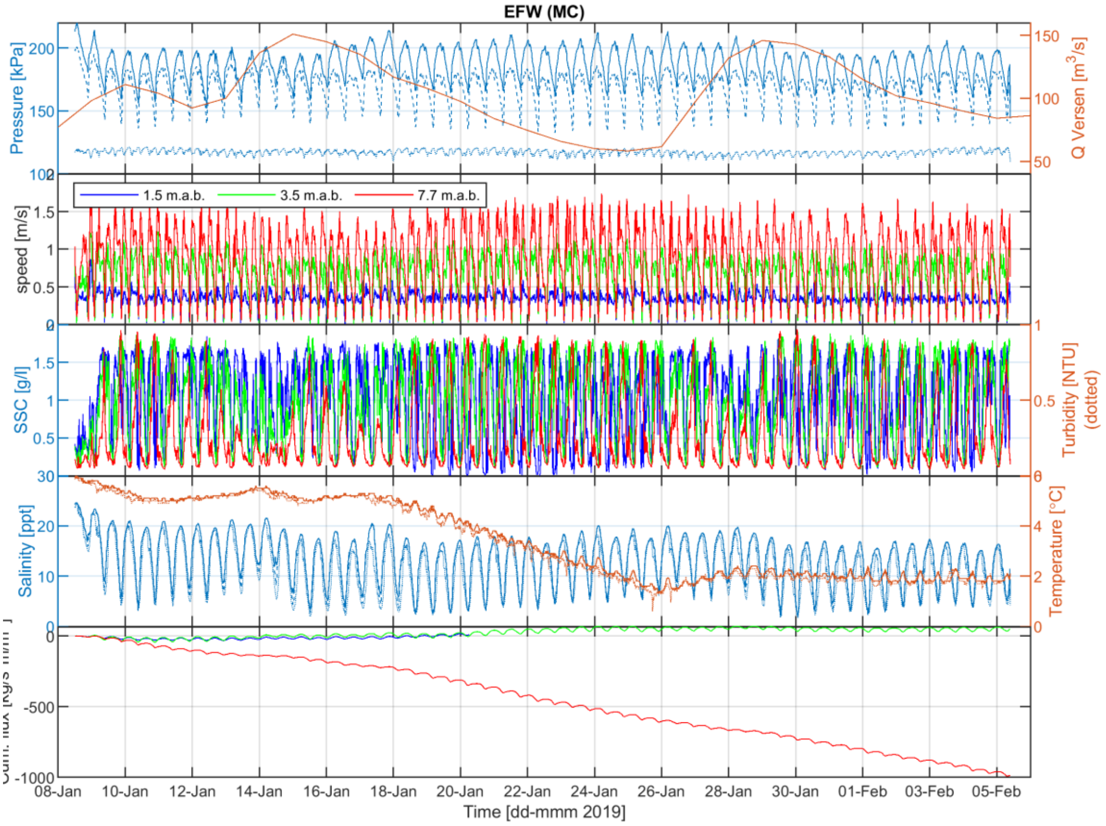
EFW (MC)
Pressure [kPa]
Q Versen [m^3/s]
speed [m/s]
1.5 m.a.b.
3.5 m.a.b.
7.7 m.a.b.
SSC [g/l]
Turbidity [NTU] (dotted)
Salinity [ppt]
Temperature [°C]
08-Jan 10-Jan 12-Jan 14-Jan 16-Jan 18-Jan 20-Jan 22-Jan 24-Jan 26-Jan 28-Jan 30-Jan 01-Feb 03-Feb 05-Feb
Time [dd-mmm 2019]

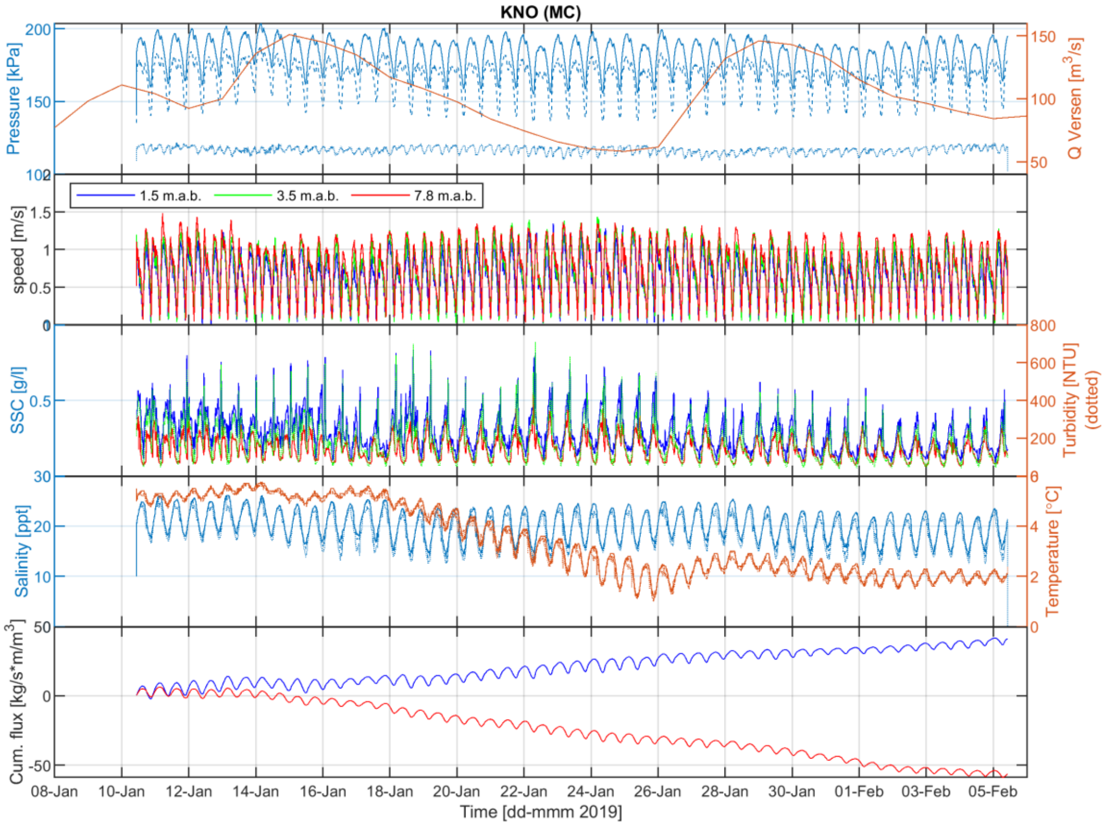
KNO (MC)
Pressure [kPa]
Q Versen [m3/s]
1.5 m.a.b.
3.5 m.a.b.
7.8 m.a.b.
speed [m/s]
SSC [g/l]
Turbidity [NTU] (dotted)
Salinity [ppt]
Temperature [°C]
Cum. flux [kg/s*m/m3]
Time [dd-mmm 2019]

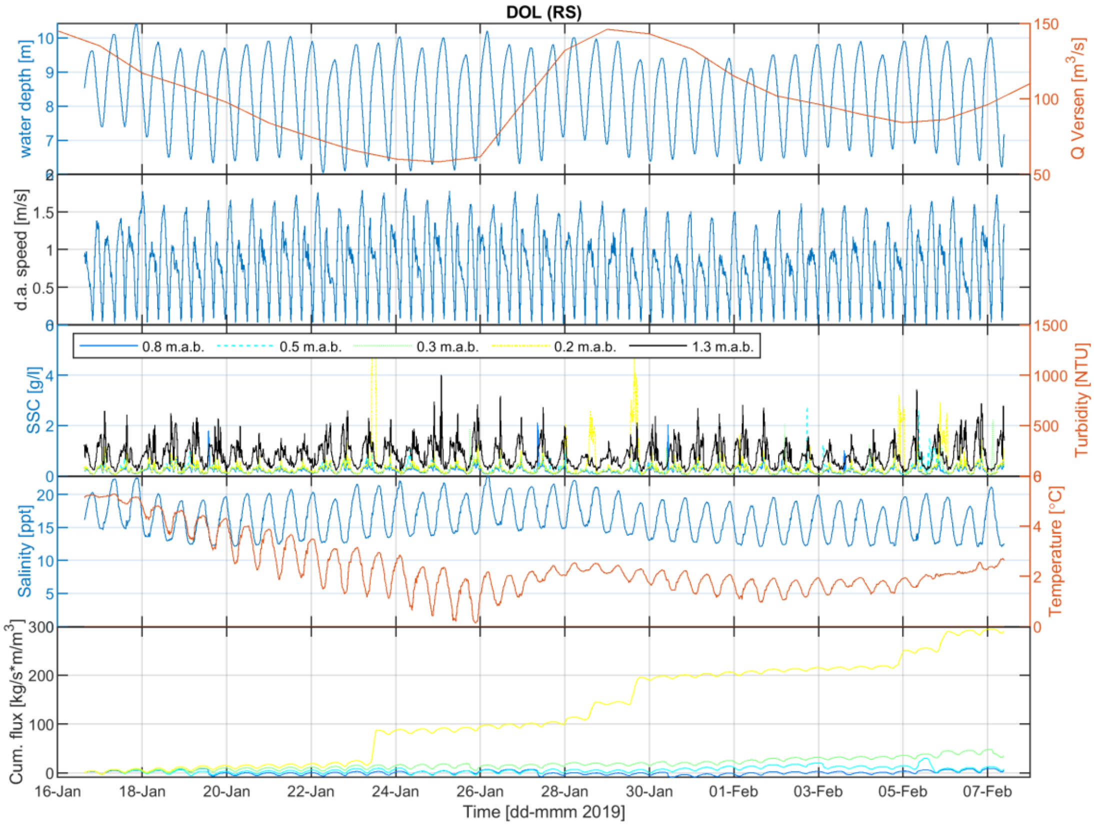

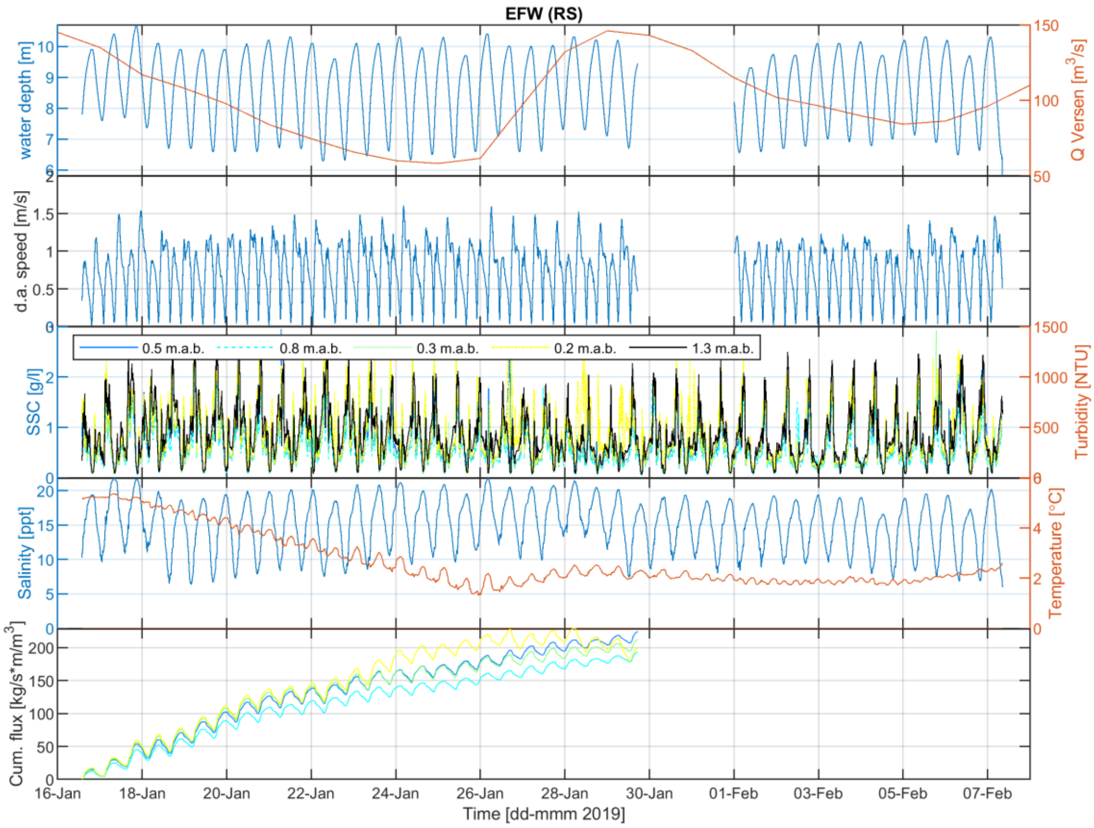

D.2.1.6. Sediment fluxes

At GAT (BM), the turbidity time series is too short (due to malfunctioning of the sensor) to compute a residual flux over a spring-neap tidal cycle.

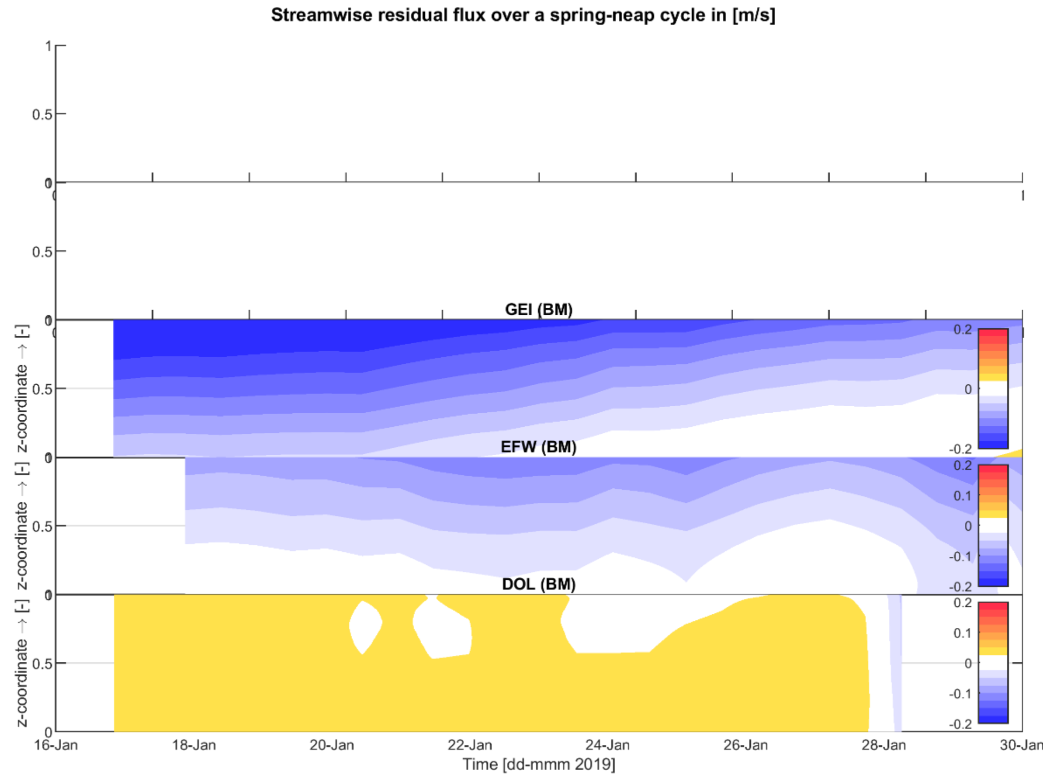
Streamwise residual flux over a spring-neap cycle in [m/s]
GEI (BM)
EFW (BM)
DOL (BM)
z-coordinate → [-]
Time [dd-mmm 2019]
16-Jan
18-Jan
20-Jan
22-Jan
24-Jan
26-Jan
28-Jan
30-Jan

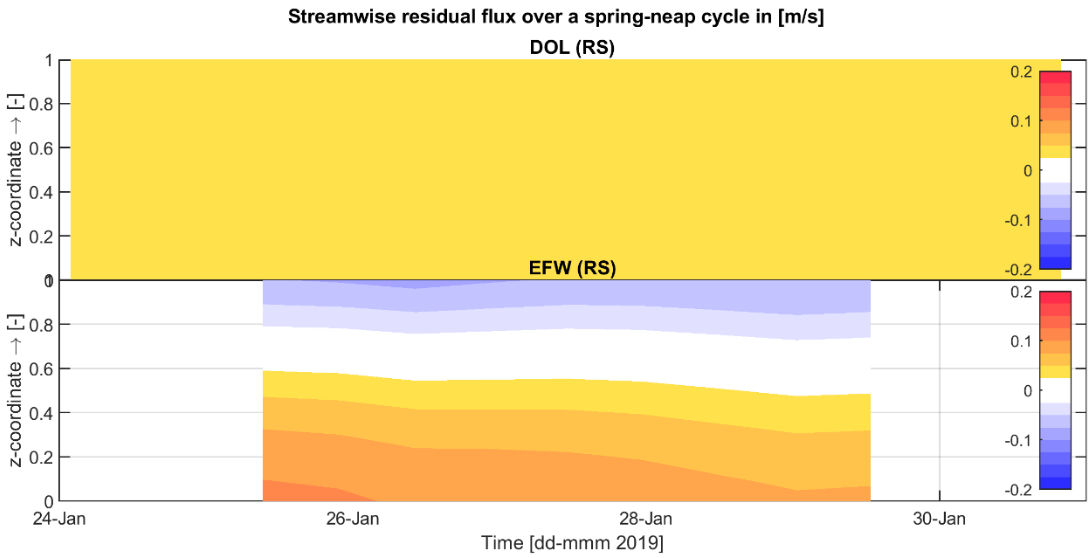
Streamwise residual flux over a spring-neap cycle in [m/s]
DOL (RS)
EFW (RS)
z-coordinate → [-]
Time [dd-mmm 2019]
24-Jan
26-Jan
28-Jan
30-Jan

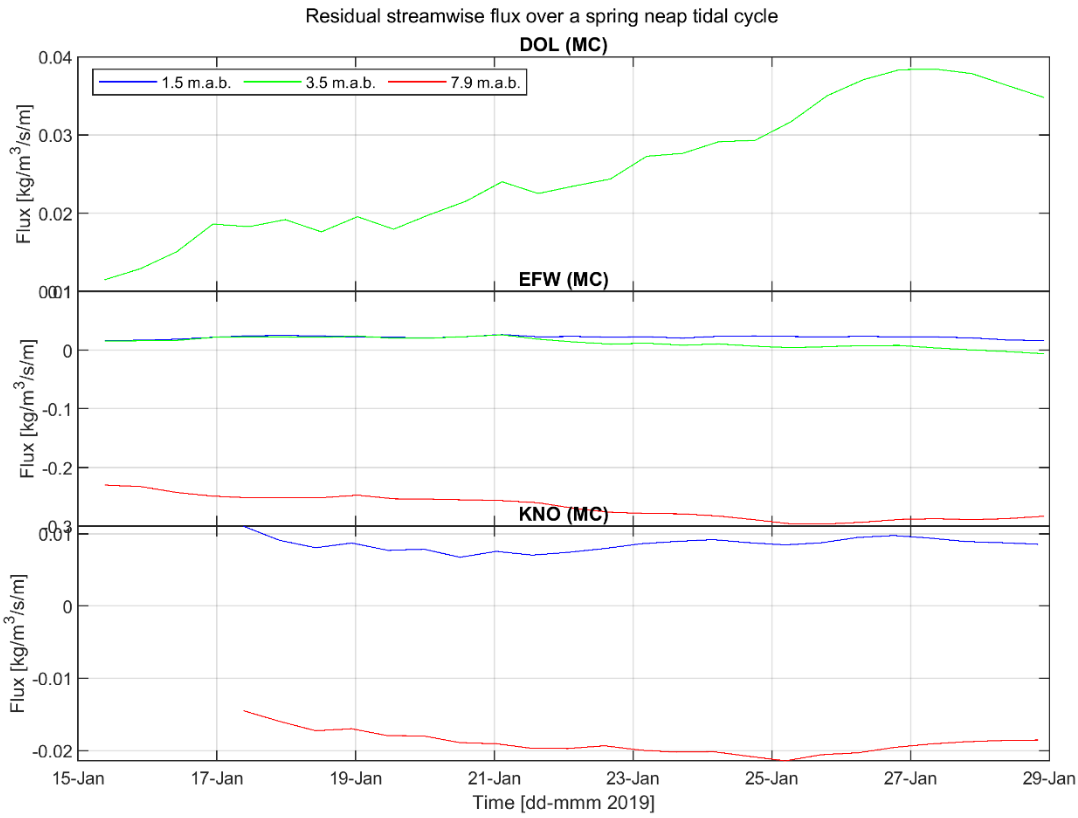

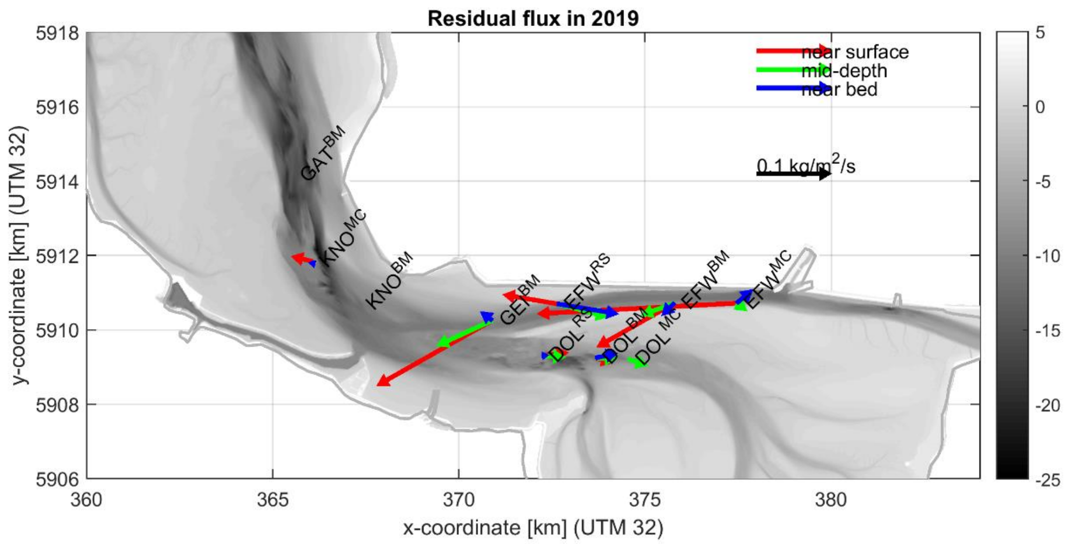

Comparison of Eastward flux profiles between 2018 and 2019

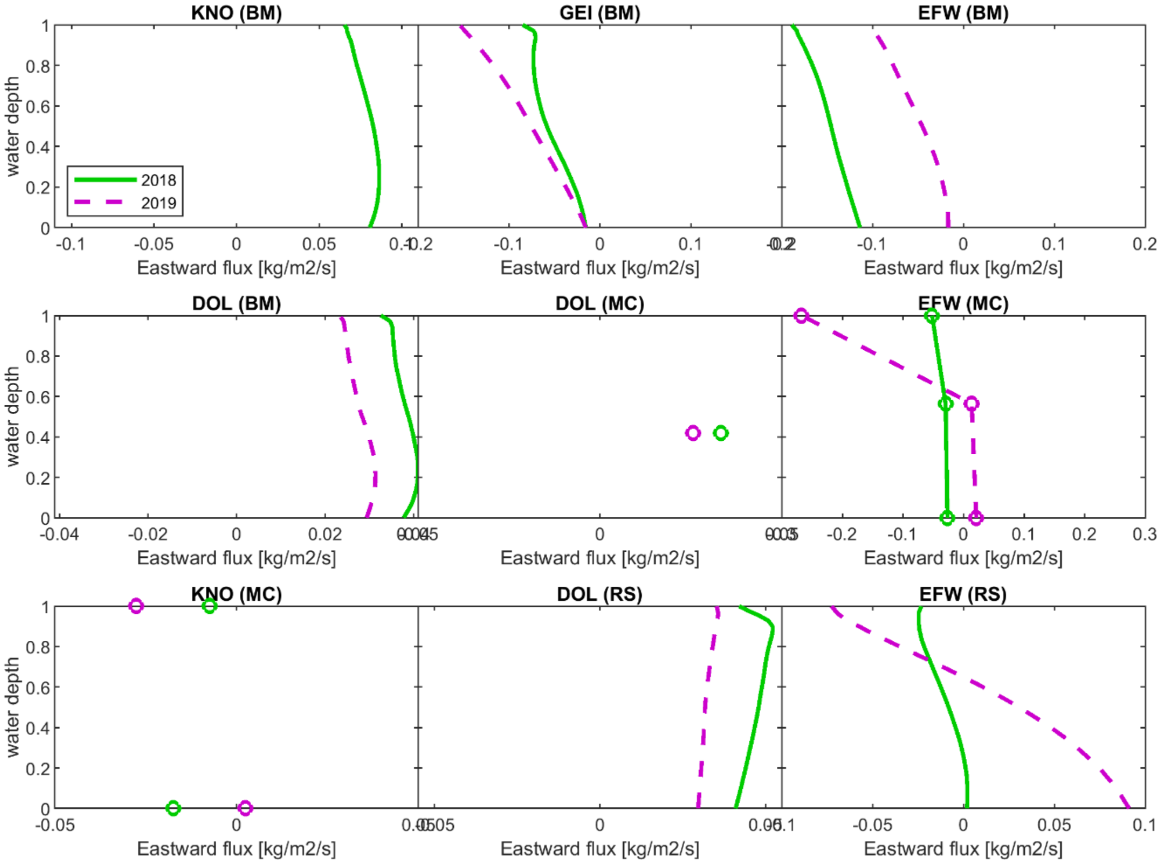

D.2.1.7. Time stack plots stream-, crosswise and upward velocities (13-hour measurements)

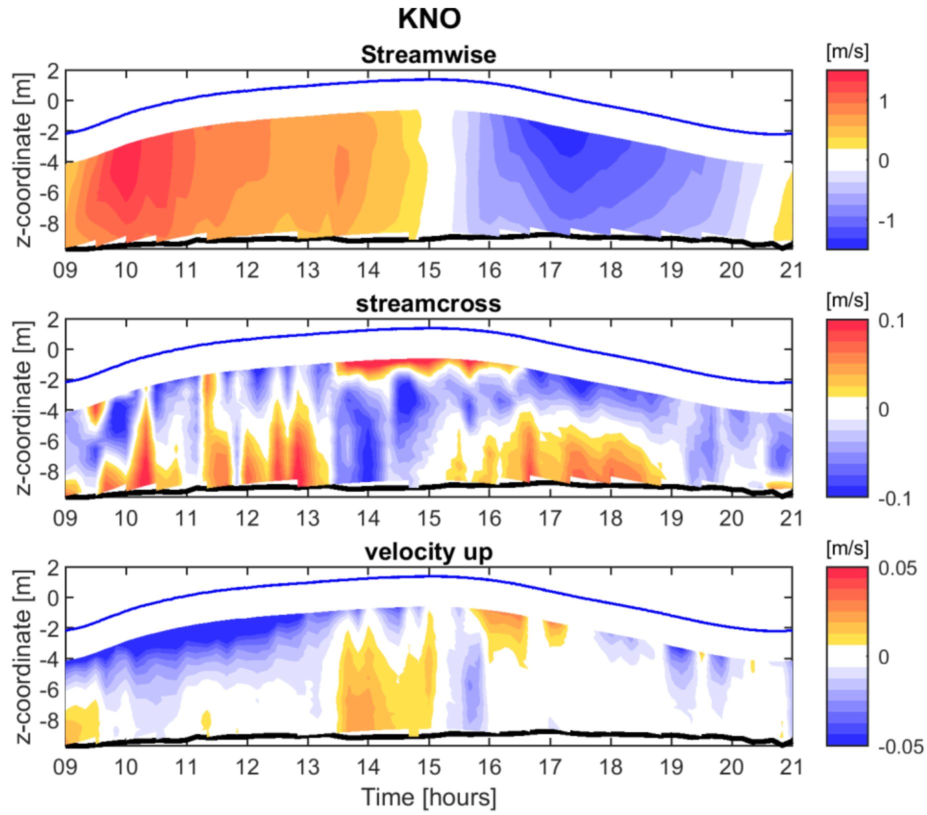
KNO
Streamwise
streamcross
velocity up
z-coordinate [m]
[m/s]
Time [hours]
09
10
11
12
13
14
15
16
17
18
19
20
21
2
0
-2
-4
-6
-8
1
-1
0.1
-0.1
0.05
-0.05

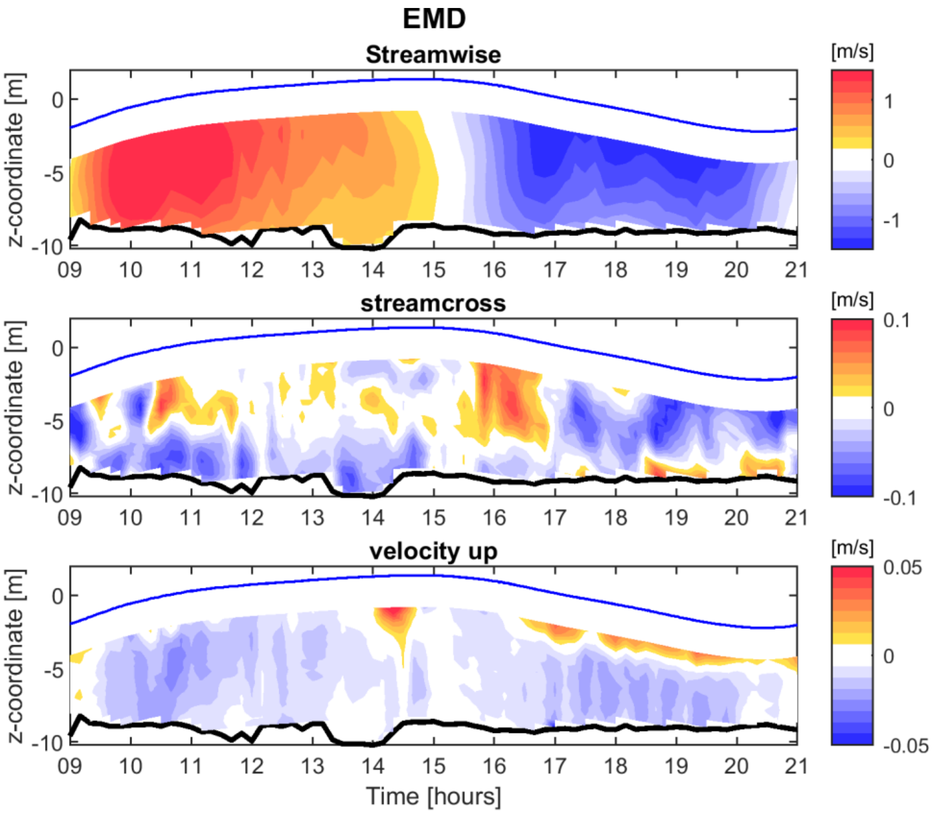
EMD
Streamwise
streamcross
velocity up
z-coordinate [m]
[m/s]
Time [hours]
09
10
11
12
13
14
15
16
17
18
19
20
21
0
-5
-10
1
-1
0.1
-0.1
0.05
-0.05

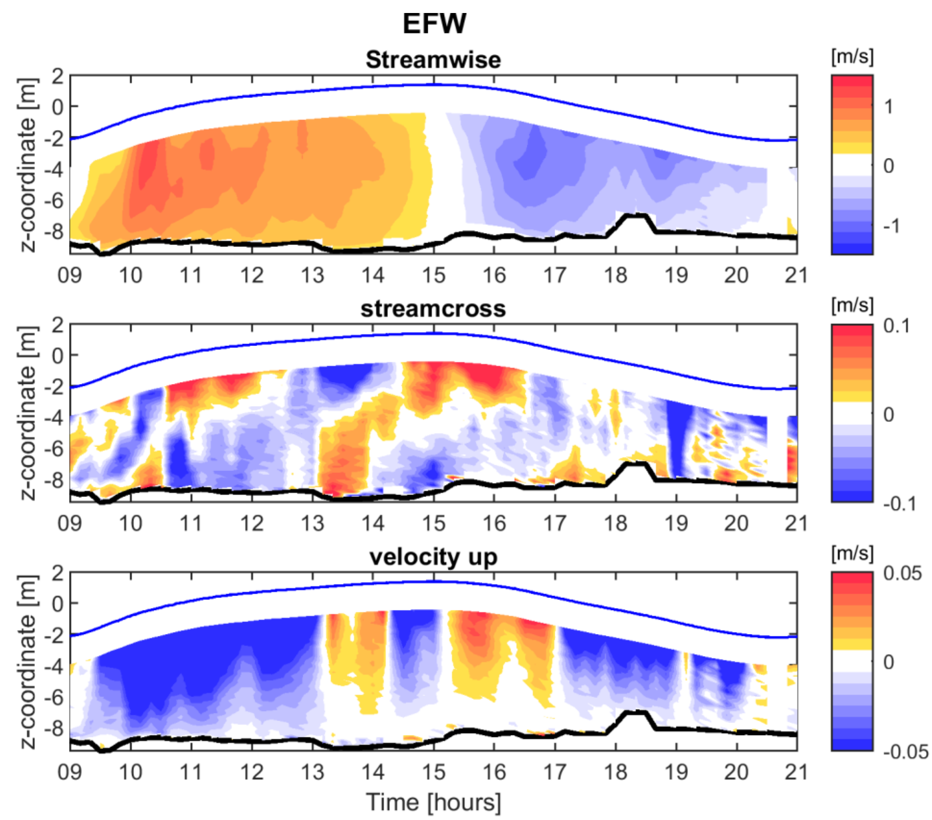
EFW
Streamwise
streamcross
velocity up
z-coordinate [m]
[m/s]
Time [hours]

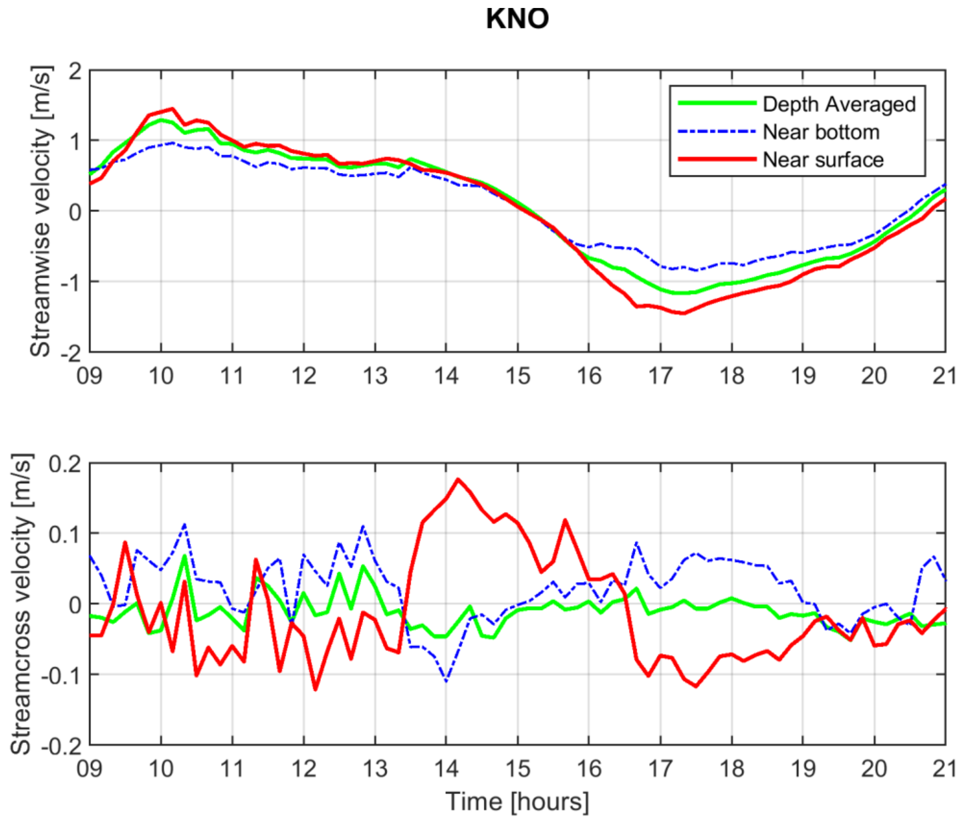
KNO
Depth Averaged
Near bottom
Near surface
Streamwise velocity [m/s]
Streamcross velocity [m/s]
Time [hours]

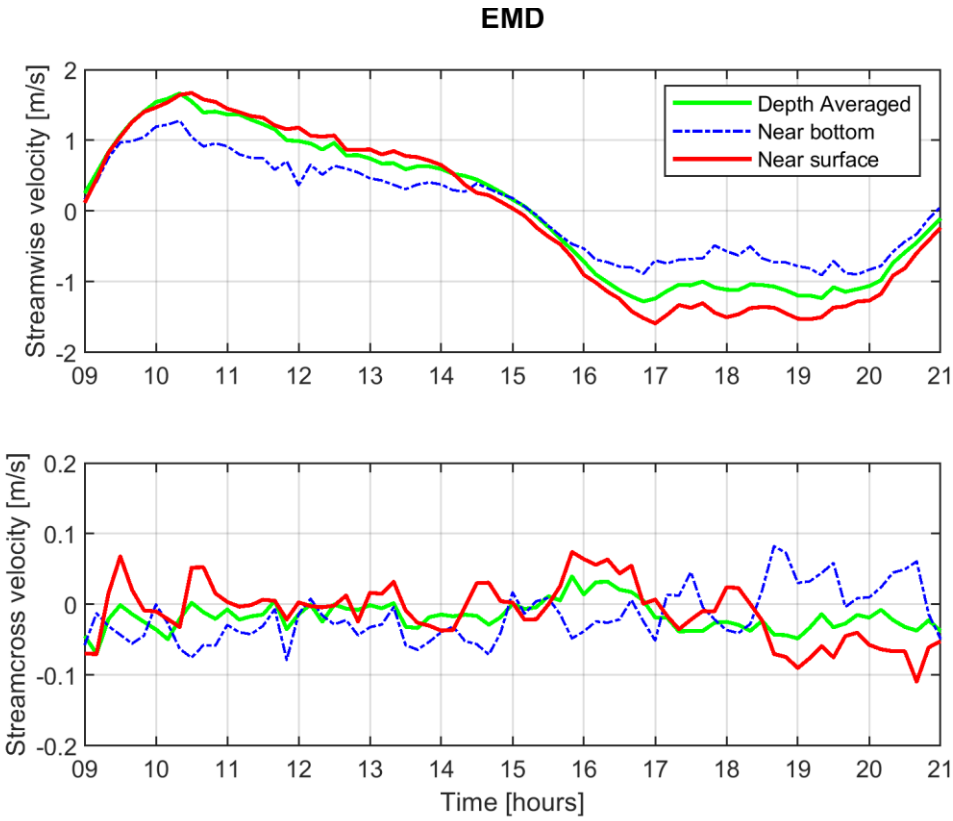
EMD
Depth Averaged
Near bottom
Near surface
Streamwise velocity [m/s]
Streamcross velocity [m/s]
Time [hours]

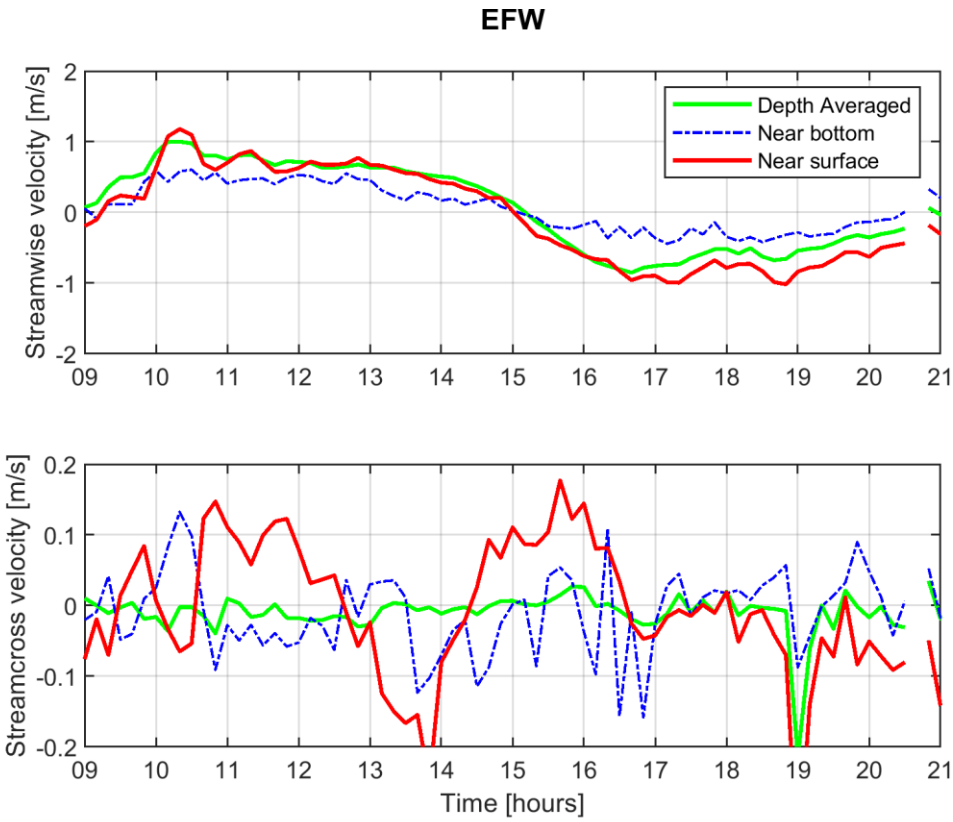
EFW
Depth Averaged
Near bottom
Near surface
Streamwise velocity [m/s]
Streamcross velocity [m/s]
Time [hours]

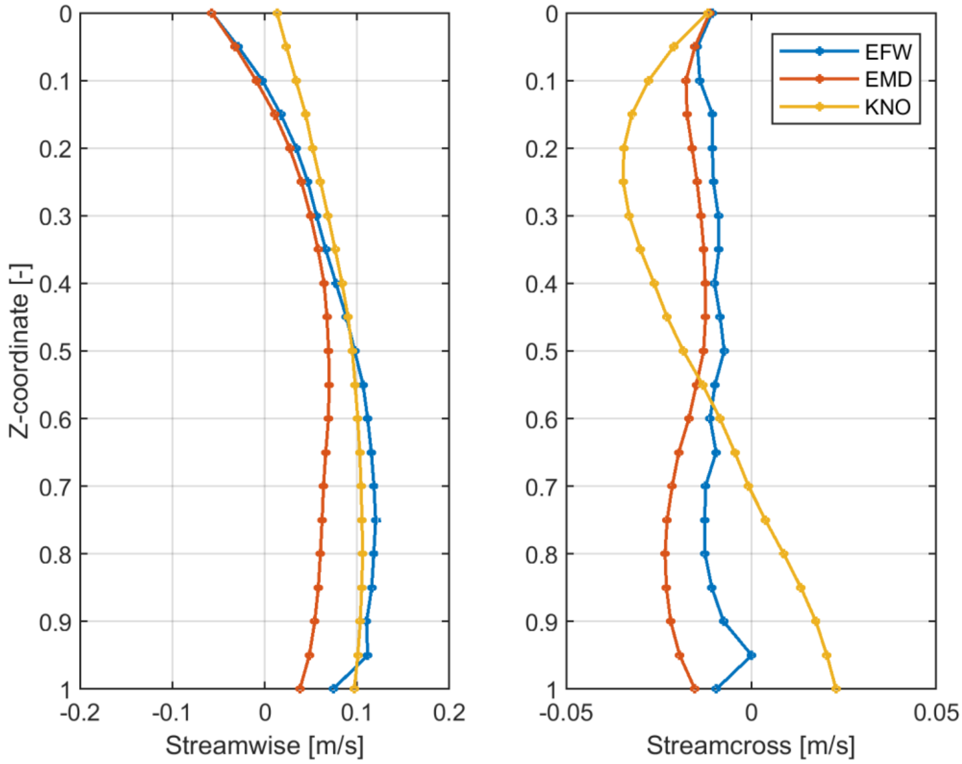

D.2.1.8. Time stack plots sediment concentrations and streamwise and upwards sediment flux

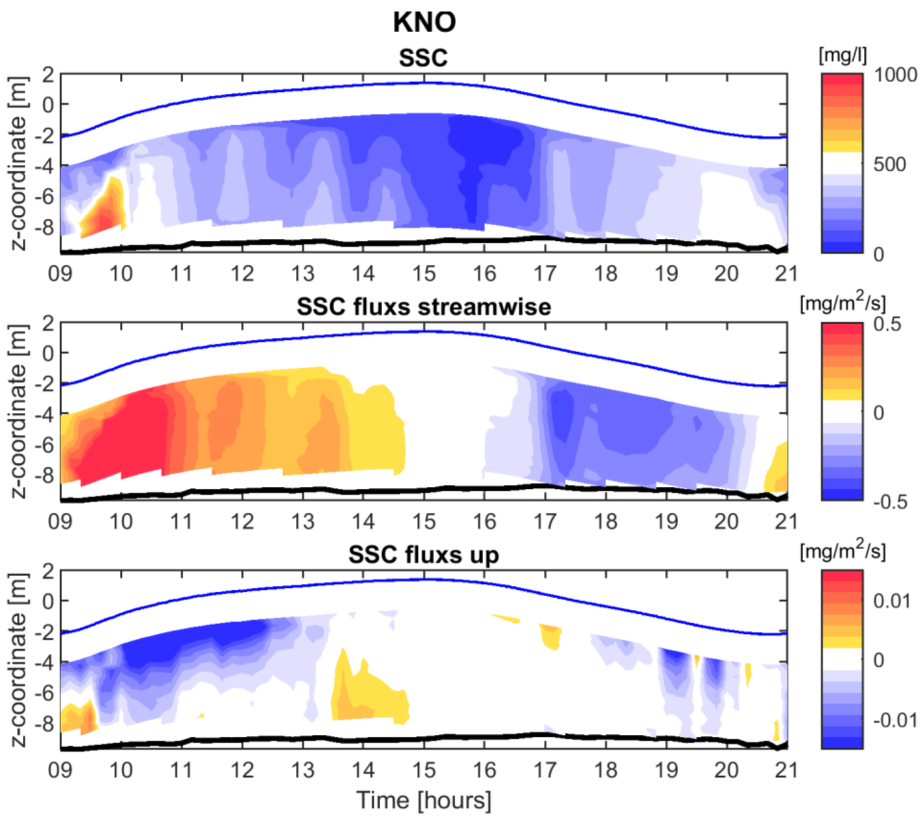

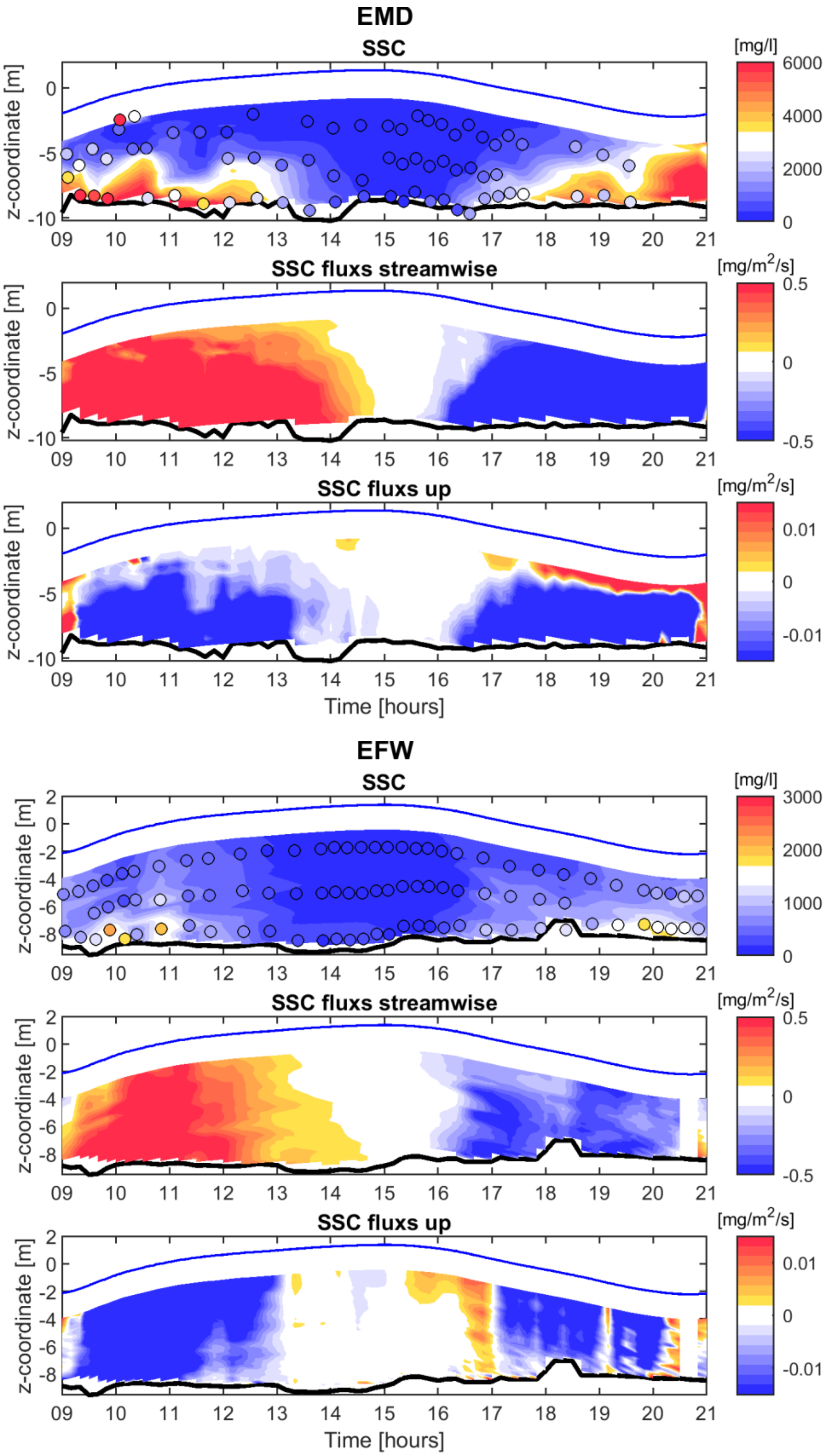
EMD
SSC
[mg/l]
SSC fluxs streamwise
[mg/m²/s]
SSC fluxs up
[mg/m²/s]
z-coordinate [m]
Time [hours]
EFW
SSC
[mg/l]
SSC fluxs streamwise
[mg/m²/s]
SSC fluxs up
[mg/m²/s]
z-coordinate [m]
Time [hours]

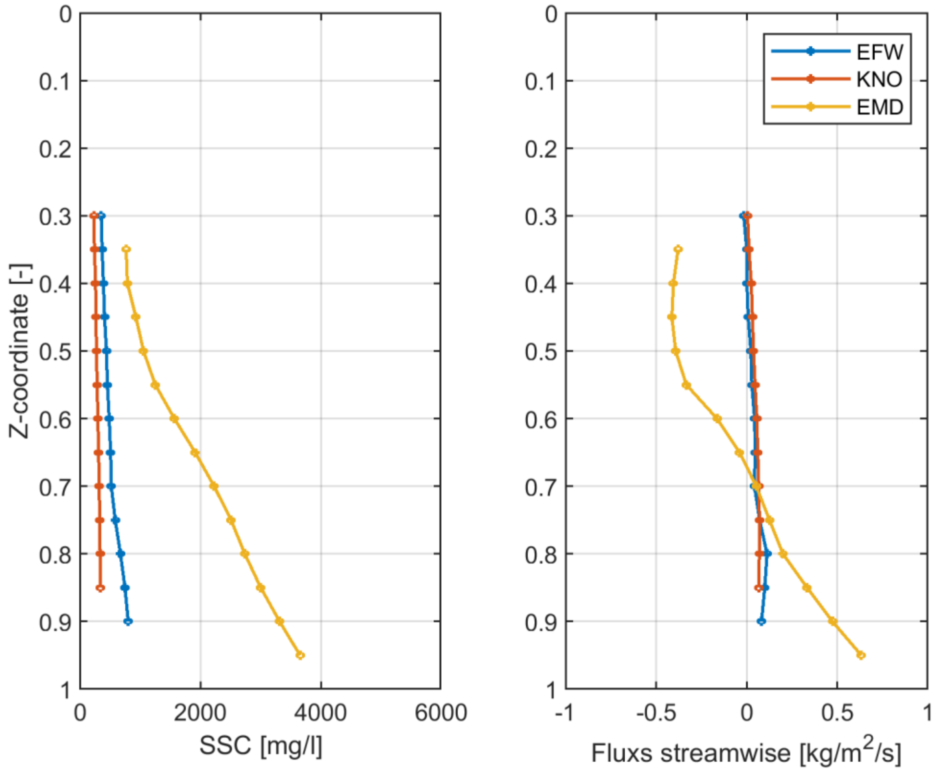

D.2.1.9. Time stack plots sediment concentrations and streamwise and upwards sediment flux (ADCP, echo intensity)

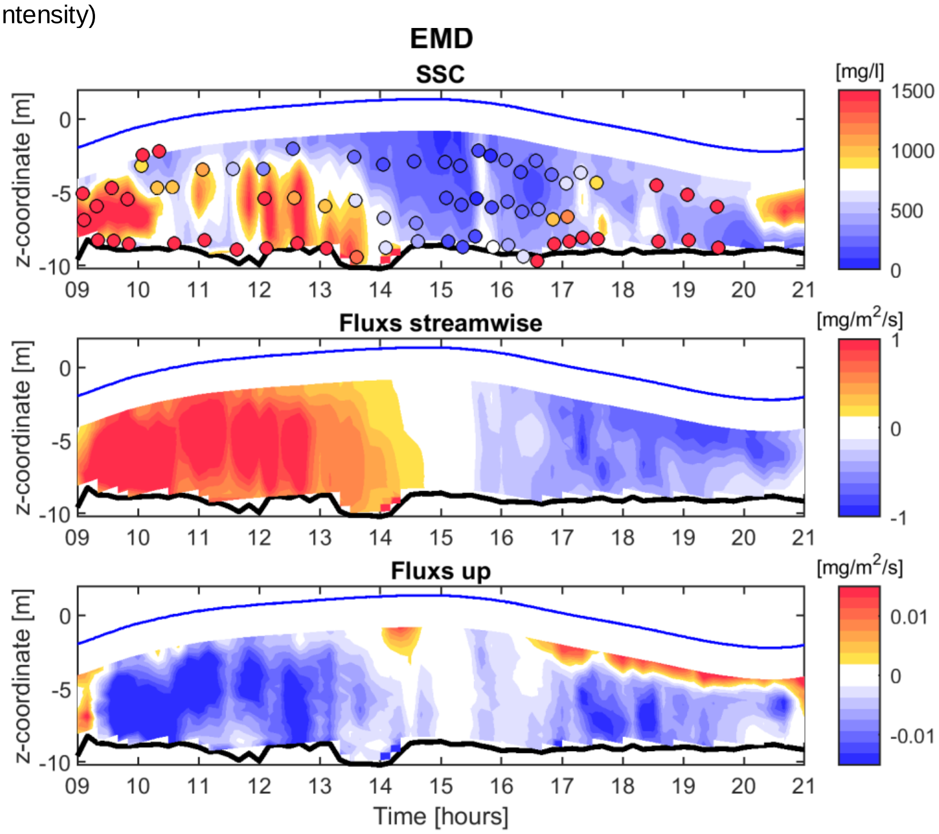

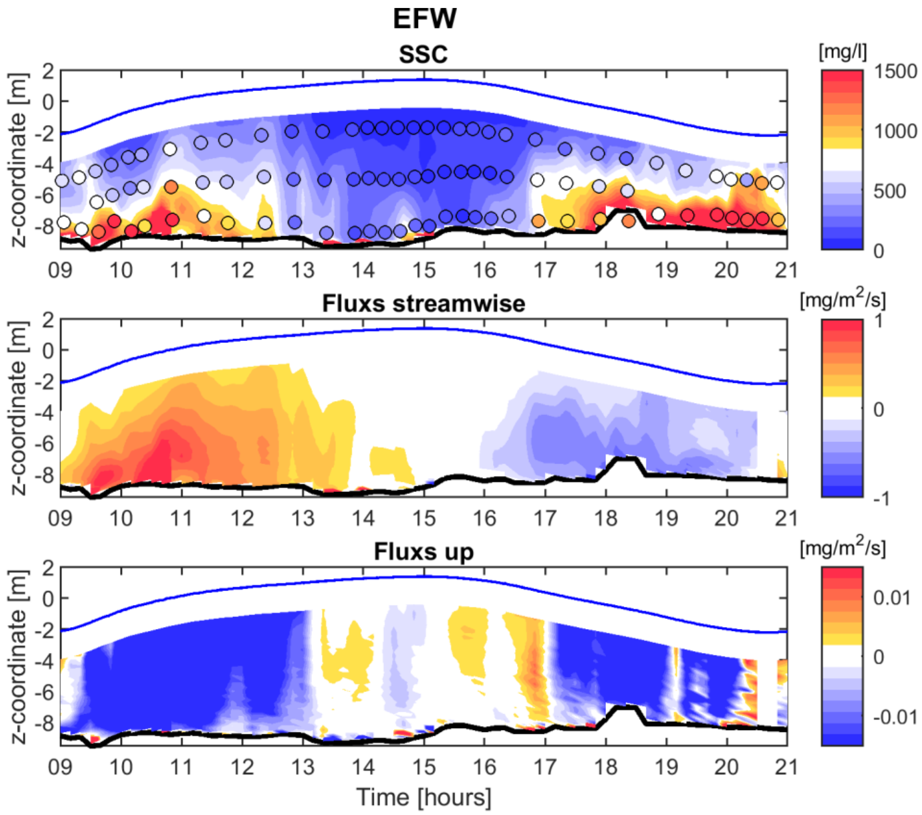

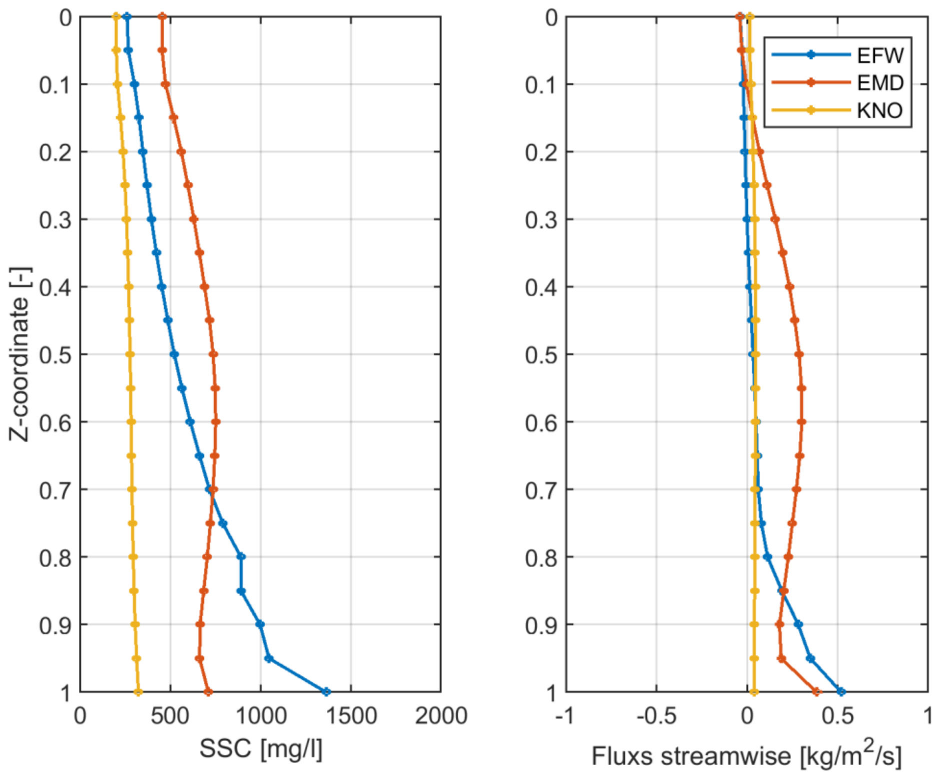

D.2.1.10. Time stack plots salinity measurement (CTD data)

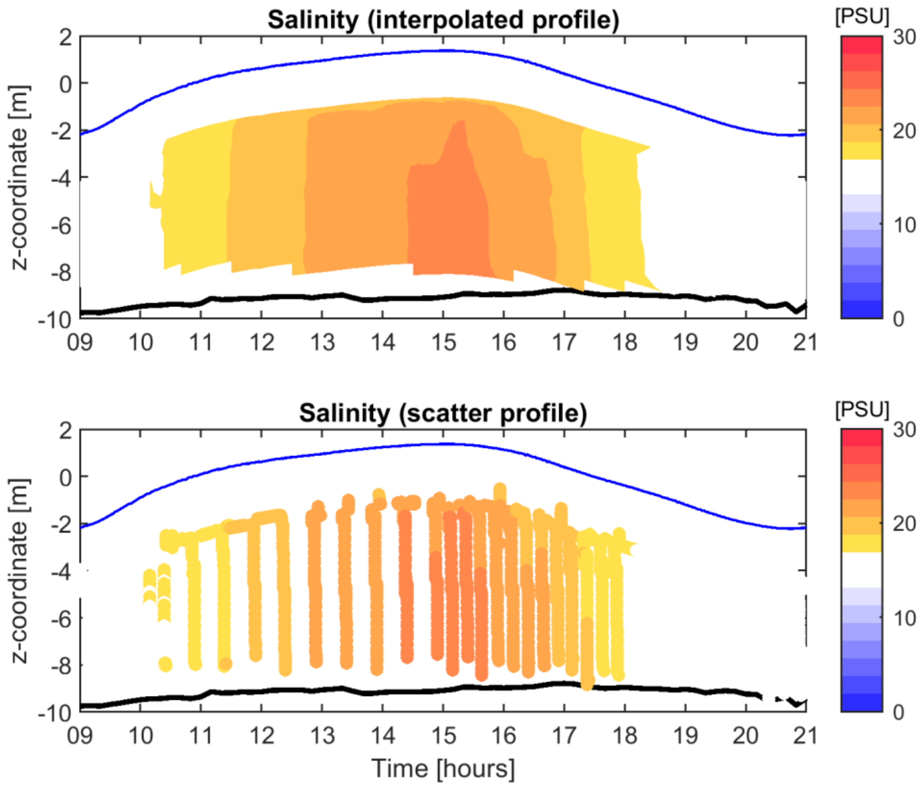

Station BM_{KNO}

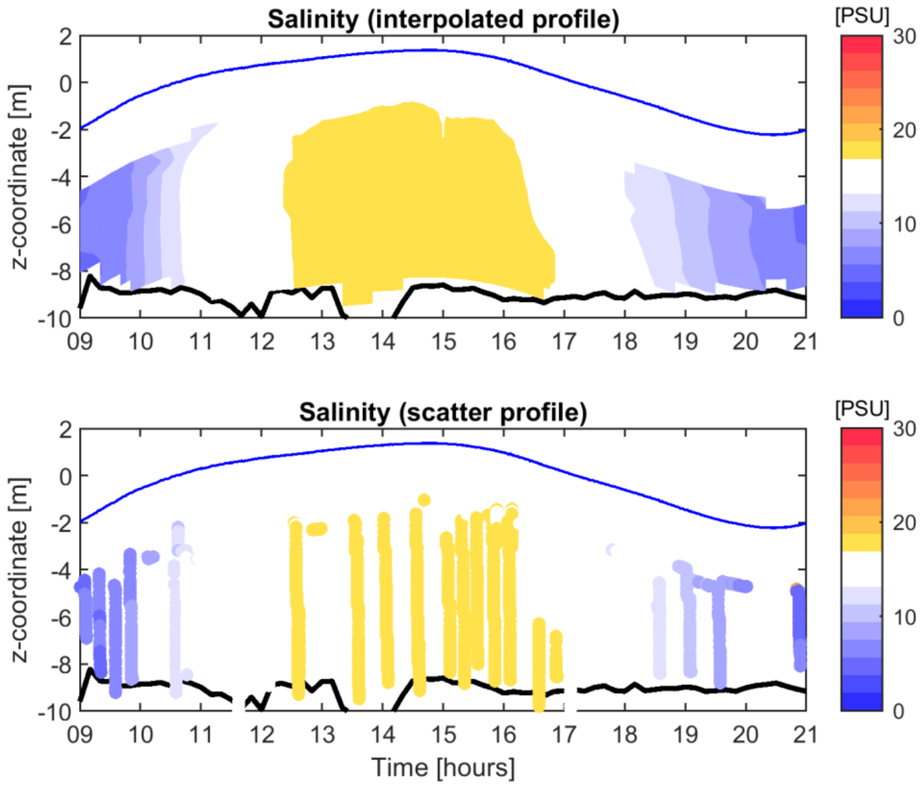

Station BM_{EMD}

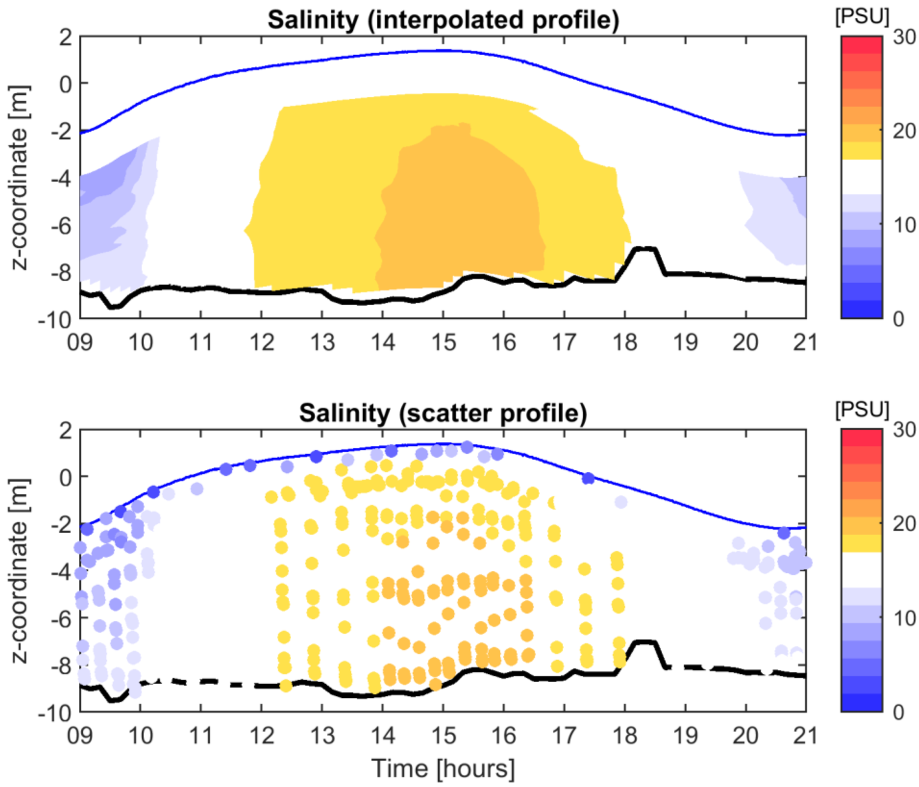

Station BM_{EFW}

D.2.1.11. Stack plots cross-sectional measurement velocities and spatial suspended sediment variability.

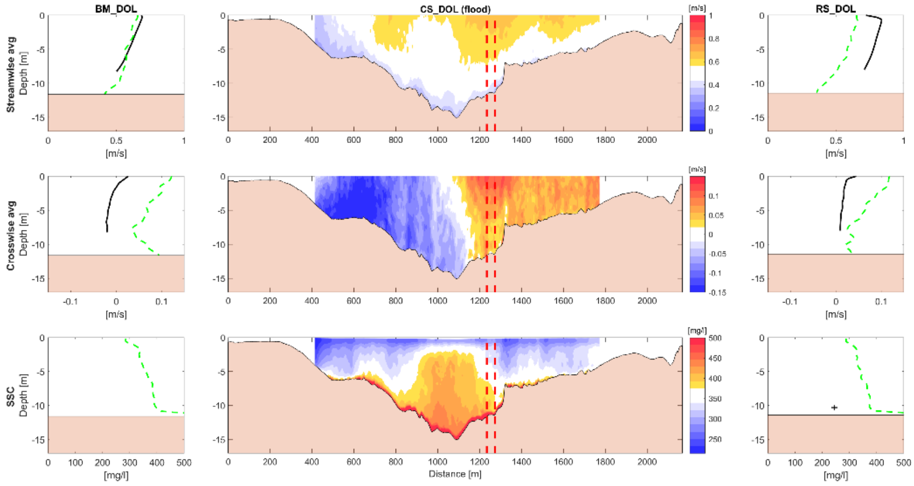

Longitudinal flow velocity (top), cross-sectional velocity (2nd panel) and SSC (based on echo intensity) (3rd panel), averaged over the flood period in the Dollard cross-section

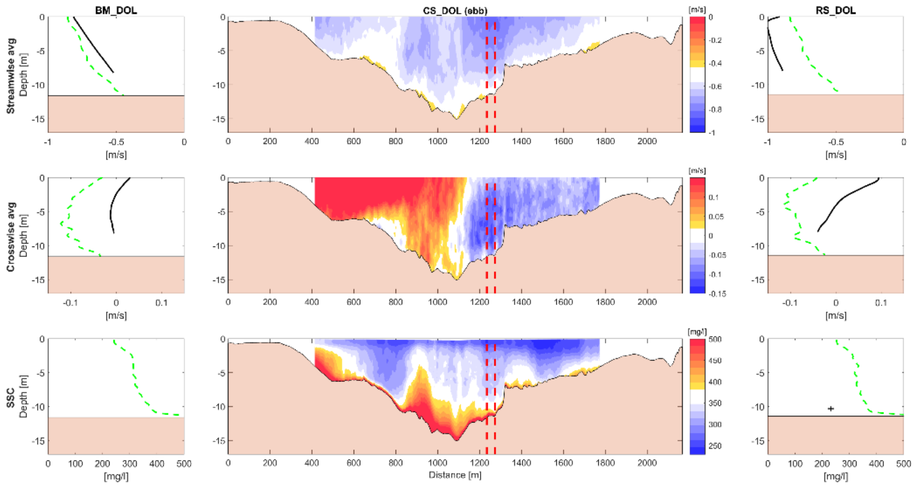

Longitudinal flow velocity (top), cross-sectional velocity (2nd panel) and SSC (based on echo intensity) (3rd panel), averaged over the ebb period in the Dollard cross-section

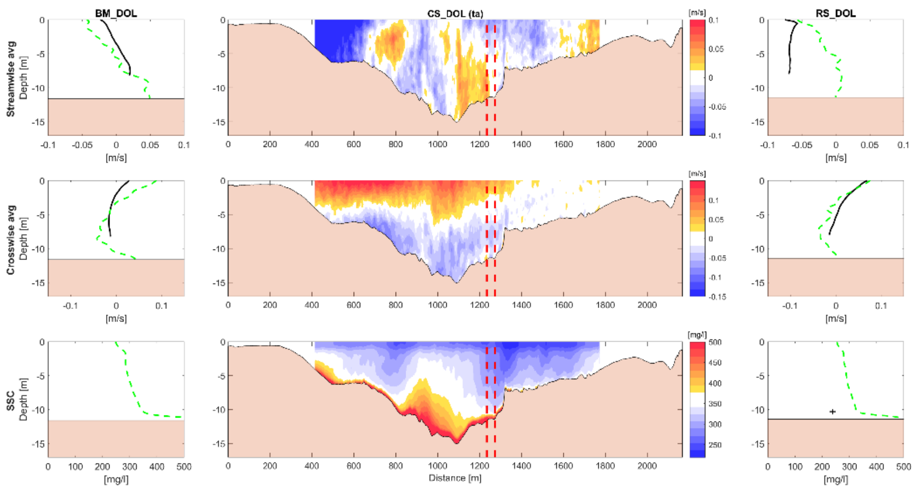

Longitudinal flow velocity (top), cross-sectional velocity (2nd panel) and SSC (based on echo intensity) (3rd panel), averaged over the full tidal period in the Dollard cross-section

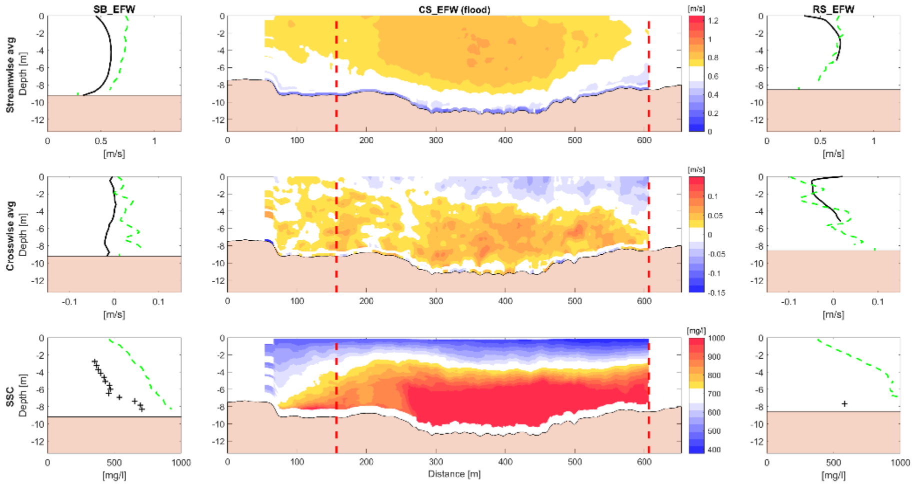

Longitudinal flow velocity (top), cross-sectional velocity (2nd panel) and SSC (based on echo intensity) (3rd panel), averaged over the flood period in the Emden Fairway cross-section

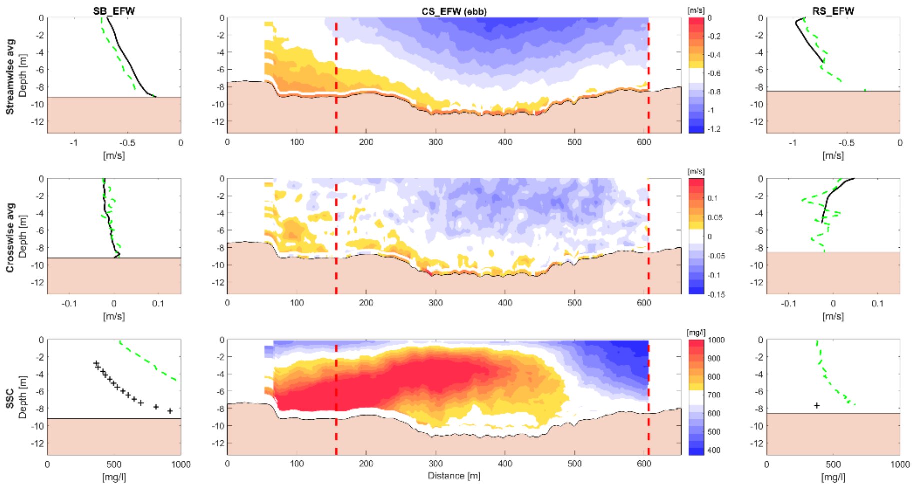

Longitudinal flow velocity (top), cross-sectional velocity (2nd panel) and SSC (based on echo intensity) (3rd panel), averaged over the ebb period in the Emden Fairway cross-section

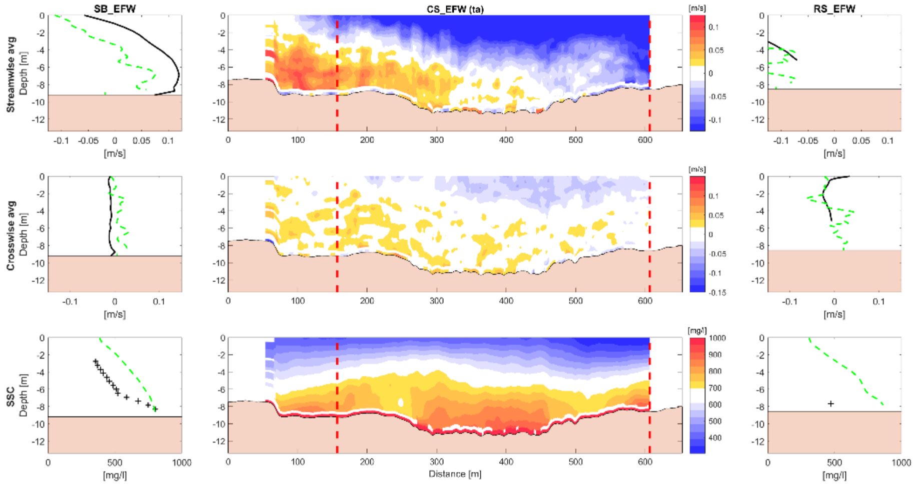

Longitudinal flow velocity (top), cross-sectional velocity (2nd panel) and SSC (based on echo intensity) (3rd panel), averaged over the full tidal period in the Emden Fairway cross-section

D.2.1.12. Stack plots cross-sectional measurement sediment fluxes and spatial suspended sediment variability.

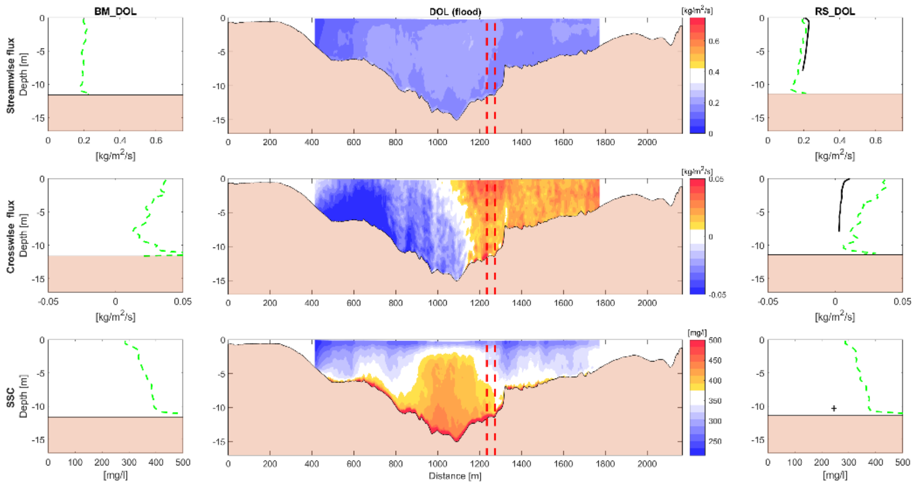

Longitudinal sediment flux (top), cross-sectional sediment flux (2nd panel) and SSC (based on echo intensity) (3rd panel), averaged over the flood period in the Dollard cross-section

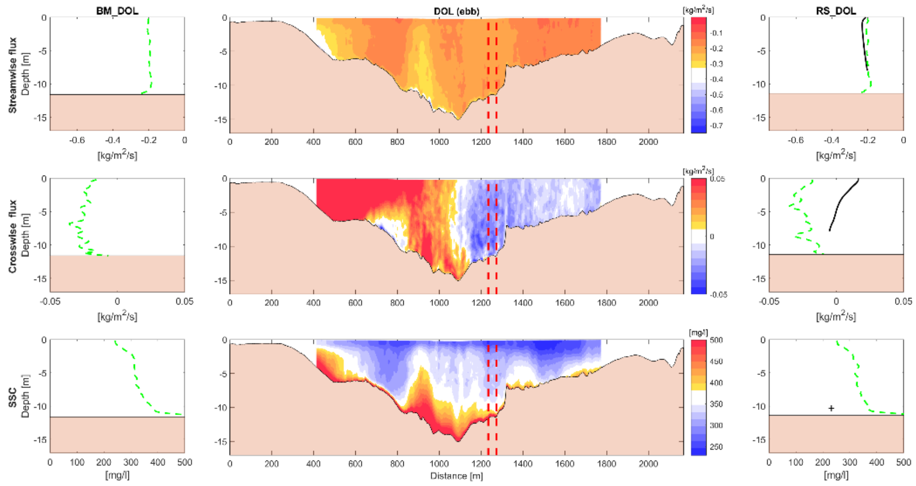

Longitudinal sediment flux (top), cross-sectional sediment flux (2nd panel) and SSC (based on echo intensity) (3rd panel), averaged over the ebb period in the Dollard cross-section

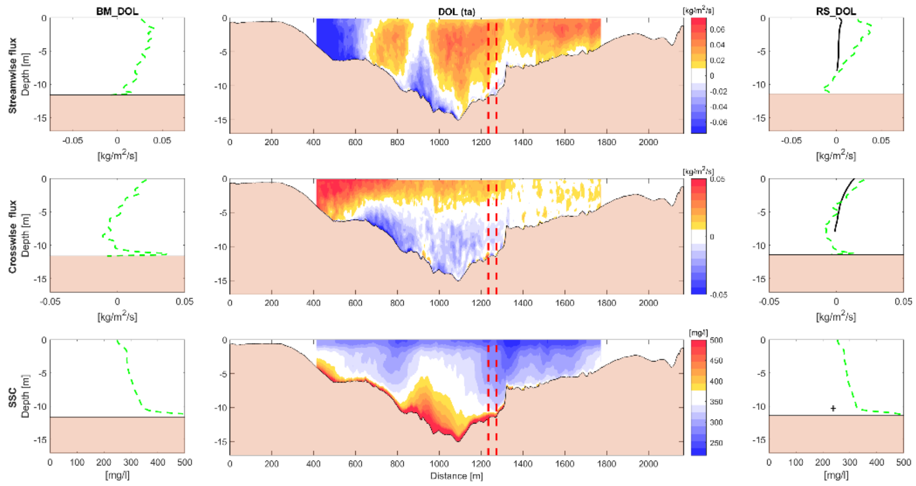

Longitudinal sediment flux (top), cross-sectional sediment flux (2nd panel) and SSC (based on echo intensity) (3rd panel), averaged over the full tidal period in the Dollard cross-section

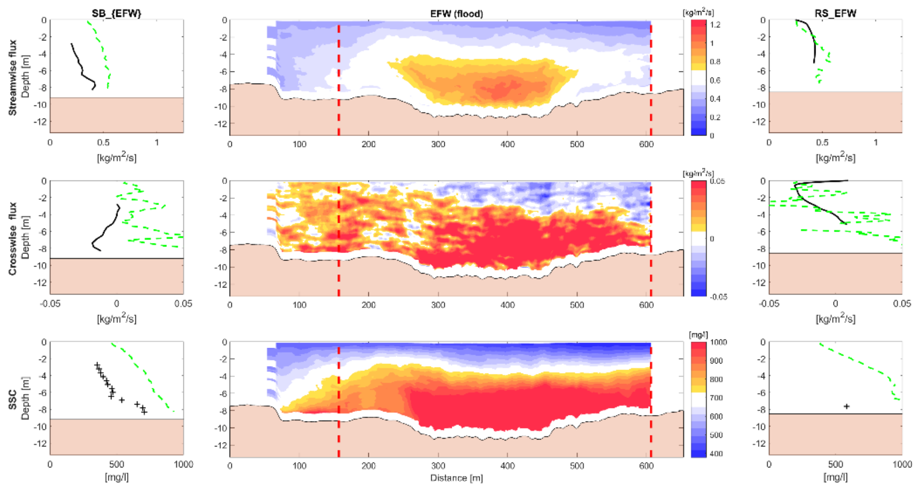

Longitudinal sediment flux (top), cross-sectional sediment flux (2nd panel) and SSC (based on echo intensity) (3rd panel), averaged over the flood period in the Emden Fairway cross-section

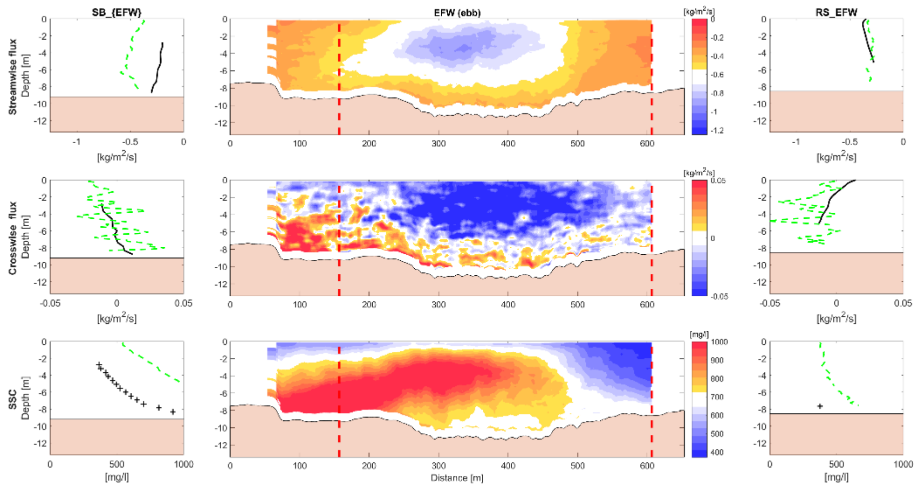

Longitudinal sediment flux (top), cross-sectional sediment flux (2nd panel) and SSC (based on echo intensity) (3rd panel), averaged over the ebb period in the Emden Fairway cross-section

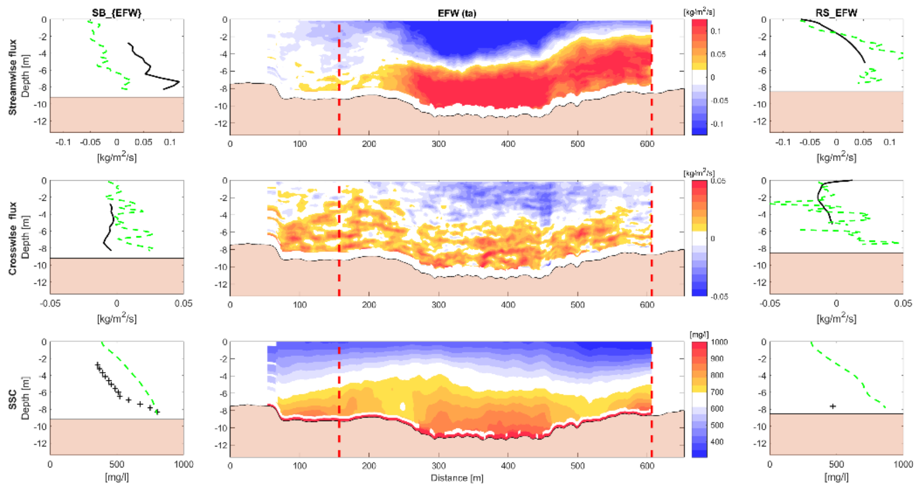

Longitudinal sediment flux (top), cross-sectional sediment flux (2nd panel) and SSC (based on echo intensity) (3rd panel), averaged over the full tidal period in the Emden Fairway cross-section

D.2.1.13. Geise dam flow measurement

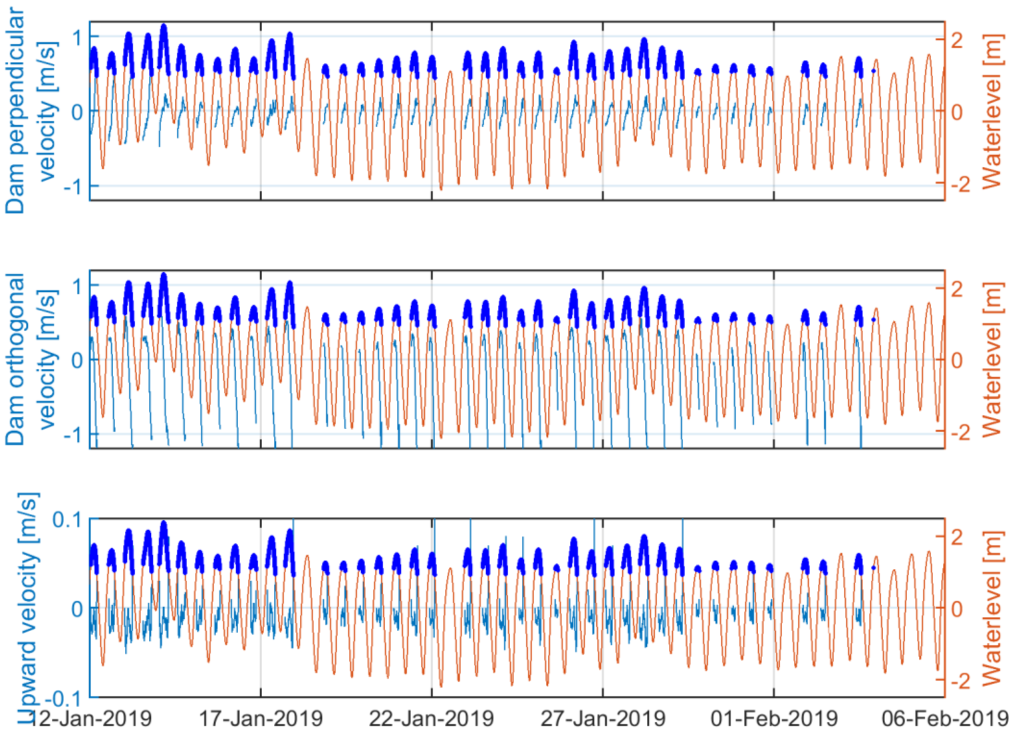

Top panel: Waterlevels (orange) measured at Emden, with dark blue waterlevels indicating the period of flow through the cross-section, at station Ems East. Flow velocities in light blue, with the velocity component perpendicular to the dam in the top panel, in the direction of the dam in the second panel, and the vertical velocity in the third panel.

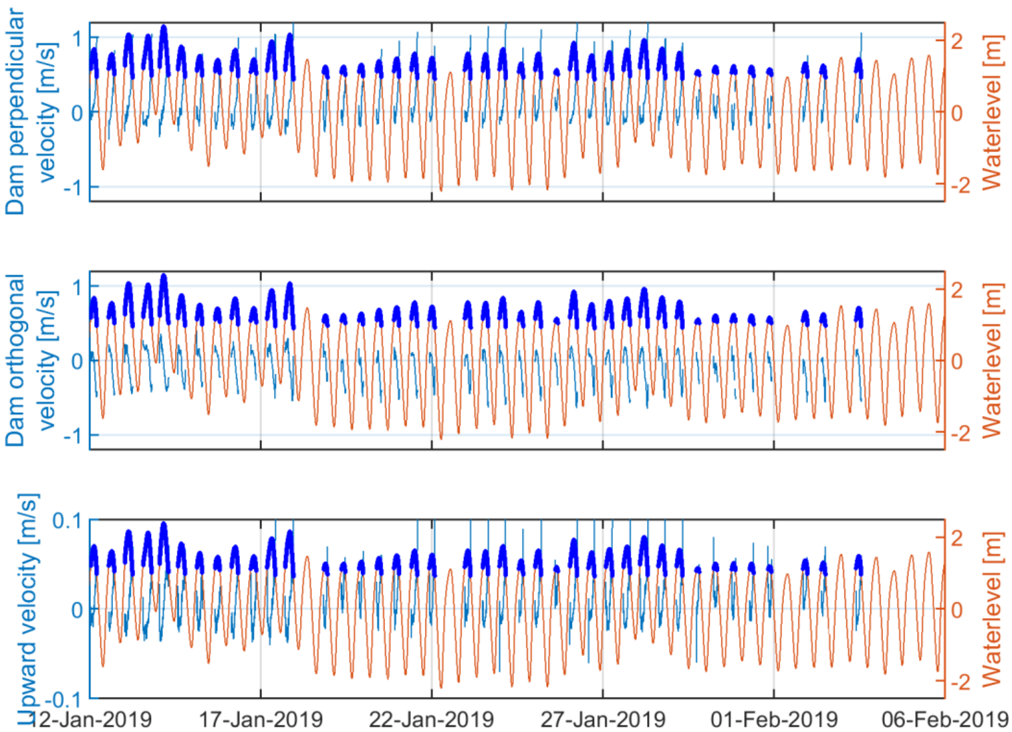

Top panel: Waterlevels (orange) measured at Emden, with dark blue waterlevels indicating the period of flow through the cross-section, at station Ems West. Flow velocities in light blue, with the velocity component perpendicular to the dam in the top panel, in the direction of the dam in the second panel, and the vertical velocity in the third panel.

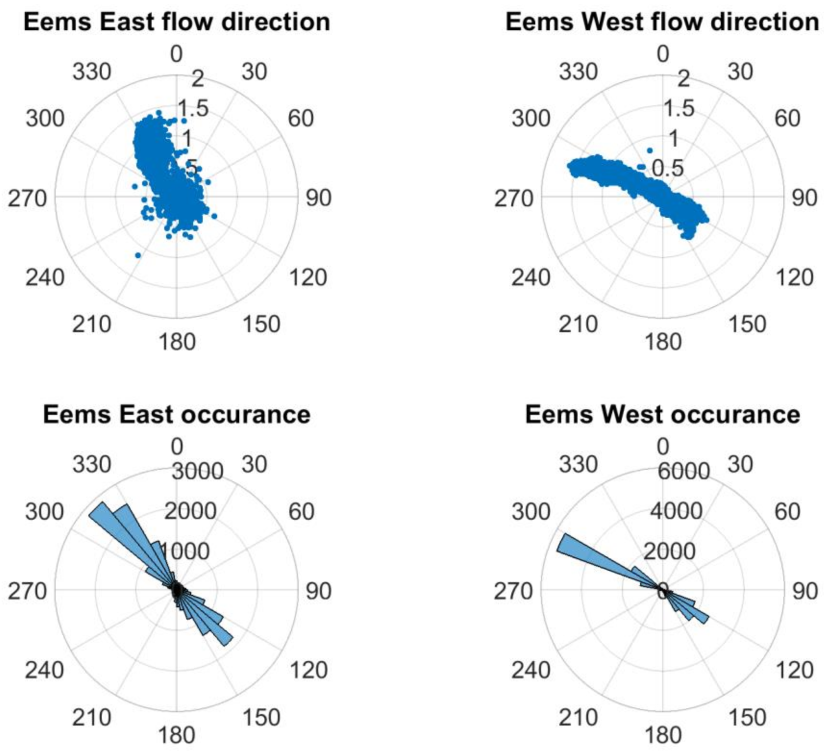

Flow velocity rose (top panels) for Geise dam observation East and West; and frequency of occurrence of flow direction (lower panels). Both the largest flow velocity and the largest frequency of occurrence are for flows towards the Northwest.

D.2.1.14. Longitudinal survey of turbidity and salinity

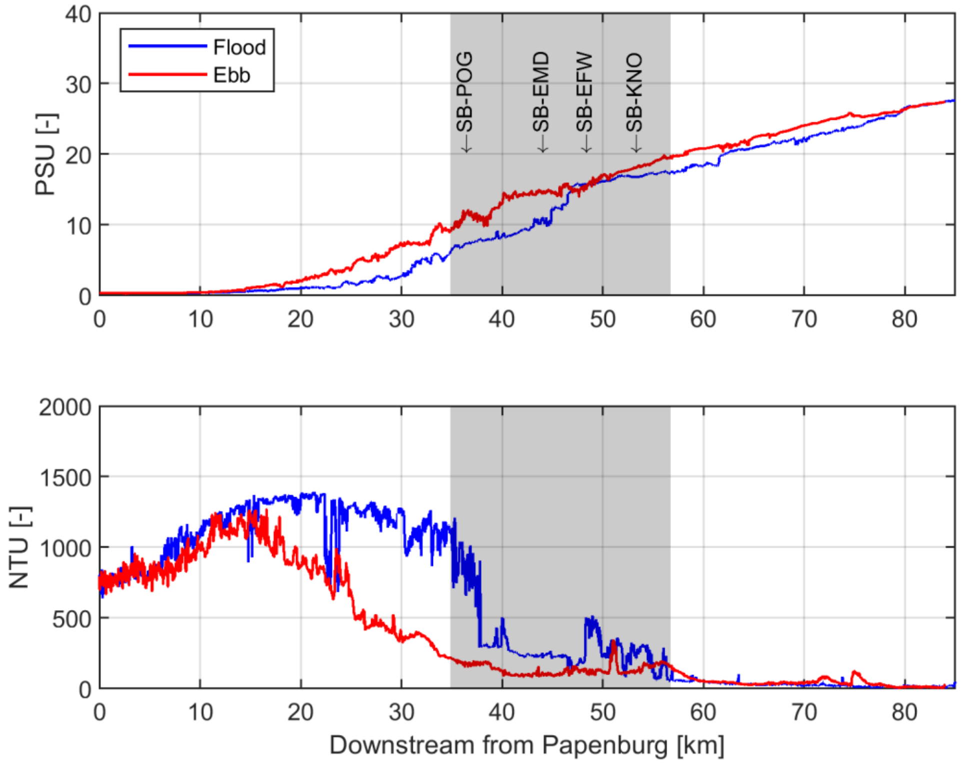

Salinity (in psu) and turbidity (in ntu) measured near-surface during the longitudinal cross-section between Papenburg and Borkum, measured on 24 January 2019.

E Observations Geise dam

E.1 Observations 1999

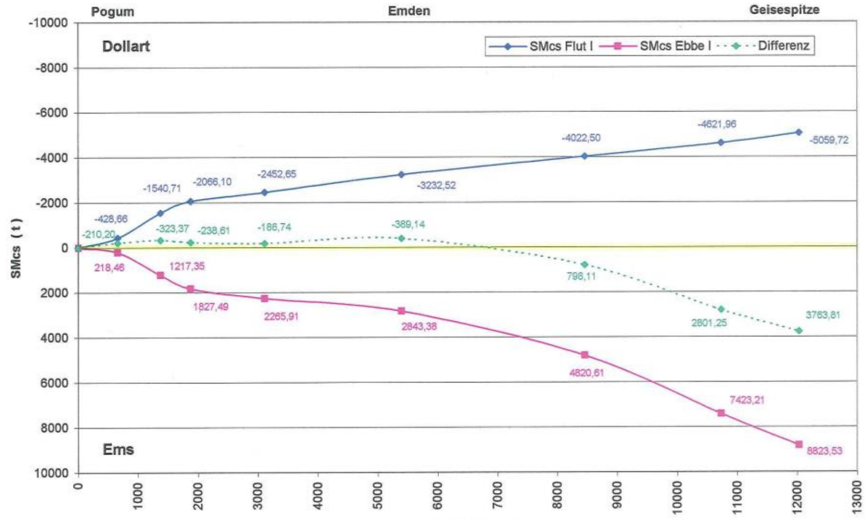

Figure 7-23 Transport over the Geise dam, averaged over one tidal cycle on 8 November 1999 (Klebanowski and Jurgens, 2001)

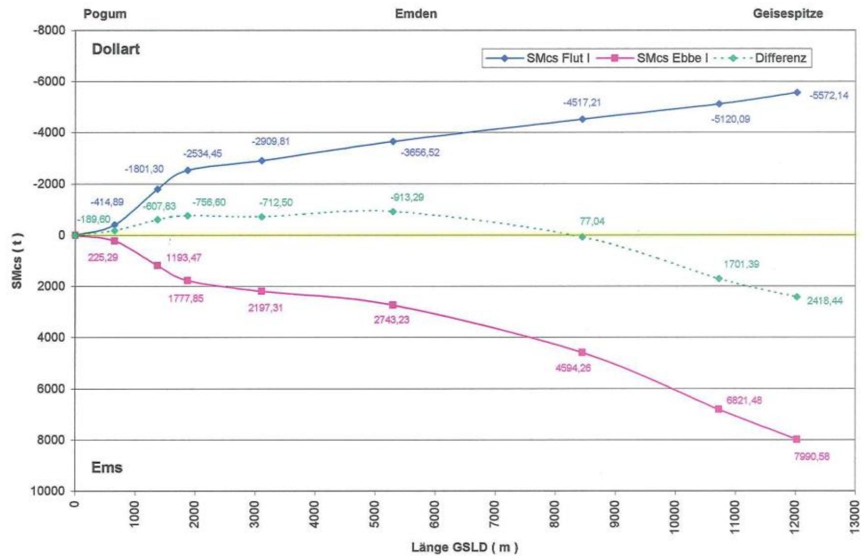

Figure 7-24 Transport over the Geise dam, averaged over tidal cycle 1 on 9 November 1999 (Klebanowski and Jurgens, 2001)

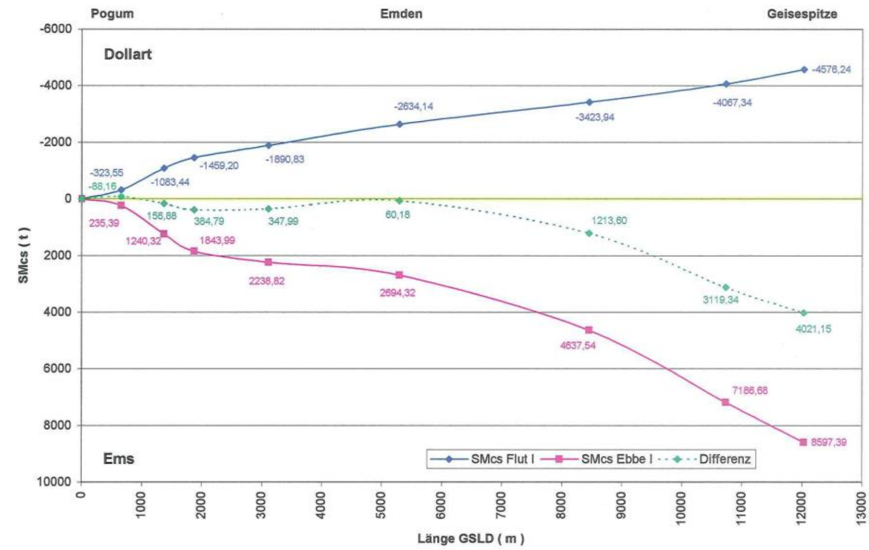

Figure 7-25 Transport over the Geise dam, averaged over tidal cycle 2 on 9 November 1999 (Klebanowski and Jurgens, 2001).

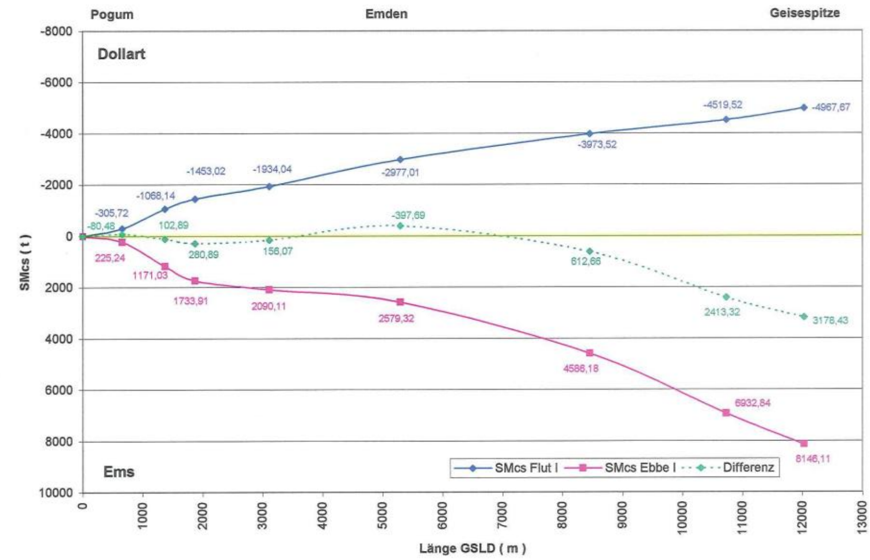

Figure 7-26 Transport over the Geise dam, averaged over one tidal cycle on 10 November 1999 (Klebanowski and Jurgens, 2001).

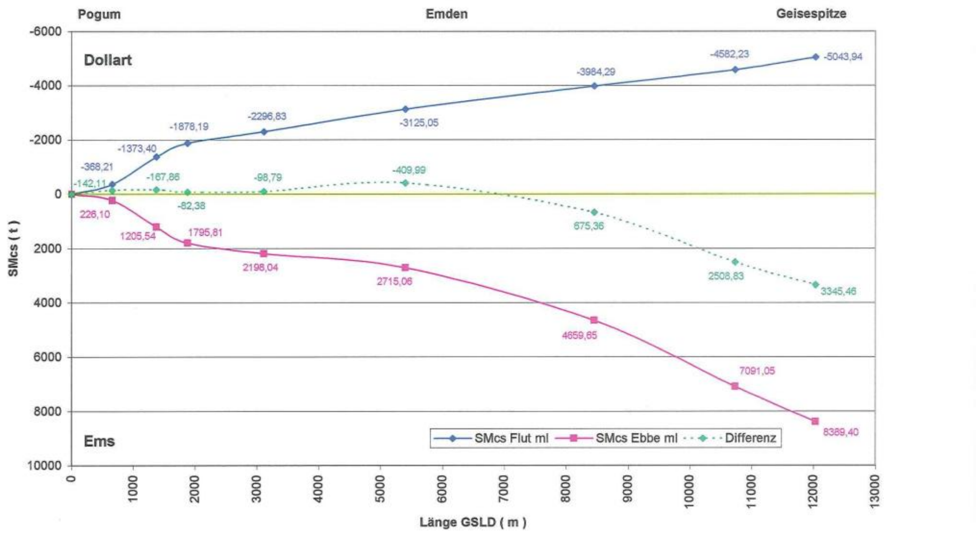

Figure 7-27 Transport over the Geise dam, averaged over 4 tides from 8 November 1999 to 10 November 1999 (Klebanowski and Jurgens, 2001)

E.2 Observations 2001

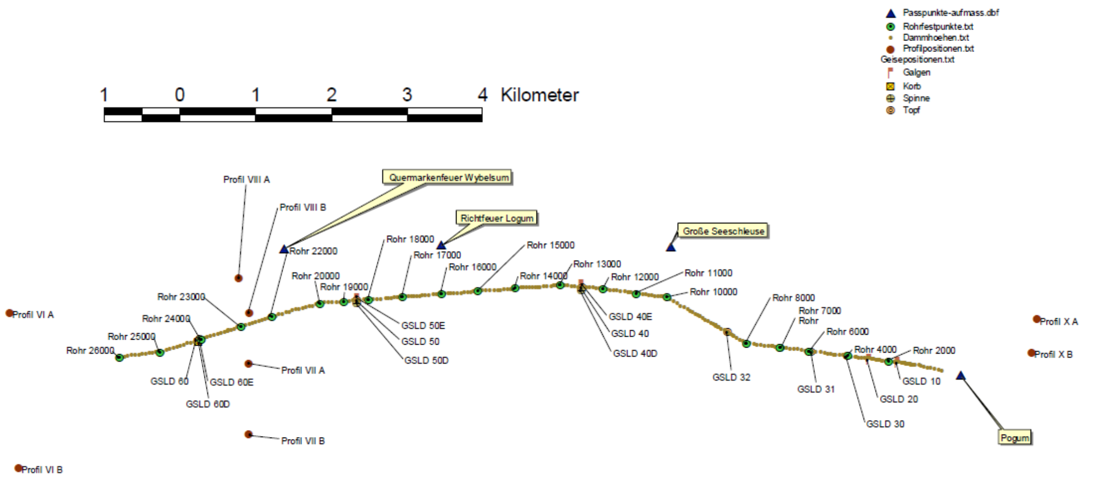

Figure 7-28 Location of observations in 2001 (Jensen et al., 2002)

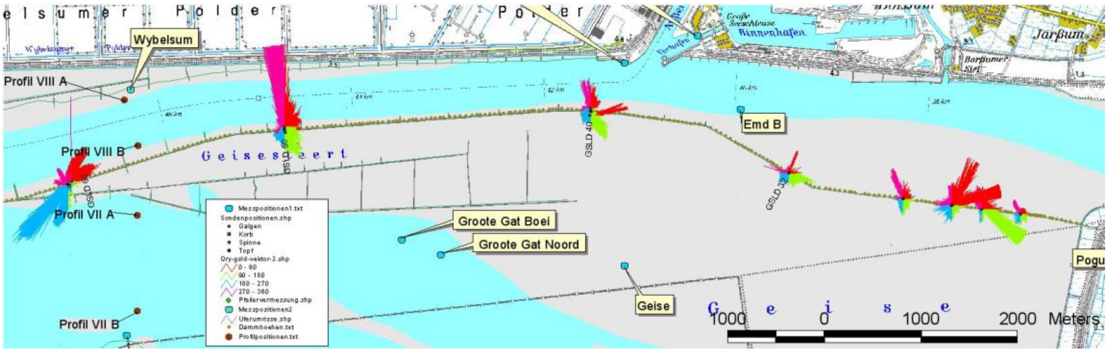

Figure 7-29 Flow velocity observations on 13 March 2001 (Jensen et al., 2002)

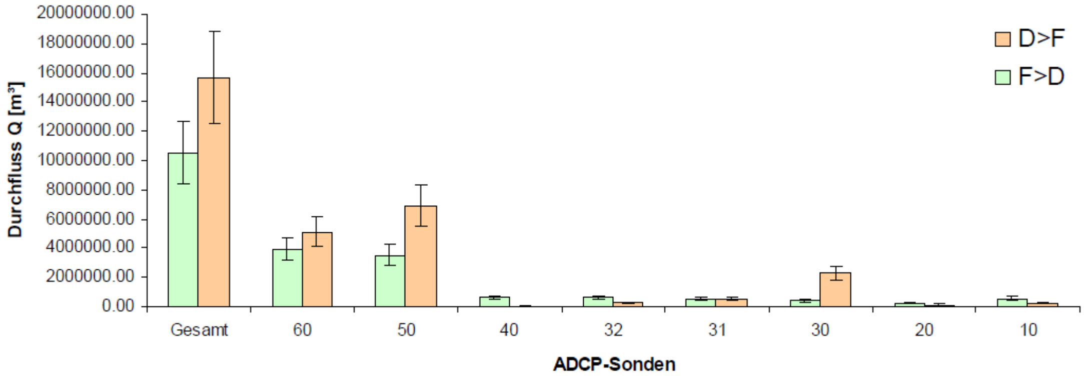

Figure 7-30 Measured discharge from Dollard to fairway (orange) and fairway to Dollard (green) on 13 March 2001 (Jensen et al., 2002).

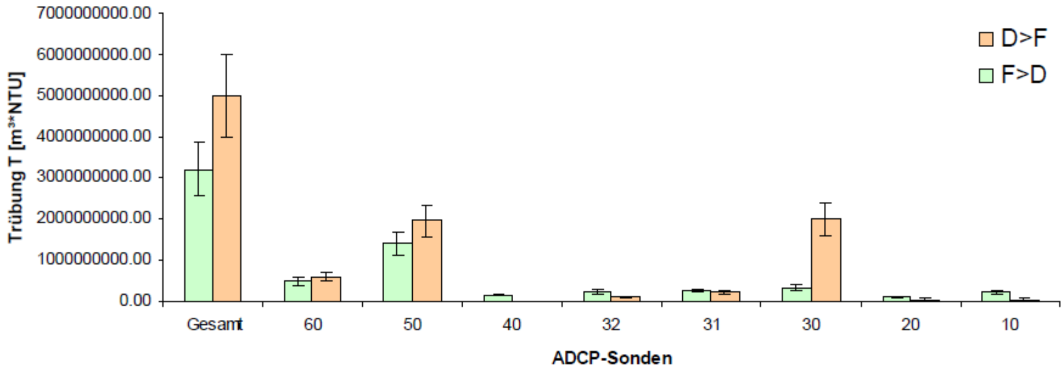

Figure 7-31 Product of measured discharge and turbidity (in NTU) from Dollard to fairway (orange) and fairway to Dollard (green) on 13 March 2001 (Jensen et al., 2002).

E.3 2019 observations

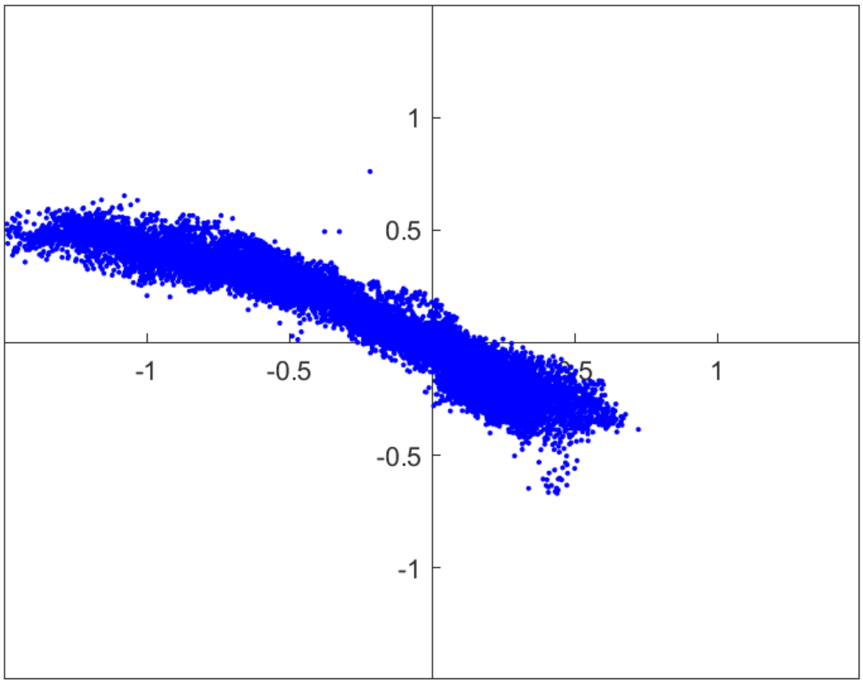

Figure 7-32 Flow velocity measured on the western Geise location

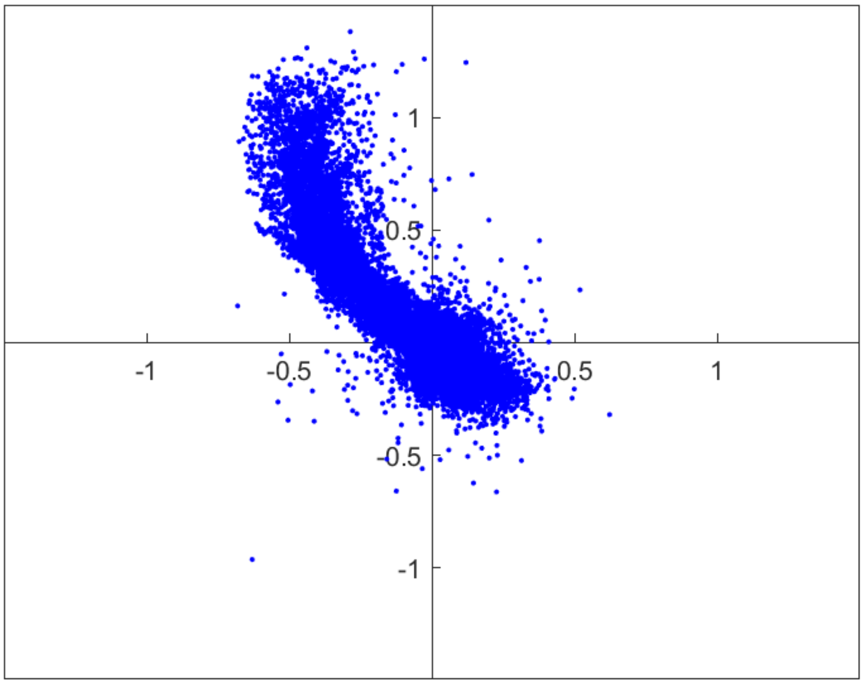

Figure 7-33 Flow velocity measured on the eastern Geise location

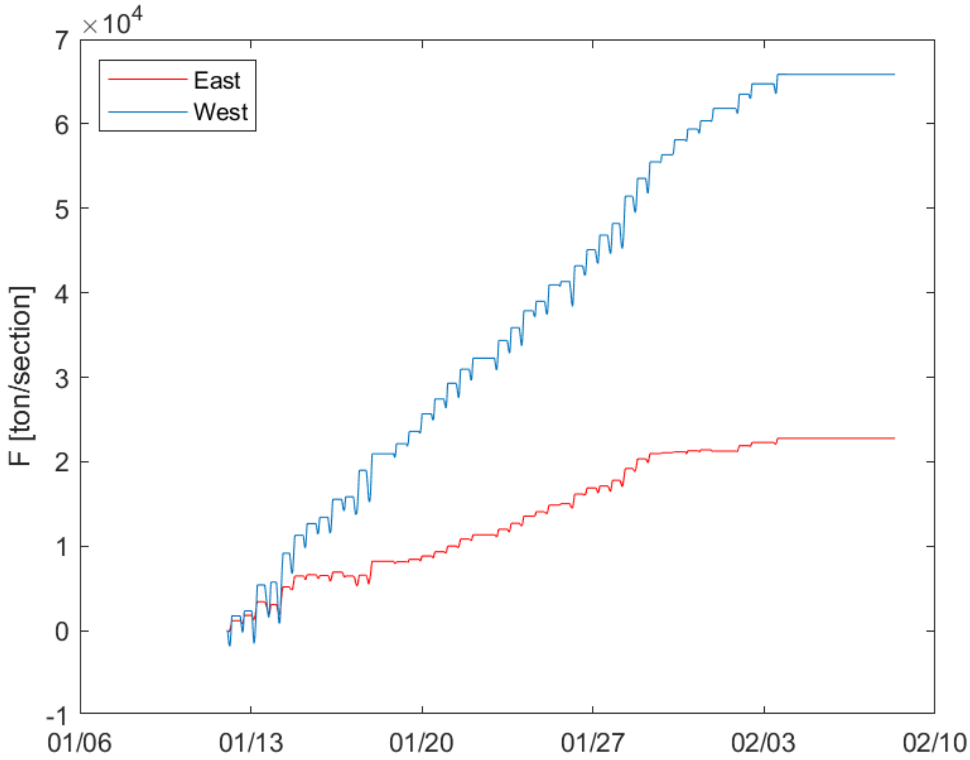

Figure 7-34 Cumulative sediment flux for the sections represented by the observation stations west and east, assuming a sediment concentration of 200 mg/l during both ebb and flood, and an average height of 20 cm above NAP for the western section and 80 cm above NAP for the eastern section

E.4 2020 observations

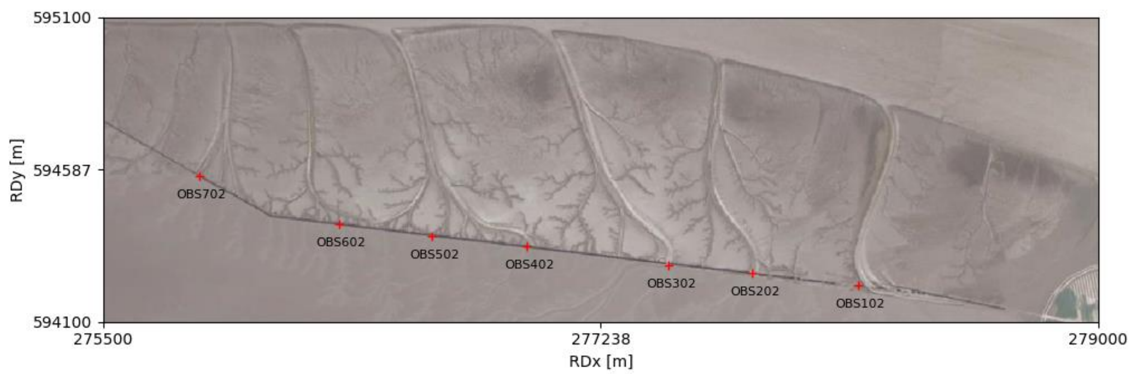

Figure 7-35 Observation stations on the Geise dam in 2020

E.4.1.1. Velocity scatterdiagram with waterlevel in colors

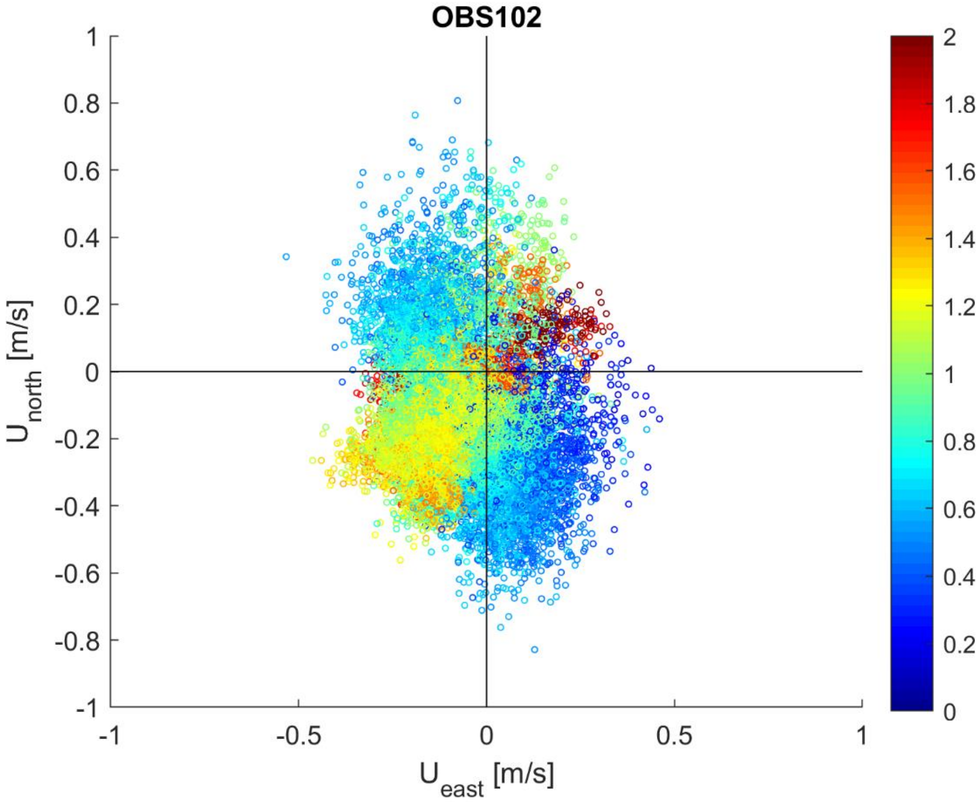

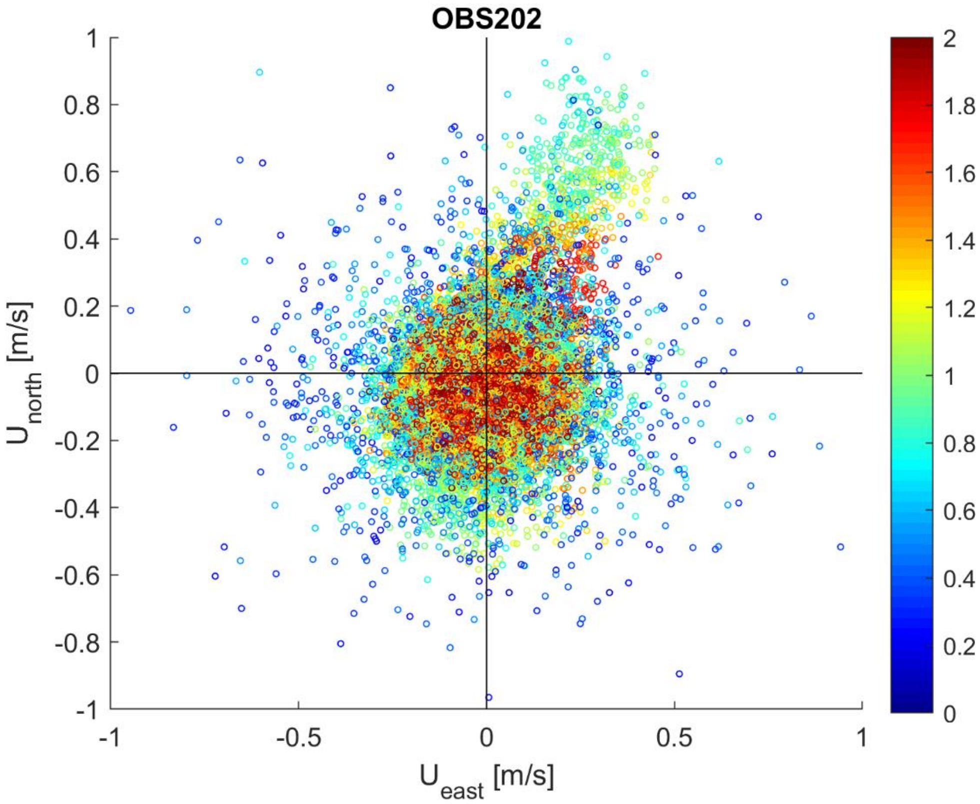

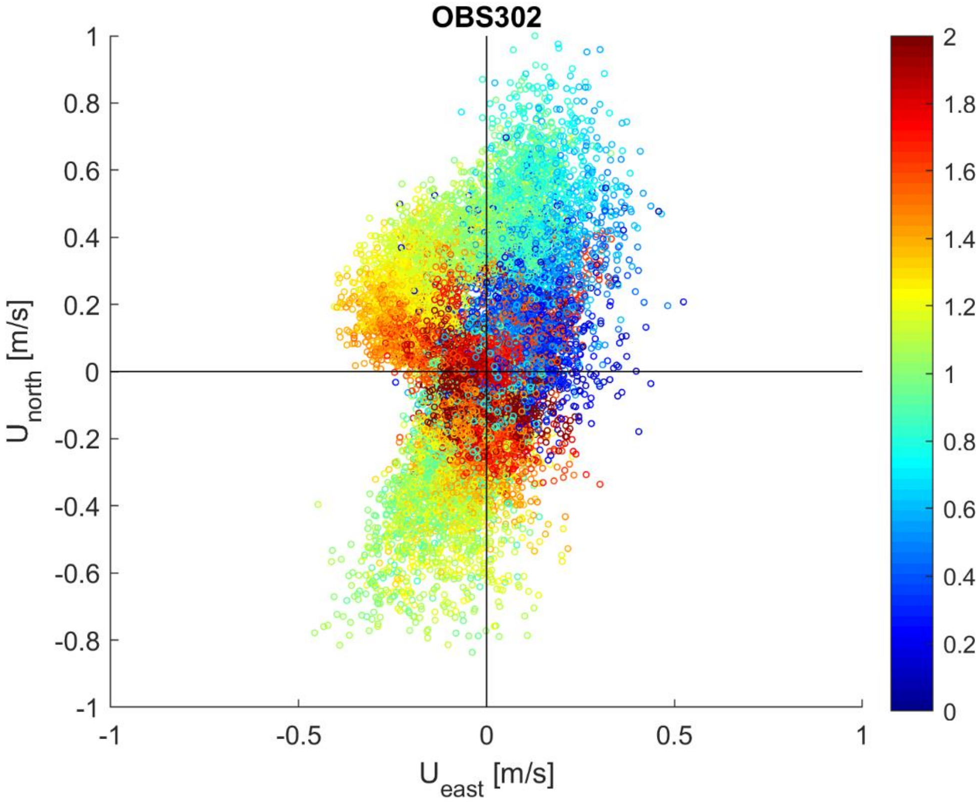
OBS302
1
0.8
0.6
0.4
0.2
0
-0.2
-0.4
-0.6
-0.8
-1
U north [m/s]
-1
-0.5
0
0.5
1
U east [m/s]
2
1.8
1.6
1.4
1.2
1
0.8
0.6
0.4
0.2
0

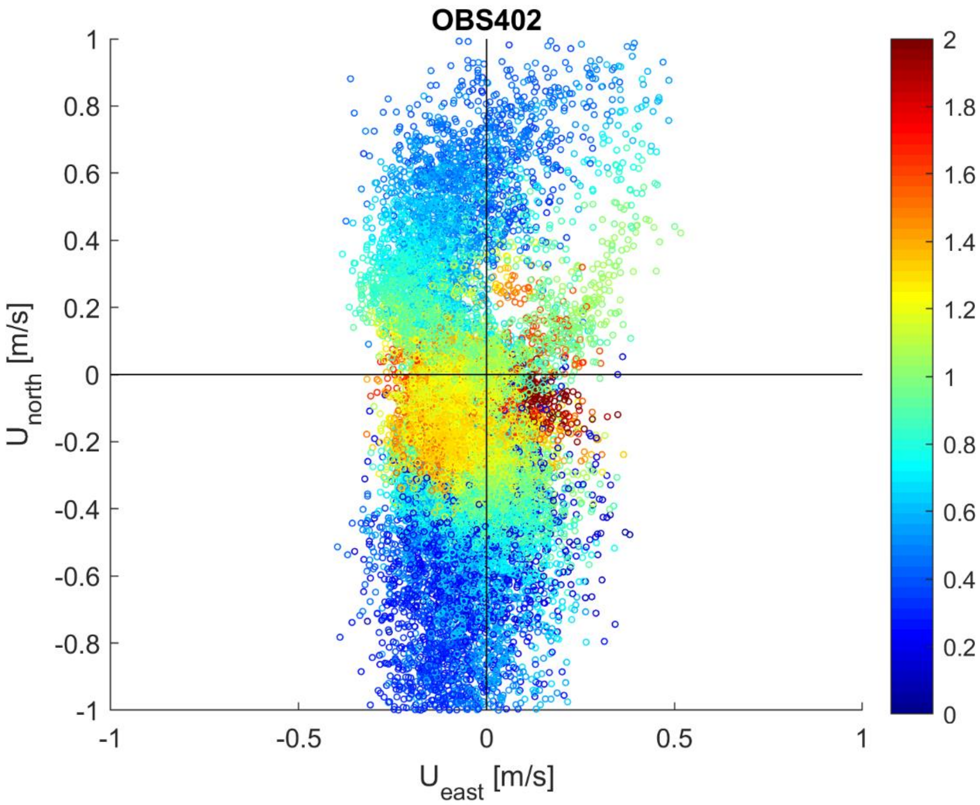
OBS402
1
0.8
0.6
0.4
0.2
0
-0.2
-0.4
-0.6
-0.8
-1
U north [m/s]
-1
-0.5
0
0.5
1
U east [m/s]
2
1.8
1.6
1.4
1.2
1
0.8
0.6
0.4
0.2
0

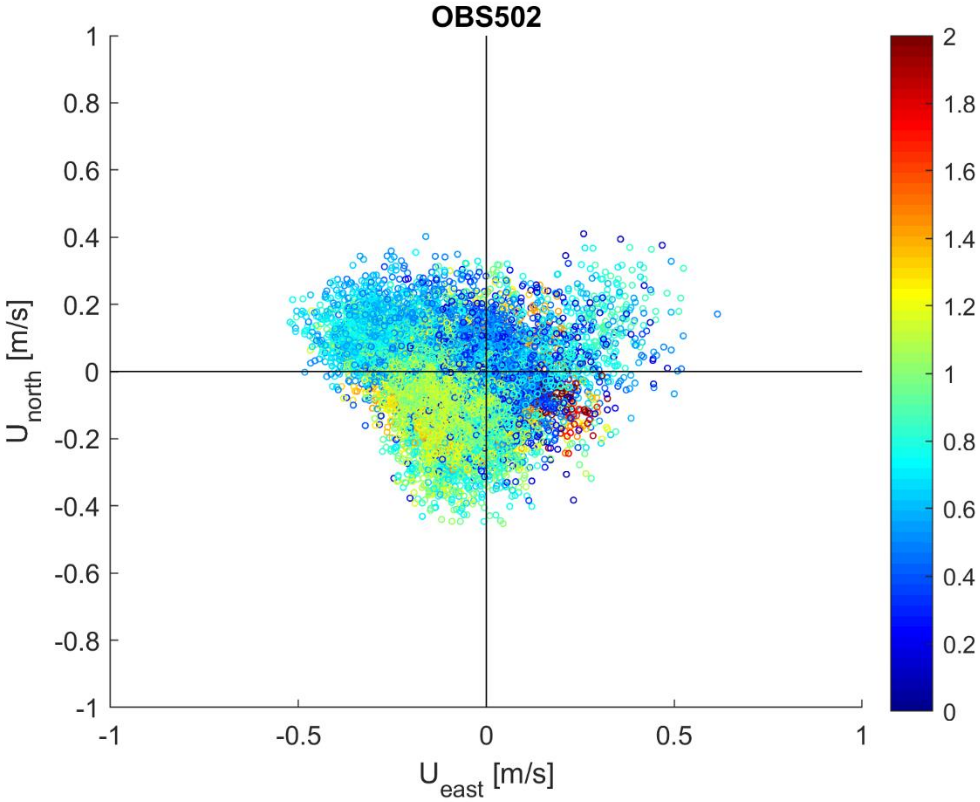
OBS502
U_north [m/s]
U_east [m/s]
1
0.8
0.6
0.4
0.2
0
-0.2
-0.4
-0.6
-0.8
-1
-0.5
0.5
2
1.8
1.6
1.4
1.2

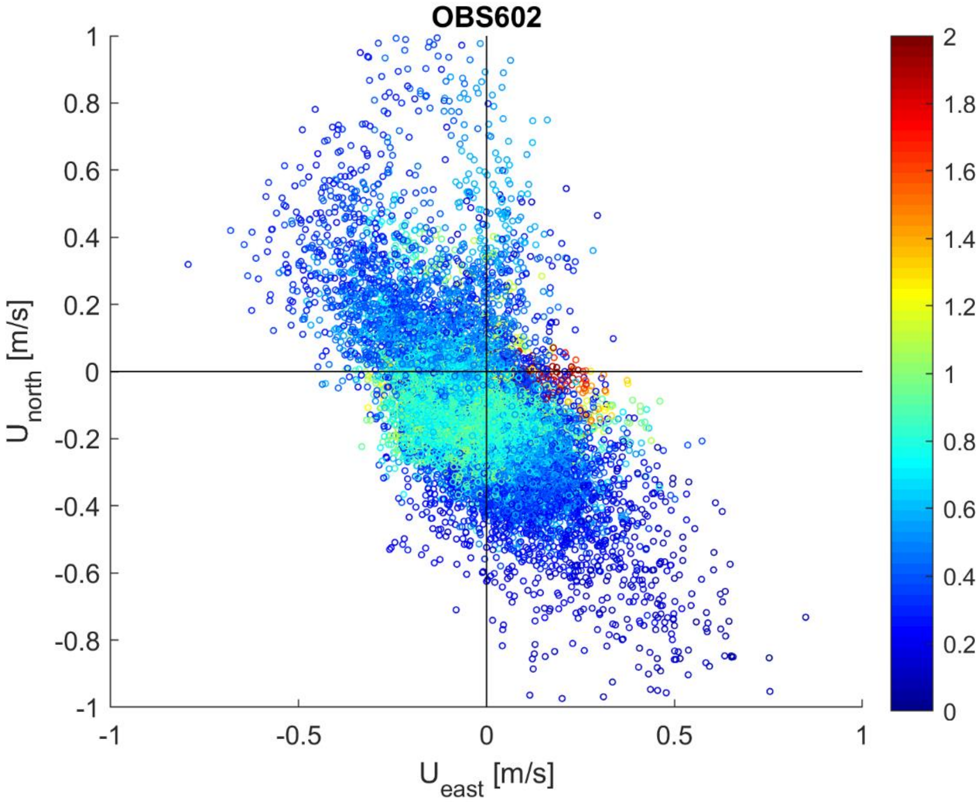
OBS602
U_north [m/s]
U_east [m/s]
1
0.8
0.6
0.4
0.2
0
-0.2
-0.4
-0.6
-0.8
-1
-0.5
0.5
2
1.8
1.6
1.4
1.2

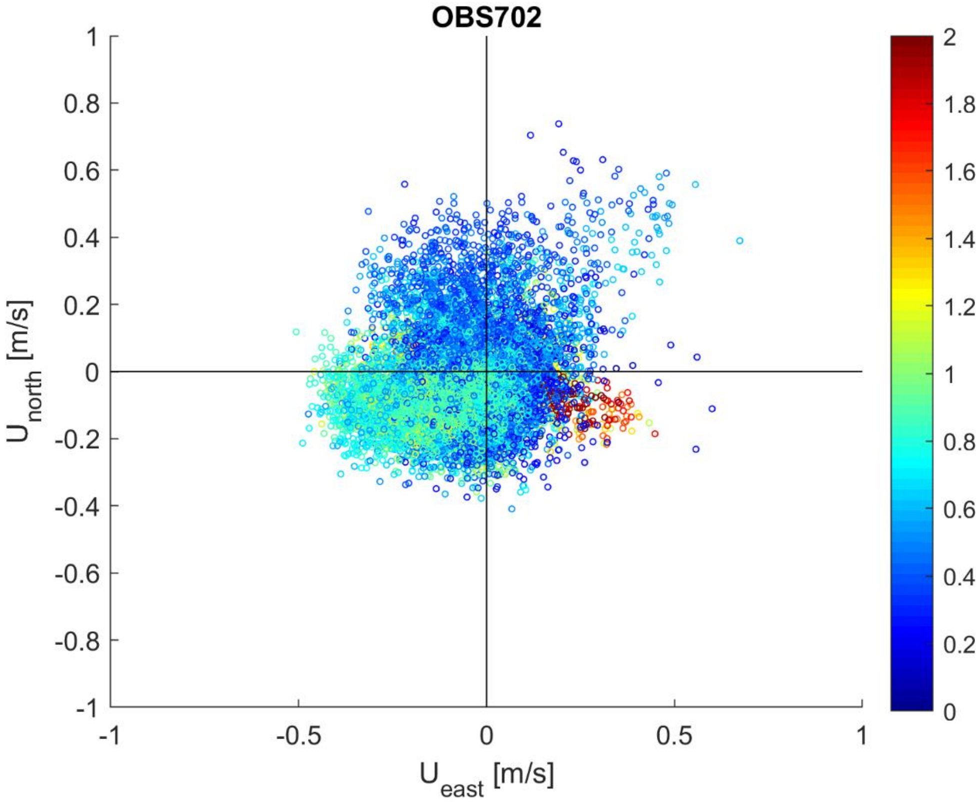
OBS702
U_{north} [m/s]
U_{east} [m/s]
1
0.8
0.6
0.4
0.2
0
-0.2
-0.4
-0.6
-0.8
-1
-1
-0.5
0
0.5
1
2
1.8
1.6
1.4
1.2
1
0.8
0.6
0.4
0.2
0

E.4.1.2.   Velocity scatterdiagram with sediment concentration in colors

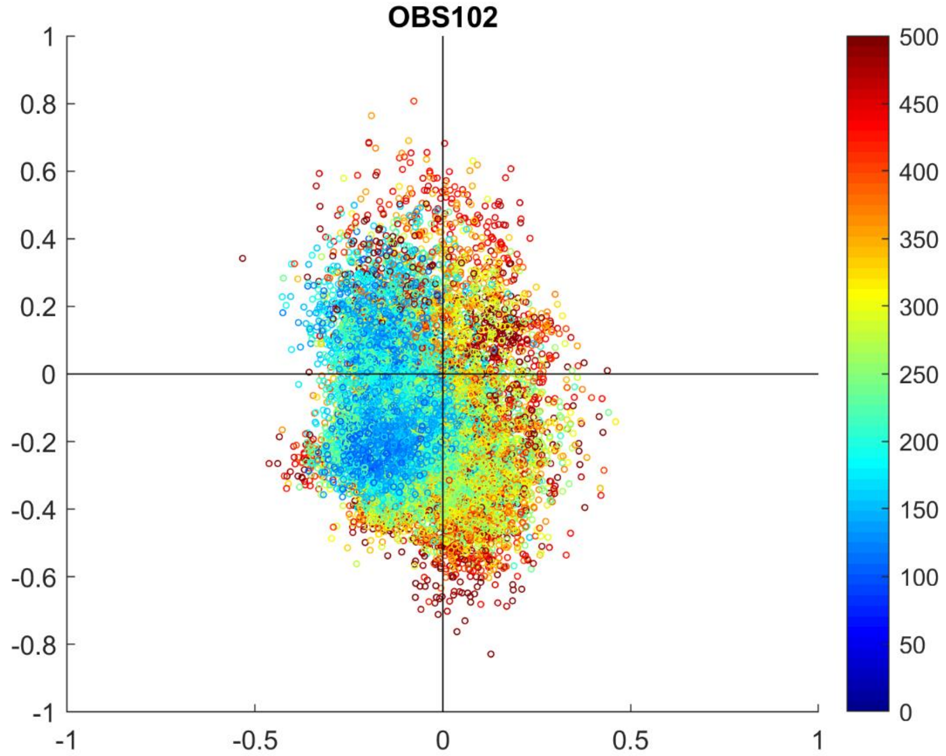

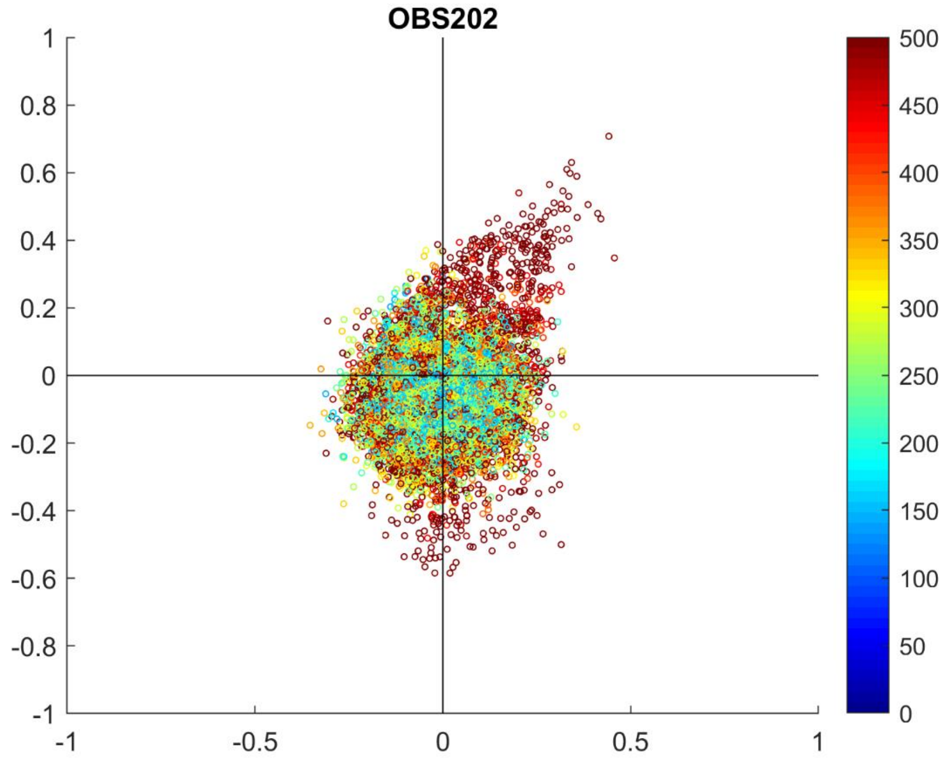

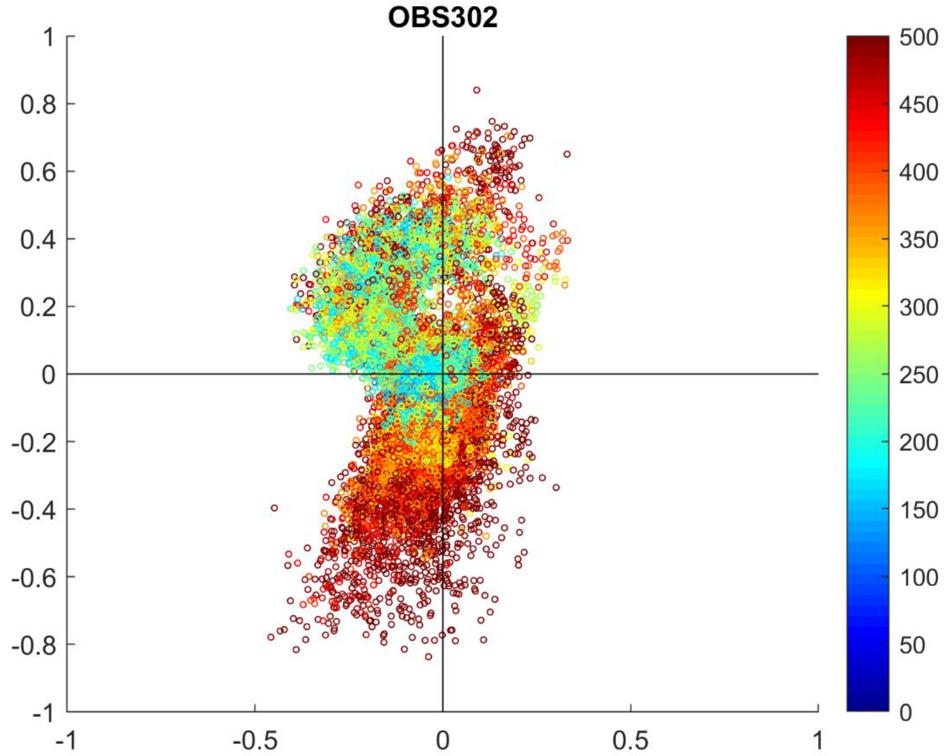
OBS302
1
0.8
0.6
0.4
0.2
0
-0.2
-0.4
-0.6
-0.8
-1
-1
-0.5
0
0.5
1
500
450
400
350
300
250
200
150
100
50
0

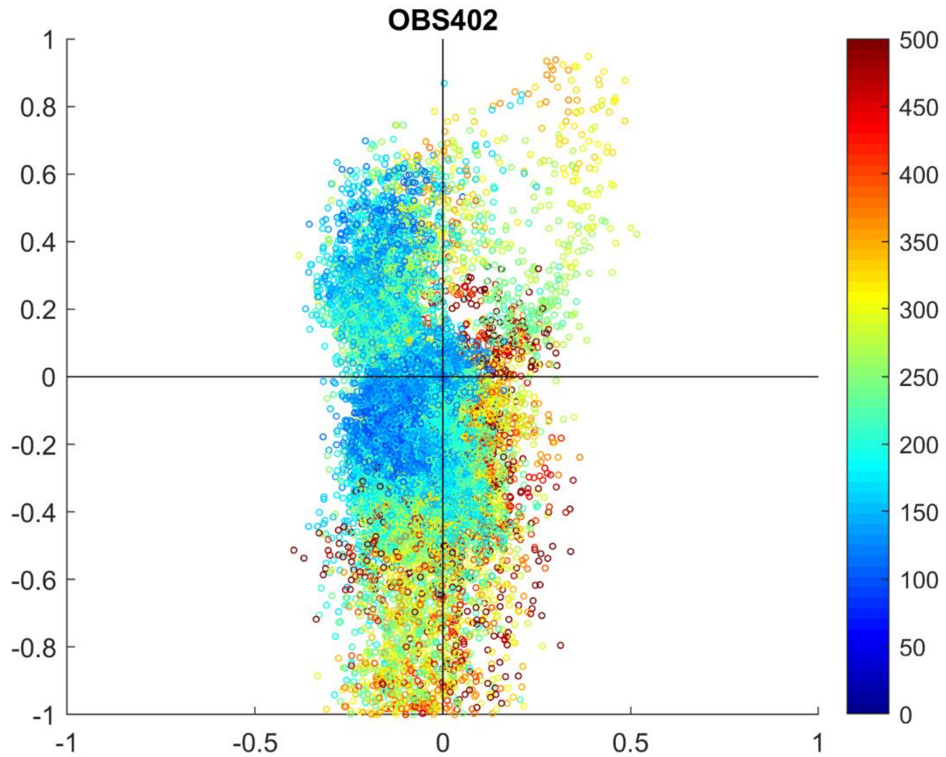
OBS402
1
0.8
0.6
0.4
0.2
0
-0.2
-0.4
-0.6
-0.8
-1
-1
-0.5
0
0.5
1
500
450
400
350
300
250
200
150
100
50
0

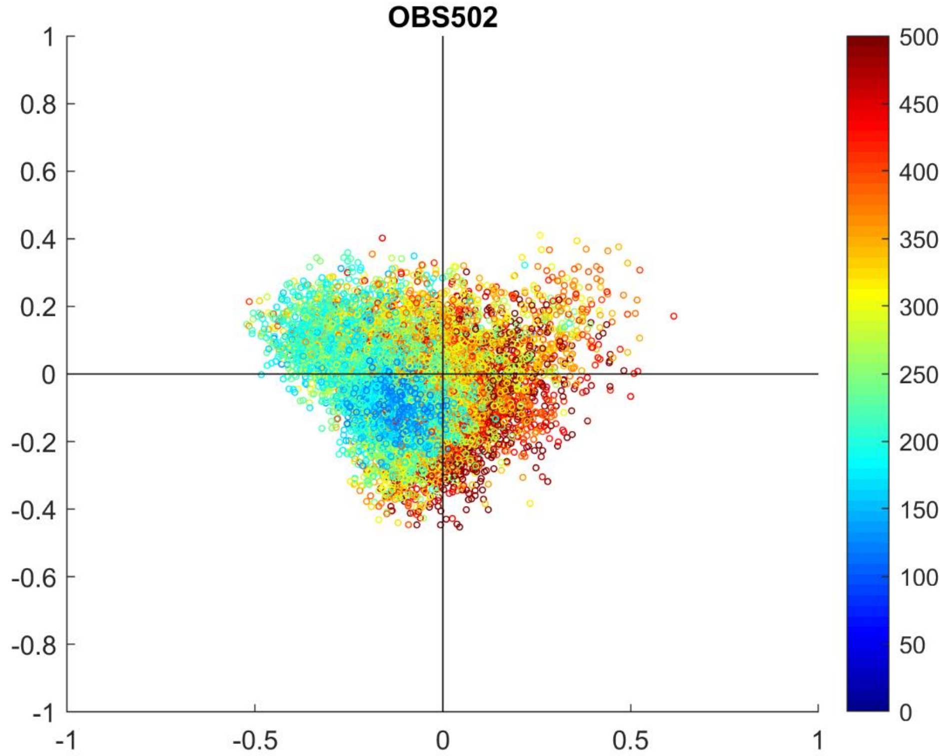
OBS502
1
0.8
0.6
0.4
0.2
0
-0.2
-0.4
-0.6
-0.8
-1
-1
-0.5
0
0.5
1
500
450
400
350
300
250
200
150
100
50
0

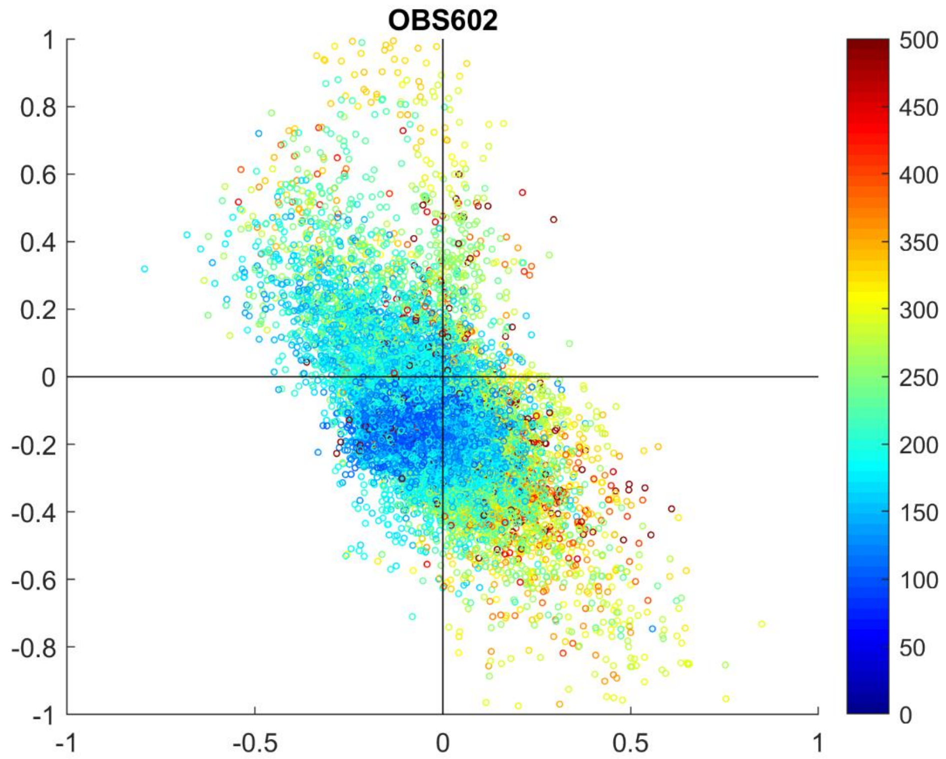
OBS602
1
0.8
0.6
0.4
0.2
0
-0.2
-0.4
-0.6
-0.8
-1
-1
-0.5
0
0.5
1
500
450
400
350
300
250
200
150
100
50
0

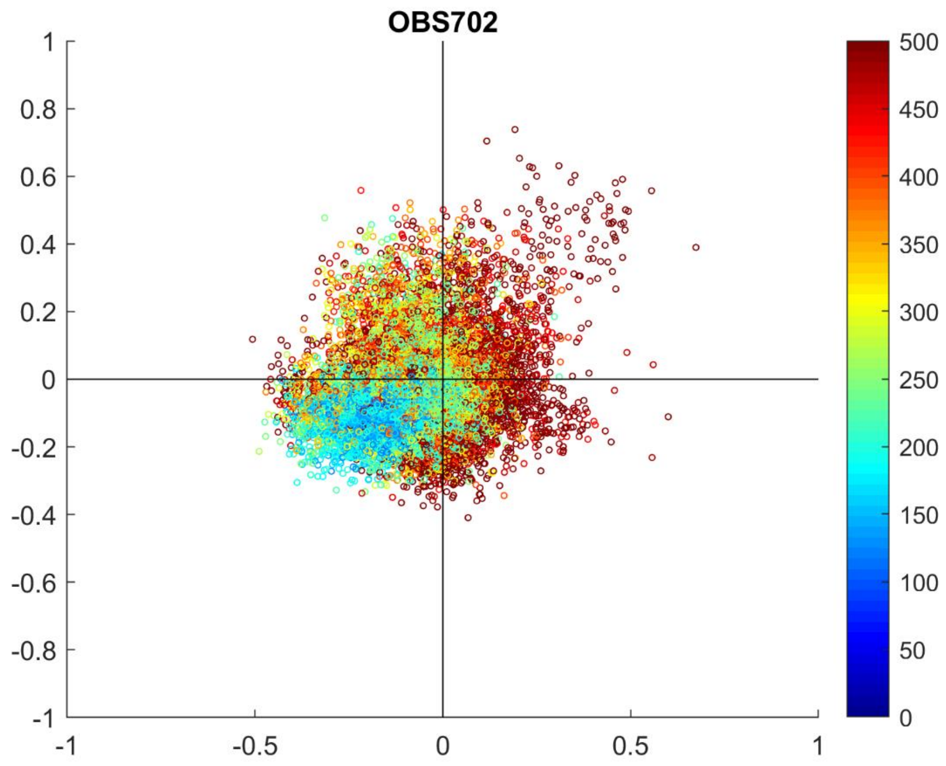
OBS702
1
0.8
0.6
0.4
0.2
0
-0.2
-0.4
-0.6
-0.8
-1
-1
-0.5
0
0.5
1
500
450
400
350
300
250
200
150
100
50
0

E.4.1.3. Cumulative sediment flux (northward positive)

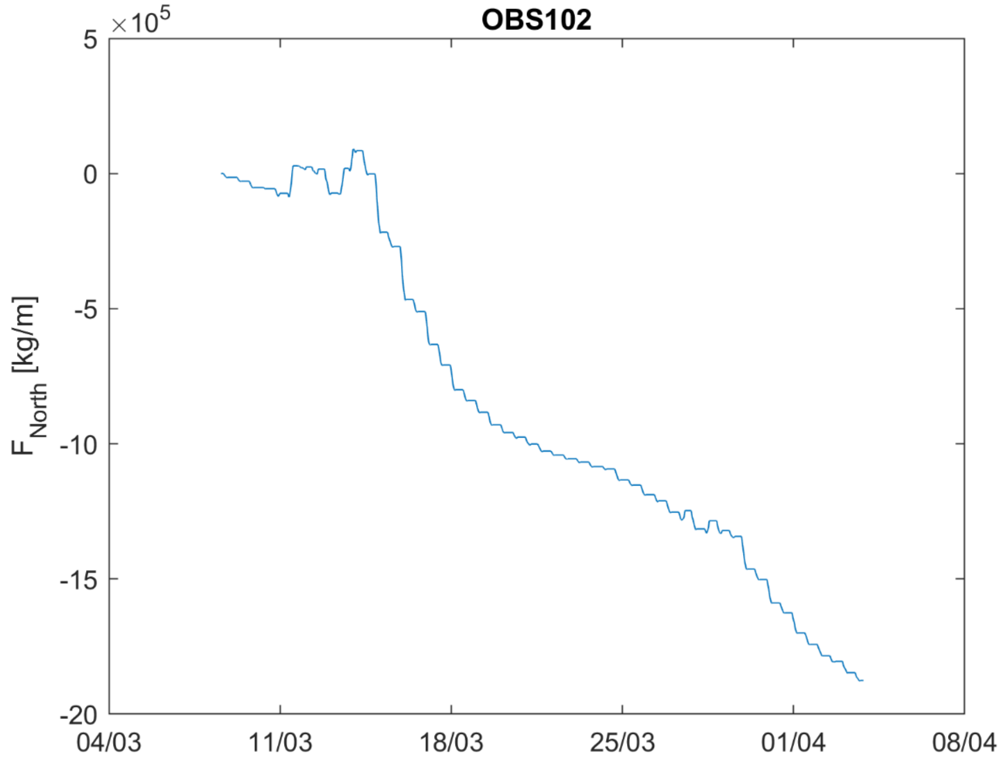

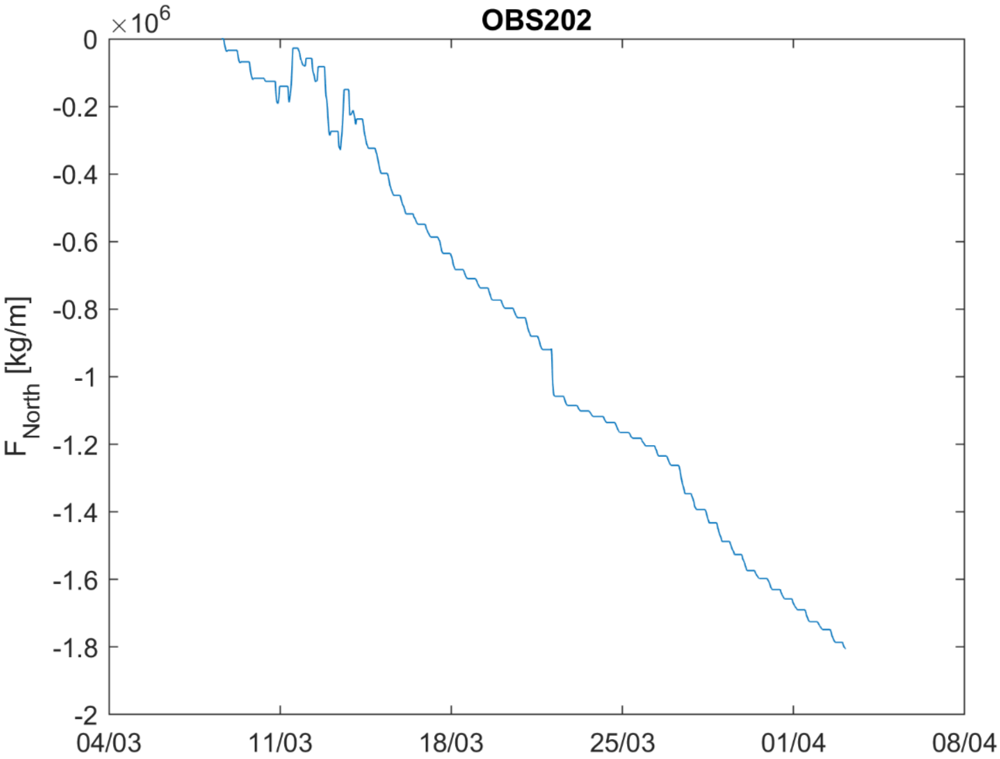

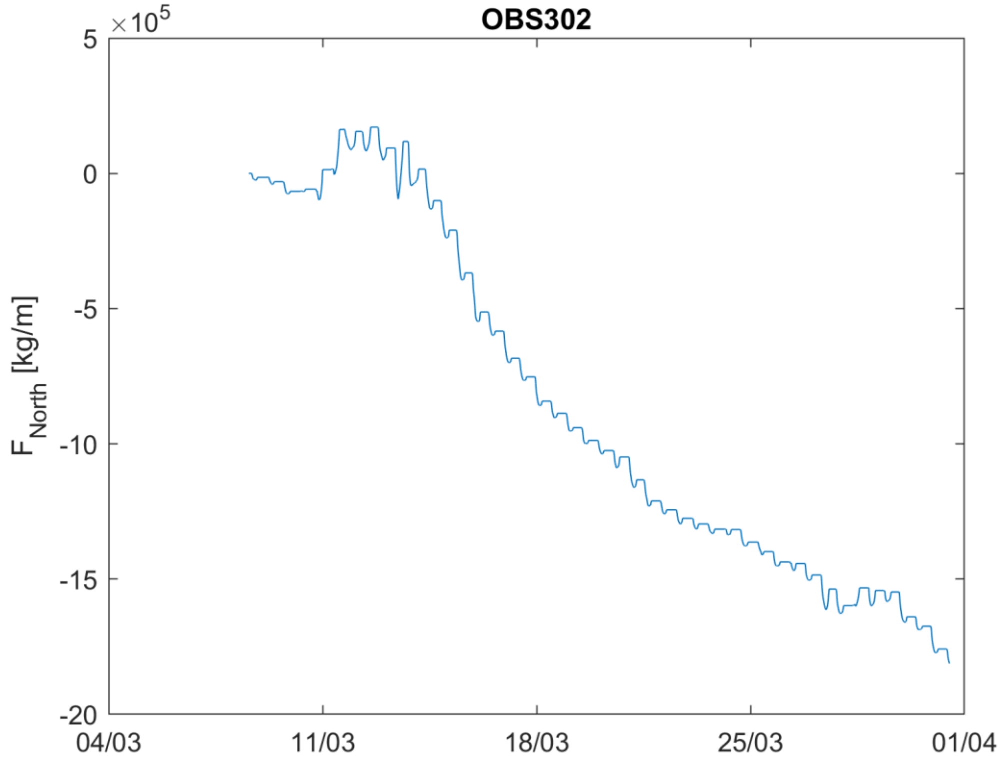
OBS302
×10^5
5
0
-5
-10
-15
-20
F_North [kg/m]
04/03
11/03
18/03
25/03
01/04

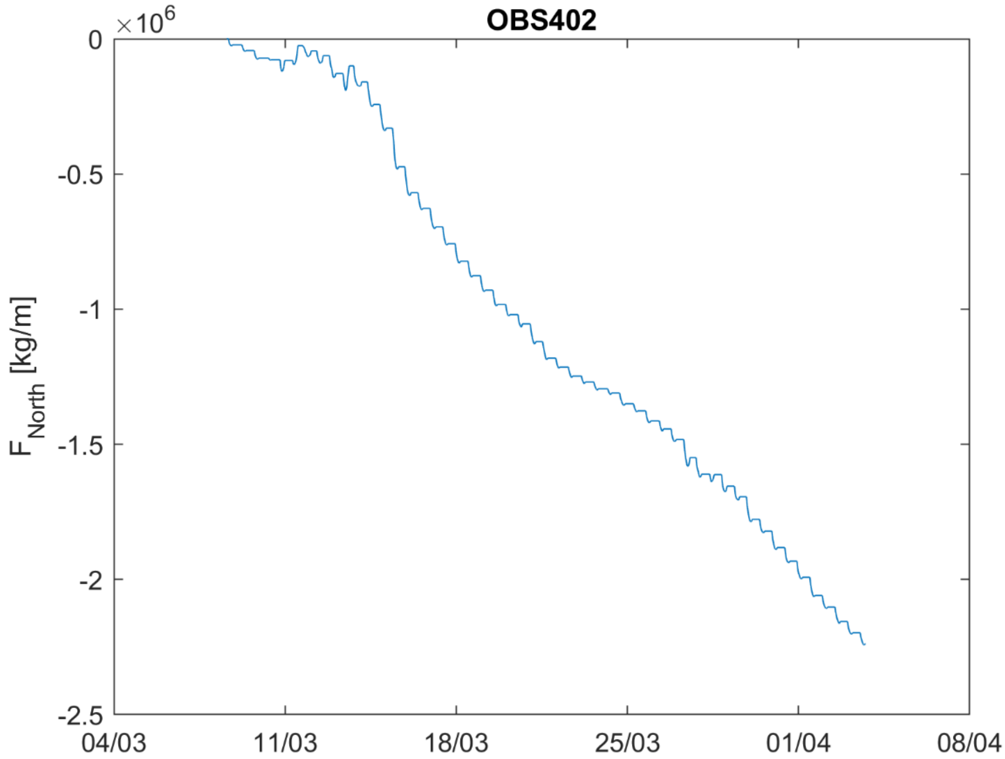
OBS402
×10^6
0
-0.5
-1
-1.5
-2
-2.5
F_North [kg/m]
04/03
11/03
18/03
25/03
01/04
08/04

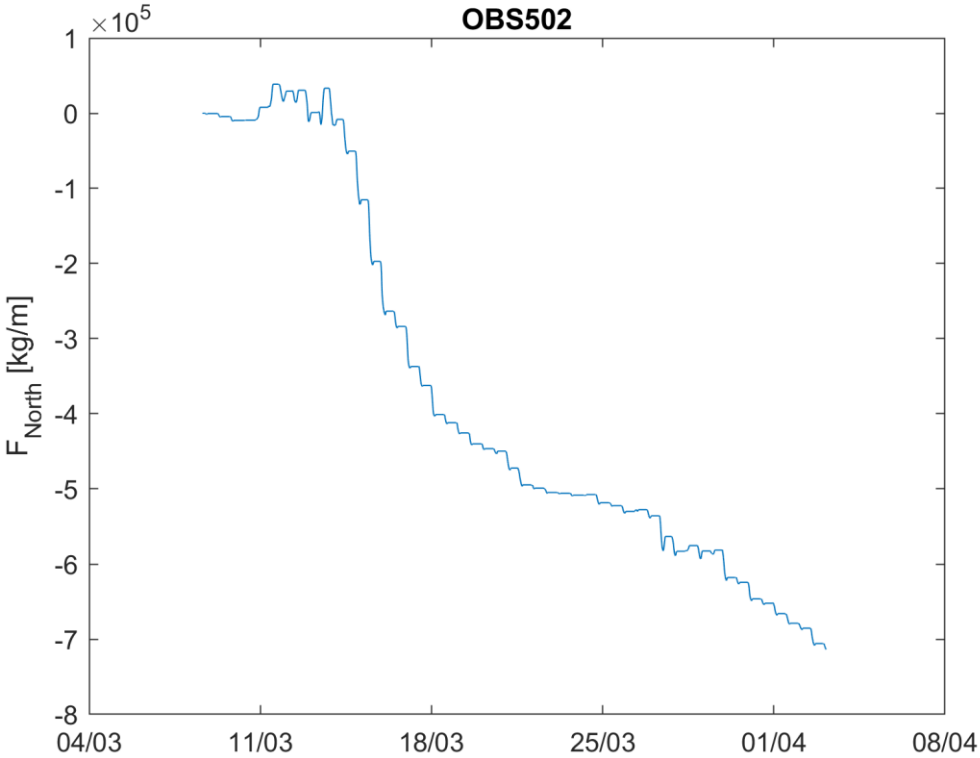
OBS502
×10^5
F_{North} [kg/m]
1
0
-1
-2
-3
-4
-5
-6
-7
-8
04/03
11/03
18/03
25/03
01/04
08/04

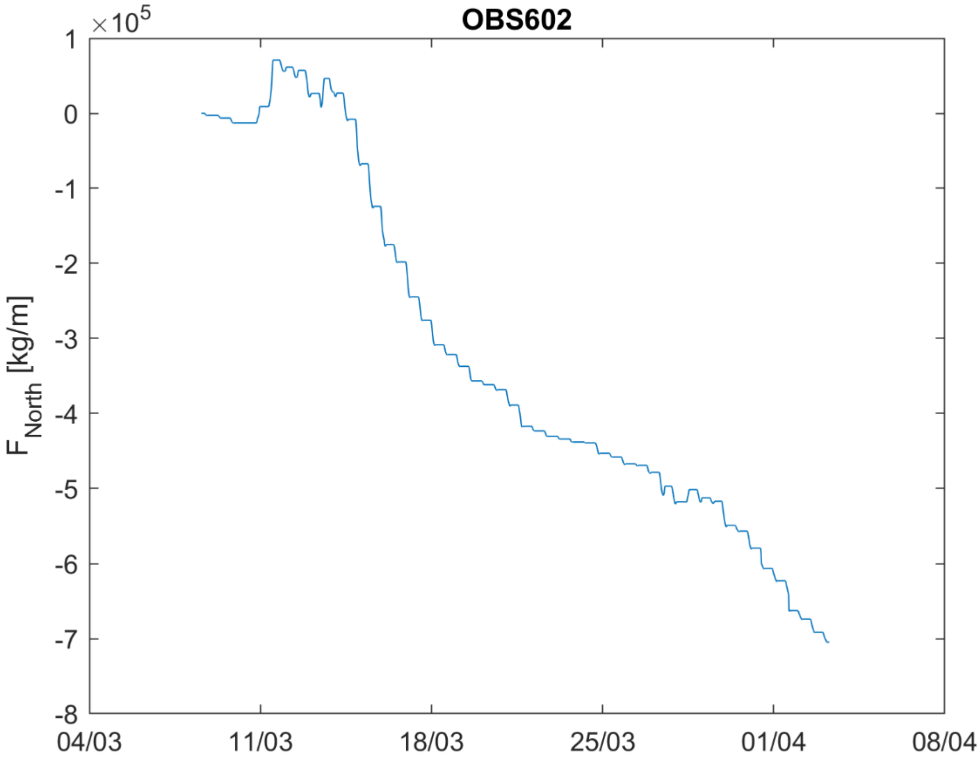
OBS602
×10^5
F_{North} [kg/m]
1
0
-1
-2
-3
-4
-5
-6
-7
-8
04/03
11/03
18/03
25/03
01/04
08/04

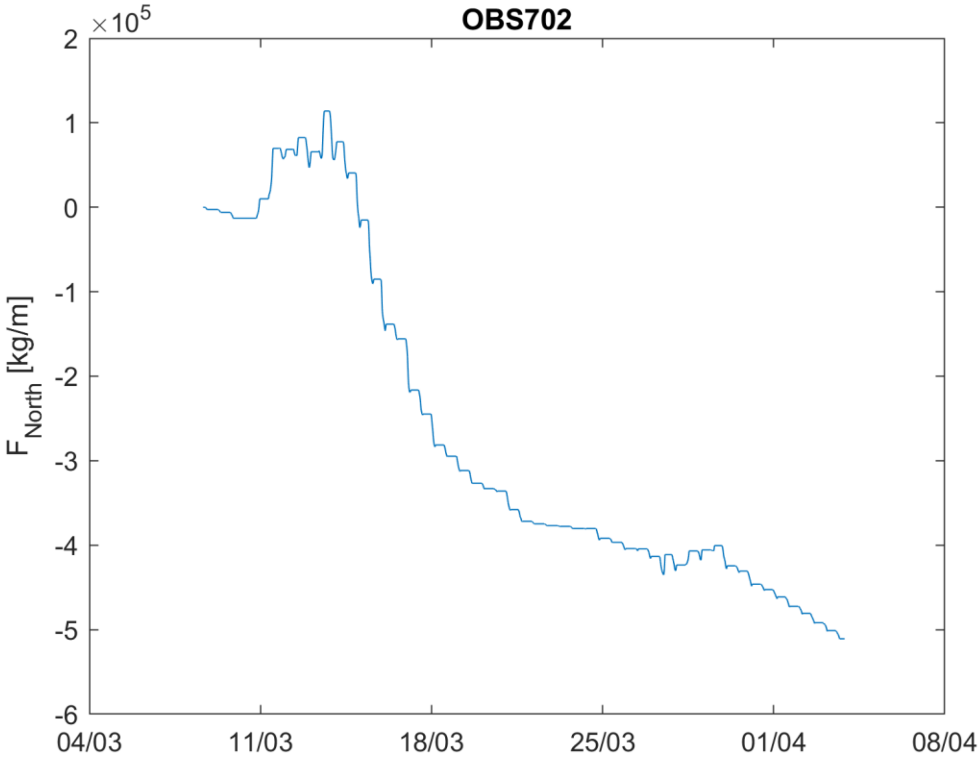
OBS702
×10^5
2
1
0
-1
-2
-3
-4
-5
-6
F_North [kg/m]
04/03
11/03
18/03
25/03
01/04
08/04

F Settling velocity observations

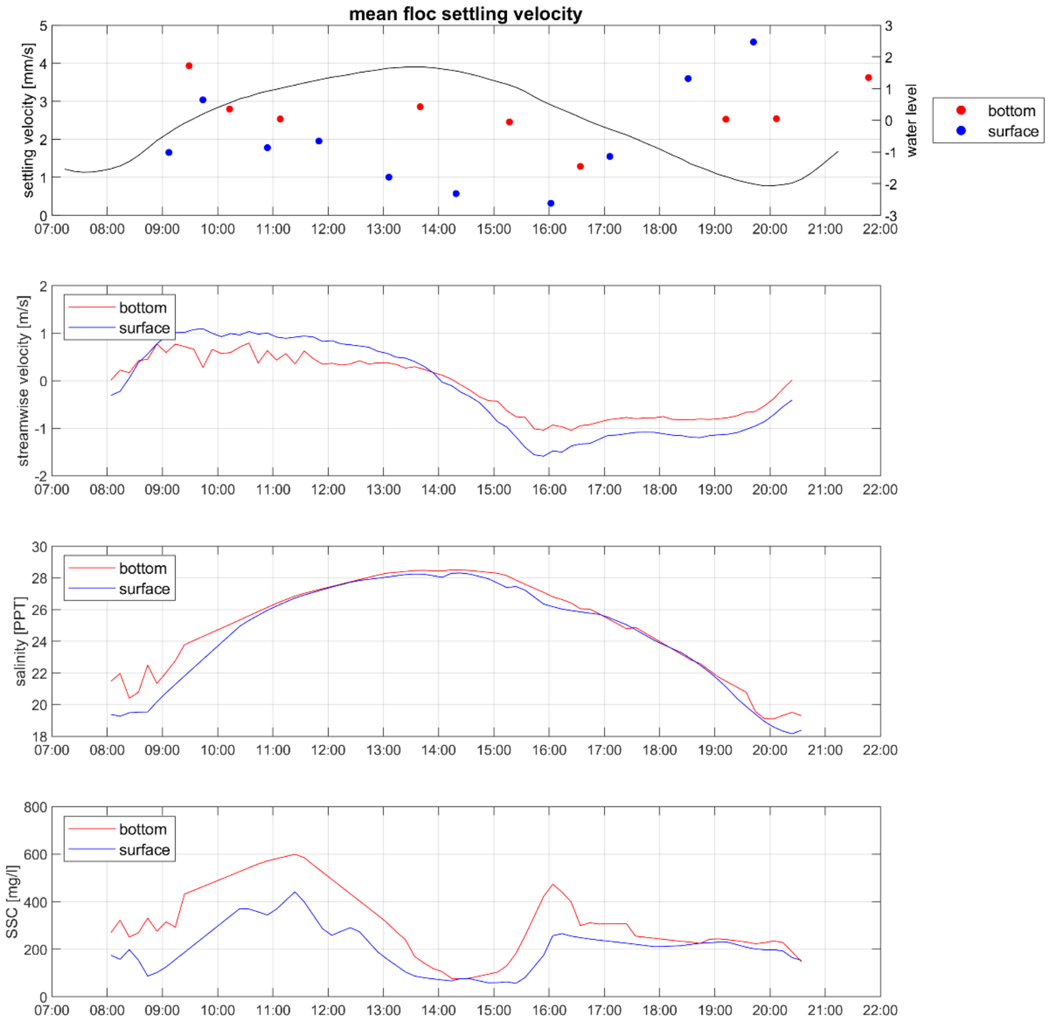

Figure 7-36 Floc settling velocity (top panel), flow velocity (second panel), salinity (third panel) and SSC (fourth panel) in august 2018 at location Emden

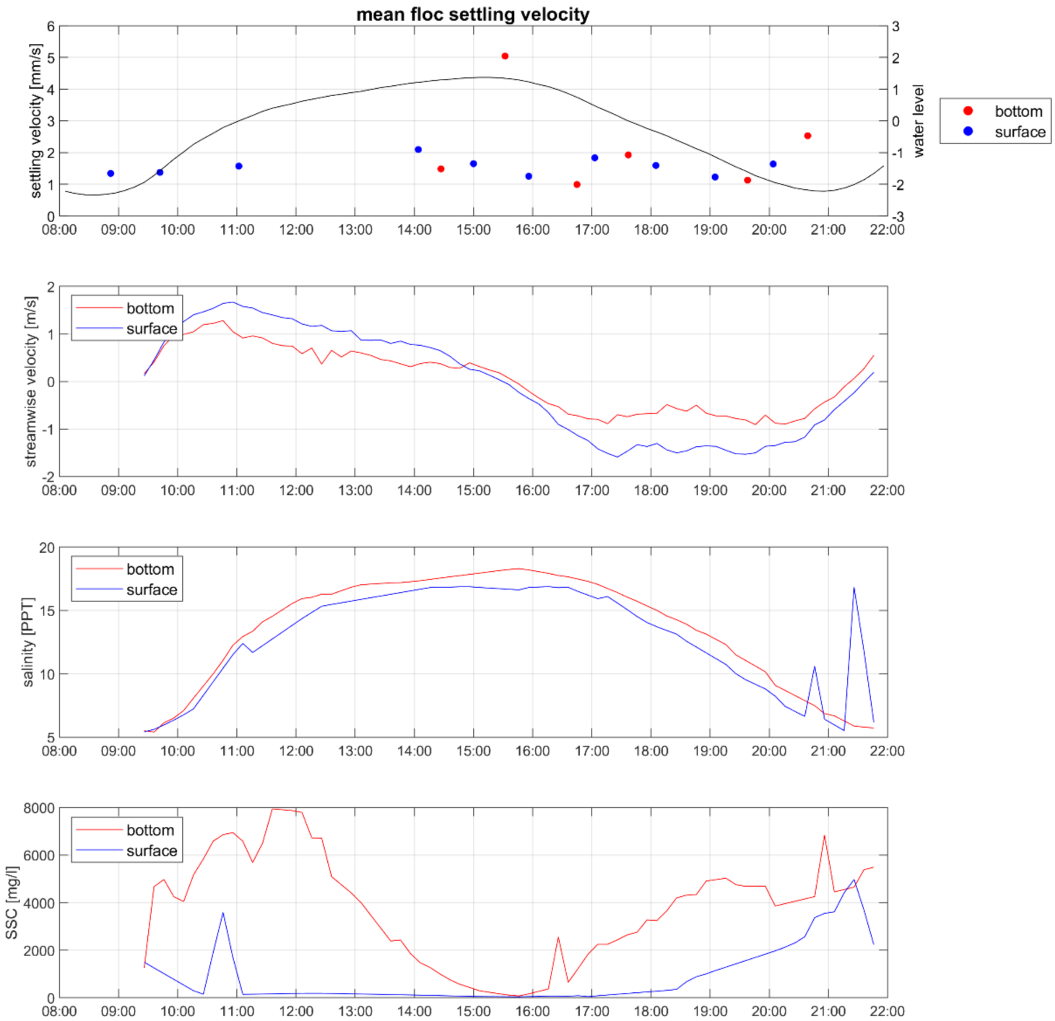

Figure 7-37 Floc settling velocity (top panel), flow velocity (second panel), salinity (third panel) and SSC (fourth panel) in January 2019 at location Emden

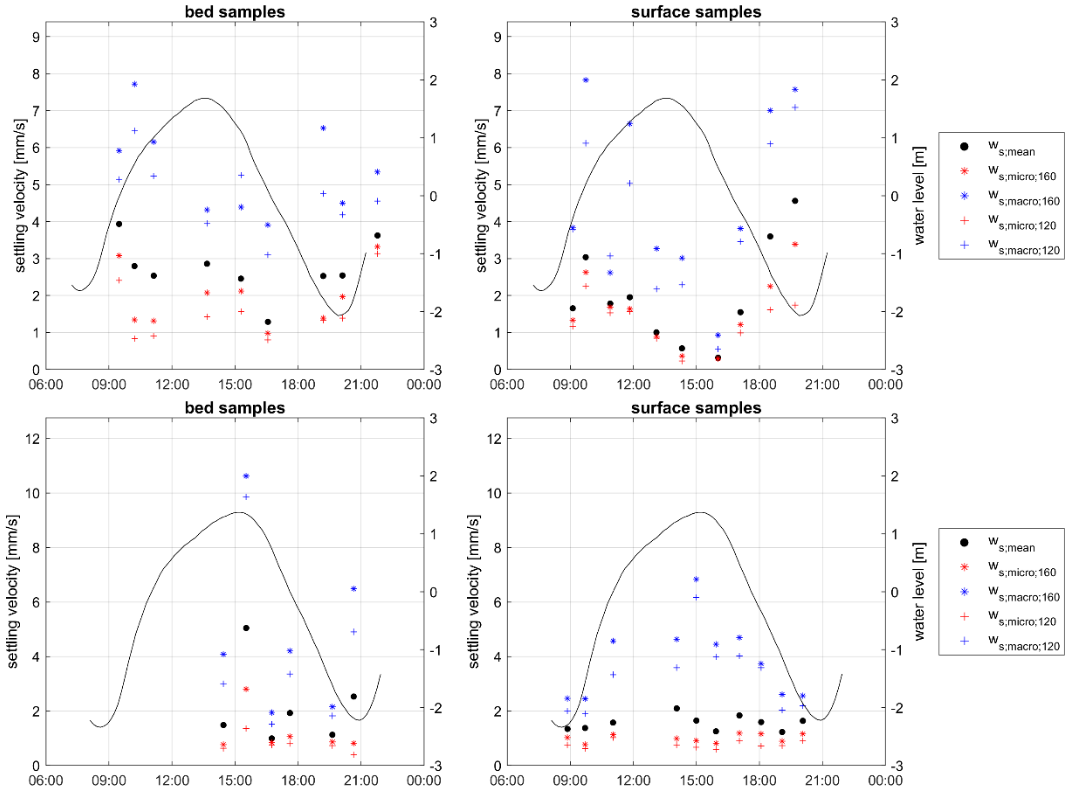

Figure 7-38 Mean. Micro, and macro floc settling velocity (using both 120 and 160 µm as a differentiator) through time near the bed (left panels) and near surface (right panels) in August 2018 (top panels) and in January 2019 (lower panels).

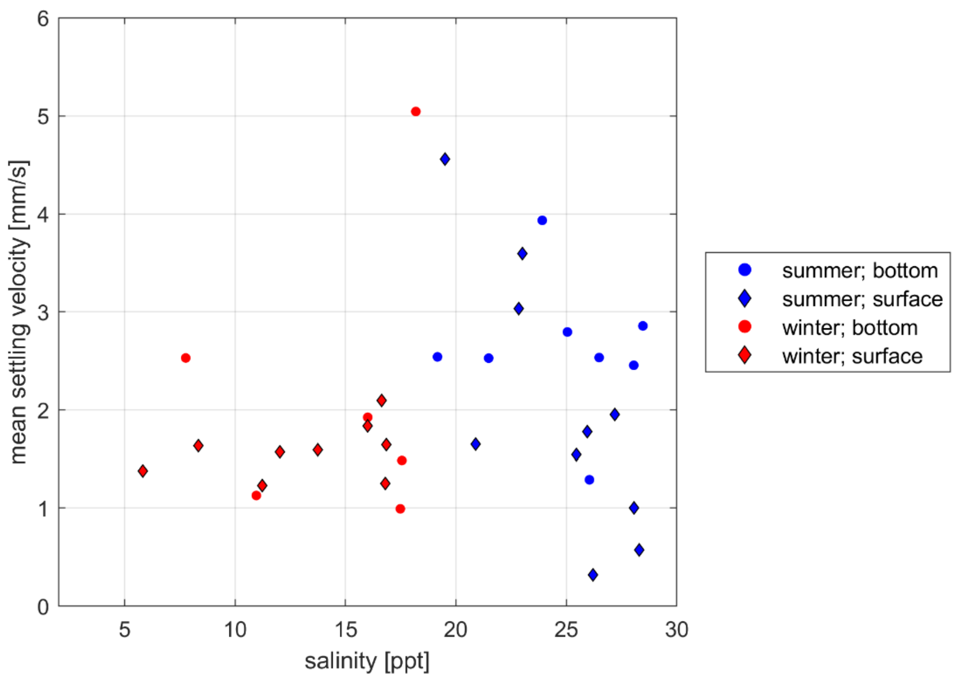

Figure 7-39 Mean floc settling velocity as a function of salinity; both measurement campaigns, near bed and near surface

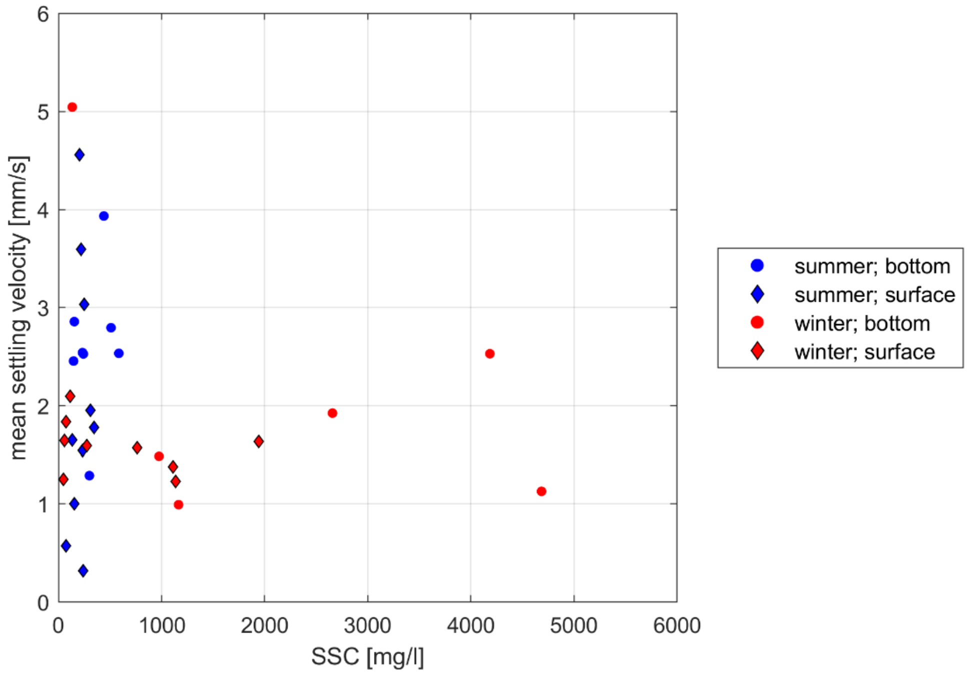

Figure 7-40 Mean floc settling velocity as a function of SSC; both measurement campaigns, near bed and near surface

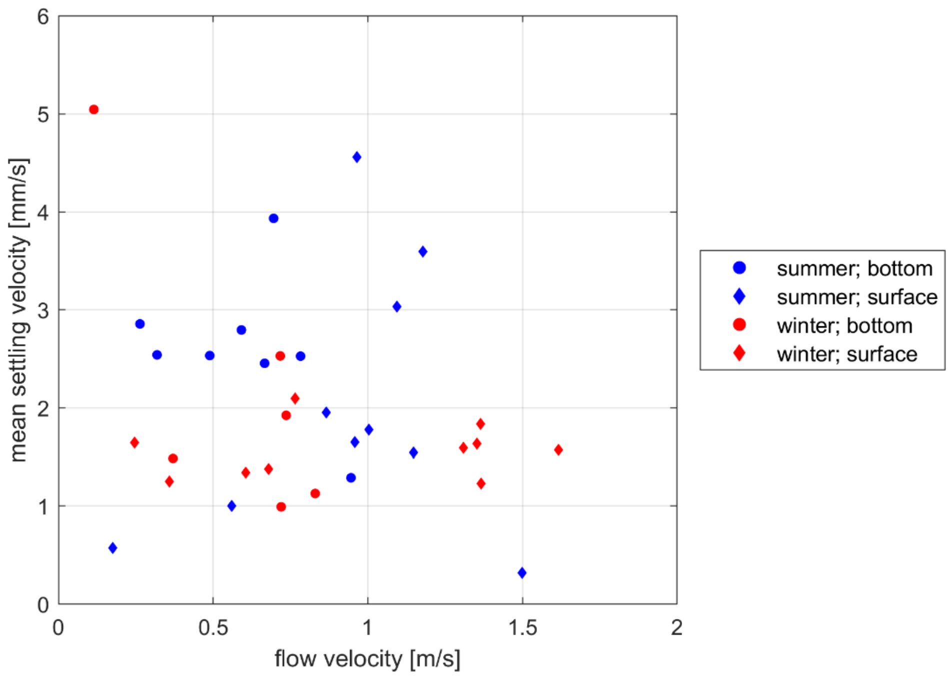

Figure 7-41 Mean floc settling velocity as a function of flow velocity; both measurement campaigns, near bed and near surface

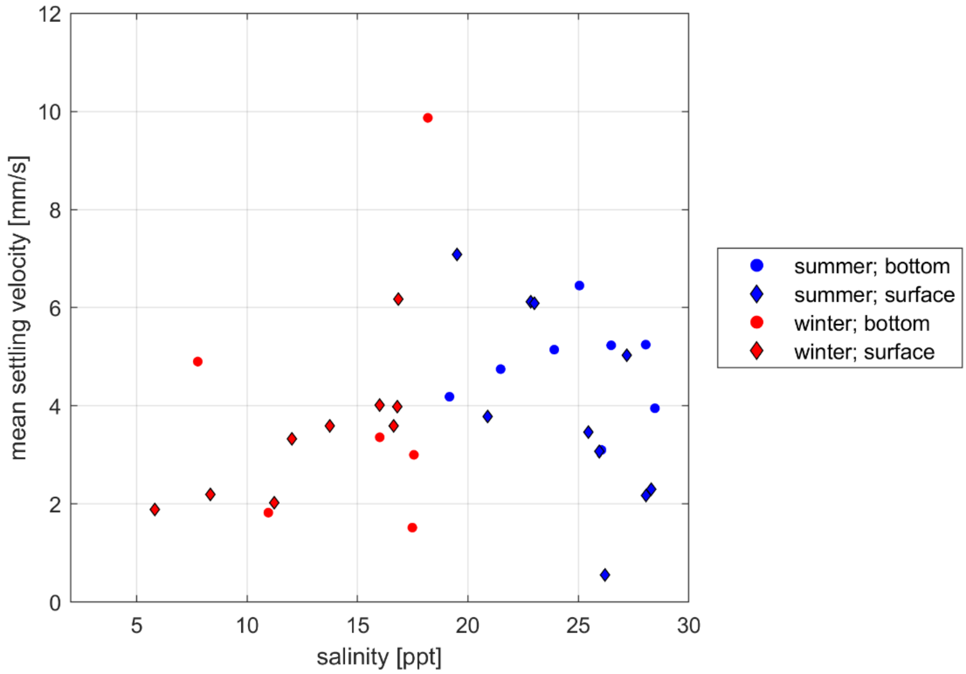

Figure 7-42 Macro floc settling velocity (defined as D > 120 micron) as a function of salinity; both measurement campaigns, near bed and near surface

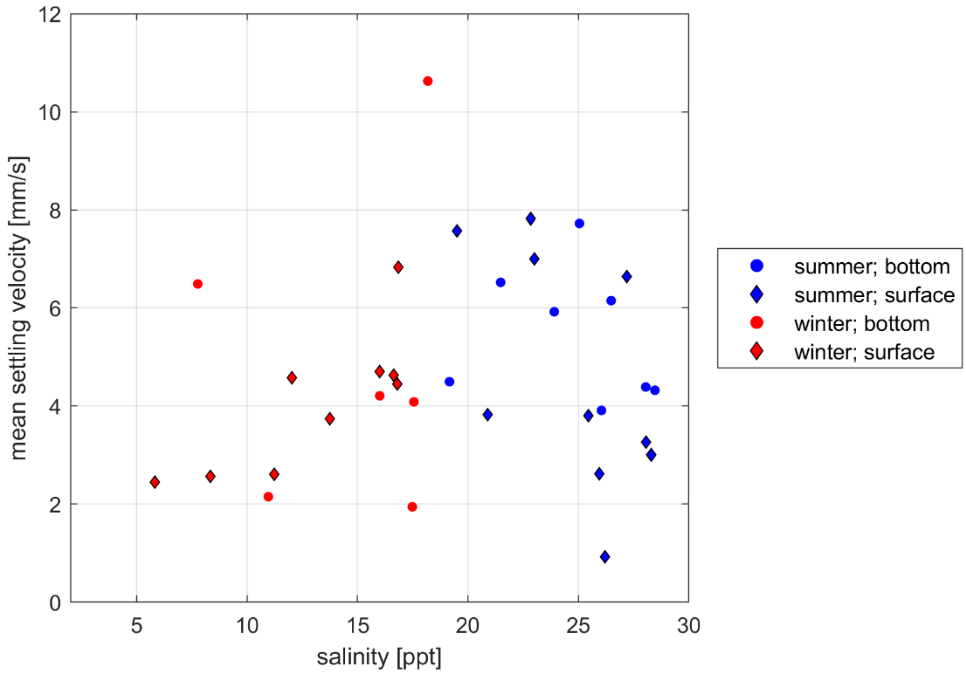

Figure 7-43 Macro floc settling velocity (defined as D > 160 micron) as a function of salinity; both measurement campaigns, near bed and near surface

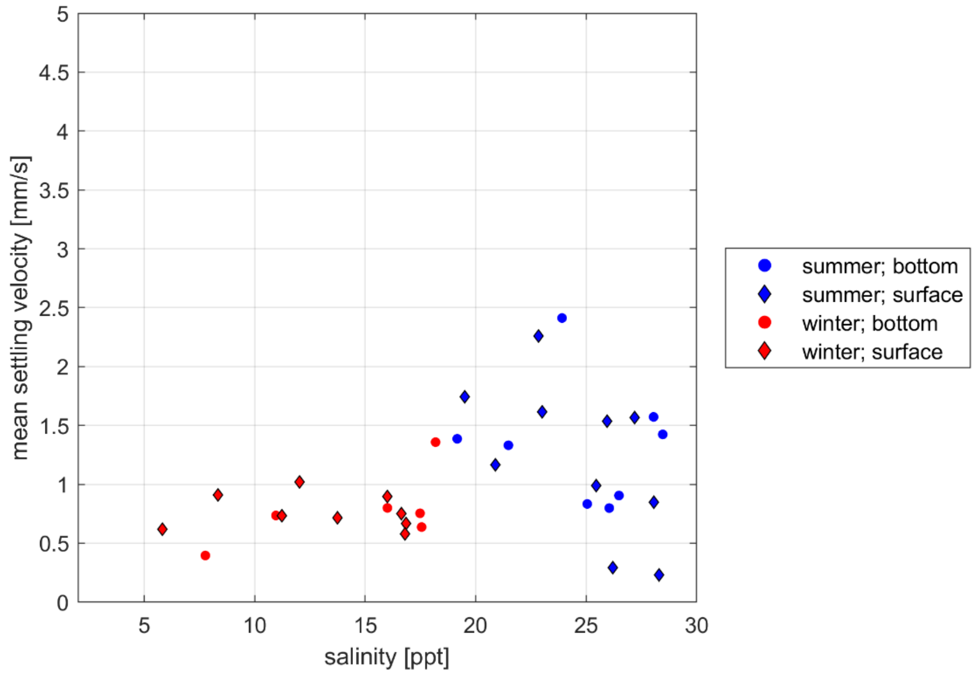

Figure 7-44 Micro floc settling velocity (defined as D > 120 micron) as a function of salinity; both measurement campaigns, near bed and near surface

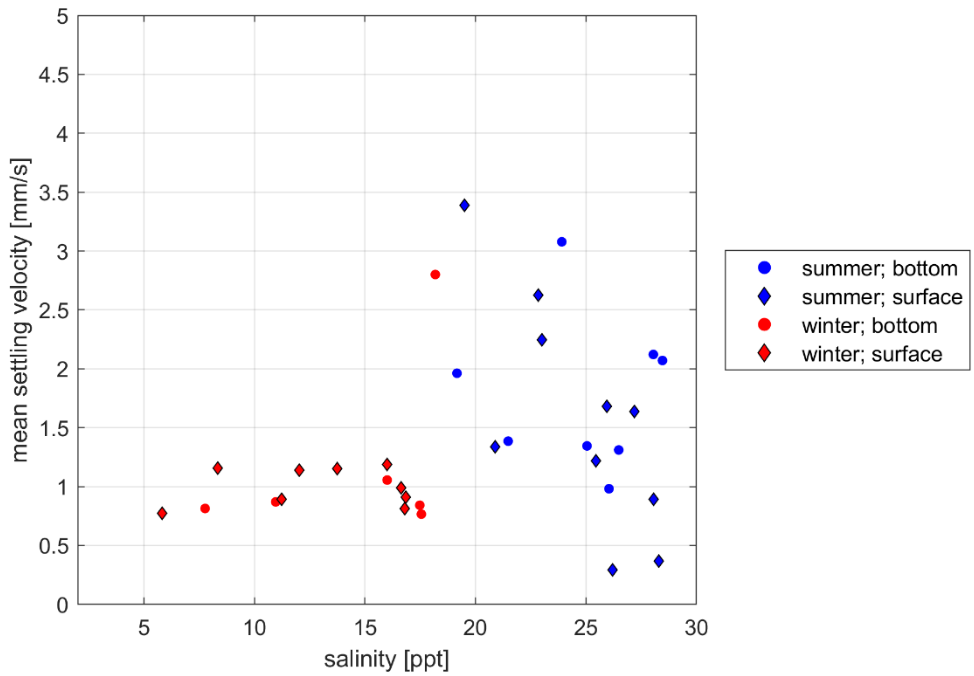

Figure 7-45 Micro floc settling velocity (defined as D > 160 micron) as a function of salinity; both measurement campaigns, near bed and near surface

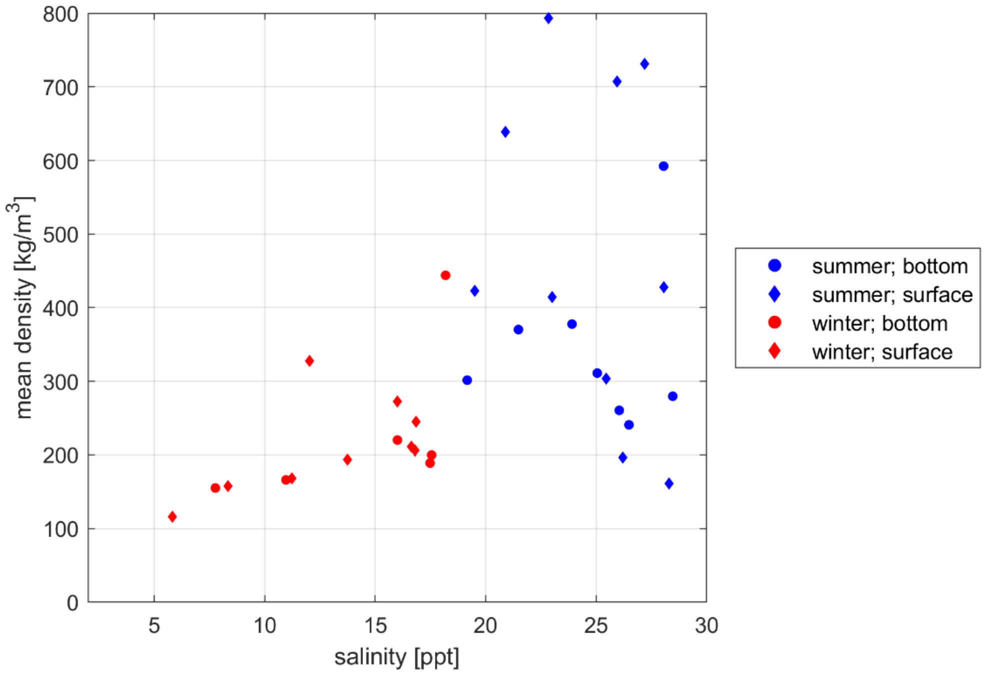

Figure 7-46 Mean density of flocs as a function of salinity

Deltares is an independent institute for applied research in the field of water and subsurface. Throughout the world, we work on smart solutions for people, environment and society.

Deltares

www.deltares.nl